2007

Improving the Prediction of the Behaviour of Masonry Wall Panels Using Model Updating and Artificial Intelligence Techniques

Sui, Chengfei

http://hdl.handle.net/10026.1/2260

Improving the Prediction of the Behaviour of Masonry Wall Panels Using Model Updating and Artificial Intelligence Techniques

By

Chengfei Sui

A thesis submitted to the University of Plymouth for the degree of

Doctor of Philosophy

School of Engineering, Faculty of Technology

May 2007

IMPROVING THE PREDICTION OF THE BEHAVIOUR OF MASONRY WALL PANELS USING MODEL UPDATING AND ARTIFICIAL INTELLIGENCE TECHNIQUES

————CHENGFEI SUI

ABSTRACT

Out-of-plane laterally loaded masonry wall panels are still much used in modern structures. However due to their anisotropic and highly composite nature, it is extremely difficult to understand their behaviour and to date there is no analytical method that is capable of accurately predicting the response of masonry panels to the applied loadings. This is one of the major obstacles in analysing and designing masonry structures. This research studied a new method that accurately predicts the response of laterally loaded masonry wall panels.

In this dissertation, the method of using corrector factors developed by previous researchers was further studied using model updating and artificial intelligence (AI) techniques based on previous experimental results of full scale wall panels tested in the University of Plymouth. A specialised non-linear finite element analysis (FEA) program was used to implement the method developed in this study. The analytical response was compared with other experimental results from different laboratories.

Initially, it was found that there was some obvious noise in the experimental load deflection data, which made comparison between FEA and the experimental results very difficult. The research therefore proposed a methodology for minimising the experimental noise based on 3D surface fitting and regression analyses applied to lateral deflection experimental data.

The next step was the detailed study of corrector factors using the numerical model updating procedure. Corrector factors were determined for various zones within a masonry panel (the Base Panel) by minimising the discrepancy between the experimental load deflection data and those obtained from non-linear FE analysis. A detailed model updating procedure was studied including the model analysis, the objective function and the constraint function for the genetic algorithm (GA). A uniqueness study to corrector factors was also carried out.

The following step was undertaken to analyse general masonry wall panels using the findings of this study. The concept of zone similarities proposed by previous researcher, which was based on the relative distance of each zone from similar boundaries, was used for applying correctors from the base panel to the new panel to be analysed. A modified cellular automata (CA) model was used to match the similar zones between the new panel and the base panel. The generality and robustness of this method was validated using a number of masonry wall panels tested by various organizations. These walls were single leaf masonry wall panels of clay bricks with different boundary types, dimensions, with and without openings.

The main finding in this research are that the boundary effects have a major influence on the response of masonry panels subjected to lateral loading, improperly defined boundary conditions in FEA are the main source of error in the past numerical analysis. Using the corrector factors that are able to properly quantify the actual boundary effects and make appropriate revisions, more accurate analysis is achieved and the predicted response of masonry walls match with their experimental results very well.

Key Words: **masonry panel, lateral loading, model updating, artificial intelligence corrector factors.**

ACKNOWLEDGEMENTS

AUTHOR'S DECLARATION

At no time during the registration for the degree of Doctor of Philosophy has the author been registered for any other University award.

This study was financed with the aid of a studentship from the Faculty of Technology, the University of Plymouth, UK.

A programme of advanced study was undertaken, which included courses on Artificial Neural Network and Evolutionary Computation. The author has acted as a demonstrator in the first year Structural Analysis laboratory

Relevant scientific seminars and conferences were regularly attended and 4 papers were presented in the Masonry International Conference in 2006,

Presentation and Conferences Attended:

- The 7th Int. Masonry Conference, London, British Masonry Society

- School internal Seminar

In total 8 papers were published as attached in this thesis

Words counted for main body of thesis: 42,484.

Signed...Chengfee. Sui

Date...18. June. 2007

NOTATIONS

As, Bs, Cs, Ds,Es   the GA variables for the contributions to corrector factors from simply supported edge

Ab, Bb, Cb, Db, Eb   the GA variables for the contributions to corrector factors from built-in edge

Ai,Bi,Ci   the GA variables for the increasing tendency formula

Ad, Bd, Cd   the GA variables for decreasing tendency formula

CR_l,CRr,CR_b   the boundary effects from the left, right and bottom edges respectively

CRl , CRr, CRb   the contribution to the corrector factors from left, right and bottom edges of the panel.

CRi, CRd   the contribution to the corrector factors from decreasing and increasing tendency formula

C_{fx}, C_{fy}   strength coefficients for the tensile strength perpendicular and parallel to the bad joints   .

D, F, G   Deflection, Load and Gradient respectively

Df, De   the deflections of FEA and experiment respectively,

EXP   experimental data

Ff, Fe   the FEA and experimental loads respectively.

j   the load level.

k   the position measurement points on the panel.

m   total load levels determined from non-linear FEA

n	number of points on masonry panel for which the deflections are considered.
wl, wd, wg	the weights of failure load, deformations and gradient respectively
Xs,Xb	distance from centre of the element to the corresponding panel edges of simply supported and built-in.
X1,X2...,	Zone position in X direction
Y1,Y2,....	Zone position in Y direction
δt	the total discrepancy between analytical and experimental results
δl, δd, δg	the discrepancy of the failure load , deformation and the discrepancy respectively between the experimental results and FEA.

TABLE OF CONTENT

LIST OF FIGURES

LIST OF TABLES

1. INTRODUCTION

1.1 THE MOTIVATIONS OF THIS RESEARCH

The motivations of studying out-of-plane laterally loaded masonry wall panels are as follows: Firstly, masonry is still preferred in many modern structures due to its advantages such as durability, low maintenance, excellent sound absorption, good insulation properties, and fire protection to say the least. To reduce the self-weight of the masonry wall to meet the needs of modern structures, thinner masonry wall panels are required which call for the more accurate design method for masonry wall panels. Secondly, the preservation of existing historical masonry buildings (walls) requires the advanced understanding of the behaviour of masonry wall panels under lateral loading. Thirdly, the study of masonry will facilitate the analyses of other complicated materials and structures due its highly composite nature.

Currently, two methods are used in the study of masonry wall panels: empirical methods and numerical methods. Empirical methods propose theories are based on the simple model and comparing the results with those of experiment. Researchers studied the behaviour of laterally loaded masonry wall panels using empirical methods such as Baker(1972, 1973, 1979, 1982a, 1982b, 1982c), Lawrence(1983, 1988, 1991a, 1994, 1995) , West, *et.al.*(1974, 1975, 1976), Sinha (1978, 1980), Anderson(1984, 1985, 1987), Edgell (1995a, 1995b, 2002, 2005), Fried(1989), Chong, *et.al.*(1992a) and Duarte(1998). By testing masonry constituents, small specimens, wallettes and full scale panels, several analytical methods were proposed such as the Empirical Strip Method (Baker 1980), Fracture Line Method (Sinha 1978) , Principal Stress Method (Baker 1982c), Elastic Plate Method (Sinha 1973, Baker 1982a), Plastic Plate Method (Sinha 1978), Yield Line Method (West 1977, Cajdert 1980, Brinker 1984), and Energy

method (Candy 1988). In the UK, the code of practice BS 5628 is based on principles derived from these research findings especially those by CERAM (former British Ceramic Research Association). Normally, the models established by empirical methods are based on a variety of simplifications, their accuracies are limited and these methods do not cover predictions of panel deflection, which is a major structural aspect that influences the behaviour of panels. Numerical methods such as finite element analyses (FEA) is more suitable to analyse complicated structure and it had been applied to study the laterally loaded masonry panels by many researchers such as Ma and May(1986), Chong, et al.(1992a), (Lourenco 1997, 2000b, 1996), Luciano and Sacco(1997, 1998), Zucchini and Lourenco(2002), Lee, et.al.(1996), Massart., et.al.(2004, 2005b), Trovalusci and Masiani(2003, 2005). Nowadays two kinds of finite element analyses (FEA) have been developed for masonry study; they are micro-modelling and macro-modelling. Micro-modelling considers the units and the mortar separately whereas macro-modelling regards masonry as homogeneous materials.

However, due to the length of time taken in micro-modelling, or the inaccuracy of the smeared material properties used in macro-modelling, the finite element analysis of laterally loaded masonry wall panels are still not accurate enough for practical usage compared with the analysis of other materials such as concrete, steel, plastic or even wood.

The difficulty of accurately analysing masonry wall panels lies in that masonry consists of two different constituents (bricks and mortar). The mechanical properties of masonry not only depend on the properties of the bricks and mortar, but also depend on other factors such as the bond strength between bricks and mortar, the volume ratio of the two components, the orientation and dimension of units, and the existence of cracks in masonry. Therefore, any material properties obtained by testing the smaller specimens

in laboratory are not able to accurately represent the characteristics of the real masonry structures (of larger dimension), which bring great difficulty to accurate analysis.

The Conceptual Modelling Research Group (CMRG) in the University of Plymouth (UoP) studied a new method that directly employs the information of full scale masonry walls to accurately predict the response of laterally loaded masonry wall panels. Using the nonlinear FEA model and Cellular Automata (CA), Zhou(2002) developed the concept of corrector factors and zone similarity based on the experimental data from some full scale laterally loaded masonry panels tested by Chong(1993) in the University of Plymouth. Corrector factors were used to summarise and revise the total discrepancies caused by all possible factors in FEA model such as material properties, physical and geometrical properties and other causes. The corrector factors were derived by comparing the analytical and experimental deflections at various locations (called zones) on a selected full scale masonry wall panel (called the base panel). Then these corrector factors were used to modify the flexural stiffness or strength in the related zones (elements) of the new panel to improve the FEA analysis based on zone similarity. Zone similarity was established based on the relative distance of zones from the similar boundaries, which mean that any zone on new masonry panels shares the same corrector factors with its similar zone on the base panel. Using the concept of zone similarity with the Cellular Automata model (CA), the corrector factors of new panels to be analysed were determined from the corrector factors derived from the base panel.

So far the method of using corrector factors is still in its infancy. The definition of corrector factors is rough, some manual modification are needed for deriving corrector factors, their physical meanings are ambiguous, and it is still not clear why and how they work, the predictions using these corrector factors may sometimes not work well. Consequently further studies are necessary to better understand the concept of corrector

factors, to achieve more accurate predictions of the response of laterally loaded masonry panels.

1.2 THE OBJECTIVE OF THIS RESEARCH

This dissertation studies corrector factors, aimed to further improve the prediction of the behaviour of laterally loaded masonry wall panels; the objective of this research includes the following:

1. Understand the nature of corrector factors particularly their physical meaning.

2. Give a scientific definition of the corrector factors.

3. Find a numerical method to derive corrector factors, using the experimental information of the full scale masonry wall panel.

4. Further improve the prediction of the behaviour of laterally loaded masonry panels.

1.3 STRUCTURE OF THE THESIS

The main works involved in this dissertation are as follows:

In chapter 1, a simplified introduction is given to the motivation, the contribution and the content of this study.

In chapter 2, a comprehensive literature survey is presented, which involves empirical methods and numerical methods used in the study of laterally loaded masonry wall panels. Finite element analysis (FEA) and model updating techniques are covered in this literature survey as it is mainly used in this research.

In chapter3, the research by Chong(1993) and Zhou(2002) is explained in detailas it is the background for this research.

In chapter 4, a method to refine the irregularities of the experimental load deflection data of the laterally loaded masonry wall panels are studied, which make the irregular deflections to be regular so as to be in accordance with the macro-modelling and provide a foundation for further numerical study to corrector factors.

In chapter 5, an initial study of the corrector factors is carried out using the definition proposed by Rafiq, *et.al.*(2003).

In chapter 6, the parametric study of the FEA model used in this research is carried out, which provide the support of using corrector factors.

In chapter 7, a method of deriving corrector factors using model updating techniques with the genetic algorithm (GA) are studied. The corrector factors are thereby obtained from the laboratory information of a full scale masonry wall panel (base panel). The physical meanings of corrector factors are disclosed.

In chapter 8, the extensive study of corrector factors is carried out by changing the definition of boundary condition in the FEA model, to verify the uniqueness of the model updating solution (corrector factors) obtained. The physical meaning of corrector factors is further confirmed.

In chapter 9, the generality and validations of the corrector factors are studied using cases from different sources.

In chapter 10, conclusions and the perspectives for future works of this research are addressed.

1.4 THE CONTRIBUTIONS OF THIS RESEARCH

Following contributions are achieved in this research.

1. A method to regularize the experimental deflection data of laterally loaded masonry wall panel is proposed. This method can also be used for panels of other materials in similar situations.

2. A numerical model updating method for the FEA model of laterally loaded masonry panels using the genetic algorithm (GA) is studied. Consequently a method of updating this kind of model (deriving corrector factors) is proposed.

3. For the first time, the major boundary effects are directly revealed by numerical method and these effects are quantified using corrector factors.

4. Using the corrector factors, discrepancies caused by boundary effects are revised. This leads to a prediction of the failure load with remarkably improved accuracy.

5. For the first time, the deflections on the whole surface of the laterally loaded masonry wall panels are reasonably predicted.

6. The physical meaning of the corrector factors is clarified. It has been found that the boundary effects strongly affect the behaviour of masonry panel of laterally loading.

7. This research starts using model updating method in this area, which could be extended to other relevant studies such as constitutive relationships and failure criteria of the masonry, micro-modelling analyses and homogeneous techniques.

2. LITERATURE REVIEW

2.1 INTRODUCTION

There have been many papers published on masonry studies. The literature reviewed here focuses on studies of out-of-plane laterally loaded masonry panels (called laterally loaded masonry panel briefly in this thesis). Finite element analysis (FEA), model updating are also involved in this literature review as they are mainly used in this research.

2.2 REVIEW ON THE RESEARCH OF LATERALLY LOADED MASONRY WALL PANELS

Currently, there are mainly two ways to study laterally loaded masonry panels, the first one is the empirical methods, and the second one is the numerical methods.

2.2.1 Empirical studies of masonry wall panels

Empirical methods were the common way to study masonry panels to estimate the first cracking and the failure load of laterally loaded masonry wall panels. Researchers such as West, et al.(1974, 1975, 1976), Baker(1972, 1973, 1979, 1982a, 1982b, 1982c), Hendry(1973, 1976, 2001), Sinha (1978, 1980, 1999), Lawrence(1983, 1988, 1991a, 1994, 1995), Ma and May(1984, 1986), May and Tellett (1986), Chong, et al.(1992a, 1992b), Fried(1989), Duarte(1993, 1998) and Edgell (1987, 2002, 2005) have made significant contributions in this area. Research groups involved in this area in UK are CERAM (the former British Ceramic Research Association), University of Edinburgh, University of Plymouth, University of Leeds, University of Swansea and University of Cardiff and the University of Kingston. So far several analytical methods have been proposed such as: (a) Elastic plate method (Hendry1973, Baker 1982a), (b) Plastic plate method (Sinha 1978), (c) Principal Stress method (Baker 1982c), (d)Yield line method

(West et al.1977, Sinha 1978, Cajdert 1980, Brinker 1984) , (e) Fracture line method (Sinha 1978), (f) Strip method (Hillerborg 1976, Baker 1980), (g) Energy method (Candy 1988). Among these methods, the yield line method that is incorporated in BS 5628 is more influential. The review of these methods will be chronologically presented in the following:

The first test on laterally loaded un-reinforced masonry panels (i.e. no steel bar embedded into the causes of masonry wall) was carried out at the National Bureau of Standards in Washington, D.C, by Stang, et.al.(1925/1926) and later was continued by Kelch (1932), and Richart, et.al.(1932). These works mainly investigated the flexural behaviour of masonry panels and examined the masonry constituent such as bricks, blocks and mortar.

The first experiment on two-way spanning un-reinforced masonry walls was carried out by Tasker (1947) in The Commonwealth Experimental Building Station in Australia in 1947, plastic behaviour was found in the two walls tested.

In Great Britain, the first laterally loaded masonry wall panels was tested by Davey and Thomas(1950), the panels were four sides simply supported without in-plane constraint. The results showed that there was no reserve of strength left in a masonry panel after the first cracking. But they also observed that the failure crack patterns were very similar to those of the yield line which was originally developed for analysing reinforced concrete slabs. Their results were also confirmed by Thomas(1953).

In 1954, Monk(1954) reported the effects of brick and mortar and workmanship on flexural behaviour of masonry walls. Brick properties such as suction rate at laying-time, water absorption, surface roughness, texture would affect the flexural strength of masonry. Mortar properties affecting the flexural behaviour of masonry include the flowing property, the water retentivity and the workability, the curing and the age. This

paper studied how the materials properties of the constituents affect the properties of masonry.

In 1964, Losberg and Johansson(1964) tested walls with four edges supported; the results showed that, under the action of lateral load, the initial cracking occurred when it reached the ultimate load. They thought this was due to the brittle nature of masonry, which would prevent true yield lines to be developed in the masonry panels.

In 1965 in Britain, Bradshaw and Entwistle (1965) presented the preliminary guidelines of wind forces on non-load bearing brickwork panels. Moment coefficients for the design of walls with various edge conditions were proposed and it was emphasised that good bond between brick and mortar was very important to get higher lateral load bearing.

In 1967 in Britain, Monk and Hallen (1967) tested the hollow clay blocks walls with lateral loading added by air bags and with no axial compression loading. They found that the failure criterion was the first appearance of the crack along horizontal joint at the mid-depth.

In 1969, both the Americans and the Australians published their first codes of practice for laterally loaded brick walls. In America, Building Code Requirements for Engineered Brick Masonry suggested the design recommendations on lateral loading (Structural Clay Products institute 1969). In Australia, The Standards Association of Australia (S.A.A.) provided guidance on the design of lateral loading (SAA brickwork code.1969).

In 1970, the publication of CP111, part 1 in the UK (*British Standards Inst 1970 ,Code of Practice for Structural Use of Masonry, Part 1*) gave initial design guidance on the values of tensile strength of masonry in UK.

In 1971 in Britain, West, et.al.(1971) carried out an extensive study of lateral-load resistance of walls by testing over 100 full scale walls of storey-height with different compression levels. The walls were of different lengths with and without returns at one or both ends. Different construction types, including single leaf, double leaf and cavity walls were studied. The following conclusions were drawn from these studies: (a) compressive strength of the constituent (bricks and mortar) had a negligible influence upon the lateral resistance; (b) the relationship between the out-of-plane lateral load and the applied vertical compression load had been clarified; (c) the effects of returns, which related to stiffening effects on the panel, change the failure mode to yield line pattern; the three-pinned arch method of calculation is only applicable in the case of no returns.

Baker(1972, 1973) suggested a simplified strip method and compared it with the existing analytical methods such as the strip method (Hillerborg 1976), the elastic isotropic plate theory (Timoshenko 1981), the yield line theory (Johansen 1972) and the tabulated elastic moment coefficient. The results showed that, the elastic plate theory generally underestimated the ultimate load, the elastic analysis of the cracked panels was inconsistent; yield line method always overestimated the strength and the tabulated moment coefficients were always conservative. He recommended empirical strip method as the most reliable method at that time, which make reasonable estimate to 4 sides supported but conservative estimate to 3 sides supported.

In 1973, Hendry(1973) suggested that yield line theory was not rational to be used for brittle masonry, because the stiffness of the wall could not remain constant after cracking. He suggested using a moment coefficient method based on a horizontal strip to predict the failure load.

In 1973, Haseltine and Hodgkinson(1973) used experimental results to check the validity of both elastic plate (Timishenko 1981) and yield line theories (Johansen 1972).

Both were found to underestimate wall strengths, which were contrary to the findings of

Baker(1972, 1973). In the same year, Haseltine, et.al.(1973) pointed out that the

supporting boundary types had a strong influence on the failure load.

In 1974, West, et al.(1974) tested the lateral resistance of fifteen clay brick walls with

various boundary conditions under compressive axial loading. The results showed that

the mortar composition is important in determining the failure load, which could be due

to the fact that mortar composition could affect the bond strength between mortar and

bricks.

In 1975, West, et al.(1975) carried out a large number of experiments on wallettes and

full-scale walls (generally a wall is defined to be 10 course by 3 bricks wide). The

lateral load resistance of walls with different lengths were studied. Based on the results

of the tests on twenty-six wallettes constructed from different brick types, it was found

by West, et al. that the ratio of ultimate flexural strength in two orthogonal directions

varied from 1.5 to 5.0. A comparison of bending moments obtained from the yield line

theory and the experiment showed good agreement. This research also showed that

boundary conditions are critical to the response of the panel to lateral loads.

In 1976, West(1976)and Haseltine and West(1976) investigated the flexural strengths

of brickwork perpendicular and parallel to the bed joints. A wide variety of bricks and

mortar designations were studied. The results showed that the type of mortar had no

significant influence on the flexural strength perpendicular to the bed joint, but the

stronger mortar results in a relatively higher flexural strength in the direction parallel to

the bed joint.

In 1976, Hendry and Kheir (1976)tested one sixth scale brick walls with various aspect

ratios and support conditions. Elastic plate theory, strip method and yield line method

were used for the analysis. They considered that the elastic plate theory underestimated

test results for panels with higher aspect ratios but the yield line method provided slightly conservative estimate of experimental strength. They suggested that although application of the yield line method lacked rational basis, it was the best method among other techniques.

In 1978, Sinha (1978) proposed a modified yield line approach called fracture line analysis, which assumed the load was distributed in proportion to the panels stiffness in the two principal directions. He found that conventional yield line theory was shown to overestimate test results, but his fracture line analysis results were in a very good agreement with the experiments; the same results were also reported in 1980 in his publication (Sinha 1980).

In 1978, the first version of the new limit state, British Masonry Code BS 5628: Part 1 was published (later was updated and republished in 1985, 1992, 2005). In this code, two design methods for laterally loaded masonry walls were introduced. The first method was based on the yield line theory which assumes constant moments of resistance along the yield lines. The second method employed arching theory that allows a masonry panel to act as an arch between suitable rigid supports. The publication of BS 5628 undoubtedly stimulated the substantial research on laterally loaded masonry panels, because researchers were confused that the yield line theory, proposed in BS 5628 results in a number of discrepancies between theoretical and experimental results.

In 1979, Baker(1979) proposed an elliptical failure criterion for brick panels subjected to bi-axial bending based on single joint specimen. He believed that this failure criterion was also feasible to the case of having the compressive vertical force. These results had been widely used for further numerical analysis.

In 1980, after an extensive study of masonry wall panels, Cajdert (1980) recommended the use of yield line method to predict the ultimate load and the elastic plate theory to predict the first cracking load. He found both methods gave reasonable results.

In 1982, Baker(1982a, 1982c) proposed the Principal Stress Method which was based on the principal moments in the panel and a partially plastic failure criterion, cracking load and failure load were predicted. Baker compared his theoretical predictions with the test results and found that his prediction of cracking load was conservative but was accurate to the ultimate load of a four sides supported panel. Other researchers such as Gairns (1983), Lawrence(1983), Brinker(1984), Anderson(1987) have made further studies of the accuracy of principal stress and yield line method, but their results were somewhat contradictory to Baker's results.

In 1986, Ma and May(1986) presented biaxial stress failure criterion for brick masonry which covered tension-tension region, tension-compression region and compression - compression region; a linear relationship between the change of stress and the change of bed joint orientation was assumed. A tri-linear stress strain relationships was assumed, which consists of a linear elastic stage, the elastic-plastic stage and the plastic stage in the compression region; in the elastic-plastic stage the panel stiffness was supposed to decrease by up to 80% compared with the elastic stage. The stress strain relationship in tension was always assumed to be linear.

In 1987, Edgell(1987) presented a review paper about effects of various factors on the strength of brick masonry. Mortar designation (mortar grade), mortar mix, mortar constancy, initial rate of suction of the bricks, adjustment of initial rate of suction, curing condition are reviewed and discussed in a detailed way. Edgell concluded the main points including: (1) when the mortar is changed from designation III to designation I, the ratio of the characteristic flexural strength taken from Table 3 of BS

5628: part 1 is not unreasonable but likely to be conservative. (2) The ratio of flexural strength when the mortar is changed from designation III to IV appears to be 0.75. (3) The ratio of flexural strength when the mortar is changed from designation III to 1:3:12 should be 0.5. (4) Increasing water retention improves the bond to bricks having higher initial rate of suction and reduces the bond with bricks having a low initial rate of suction.

In 1988, Candy(1988) developed another new analytical method, the Energy Method. This method was based on such assumptions as: (a)The panel is regarded as several planar plates as in yield line analysis when it is under ultimate lateral pressure.(b) The geometry of the panel and its units determine the position of energy lines but not the minimum energy as in the yield line method.(c) The virtual work due to the increased unit deflection is the integral of the pressure times incremental deflection.(d) The rotation around the energy lines due to the increased unit deflection is associated with horizontally acting moments which results from bed-joint torsional stresses; these horizontal moments vary linearly from a maximum at the supported corner to zero at the end of the diagonal energy lines. The integral of the product of horizontal moment and incremental rotation on the energy lines provides the internal work done in the panel. Candy found that the scatter of the predictions by his method was significantly less than that by the Strip method. However, the nature of this method was still similar to the yield line method which was based on similar assumptions, its effectiveness still needed to be further checked.

In 1989, Fried(1989) carried out more than forty experiments on masonry elements and panels in his PhD research. He made a summary of the existing analytical methods in the UK, Canada, the USA, Australia, Sweden and other countries since 1932. He also compared the predicted lateral load capacity of panels by the yield line method, the strip

method, the principal stress method and the elastic plate method using the same assumed materials. Meanwhile, he investigated the effects of the aspect ratios, the orthogonal ratio, and the boundary conditions on the different methods. His comparisons clearly showed the advantages and shortcomings of these methods. He suggested that, the yield line method and strip method (called strip 3 method in his thesis) are more feasible to obtain the ultimate load capacity while the elastic and principal stress method are found to be more suitable for predicting the first cracking load. He pointed out that masonry research had been mainly experimental rather than theoretical because of the difficulties in analysing panels consisting of two different components. Fried's research clearly expressed the practical application of the existing analytical techniques at that time, and he also mentioned that these methods are not applicable for all cases and the reasons are still not very clear, e.g. the yield line method produces accurate results for totally simply supported panels, but is not accurate enough for panels with even one side built-in.

In 1991, Lawrence and Lu(1991b) presented their analysis of the cracking pressure for 32 panels using isotropic elastic plate analysis. Monte Carlo simulation (Rubinstein 1981) was used to model the random variation of flexural strength. The analyses agreed with the experimental results very well.

In 1991, Golding(1991) presented an integrated and practical approach to the design of laterally loaded masonry panels. Un-reinforced, reinforced and prestressed masonry wall panels with variable fixity along two, three and four sides were studied. He suggested that all masonry whether un-reinforced, reinforced or prestressed should be regarded as one material rather than two or three. He suggested that the yield line method provided a unified approach.

In 1992, Chong, et al.(1992a) studied the behaviour of laterally loaded masonry panels with and without openings by testing 18 full-scale masonry wall panels. Yield line theory and finite element analysis (FEA) established by Ma and May(1986) were used for the comparison. He found that the yield line approach, as suggested in BS 5628, tends to overestimate the failure load but the non-linear finite element analysis gave reasonable agreement with the experimental failure loads and the failure patterns.

In 1993, Duarte(1993) presented his PhD thesis on the study of the lateral strength of brickwork panels with openings, 160 wallettes, 24 cross beams and 16 panels were tested. It was found that under bi-axial bending, the flexural strength perpendicular to bed joints increased dramatically compared to the strength in the uni-axial test. This was a significant finding, which means that the present method of obtaining material properties of masonry panels might not be suitable for FEA analysis. In his works, the biaxial cracking criterion for brickworks was established through the cross-beam experiments and was used in a finite element analysis program which proved to give reasonable results. The strip method and yield line analysis were also used to predict the ultimate failure pressure of the panel, the yield line analysis agreed with the experimental results but the strip method did not. Another interesting point of this method was that the moment in two directions (parallel and perpendicular to the bed joint) were measured directly, and it was proved that after cracking, the redistribution of moment took place from the weaker direction to the stronger direction. His experiments and the findings were very helpful in understanding the reality of the behaviour of laterally loaded masonry wall panels.

In 1994, Lawrence(1994) carried out an investigation into 32 full-scale single-leaf masonry panels of three and four sides supported, together with a large number of tests on small brickwork specimens. Lawrence made some recommendations for the design

of two-way spanning panels without openings based on the comparison of various analytical methods. He believed that the empirical approach given in The Australian Standard AS 3700-1988 was the best method available at that time. He also suggested that the biaxial bending failure criterion for masonry should be further developed and the random variation of masonry material properties should be considered.

Christiansen (1996) studied a theoretical way to acquire accurate flexural strength values of masonry using such experimental results as the properties of bricks, the pre-watering of the bricks, mortar, the cement content and the water content in the mortar. The proposed method was still not successful since all the possible factors affecting the flexural strength of the masonry could not be incorporated in practical usage.

In 1998, Brooks and Baber(1998) established a method to evaluate the modulus of elasticity of clay and calcium silicate brickwork. In their method, a composite model was used to express the modulus of masonry in terms of properties that are generally known to the designer such as the strengths of the unit and the mortar and the water absorption of the unit. Using the previously published and new test data, it was shown that the proposed method was to be more accurate than the current methods of prediction including BS 5628 and Eurocode 6.

In 1998, Duarte(1998) investigated the design of laterally loaded brickwork panels with openings. Analytical methods such as the Yield Line Theory, the Fracture Line Method, the Strip Method and those in BS 5628 were used and compared with the experimental results of 16 half-scale masonry panels. The variables used included aspect ratio, boundary conditions and the dispositions of window openings. It was found that the yield line method provided a reasonable prediction to the failure load.

In 1999, Liang(1999) made a comprehensive study of the flexural strength and modulus of elasticity of masonry both parallel and perpendicular to the bed joints by testing

brickwork crossbeams which provided new constitutive relationships and failure criteria. Agreements were achieved between FEA and experimental results both in analysing the cross-beam specimen and masonry wall panels of half scale. Liang found that the variation of modulus of elasticity in two directions determined the distribution of the load applied in two directions which would be the main reason for the discrepancy of most FEA models.

In 2005, Edgell (2005)described the importance of testing in the development of Code of Practice guidance for the structural design of masonry structures. Two projects were described which used the test results to develop designs beyond the scope of the guidance in current codes. The role of testing in supporting guidance is explained because this cannot be done by calculation. An approach to the appraisal of existing structures is illustrated.

In 2006, Kanyeto, *et.al.*(2006) presented their research on laterally loaded block masonry panel using the thin layer mortar. Kanyeto, *et.al* suggested that the yield line method is unlikely to be appropriate to analyse the behaviour of wall panels constructed using thin bed joints because the panels behave more as concrete plates, which would necessitate the use of elastic plate theory for their design and the paper recommended that an elastic theory based-method be considered for the design of laterally loaded concrete block work panels constructed with thin layer mortar.

From the literature review in this section, it can be concluded that, though several analytical method have been proposed by previous researchers, the results of using these methods are some times contradictory, and the deflections of the masonry panel are not involved. Therefore, other methods are quite necessary to be further studied.

2.2.2 Numerical studies of masonry wall panels

The main numerical methods in masonry research is the finite element analysis (FEA) (Brenner 2002) which has been widely used for structural analysis. Other methods which have been used in concrete such as spectral methods (Bertrand 1989), boundary element method (BEM) (Watson 2003)have not yet been used in masonry study. More general bibliography on finite element analysis can be found elsewhere (Mackerle 1998, 2000, 2000a, 2001, 2002, 2002b, 2004, 2005).

In masonry studies, two kinds of FEA are commonly used: macro-modelling and micro-modelling. In macro modelling the masonry is regarded as a homogeneous material, whereas in micro modelling the brick and joints are separately modelled. At present, micro-modelling is not feasible for real masonry structures because modelling the units and the mortar joints separately needs a very long time for model preparation and calculation. Therefore, most practical analyses of masonry structures use macro-modelling which uses smeared material properties. To acquire smeared material properties of masonry, homogenisation techniques (Bakvalov and Panasenko 1989) are used, which have also been extensively studied and are becoming popular in the masonry community (Zucchini and Lourenco 2002). The literature survey carried out here will cover macro modelling, micro modelling and homogeneous techniques in the chronological order.

In 1985, Essawy, et.al.(1985) developed a finite element program for analysing laterally loaded block masonry wall panels in which a multi-layered model was used in the program which could track the progress of cracking in a way that the stiffness of each cracked element was modified only in that particular cracked layer.

In 1986, May and Tellett (1986) introduced a non-linear finite element program for reinforced and unreinforced masonry panels subjected to lateral load. The masonry was

modelled as a homogeneous material in the elastic range. When the cracks were initiated or the stress reached its maximum level, the Poisson's ratio was assumed to be zero. The "square" failure criteria were adopted in all tension-tension, compression-compression and compression-tension regions but they realized that assuming a "square" failure criterion in the tension–tension region was not reasonable.

In 1989, Pande, *et.al.*(1989) presented a method to simulate masonry using homogenization techniques. In this technique, the homogeneous material properties of the elastic equivalent of the anisotropic masonry were acquired; subsequently the masonry was regarded as an isotropic material for further numerical analysis.

In 1991, Liang(1991) in his PhD thesis addressed more details of his work based on Pande, *et al.*(1989) which extended the homogenisation techniques to the constitutive relationships at the non-linear region (visco-elasticity) of masonry with the consideration of failure criteria. The homogenization was applied to kinds of masonry specimens and the comparison was made between the experiments and the FEA. The results show that the proposed homogenization technique was credible. Based on the equivalent isotropic features obtained by the homogenization technique, the FEA was carried out to analyse two masonry panels with vertical loading, and very good results were obtained. This homogenization technique was based on many assumptions such as: masonry and mortar are linear isotropic materials, a structure is much larger than its components (masonry units and mortar joints), the constituents are perfectly bonded without any debonding effects; the bed joints are continuous. Obviously, these assumptions affect the accuracy of the analysis, e.g. debonding is a very common phenomenon during the failure of a masonry structure but this method did not consider its occurrence. Therefore, based on Liang's work, Lee, *et al.*(1996) further studied the

numerical simulation of cracking and collapse of masonry panels based on the homogenisation techniques.

In 1991, Lawrence and Lu(1991a) presented a finite element analysis specially for laterally loaded masonry wall panels with openings. A computer program was developed accompanied by a Monte Carlo simulation approach to account for the random variation of flexural strength of masonry. The influence of self-weight was included and good agreements to the experimental results were achieved.

In 1991, Chong(1993) analysed 18 masonry panels that he tested in the University of Plymouth using the revised program which was initially created by May and Tellett (1986). He found out that, the FEA was close to the experimental results. However, he was confused that, the load deflection curve of FEA suddenly drops after the first cracking whereas the experimental results did not. The cause of this phenomenon will be illustrated in this research.

In 1996, research by Lee, *et al.*(1996) presented a homogenisation technique based on the previous work carried out by Pande, *et al.*(1989, 1991). In his work, two stages of homogenisation were used: one for the orthotropic material properties and the other one for the cracking of the material. In this model, tensile cracking was considered as the non-linearity parameter. He also compared the analytical and the experimental results and it was found that the failure patterns obtained by FEA reasonably agreed with the experimental results. He concluded that the analytical model could successfully predict the physical behaviour of laterally loaded masonry panels.

In 1996, Lourenco(1996) presented a systematic study on the analysis of masonry using computational methods in his PhD thesis. Techniques such as numerical algorithms, micro-modelling, homogenization techniques and macro-modelling were studied. The non-linear equilibrium problem was solved by a constrained Newton-

Raphson method with a line-search technique. Non-symmetric tangent stiffness matrix, raised from non-associated plastic flow (hardening/softening), was used in all analysis to trace the complete loading process. In his micro-modelling, the inelastic phenomena were "lumped" in the weaker joints through a composite interface model which regarded the joint as zero-thickness interface. There were three failure mechanisms for the three failure modes in this model. The internal damage associated with each failure mechanism was modelled using internal parameters related to fracture energy in tension, compression and in shear. In the homogenization process, two steps were adopted: the homogenisation is carried out in one direction first (either parallel or perpendicular to the bed joints); and then it is carried out in another direction. The behaviour of masonry cells predicted by macro-modelling with homogenisation is quite close to those by micro-modelling, but Lourenco stated that the experiments should be carried out to confirm the homogenisation results. In the macro-modelling, an orthotropic continuum model was developed, which consists of a Rankin type yield criterion for tensile failure and Hill type yield criterion for compressive failure. Again the internal damage associated with each failure mechanism can be modelled using internal parameters related to tensile and compressive fracture energy. However, Lourenco demonstrated that the macro-model performs badly for the case when the failure mode is governed by the interaction of a few units and mortar; therefore, the adoption of macro-modelling must be associated with a composite failure process. More comprehensive research by Lourenco in this area could be found elsewhere (Lourenco 1994, 1996, 1997b, 1998, 1999, 2000a, 2000, 2001, 2004, 2005).

In 1999, Pluijm (1999) made a comprehensive study to the flexural failure mode under different directions of masonry subjected to lateral loading, which provided the basic data for the numerical analysis of laterally loaded masonry wall panels.

In 1999, Mathew, *et al.*(1999) published his research results on predicting failure loads using artificial intelligence. A hybrid system, which combines a case-based reasoning technique and a neural network (NN) based model was used in this study. The trained NN was able to match the failure load of a masonry panel under lateral pressure when the wall was subjected to biaxial bending, for instance, masonry cladding panels supported on three or four sides.

In 2000, Edgell and Kjaer (2000) presented their yield line analyses on lateral load behaviour of walls with openings using various computing software package such as Tedds, DTI (developed by Danish technology institute), PSA Guide. They compared the analytical results from three approaches with the experimental ones. The multipliers (ranged 1.14-5.7) were used in the DTI analysis to revise the input flexural strength. They concluded that the three software packages (Tedds, DTI, PSA Guide) were in general conservative but could be used to predict the failure load of walls subjected to lateral loading. The DTI could well predict the failure pattern of the masonry panel of lateral loading.

In 2001, Lourenco(2001) briefly reviewed the out-of-plane behaviour of masonry panel which including one-way and biaxial bending, the influence of normal bending and the size effects and randomness of material were also discussed. Lourenco advocated that the existing experimental results are not suitable for deriving the constitutive behaviour of masonry and he suggested to using deformation controlled tests.

In 2001-2004, Cecchi and Rizzi (2001, 2002b, 2002a, 2004) presented an extensive study on homogeneous 3D model periodic heterogeneous bodies (such as masonry) with multi-parameters and regarded masonry as periodic in the middle plane, i.e. in the orthogonal directions to the thickness. The model could be successfully used for analysing both in-plane and out-of-plane load.

In 2002, Zucchini and Lourenco(2002) summarised the methods of homogenization techniques into three kinds: (a) to handle the masonry by considering their special feature of the discontinuum within the frame work of a generalised/Cosserat continuum theory by Besdo (1985). This method possesses some inherent mathematical complexity and is able to handle the mortar interface and true discontinuous behaviour, but so far this method is not yet adopted by researchers and its practical applications still need further research. (b) To apply the homogeneous theory for periodic media to the basic cell, i.e. to carry out single step homogenisation with adequate boundary conditions and exact geometry (Arthoine 1995, 1997); the interfaces between unit and mortar are not yet accounted for, the complexity of the basic cell of the masonry implies the solution which could be obtained by using the FEA method and thus the macro-parameter could be obtained, (c) as an "engineering approach" aimed at substituting the complex geometry of the basic cells by a simplified geometry, such as work done by Pande, et al.(1989) ,this approach is performed in two steps (two directions) and masonry is assumed to be a layered materials so as to simplify the problem; this method performs very satisfactory in the case of linear elastic analysis, but the defect of this method is that the final results are affected by the order of the two steps of homogenisation, and for the case when the stiffness ratio between units and mortar becomes too large(>10), unacceptable errors are caused. To improve the homogenisation techniques, Pande, et al.(1989) in his work presented a micro-mechanical homogenization model for masonry which included the additional deformation of the basic cells and the elastic-plastic deformation on the units and mortar was assumed. The proposed homogenization techniques avoided the big error caused when the stiffness ratio between units and mortar becomes too large (>10).

In 2003, Rafiq, *et al.*(2003), Zhou, *et.al.*(2003) proposed a novel method of using corrector factors. The corrector factors were derived by comparing the deflections of FEA and experimental deflections and were used to revise the flexural stiffness or strength in the zones of the panel to improve the FEA analysis. To apply the corrector factors from a known base panel to more general masonry panel of different boundary conditions and sizes and with openings, zone similarity are established using a cellular automata (CA) model. Improved analyses were achieved both for the failure load and failure pattern.

In 2003, Trovalusci and Masiani (2003) presented a non-linear anisotropic continua which is equivalent to masonry-like materials. An integral procedure of equivalence in terms of mechanical power has been adopted to identify the effective elastic moduli of the two continuous models. Non-linear constitutive functions for the interactions in the Lagrangian system are defined to take into account both the low capability to carry tension and the friction at the interfaces between elements. The non-linear problem is solved through a finite element procedure. Differences between the classical analysis and his model were investigated with the aid of numerical analyses models carried out on masonry walls made of blocks of different size; good results were achieved.

In 2004 and 2005, Massart, *et.al.*(2004, 2005a) presented his comprehensive study on modelling masonry structures of different scales (i.e. mesoscopic modelling). He first made the micro-modelling based on homogeneous techniques to get the isotropic material properties which were used for further macro-modelling later, good results was achieved. Similar studies were carried out by Larbi (2004) and Trovalusci and Masiani(2005).

In 2004, Bigoni and Piccolroaz (2004) proposed a novel yield/damage function for modelling the inelastic behaviour of materials ranging from pressure-sensitive, frictional,

ductile to brittle-cohesive ones. The yield function was able to describe the transition between the shapes of a yield surface from one class of materials to another class of materials. The proposed yield function was shown to agree with a variety of experimental data such as soil, concrete, rock, metallic and composite powders, polymers, metallic foams and porous metals. The yield function is therefore a generalization of several criteria, including von Mises, Drucker–Prager, Tresca, modified Tresca, Coulomb–Mohr, modified Cam-clay, and concerning the deviatoric section—Rankine and Ottosen. Obviously it would be meaningful to apply this yield function to masonry study.

In 2005, Sing-Sang, et.al.(2005) summarised that, the FEA models used for analysing masonry differ from each other mainly in the following ways:(1) different equations to define the yield surface to fit the experimental data; (2) the adoption of classical yield surfaces, such as Drucker-Prager, Hill, Hoffman, Mohr-Coulomb, Rankine , and Von Mises , which are calibrated with test results; (3) whether masonry is regarded as a material with or without softening properties. In the same report, Sing-Sang, et.al made a 3D implementation of the masonry panels with in-plane and out-of-plane loading based on the model proposed by Lourenco(1997a, 1996) . The implementation was carried out in DIANA 9.0 (2005 published) with a subroutine added, in which, for each integration point of the structure, the stress vector and stiffness matrix was defined in accordance with material behaviour. The stress vector and stiffness matrix are updated in the subroutine according to the yield surface, and then returned to the software, which then determines the nodal equilibrium forces and the resulting strain vector. Lourenco claimed that improvement had been obtained compared with the original implementation by Lourenco(1996).

From the literature review in this section, it can be found that, there are some different judgements to empirical methods, some times the results from different laboratories are contradictory. Though the yield line method appears to produce better predictions and is suggested by the BS 5628, it is still a method that based on the summary to experiments and cannot be accurate enough. It can be concluded that empirical method are not likely to result in more accurate analyses.

Finite element analysis (FEA) is an advanced method, and much research has been carried out on the study of this method. However, due to the highly anisotropic nature of masonry, it is very difficult to get suitable material properties and constitutive relationships of masonry materials. Although homogeneous techniques were studied by many researchers for solving this problem, there is still a long way before reach to the practical usage because the dimensions of masonry structure affect its characteristics.

Boundary conditions have a strong role in the response of the masonry panels to lateral loads. Accurate modelling of the boundary types for masonry panel is almost impossible. Consequently new ways should be explored to take accounts of this issue.

2.3 MODEL UPDATING TECHNIQUES

Model updating (Sinha and Friswell 2002) is a method which refines the mathematical model using experimental results. The refinements were carried out by adjusting some chosen parameters (input data) in the FEA model such as mass matrix, stiffness matrix, damping matrix (only for dynamic analyses), or geometric and material properties (Visser 1992, Mottershead and Friswell 1998) to minimise the discrepancies between the FEA model and the test measurements. In this procedure, the model is analysed and the error in it is located and then revised accordingly using the updated parameters; hence the prediction of the response of the structure is improved. Usually changes are introduced in the structural stiffness matrix.

The model updating technique was firstly raised as a system identification (Asterom and Eykhff 1971, Robert-Nicoud, et.al, 2004) in the control engineering community and later this was extended to structural dynamics. In the past twenty years, there have been a large number of papers published in the fields such as: model updating, model calibration, parameter estimation and damage detection. Friswell and Mottershead (1995), Mottershead and Friswell (1993) Maia and Silva(1997) made comprehensive reviews and detailed introductions to model updating techniques. Model updating could be simply divided into two main categories (Jaishi 2005): the direct method and the sensitivity based method. The direct method means that the total stiffness and/or mass matrix in the FEA model are updated based on some measured modal parameters. The typical direct methods include optical matrix updating method (Braruch 1982), the matrix mixing method (Caesar 1987), the eigen–structure assignment method (Minas and Innman1988), the inverse eigenvalue method (Starek 1991). The direct method is seldom used in structural dynamics. The sensitivity based method (Banan 1999) uses the sensitivity matrices that correlate the perturbation between the modal parameters and the structural parameters to be updated in the updating process (Link 1993, 1999). The typical sensitivity based methods are the iterative method (Chang 2000), the optimisation method (Echert 1991) and the Bayesian estimation method (Zhang 2000). The sensitivity based method has been commonly used in structural dynamics because the model updating problems are changed to be an optimisation process; the objective function is set to minimise the error between experimental and analytical data. When using sensitivity based model-updating techniques, selecting the proper parameters for updating is vital (Sandink 2001). Normally, the parameters that most strongly affect the model/outputs are selected. The selected parameters can be material properties of the structure and their updated values would be more close to their real values. If model

updating techniques are used to determine the values of parameters such as material properties (Papazoglou 1996, Chakraborty, et.al. 2002) and boundary conditions (Ahmadian 2001) this procedure is called parameter estimation or parameter identification (Mahnken, et.al.1998, Hjelmstad, et.al.1999, Prells and Friswell 1999, Chakraborty and Mukhopadhyay 2000, Angelis, et.al. 2002, Koh, et.al. 2003, Morbiducci 2003, Wu and Li 2006). Model updating techniques are also widely used as damage identification/detection (Freswell et. al 1998, Santos et al, 2000b, Santos,et.al 2000a, Hu 2001, Hanganu,et.al, 2002, (Lauwagie.et.al 2002, Li,et.al, 2002, Zabaydi 2002, Al-Qaisia.et.al 2003, Lee,et.al, 2003, Necholas and Abell2003, Titurs et al 2003b, Epureanu and Yin 2004, Fang,et.al, 2005, Ge and Liu2005, Kolakowski,et.al,2006) or structural health monitoring (Titurus,et.al 2003a) because if a structure were damaged, the vibration frequencies or the stiffness matrix would be changed at damaged locations, which could be used to identify and locate the damaged parts of the structure.

Though in most of model updating cases, a vibration frequency from the structural dynamic experiments were used as the output data and is used for models updating, there are still a lot of studies using static loading or deflections. In 1982, Sheena Sheena, et.al.(1982) theoretically studied the method of correcting the stiffness matrix using a traditional Lagrangian matrix, to improve the agreements between the deflections of the analytical model and the experimental ones. He applied his method to several wings of aircrafts and the method was proved to be reliable. In 1989, Hajela and Soeio(1989) presented his study on damage detection using static deflections and vibration modes of truss structures, The position of damage on the structure were detected and located based on the changes of the stiffness matrix and damping matrix caused by the damage of the structure. However, Hajela specially pointed out that a static load distribution can affect some structural components more significantly than others. If the damaged

member in a frame structure was the member that does not play the major role on the load bearing process, the use of static displacement in damage detection might yield erroneous results. In 1991, Sanayei and Onipede (1991) presented his study on identifying properties of structural elements using static test data. A set of static forces was applied to the structure (frame) with a set of degrees of freedom (DOF). The displacements were measured as another set of DOF. The stiffness of each element was identified, which could identify the change of stiffness of the element and the failure of the element. In 1992, Banan, et.al. (1992) presented a parameter estimation method to simultaneously compute the element's constitutive parameters and unmeasured displacements from the measured static response. The work was based on a planar bowstring truss with known geometry and topology. The objective function was defined as the discrepancy between the applied force and inner resistance. The general concept of non-linear least-square theory was used to construct the objective function. The parameter estimation was finished by solving a constraint optimisation problem. The result was robust. In 1992, Berret and Cogan (1992) presented a typical FEA model updating study using static deflections of the structure. A detailed illustration of the definition and calculation to the sensitivity matrix, test case, damage localization techniques and parametric optimisation were involved in the study. In 1994, Banan, et.al.(1994a, b) presented his study on parameter estimation using measured displacements, to minimise the difference between the measured response subjected to several load cases of static loading. Displacement error estimator (DEE) was used to measure the error between the displacements from model-computing and the measured response. An algorithm was proposed to estimate the constitutive properties. In 1997, Liu and Chian(1997) made parameter identification of a truss structure using static strains. The axial strains of the truss element were measured for the identification

process and the error normal to the equilibrium equation was minimised. The identifiability of the inverse problem was also studied by a perturbation method.

In 1997, Sanayei, *et.al.*(1997) presented his experiments on small scale steel frame models to support his previous method of parameter estimation using static deflections (Sanayei 1992, 1996a, 1996b). Static displacements and static strain measurements were used to evaluate the unknown stiffness parameters of the structural components. Weight factors from the variance of measured data were applied. Similar work was also addressed in other papers (Sanayei 1996a, 1996b, Hjelmstad 1997, Potisiri 2003) which involved the damage detection and assessment algorithm based on parameter estimations using static response such as deflections and static strain.

From 2000, much research on system identification using static deflections of beams was carried out in the Swiss Federal Institute of Technology. Robert-Nicoud, *et.al.*(2000, 2002, 2005) introduced model composition and stochastic search. In their other papers (Robert-Nicoud,et.al. Robert-Nicoud, *et al.*(2000, 2002, 2005), static deflections and rotations of a bridge from the fibre optic sensor were used for the model identification.

In 2002, Zhou(2002) and Rafiq, *et al.*(2003) used the defined corrector factors to revise stiffness/ strength values of laterally loaded masonry panels to improve the FEA analyses. The concept of zone similarity was also proposed by Zhou, *et al.*(2003) to apply the corrector factors derived from the base panel to new panels using a cellular automata (CA) model. The improved prediction on failure load and failure pattern was obtained.

In 2005, Chen, *et.al.*(2005) proposed a new structural damage identification method using limited test static displacement based on grey system theory. The grey relation coefficient of displacement curvature is defined and used to locate damage in the

structure, and an iterative estimation scheme for solving nonlinear optimization programming problems is used to identify the damage magnitude. The advantage of the proposed method is that only limited static test data are required. A cantilever beam is used to validate the proposed method. The numerical results showed that damage in the structure can be localized successfully with high accuracy of damage magnitude identified.

2.4 SUMMARY

From the above literature review, it can be concluded that, the empirical methods of analysing masonry panels focus on summarizing experimental results using simplified models. These methods are easy to implement and easy to understand and they are still meaningful in practical estimation where high accuracy is not required. However, due to the complexity of the masonry panel, the models used in the empirical methods are not able to provide more accurate analyses to the complicated masonry panels. Moreover, the empirical methods are not able to work out the deflections of masonry panels. Therefore, it is advisable to carry out masonry study in a numerical way with the development of modern computing techniques.

Finite element analysis (FEA) should have been able to provide more accurate analyses to masonry due to the advanced model used. However, because the macroscopic modelling uses homogeneous material information but masonry is an anisotropic one and the substitution of this homogeneous information such as the failure criteria and constitutive relationships are very difficult to be determined properly, it is very difficult to acquire the accurate analyses of masonry structures, even by means of the microscopic modelling and homogeneous techniques. Model updating, which directly uses the information of real structures, is suitable to diagnose, revise and improve the existing FEA model. Model updating should be a novel way for modelling complicated

masonry structures such as masonry panels. This issue will be studied in details in this thesis.

In fact, using corrector factors, introduced by Rafiq, *et al.*(2003) is a way of model updating, because it works in the same way of revising stiffness matrix to achieve the improved analytical results. The only difference is that, model updating uses optimisation to get the revising coefficient but in Zhou and Rafiq's work, corrector factors are derived using a new definition. Zhou and Rafiq's work is the basis of this research and its details will be introduced in the following Chapters.

3. THE FINITE ELEMENT ANALYSIS AND CORRECTOR FACTORS

3.1 INTRODUCTIONS

This chapter introduces the research carried out in the University of Plymouth that directly related to this research.

Chong (1993) tested 18 laterally loaded masonry wall panels with and without opening in the University of Plymouth and analysed them using a smeared FEA model. Based on the test results and the FEA model initially proposed by May and Tellett (1986) and updated by Chong(1993), Rafiq, *et al.*(2003) and Zhou, *et al.*(2003) developed a new way of using the concept of corrector factors and zone similarity to improve the analysis of masonry panel.

The FEA model has been used by Chong(1993) and Rafiq, *et al.*(2003), along with the concept of corrector factors and zone similarity. Zhou, *et al.*(2003) formed the foundation of this research. This chapter will introduce a detailed study of this new concept.

3.2 THE FEA MODEL OF ANALYSING LATERALLY LOADED MASONRY WALL PANELS

A suitable FEA model is the fundamental requirement for making nonlinear analyses. It is well known that any numerical FEA model used should involve the following: (1), a stress-strain relationship to simulate the behaviour of masonry up to failure; (2) a failure criteria representing the ultimate strength (or strain) of masonry under different loading states and to judge masonry failure; (3) a post stress strain relationship is needed to account for the change of the behaviour, to make a full loading process analysis; this has

been more concerned in recent years;(4) a crack model to define the direction and propagation of cracks is very necessary because the occurrence of cracks affects masonry behaviour very much. Moreover, to implement a FEA program, others are also needed such as: (a) the integration rules, (b) the non-linear solution algorithms, (c), the convergence criteria, (d), terminated conditions of the program. These will be reviewed in the followings sections.

3.2.1 Stress-strain models

In the FEA model used, masonry is regarded as a tri-linear elastic-plastic material in compression and as a uniaxial material in tension; the strain-stress relationship is shown in Figure 3.1. For tension, it is assumed that masonry always behaves linearly; for compression, masonry is assumed to behave linearly and then reach the plastic stage when strain increases without load increasing and then reach the maximum strain ε_b, after which it lose its load bearing ability and the stress becomes zero. Also, in the linear stage, when the stresses reach half of the plastic strength, the stiffness E decreased by 20%. For bending, because the tensile strength of masonry is much smaller than that of the compressive strength, the linear elastic-brittle behaviour was assumed both parallel and normal to the bed joint as shown in the tension region in Figure 3.1.

The biaxial stress-strain relationship for isotropic linear elastic materials is given by where, E_b is the elastic modulus of brickwork and v is the Poisson's ratio; σ_x and σ_y are stresses parallel and normal to the bed joint, τ_{xy} is the shear stress; ε_x, ε_y, and γ_{xy} are the strains to σ_x, σ_y and τ_{xy}.

$$\begin{Bmatrix} \sigma_x \\ \sigma_y \\ \tau_{xy} \end{Bmatrix} = \frac{E_b}{1-v^2} \begin{bmatrix} 1 & v & 0 \\ v & 1 & 0 \\ 0 & 0 & (1-v)/2 \end{bmatrix} \begin{Bmatrix} \varepsilon_x \\ \varepsilon_y \\ \gamma_{xy} \end{Bmatrix} \qquad (3.1)$$
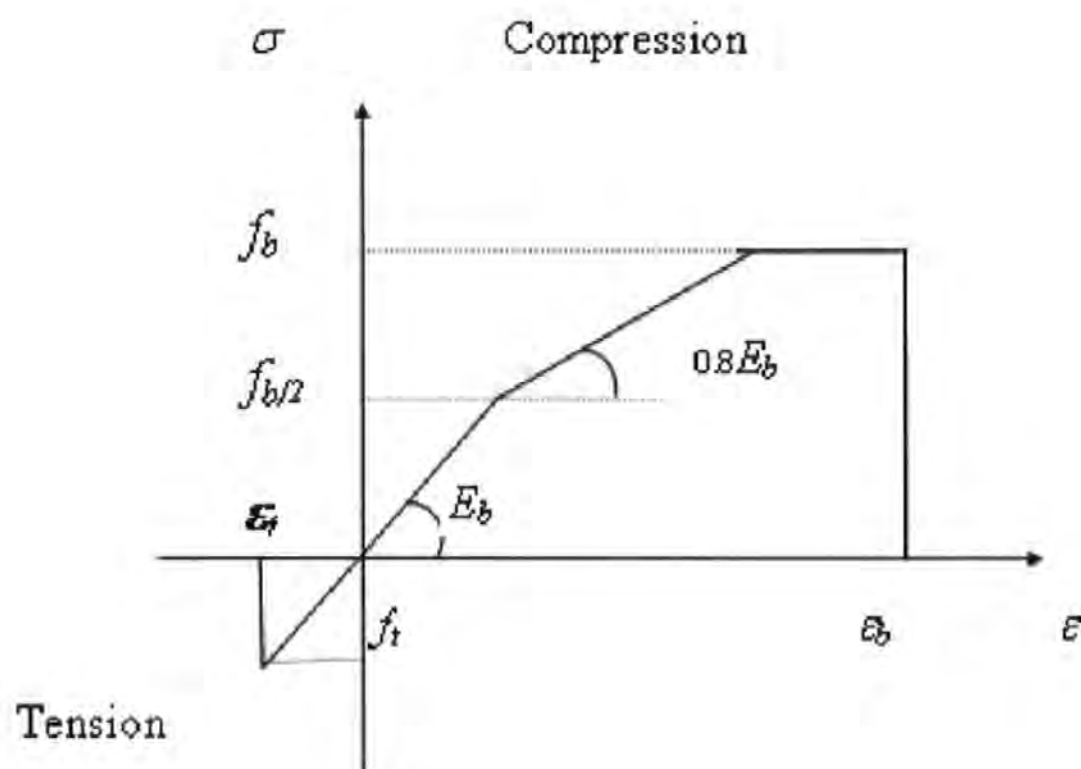
Figure 3.1 Uniaxial stress-strain relationships of masonry (Chong 1993)

3.2.2 Biaxial stress failure criterion

The biaxial stress failure criterion (Ma and May1986) used in the model includes the

compression-compression, compression-tension, and tension-tension zone

The finite element analysis of masonry panels from zero up to collapse requires:

1. A biaxial failure criterion for the flexural stresses, including the directional

    properties of masonry;

2. The flexural stresses in terms of the two principal stresses and their

    orientation to the bed joints;

3. A complete failure criterion which should cover the compression-

    compression, compression-tension, and tension-tension zones;

4. A relationship between the change of stresses and the change of bed joint

    orientation (Chong assumed a linear relationship).

Comparison of the Biaxial Relationship with the Proposed Biaxial Failure Criterion.
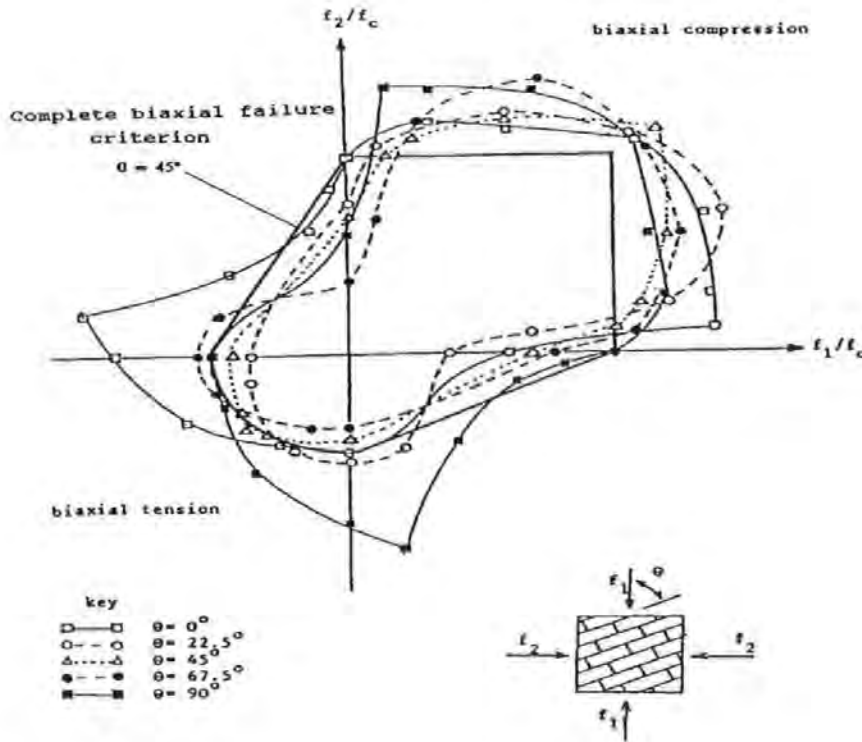
Figure 3.2 Complete biaxial failure criterion (Chong 1993)

Based on the above requirements, Equation (3.2) was used to govern the surface of the failure criterion

$$\frac{\sigma_x^2}{\sigma_{1\alpha}^2} + \frac{\sigma_y^2}{\sigma_{2\alpha}^2} = 1 \qquad (3.2)$$

where $\sigma_{1\alpha} = \sigma_{10} - (\sigma_{10} - \sigma_{1\pi/2}) 2\alpha/\pi$

$\sigma_{2\alpha} = \sigma_{20} - (\sigma_{20} - \sigma_{2\pi/2}) 2\alpha/\pi$

σ_x, σ_y are the failure stresses at a particular angle θ,

and α is the angle between the direction of the maximum prescribed stress and

the bed joints. $\sigma_{1\alpha}$, $\sigma_{2\alpha}$ are the maximum prescribed stresses in the directions x

and y at the angle (the first and the second principal stress at the angle α). σ_{10},

and $\sigma_{1\pi/2}$ are the first principal stress when α equal to zero and $\pi/2$, $\sigma_{20,}$ *and* $\sigma_{2\pi/2}$

are the second principal stress when α equal to zero and $\pi/2$.

The biaxial stress failure surfaces in the tension-tension, compression-tension, and

compression-compression zones are shown in Figure 3.2

3.2.3 Modelling of cracking and crushing

Failure can be divided into crushing in compression or cracking in tension as shown in

Figure 3.1. Masonry is assumed to crush when the deformation level reaches its ultimate

capacity and leads to a complete disintegration of the material. After crushing, the

stresses drop abruptly to zero, and the masonry is assumed to completely lose its

resistance against further deformation in any direction.

Cracking is assumed to occur when the tensile stress in an element reaches the tensile

strength limit given by the biaxial failure envelope (see section 3.2.2). The direction of

the crack is fixed normal to the direction of the principal stress. After cracking, the

masonry abruptly loses its strength normal to the crack direction. In the direction

parallel to crack, the cracked material is assumed to carry stress according to the

uniaxial conditions.

In the tension-compression zone, only tensile failure is assumed to occur. Once a crack

has formed, the material sustains compressive stress parallel to the direction of the crack

according to the uniaxial compressive failure condition.

The tensile failure causes the highly anisotropic conditions to develop. After cracking

occurs, the material property matrix in the cracked zones is given by Equation (3.3)

$$\begin{Bmatrix} \sigma_n \\ \sigma_p \\ \tau_{np} \end{Bmatrix} = \begin{bmatrix} 0 & 0 & 0 \\ 0 & E_b & 0 \\ 0 & 0 & 0 \end{bmatrix} \begin{Bmatrix} \varepsilon_n \\ \varepsilon_p \\ \gamma_{np} \end{Bmatrix} \qquad (3.3)$$

where, σ_n and ε_n are the stress and strain normal to the crack direction, and σ_p and ε_p are the stress and strain parallel to the crack direction.

This equation allows no shear stresses thus the biaxial stress system for uncracked masonry is converts into a uniaxial one after cracking.

3.2.4 Masonry representation and integration rules

The FEA program used in this study is a specialised non-linear FEA program developed by May and Tellett (1986). In this FEA model, masonry panels use a quadrilateral four-node flat shell element with offset axes, in which masonry is treated as an isotropic material; its properties are modelled based on the data of wallette tests. In this model, each node has six degrees of freedom, three axial displacements u, v and w in the x, y and z directions respectively and three rotations θx, θy and θz. Supports conditions are defined (1) if a particular freedom is restrained and (0) if is free.

Out of plane lateral loading is applied perpendicular to the surface of the wall. This load was applied in increments of 0.2 kN/m^2. The effect of self weight of the wall was also considered in the FEA analysis.

In the FEA model, elements are permitted to be stacked with layers of different material properties, and each element having a common reference surface which may be offset from the mid plane of the element.

Plane

Gauss points on a plane

Thickness of element
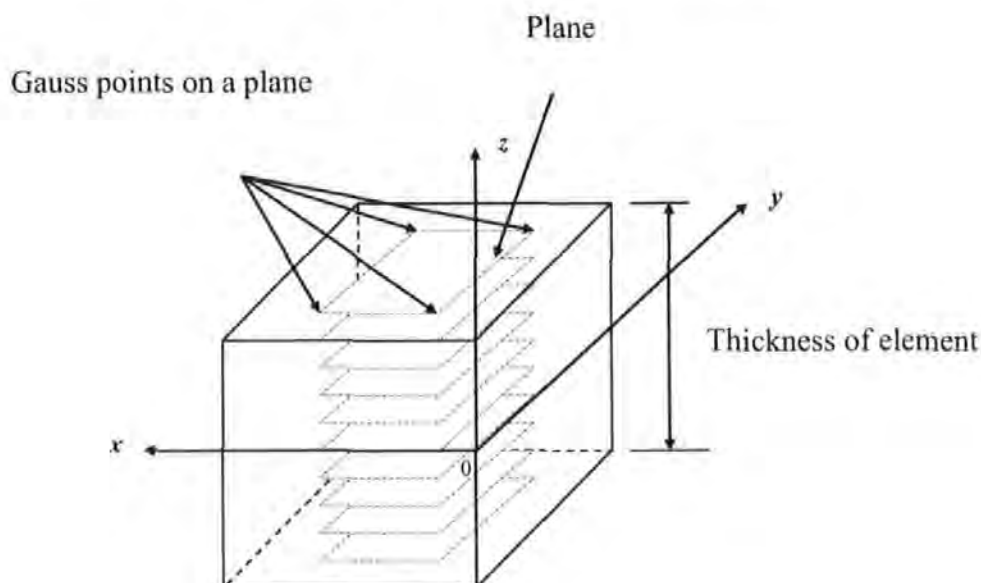
Figure 3.3 The planes through the depth of element (Zhou 2002)

In plane a 2 × 2 point Gauss-quadrature integration scheme was employed. In addition to sampling the strain on the x-y plane, it is sampled at ten points to detect non-linear behaviour (cracks) and to determine the variation in the magnitude of stress through the depth of the element (out of plane), as cracks develop along the wall thickness, see Figure 3.3.

3.2.5 Non-linear algorithms, convergence criteria and termination

An incremental iterative approach with a constant stiffness matrix was used in the program. Line search techniques are used to reduce the number of iterations required, and hence accelerate convergence.

The convergence criteria adopted in this work are based on a residual displacement norm, Equation (3.4) and a residual rotation norm. Equation (3.5) (Chong 1993)

$$TOD > \sqrt{\frac{\sum (Change\ in\ Incremental\ Displacement)^2}{\sum (Total\ Displacement)^2}} \qquad (3.4)$$

$$TOR > \sqrt{\frac{\sum (Change\ in\ Incremental\ Rotation)^2}{\sum (Total\ Rotation)^2}} \qquad (3.5)$$

where *TOD* and *TOR* are pre-selected convergence tolerance. A value of 0.002 was found to be suitable for both *TOD* and *TOR*. Both criteria have to be satisfied simultaneously before convergence is achieved.

In the non-linear analysis, load is increased in increments and the analysis is terminated when any of the following criteria is satisfied:

1. The number of load increments exceeds a maximum specified number.

2. Convergence is not achieved after the load increment has been reduced three times, each time the new increment being 1/4 of the previous increment. The load value just before this load increment is defined as the failure load of the panel.

3. Convergence is not achieved after 120 iterations.

3.3 CORRECTOR FACTORS USED FOR IMPROVING THE FEA

Rafiq, et al.(2003) and Zhou(2002) developed the concept of corrector factors based on the research carried out by Chong (1993) who tested in total 18 full-scale masonry wall panels with and without opening in the University of Plymouth. The vertical sides of these panels were supported on a steel angle connected to the test frame abutment to simulate a simply supported support edge. The base of the wall was enclosed in a steel channel packed with bed joint mortar (refer to Figure 3.4 for support details). It was assumed that the combined effect of the support details shown and the self-weight of the wall would provide sufficient restraint to the base of the panel to simulate a fixed support type.

From Figure 3.4 it is clear that vertical supports are not fully free in rotation, therefore assuming these sides as simply supported is not a correct model as there is some degree

of restrain against rotation. Although details shown in Figure 3.4 at the base of the panel is accepted by the masonry experts to be a fixed support our analytical study results has proved that this is not a fully fixed support and there is some degree of rotation at this support (see Chapter 7 for full details).

The deflections were measured at points across the whole panel at each load level, which provided more information than previous tests on panels that consist of one or several limited reading points.

Vertical Edge Support details

Support detail at Base
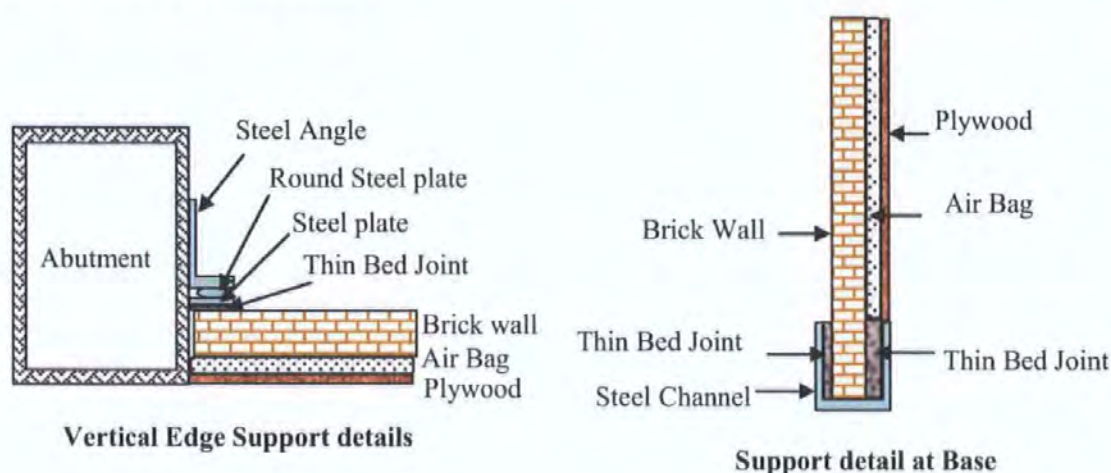
Figure 3.4. the support details for panel's test (Rafiq,et.al. 2006)

3.3.1 The concept of corrector factors

The concept of corrector factors rose from the fact that, when examining the FEA and experimental load deflections of several panels, it was found that, after a specific load level, their ratio tends to be approximately a stable value (refer to Figure 3.5). This paragraph is limited in explaining the concept. The corrector factors were defined by Eq (3-1) at higher load level, and were used to amend the global stiffness or strength by Eqs (3-2), (3-3) showed; by either revised stiffness or strength values, the prediction to failure load and failure pattern were improved thereby.

$$\psi = \frac{\omega_{FEA}}{\omega_{EXP}} \qquad (3-1)$$

$$\{D_{\psi 0}\} = \{D_\psi\} * \{\frac{\omega_{FEA}}{\omega_{EXP}}\} \qquad (3\text{-}2)$$

$$\{f_\psi\} = \{f_{\psi 0}\} * \{\frac{\omega_{FEA}}{\omega_{EXP}}\} \qquad (3\text{-}3)$$

Where

$D_{\psi 0}$: the global (smeared) rigidity D_ψ: the revised rigidity of the masonry panel.

$f_{\psi 0}$: the flexural strength f_ψ: the revised flexural strength f,

ω_{FEA} : The deflections of the FEA using a globally smeared $D_{\psi 0}$ or $f_{\psi 0}$

ω_{EXP} :   The experimental deflection recorded in the laboratory.

A full-scale single leaf masonry wall panel SBO1 tested by Chong (1993), as shown in Figure 3.6, was selected as the 'base panel'. This panel was constructed using perforate class B facing bricks, set in 1:1:6 designation (iii) mortar the bricks were docked before laying. Details of material properties of the panels measured by Chong is as Table 3.1, Table 3.3 and Table 3.3 as have been presented by Chong (1993).

Table 3.1 Material properties of masonry panel tested by Chong (1993)

Type of Strength	Type of masonry	Condition of specimen	Number of test specimen	Number of valid specimen	Flexural strength(N/mm^2)		
					Experimental wallette	analytical	
						joint	wallette
Vertical	Class B fac.Bricks	undocked	5	4	0.474	0.792	0.474
		docked	10	7	0.740	0.965	0.740

Horizontal	Class B fac.Bricks	undocked	5	4	1.670	2.214	1.670
		docked	15	13	1.700	2.017	1.700
		Docked*	10	9	2.090	2.28	2.090

*Six courses high specimens

Corrector factors for this base panel were derived. The reason for selecting this panel was that this panel involved all kinds of boundaries types such as free edge, simply supported and built-in. Details discussions of analytical results are given in section 6.5 of this thesis.

Since there were 36 measuring points on SBO1, accordingly the panel was divided into 36 zones (See Figure 3.7) and the 36 FEA deflection values were used in the zones to get 36 corresponding corrector factor values in every zone as shown in Table 3.2 and Figure 3.8 (with some manual modification so as to agree to the symmetry of the panel), they are in fact 20 independent values. These values were used to revise the global smeared modulus E or strength f in the corresponding 36 zones to improve the FEA analysis, and were extended to more general panels by the concept of similar zones proposed by Zhou (2002) as well.
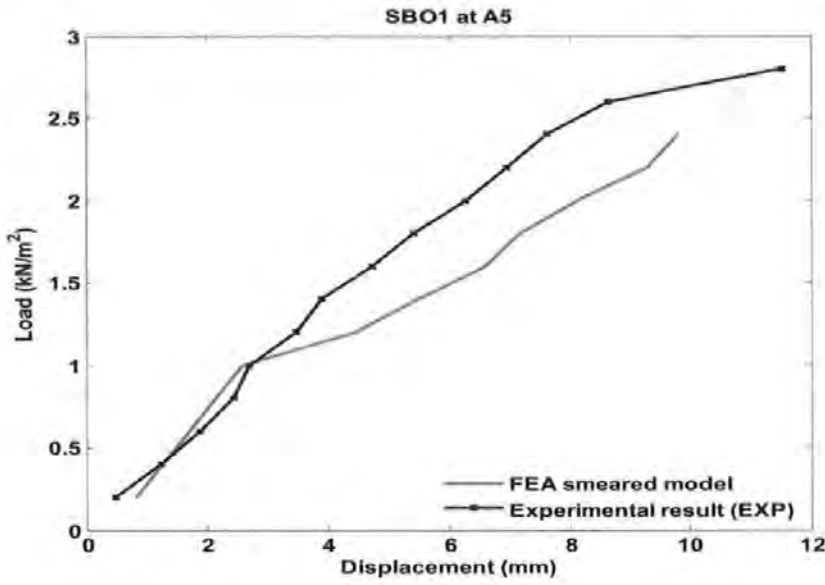
Figure 3.5 the experimental and FEA's load deflection relationships of the base panel

0 100   775   1450   2125   2800   3475   4150   4825   5500 5600

Free edge   Simply supported   Built-in
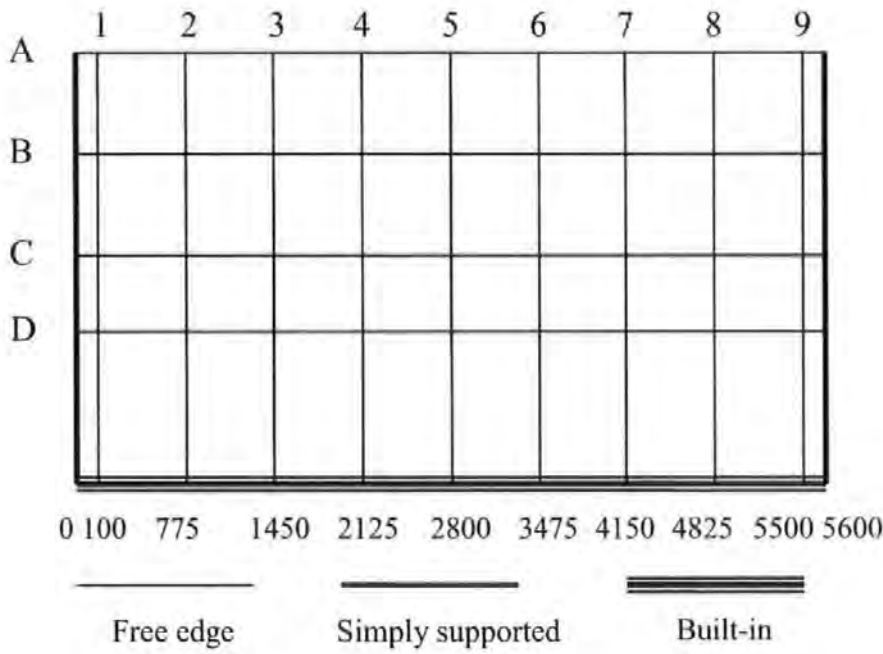
Figure 3.6 Configuration of the base panel
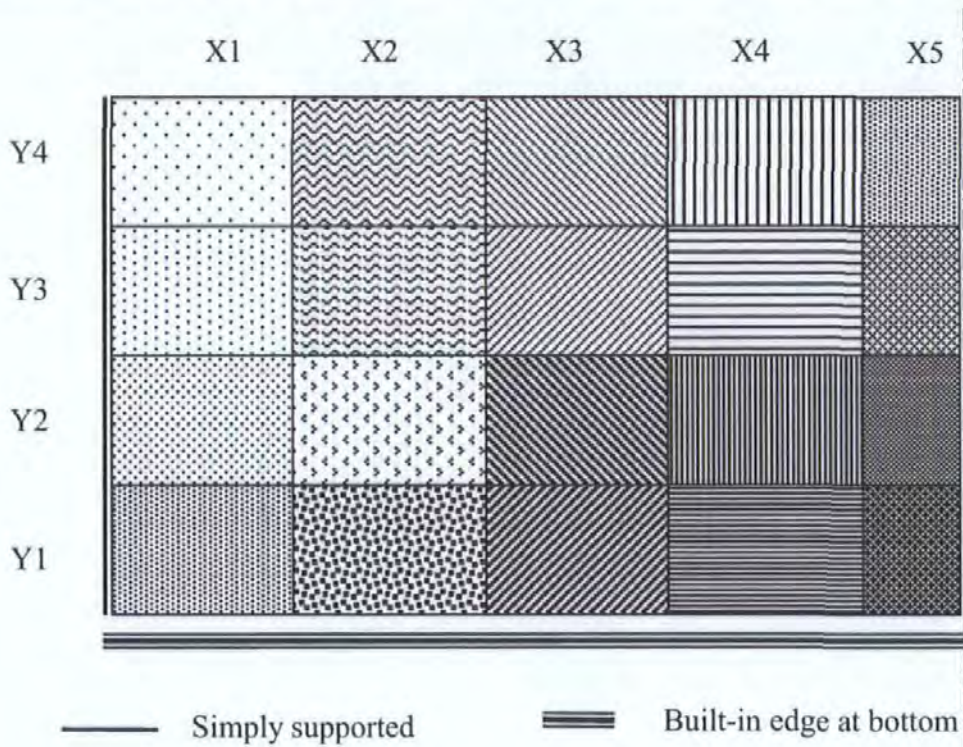
Figure 3.7 Zones division on the left symmetrical half of panel SBO1

Table 3.2 the corrector factors proposed by Zhou (2002)

q=2.4kN/m²	Corrector factors at measuring points								
	1	2	3	4	5	6	7	8	9
A	0.637	0.819	1.198	1.262	1.313	1.262	1.198	0.819	0.637
B	0.553	0.706	0.935	1.027	1.059	1.027	0.935	0.706	0.553
C	0.689	0.759	0.957	1.114	1.218	1.114	0.957	0.759	0.689
D	0.530	0.540	0.916	1.268	1.247	1.268	0.916	0.540	0.530
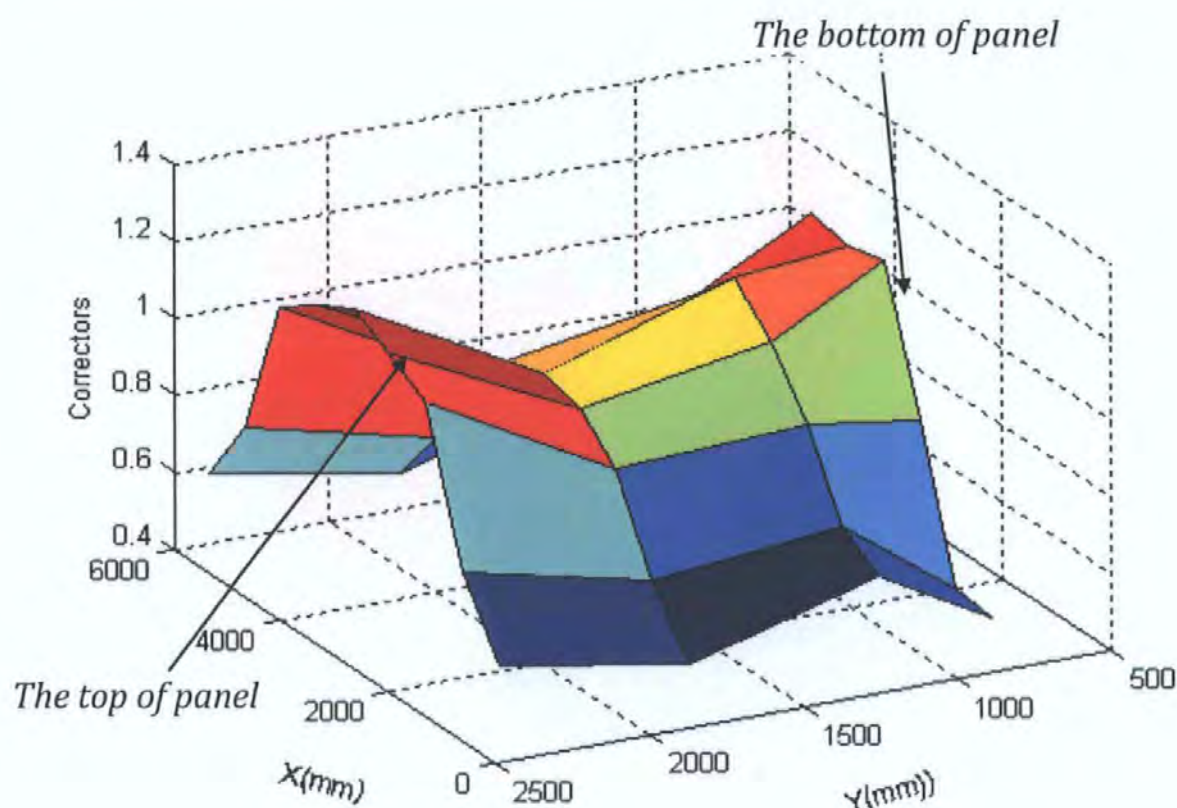
Figure 3.8 3D-plot of corrector factors given by Zhou (2002)

3.3.2 The concept of similar zone

To apply the corrector factors obtained from SBO1 to more general masonry panels (called new panel in Zhou's work and in this thesis), the concept of similar zones was proposed by Zhou, *et al.*(2003) based on the finding that, when comparing the corrector factors obtained by (3-1) between SBO1 and SBO6, their values have much correlation from each other and they also have much concerns with boundary conditions, i.e. among panels, zones near the same kinds of boundaries tend to have similar corrector factor values. More generally, any zones within two panels which share similar boundary conditions would have similar corrector factor values. Zhou designates the state value in a panel by the formulae (3-4),(3-5), (3-6),(3-7), (3-8) (Zhou 2002).

Li,j = Li,j-1 + μ(1 – Li,j-1)   *(3-4)*

Ri,j = Ri,j+1 + μ (1 – Ri,j+1)   *(3-5)*

Bi,j = Bi-1,j+ μ (1 – Bi-1,j)   *(3-6)*

Ti,j = Ti+1,j + μ (1 – Ti+1,j)   *(3-7)*

Where

μ = coefficient of transition, μ=0.2.

L --- state value of zone changes from the left boundary effect

R --- state value of zone changes from the right boundary effect

B --- state value of zone changes from the bottom boundary effect

T --- state value of zone changes from the top boundary effect,

i,j…element number in i row and j column

For free edge, $L_{i,0}$=0; $R_{i,0}$=0; $B_{0,j}$=0; $T_{0,j}$=0;

For simply supported edge, $L_{i,0}$=0.2; $R_{i,0}$=0.2; $B_{0,j}$=0.2; $T_{0,j}$=0.2;

For built-in edge, $L_{i,0}$=0.4; $R_{i,0}$=0.4; $B_{0,j}$=0.4; $T_{0,j}$=0.4;

The local rule for the calculation of the state value Si,j of the individual zones within the panel are described as:

$$S_{i,j} = \frac{(L_{i,j} + R_{i,j} + B_{i,j} + T_{i,j})}{4}$$ (3-8)

The state value, $S_{i,j}$ is the average effect from neighbourhood cells. It sums up the effect of all four boundaries at the four edges of the panel on a zone (i, j) within the panel. Cellular Automata (CA) was used to model the boundary effects and match the similar zones between two panels. Consequently, corrector factors in the zones of new masonry panels that have the different boundary condition and dimensions are derived from Table 3.2 and are used to improve the FEA of the new panel.

3.4 THE PROBLEM LEFT BY THE PREVIOUS RESEARCHERS

In Chong's analysis of laterally loaded masonry panels, a sudden decrease was always found on the load deflection curves. However, the experimental load deflection curve appears as a comparatively smooth curve (see Figure 3.5). This difference appeared on all the 18 panels he tested. He cannot make a reasonable illustration and therefore he attributed that the difference were due to :(a) the existence of self weight of the masonry panel, (b) the bond strength of mortar had increased in the bottom of the panel due to the pre-compression by self weight, (c) the biaxial failure criteria might not suitable at all for masonry Chong, et al.(1992b). Obviously his attributes are subjective.

In Zhou's work, several points are still not clear when using corrector factors:

- Defining corrector factors to be the ratio of the deflections of FEA and the experimental ones needs further theoretical verifications under the situation of larger deformations.

- The values of corrector factors were directly derived from the experimental deflections. As the experimental data appears irregular, the obtained corrector factors need some manual modification, which needs some personal experience.

- The physical meaning of corrector factors is still not clear although it is intended to express the boundary condition and the variation of material properties.

- The load deflection relationships of the FEA appear a sudden decrease but the experimental one hasn't (see Figure 3.9).The problem existed in Chong's work is still not solved in Zhou's work.

SBO1 at A5
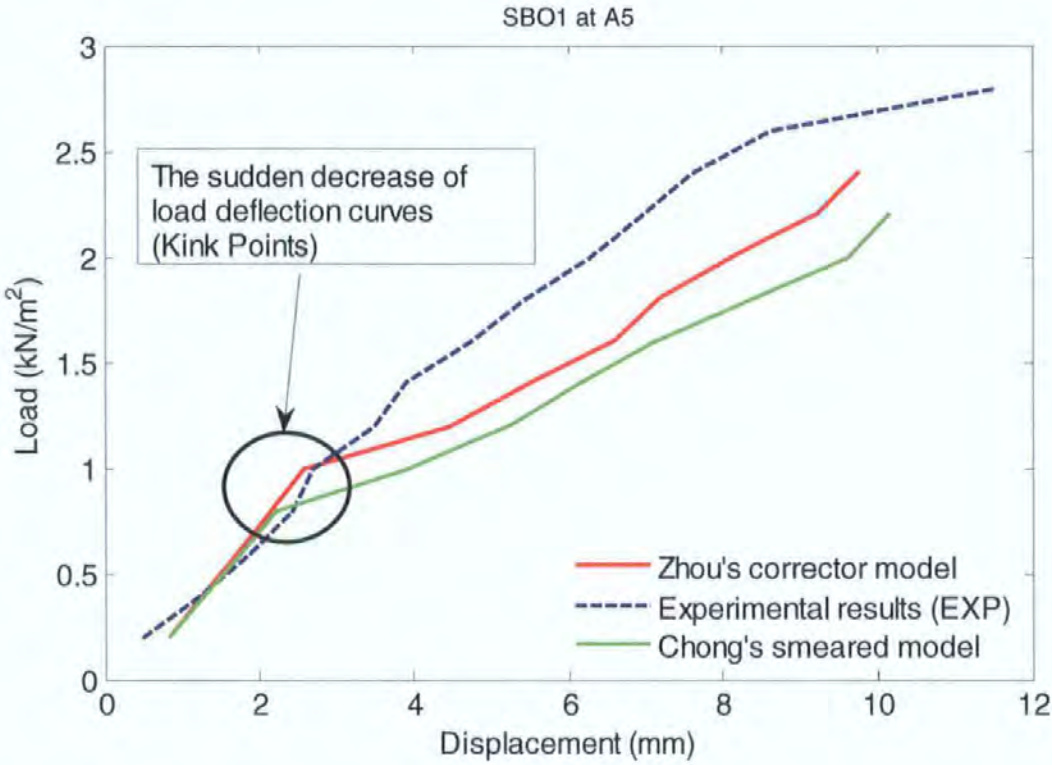
Figure 3.9 Typical load deflection relationships by experiment and FEA

To solve the problems left and to further improve the numerical prediction of the behaviour of laterally loaded masonry panels, research will be carried out in the following Chapters. Before any numerical study is undertaken, the experimental deflections of the masonry panels should be refined to appear regular to in accordance with the FEA model used, as will be introduced in Chapter 4.

4. REFINING EXPERIMENTAL DEFLECTION DATA OF MASONRY PANELS

4.1 INTRODUCTION

From Chapter 3 it is known that the concept of corrector factors developed by Rafiq, *et al.*(2003) and Zhou (2002) is directly related to the deflections of the masonry wall panel. However, it is found that the experimental deflection data of the masonry panels tested by Chong(1993) are irregular (see Figure 4.2, 4.3, 4.4), especially in locations close to the supporting edges and at the lower load levels, which resulted in the manual revision for getting the corrector factors values in Zhou's work. One reason to refine the experimental data is that, when analysing and evaluating the behaviour of masonry wall panels in numerical way, lateral deflections are an important feature beside the load bearing ability. Experimental load deflection relationships of laterally loaded masonry panels are very commonly used to verify the FEA models; obviously that using the load deflection relationships of many measuring points would be more reliable than using that for the measuring point with maximum deflection. The irregularity of experimental deflection data results in difficulty for any further numerical analysis. Besides, the physical meaning of these data might be difficult to understand. Consequently, using mathematical method to investigate the characteristics hidden in these data becomes necessary.

Another necessity for regularize the deflection data is that, in Chong's FEA model, masonry is regarded as an isotropic material, and it is well known that deflection data of the isotropic plate should be regular, such as appearing symmetry and so on.

The method presented in this chapter is based on such assumption that, data representing the behaviour of the isotropic model of the masonry wall panels are hidden

in the irregular experimental data accompanied with those noise caused by unknown factors.

It should clear that the main reason for smoothening the experimental data is that it is ONLY used to minimise the error between the experimental data and the FEA results. This was necessary for deriving corrector factors using the genetic algorithm. One reason for this was that the error between the FEA deflected surface and the experimental results were more sensitive to the irregularities of the deformed surface, particularly at locations near the boundaries of the panel.

Once the corrector factors were derived using the GA the comparison between the FEA results were made with the actual experimental data (see Chapter 9 for evidence.)

4.2 THE IRREGULAR EXPERIMENTAL DEFLECTIONS

Panel SBO1 is a solid single leaf masonry panel constructed with perforated class B facing bricks. The panel (See Figure 4.1) is 5600mm long, 2472mm high and 102.5 mm thick, with the two vertical edges simply supported, the bottom edge built-in and the top edge free Chong(1993). Deflections were measured at intersections of gridline A~D and 1~9. Figures 4.2 shows the load deflection relationships at all measuring locations along grid C. Figure 4.3 shows deflections along gridline C at all load levels and Figure 4.4 shows the surface plot of the deflections at 1.8 kN/m^2 load level.

From Figures 4.2, 4.3 and 4.4, it is clear that the experimental data contain much noise which make the deflections appear irregular, especially those near the supporting edges and at lower load levels.
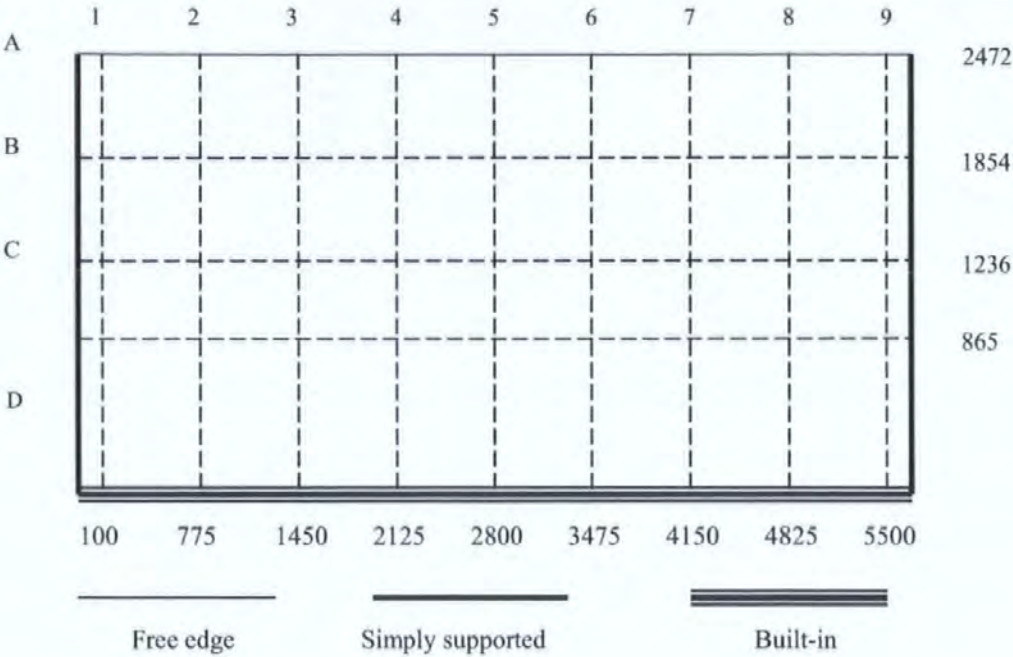
Figure 4.1 the configuration of masonry panel SBO1
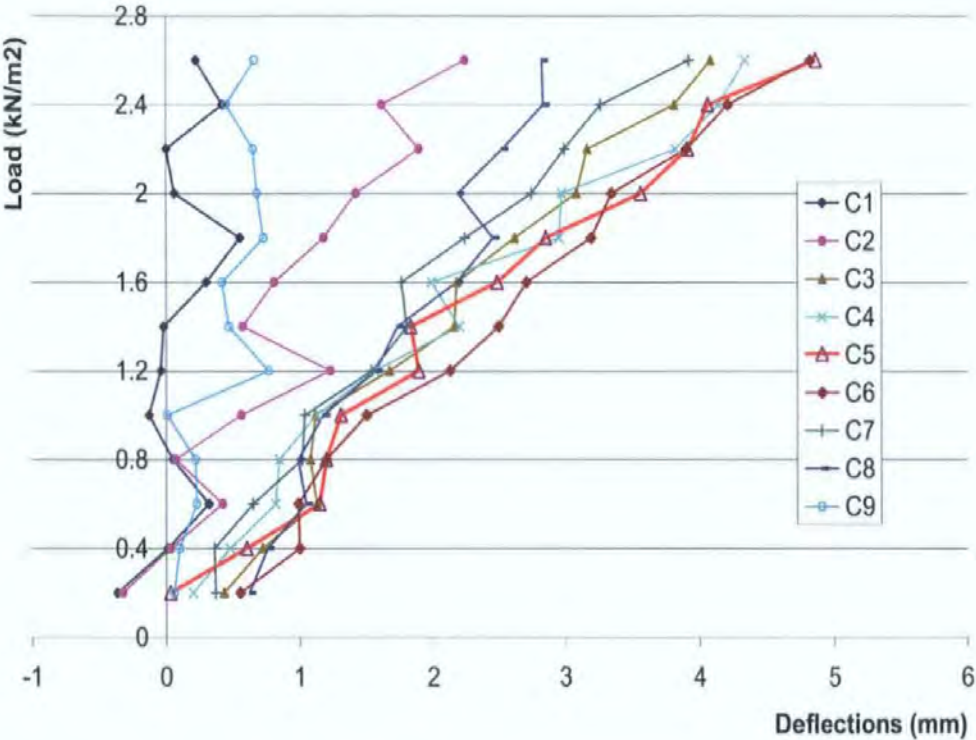
Figure 4.2 Experimental load-deflection relationships on grid C of SBO1
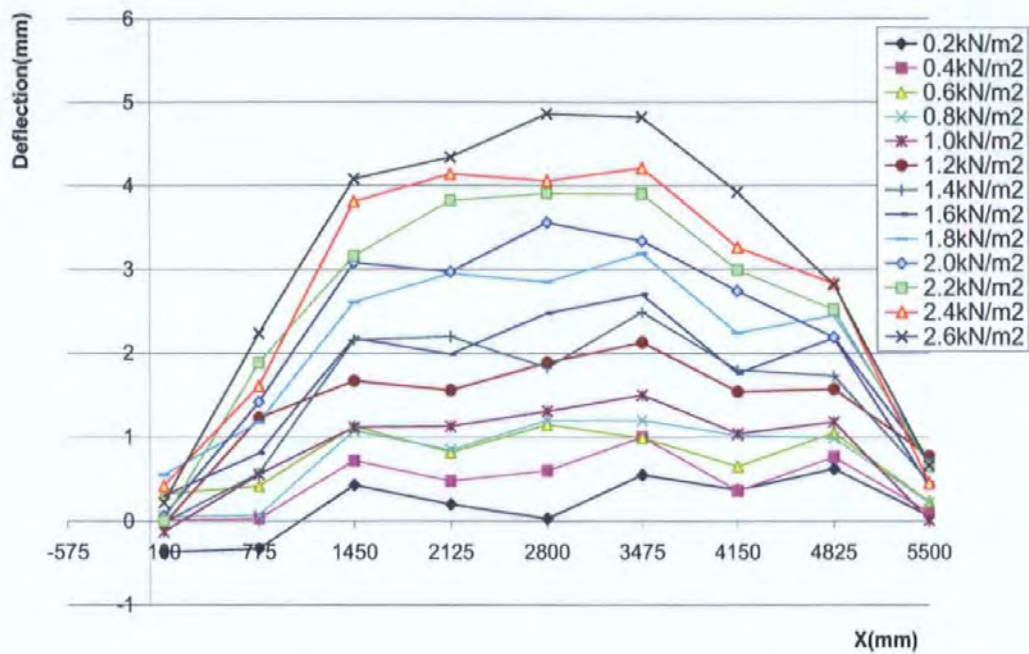
Figure 4.3 Experimental deflections on grid C of SBO1
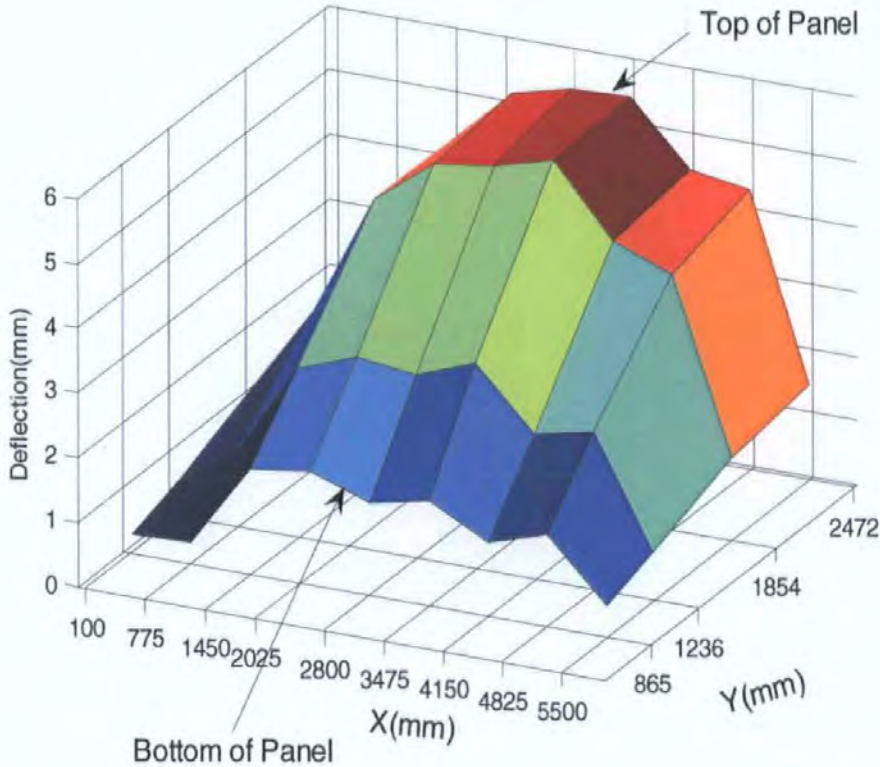
Figure 4.4 Experimental deflection surface of SBO1 (1.8kN/m²)

4.3. THE WAY OF REFINING EXPERIMENTAL DATA

In order to get rid of the noise, the experimental data and the panel itself are carefully examined. In fact, the deformations of any panel with specific boundary conditions have their own regularity. For masonry panel such as SBO1 as shown as Figure.4.1, it could be argued that the deflections of the panel should comply with the following rules:

1. The experimental deflections should be symmetrical about the central gridline at X=2800, as the supported boundary conditions are symmetric.

2. Deflections should increase from the bottom to the top and from the two vertical edges to the centre of the panel, because the top edge of the panel is free.

3. Deflections should increase as the load increases.

The above rules could be classified into two categories: the rule of deformation and the rule of load-deflection relationship. These two rules are the basis of refining the deflection data and accordingly two kinds of refinement using regression are proposed:

1. Deflection-surface refinement (the first refining): using regression with corresponding rules to fit the experimental data to get smooth surfaces at all load levels.

2. Load-deflection curve refinement (the second refining): using regression to make sure that load deflection relationships at each recording location closely follow common sense, i.e. deflections increase as load increases.

The regressions are implemented using mathematical formulae that will be introduced in the following sections. Furthermore, it would be justifiable that different weights are applied when implementing the regression, to express different reliability of data from different measuring points and load levels.

Our experience suggests to always undertake the deflection-surface refinement first, the load-deflection curve refinement is implemented only when the results of the deflection-surface refinement still in disorder; the reason is that changing load-deflection curves might be at the higher risk of changing the characteristics of the panel.

The flowchart of the refinement procedure is shown as Figure 4.5.

```
                    ┌─────────────────────────────┐
                    │ The experimental deflections of │
                    │   SBO1 tested by Chong (1993)   │
                    └─────────────────────────────┘
                                  │
                                  ▼
┌──────────────────────┐  ┌─────────────────────┐  ┌──────────────────────┐
│ Formula for regression│─▶│  Deflection-Surface │◀─│  Weights to different │
│                      │  │ Refining (first refining)│  │   measuring points   │
└──────────────────────┘  └─────────────────────┘  └──────────────────────┘
                                  │
                                  ▼
┌──────────────────────┐  ┌─────────────────────┐  ┌──────────────────────┐
│ Formula for regression│─▶│ Load-Deflection Curves│◀─│ Weights to different load│
│                      │  │Refining (second refining, if│  │        levels        │
│                      │  │      necessary)     │  │                      │
└──────────────────────┘  └─────────────────────┘  └──────────────────────┘
                                  │
                                  ▼
┌──────────────────────┐  ┌─────────────────────┐  ┌──────────────────────┐
│Mathematical expression│◀─│    The refined      │─▶│Mathematical expression│
│ at each load level (by│  │                     │  │  at any points (by load-│
│  deflection surfaces) │  │  deflection data    │  │   deflection curves)  │
└──────────────────────┘  └─────────────────────┘  └──────────────────────┘
```

Figure 4.5 Flow chart for refining the deflections of the masonry panels

4.4 DEFLECTION-SURFACE REFINING (THE FIRST REFINING)

Deflection-surface refinement is based on the fact that the deformation of the masonry panel should follow some principles as introduced in section 4.3. It has been considered that the reliability of deflection data for different locations on the panel is different, therefore, weight values are considered for regression.

4.4.1 Weights of different measuring points

After carefully examining all the experimental deflection data, including those shown in Figures 4.2, 4.3 and 4.4, two features are observed.

1. The deflections at the central part of the panel are comparatively more regular, such as C3-C7 in Figure.4.2; the deflections always increase as the load increases.

2. On the other hand, deflections near the supporting edges are more irregular such as C1-C2 and C8-C9 in Figure 4.2; the deflections sometimes decrease as the load increase.

The cause of the above is that for the measuring points far from the supported edges, their larger deflections would be less sensitive to the influence of the supported edges; however, for the measuring points close to the supported edges, their deflections are smaller, which are more sensitive to the influence of the supported edges.

Table 4.1 Weights Dissemination in the Panel

Positions	1	2	3	4	5	6	7	8	9
A	1.0	1.0	1.0	1.0	1.0	1.0	1.0	1.0	1.0
B	0.5	1.0	1.0	1.0	1.0	1.0	1.0	1.0	0.5
C	0.5	0.5	1.0	1.0	1.0	1.0	1.0	0.5	0.5
D	0.5	0.5	0.5	0.5	0.5	0.5	0.5	0.5	0.5

It is justifiable to let the more regular data make a higher contribution to the regression analysis and the less regular data a make smaller contribution to the regression analysis; therefore different weights are applied to the different measuring points on the panel. In this study, the points far from the supporting edges are given comparatively higher values, and those points close to the supported edges are given smaller values as shown in Table 4.1 which is based on examining all experimental deflection data thoroughly.

4.4.2 Candidate Formulae for deflection-surface refining

Formulae are needed for implementing regression analysis. In theory, there are many formulae that might be used for regression, but in practice, only those formulae that better represent a panel's deformation can be used.

For panel SBO1 with the boundary condition as shown in Figure 4.1 which bears the uniformly distributed lateral load, its deformations should have the following features:

- Deflections increase from the bottom edge to the top free edge.

- Deflections are symmetric about the centreline in X direction.

- Deflections along this centreline produce the highest values compared with others on the gridlines at the same height.

- In the X direction, deflections are mono-increasing from the left edge to the centreline, and reach the highest value then mono-decreasing from the centreline to the right edge.

Therefore, any formulae used for regression should produce the features above.

After some initial studies, three kinds of formulae were selected as the initial tool for regression analysis because they express the feature of deformation well. They are: the polynomial expression, the trigonometric expression, and the Timoshenko basic plate theory expression. A study of selecting the best formulae for regression is covered in the next section.

(a) Polynomial

$$\textit{Let } F1 = \sum_{i=1}^{m} Ai * (ABS(X/L_x))^i \quad \textit{and} \quad F2 = \sum_{i=0}^{n} Bi * (Y/L_y)^i ,$$

$$\textit{Then } \omega = A0*F1*F2+C \tag{4-1}$$

It has been found that, too many terms in polynomial functions would lead to over fitting, i.e. fit the disordered data too closely but do not produce a smooth surface; therefore, only 3 terms are used for the regression analysis.

(b) Trigonometric function

Defining $F_1 = COS^2 (ABS (\pi /2*(X/ (0.5*L_x)*A1))^{A2})$ *and* $F_2 = \sum_{i=1}^{m} Bi *(Y / L_y)^i$

Then $\omega = A0*F1*F2 + C$ ⠀⠀⠀⠀⠀⠀⠀⠀⠀⠀⠀⠀⠀⠀⠀⠀⠀⠀⠀⠀⠀⠀⠀⠀⠀ *(4-2)*

The definitions of the terms above are shown in notation of this thesis. In this case, similar to the case of polynomial functions, too many terms would result in an over fitting; therefore, it is also limited to 3 terms only.

(c) Formula based on Timoshenko-like formula (Timoshenko 1981)

A Timoshenko formula is suitable for deriving the deflections of isotropic plates and shells with various kinds of boundary types. The formula involves trigonometric and hyperbolic terms with constants of material properties such as modulus E and Poisson ratio v. An advantage of the Timoshenko like function is that it can satisfy the boundary conditions better than other functions.

When the panel's boundary conditions are such that the two vertical edges simply supported, the bottom edge built-in and the top edge free, and subjected to uniformly distributed load, the following expression is given by Timoshenko:

$$\omega = \left(\frac{4qa^4}{\pi^5 D} \sum_{m=1,3,5...}^{\infty} m^{-5} \sin\frac{m\pi x}{a}\right) + \left(\sum_{m=1,3,5...}^{\infty} Y_m \sin\frac{m\pi x}{a}\right)$$

$$Y_m = \frac{qa^4}{D}\left(A_m \cosh\frac{m\pi y}{a} + B_m \frac{m\pi y}{a}\sinh\frac{m\pi y}{a} + C_m \sinh\frac{m\pi y}{a} + D_m \frac{m\pi y}{a}\cosh\frac{m\pi y}{a}\right)$$

Where A_m B_m C_m D_m are the constants, a is the length of the plate, $m = 1, 3, 5, 7.....$

Again similar to the case of using polynomial and trigonometric functions, if *m* is over 5, over-fitting happens. It was decided to use *m=5* in this investigation and the Timoshenko's formula becomes as follows:

ω =A₉•[sin (πx/a) +sin (3πx/a)/243+ sin (5πx)/3125] + F₁*sin (πx/a) + F₂*sin (3πx/a)

+ F₃*sin (5πx/a) +A₁₀   *(4-3)*

Where

F₁= A₀•cosh (πy/a) +A₁*(πy/a)*sinh (πy/a) +A₂• sinh (πy/a)-A₂ (πy/a) cosh (πy/a)

F₂= A₃•cosh (3πy/a) +A₄*(3πy/a)*sinh (3πy/a) +A₅•sinh (3πy/a)-A₅*(3πy/a)*

cosh(3πy/a)

F_3= A₆*cosh (5πy/a) +A₇*(5πy/a)*sinh (5πy/a)+A₈* sinh (5πy/a)-A₈*(5y π/a)*cosh(5πy/a)

4.4.3 Determine the best formula for deflection surface refining.

The best formula is determined by comparing the regression results using the three candidate formulae at each load level such as shown in Figures.4.6, 4.7, 4.8 and 4.9. By examining these figures, the following conclusions are drawn:

1. At the lower load levels the deflection curves formed by the polynomial function and trigonometric function appear to be flat at the central part of the panel, which does not fit the anticipated form, but the Timoshenko's formula produces a reasonable fitting curve (see Figures 4.6 and 4.7).

2. At the higher load levels the deflection curves of all three formulae are very similar (see Figures 4.8 and 4.9).

Consequently, the Timoshenko-like formula (4-3) is selected as the best one for surface regressions.
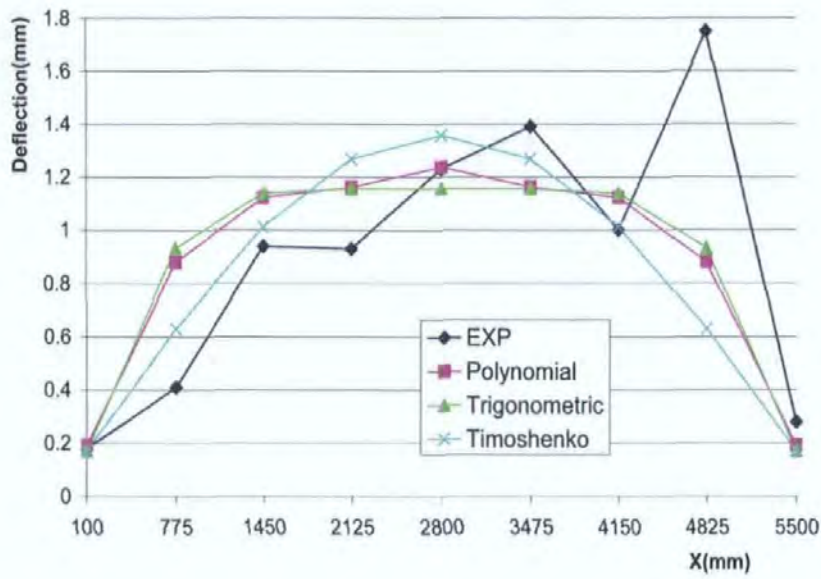
Figure.4.6 The refined deflections at 0.4 kN/m^2 on grid A
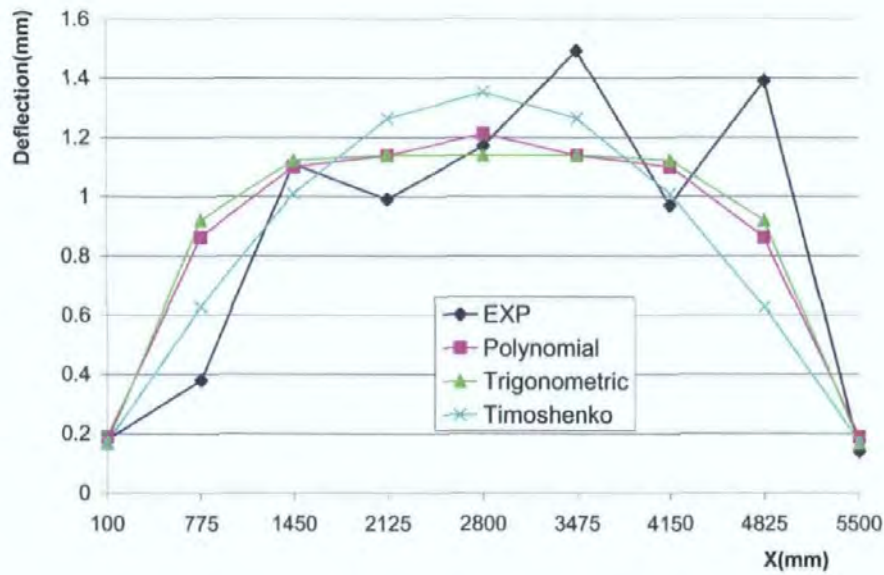
Figure.4.7, The refined deflections at 0.4 kN/m^2 on grid C
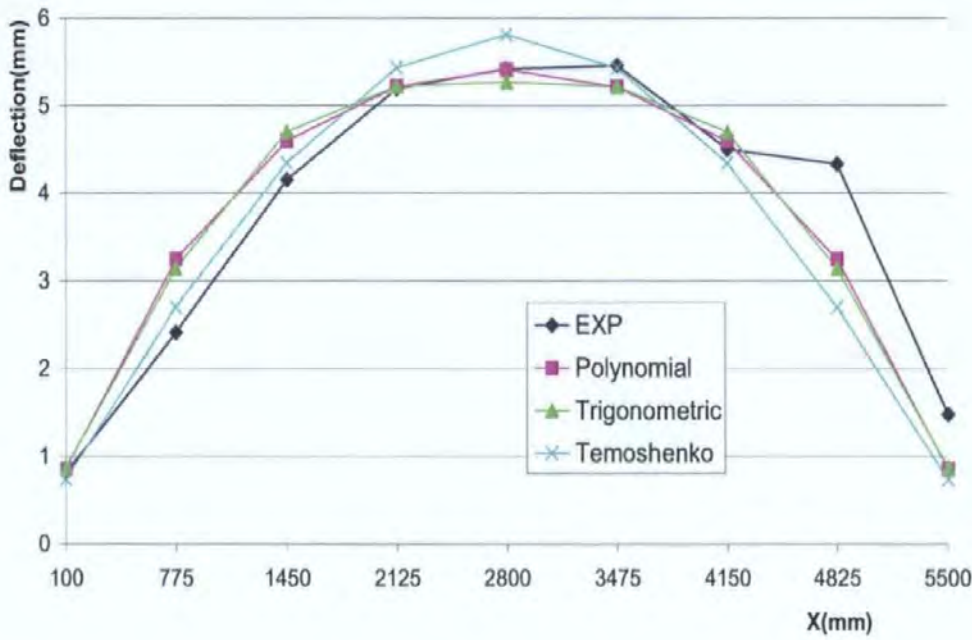
Figure 4.8 The refined deflections at 1.8kN/m^2 in grid A
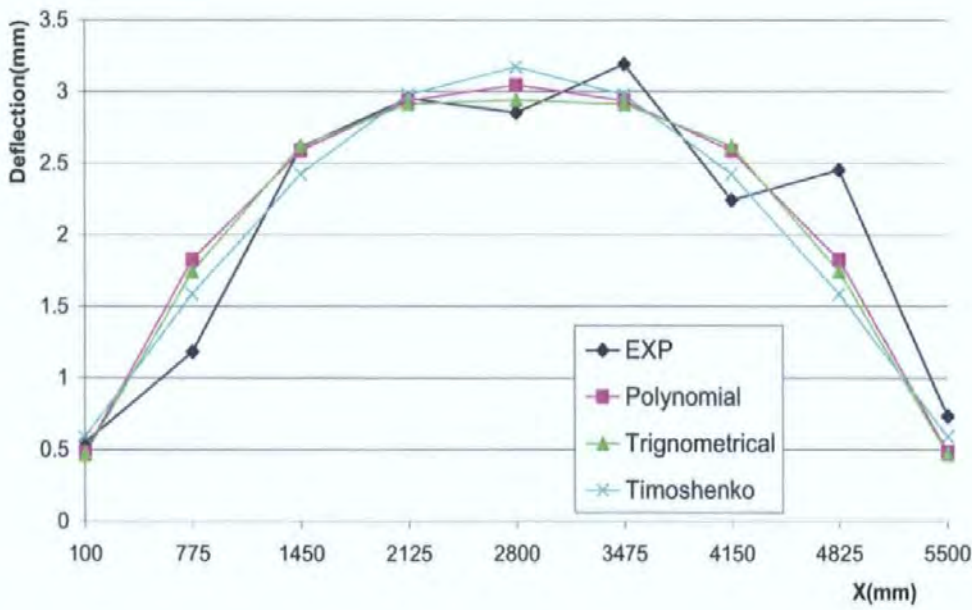
Figure.4.9, The refined deflection at 1.8kN/m^2 in grid C

4.4.4. The validity of deflection-surface refining

Figures 4.10, 4.11 and 4.12 show the refined deflection data using deflection-surface refining by formula (4-3). In figure 4.10, it is clear that the deflections appear more regular; and from Figures 4.11, 4.12, the load-deflection curves become comparatively regular as well.

However, from further examination of the load-deflection curves such as in Figure 4.11, 4.12, it can be seen that load-deflection curves at the points far away from the supported boundaries are regular, such as B3, B5 in Figure 4.11 and A4 in Figure 4.12; but those close to the supported boundaries, such as B1 in Figure 4.11 and D1 in Figure 4.12, the deflections still decrease as the load increases, which means that further refining is necessary. Obviously the deflection-surface refinement would not be valid again, therefore load-deflection curve refining is proposed as will be introduced in the next section.
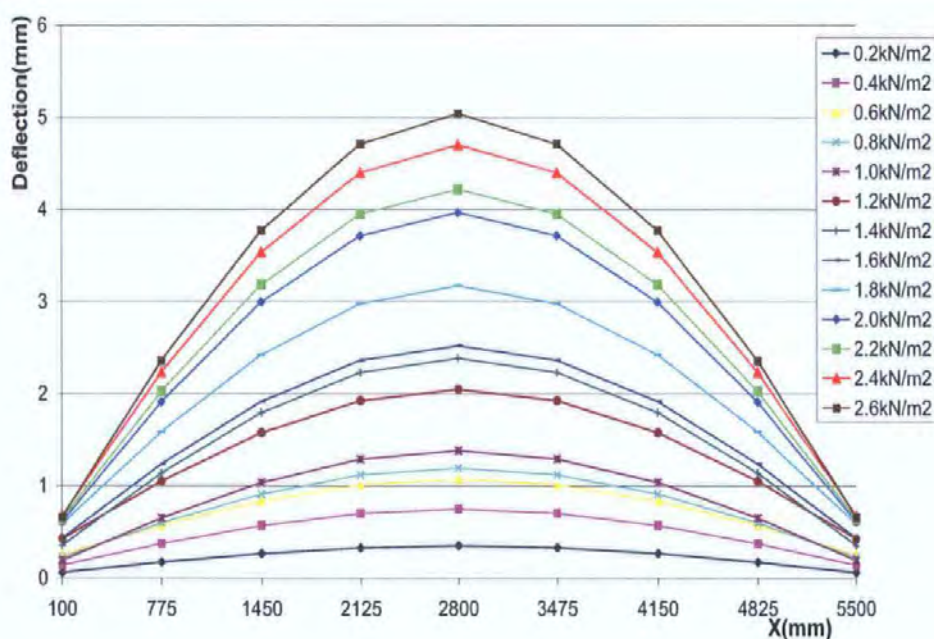
Figure.4.10 The refined deflections in grid C
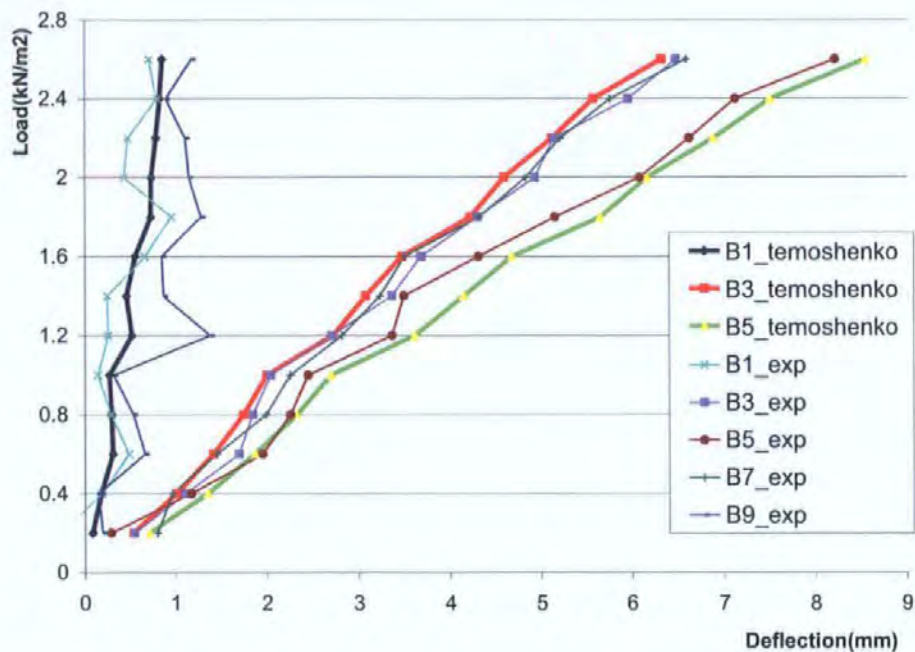
Figure.4.11 The load-deflection relationships after deflection surface refining in grid B
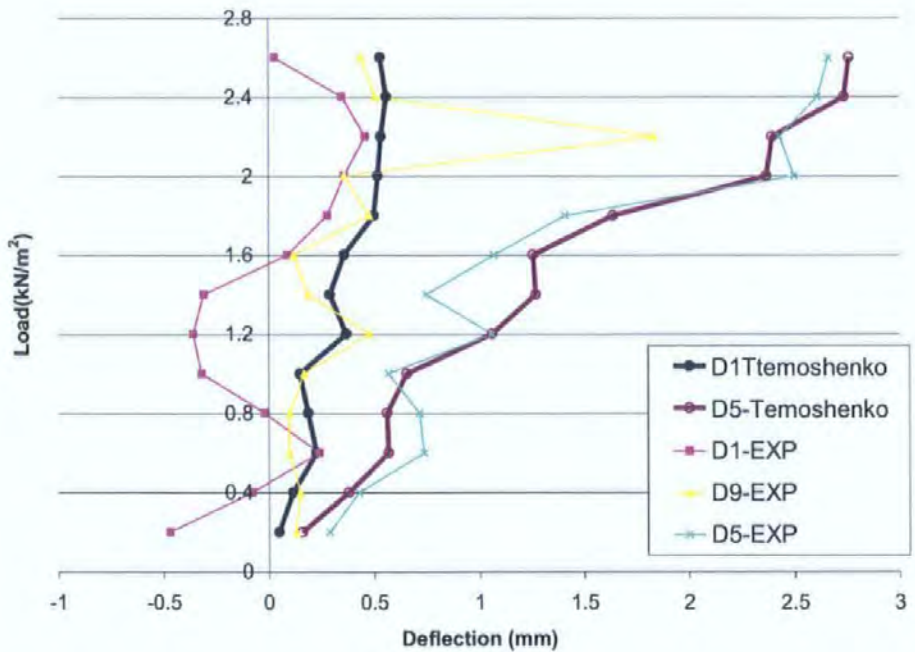
Figure.4.12 The load-deflection relationships after deflection surface refining in grid D

4.5 LOAD-DEFLECTION CURVE REFINING (THE SECOND REFINING)

Because some of the data after the first refining are still illogical, it needs to be refined again, i.e. the load deflection curves refining should be carried out.

4.5.1 Weights at different load levels

Similar to the first refinement in section 4.4.1, it is also preferable to use weight values in the second refinement.

It could be seen that the load-deflection curves are comparatively irregular at lower load level but are more regular at higher load level (see Figure 4.3, 4.4, 4.11, 4.12). In Figure 4.10, when the load level exceeds $1.6kN/m^2$, the gap between deflection lines is distinct, but for the lower load levels such as at $1.2 -1.4kN/m^2$, $0.6- 1.0 kN/m^2$, the deflection lines meet each other at two ends. When making the load-deflection curve refining, obviously deflection data at higher load levels are more reliable compared with those at lower load levels. It is justifiable that smaller weight values are applied to these less reliable data so that they make a smaller contribution to the regression analysis; on the other hand, bigger weight values are applied to those more reliable data so that they give larger contribution to the regression analysis. Weight values as shown in Table 4.2 are used for load-deflection curve regressions due to the common sense.

Table 4.2 Weights for load-deflection regression

Load(kN/m^2)	0.2	0.4	0.6	0.8	1	1.2	1.4
Weight	0.5	0.5	0.5	0.5	0.5	0.5	0.5
Load(kN/m^2)	1.6	1.8	2	2.2	2.4	2.6	------
Weight	1	1	1	1	1	1	------

4.5.2 Determine the Formula for load deflection curve refining

To further refine the data from the first refining, a suitable formula is needed. The principle to find a suitable formula for load-deflection regression is that the shape of the curves of the selected formulae are close to the general load-deflection curves and they achieve a smaller error.

4.5.2.1 Study of the polynomial formula

The polynomial is the most commonly used formula for describing a line and others; therefore, it is studied for the first instance. A typical polynomial could be expressed as (4-4)

$$\omega = \sum_{i=0}^{n} Ai * (Qi)^i \qquad (4\text{-}4)$$

Where,

Q: the load. ω: the deflection.

Ai: constants to be determined   *i* : the number and the order of the terms.

n: the total number of the term.

It has been found that, when using a polynomial to describe a load deflection relationship, the order of the selected equation expressed by equation (4-4) should be smaller than 4, because for the order equal to 4 or above, its second derivative could be negative, which means that under positive loading, the load deflection curve might fall before failure (see Figure 4.13, the 4th order). Therefore polynomials of the order of 4 and above are not suitable to represent the load- deflection curve and therefore, polynomials of two-order and three-order are selected. It also has been found that polynomial equations of two-order and three-order give very similar results (difference

<= 5%). Subsequently, a polynomial equation of two-order is suggested for load-deflection refining as shown in (4-5).

$$\omega = A0 + A1*Q + A2*Q^2 \qquad\qquad (4\text{-}5)$$

Where

ω: deflections, Q: Load, $A0, A1, A2$: constants to be determined by regression.
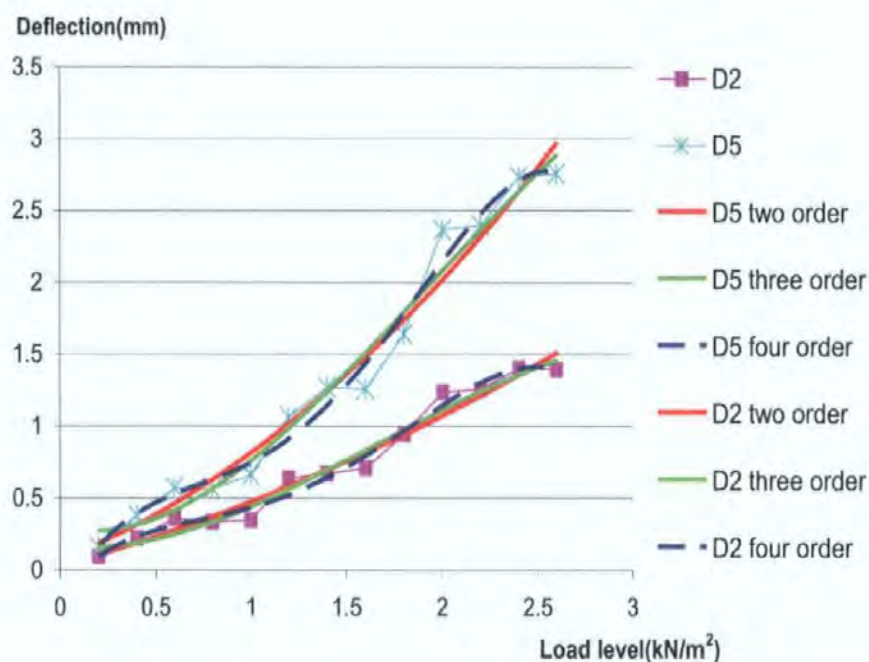
Figure.4.13 Using the polynomials of different order

(Note: The vertical coordinate is deflection and D2, D5 are deflections after surface refining)

4.5.2.2 Considering of other formulae

Because common load deflection curves of laterally loaded masonry panels appear to increase linearly in the beginning and then keep increasing with lower increasing rate after a specific load level, there is also such possibly that other kinds of formulae could better describe the load deflection relationship of laterally loaded masonry panels, such as logarithmic curves, power curves, exponential curves, and polynomial curves. Therefore, comparison is made among these formulae and the second-order polynomial.

The results of using these formulae are shown in Figure 4.14. It is very clear that the polynomial gives the smallest error, and its shape is close to the shape of the common load deflection curve; a polynomial style formula (4-4) is proved to be the better one for load deflection curve regression.
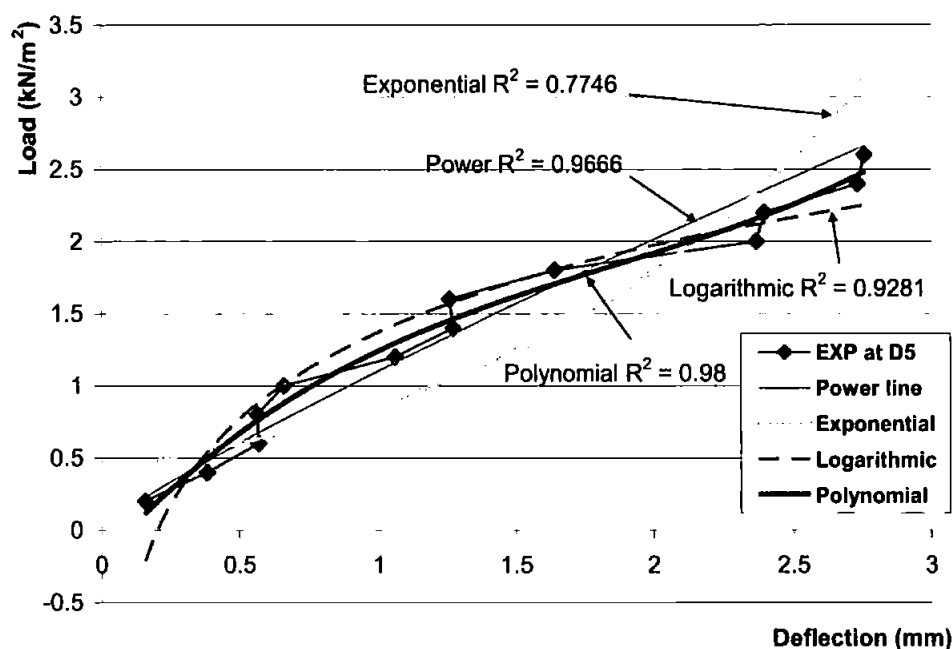
Figure.4.14, Comparison among using different kinds of formulae

4.5.2.3 Using two formulae for regression

Masonry behaves linearly at lower load levels and nonlinearly at higher load levels; therefore, using two lines might describe the load deflection curves better. To check this possibility, regressions using one line and two lines are compared.

1. Only use one line of a second-order polynomial formula.

2. Two lines are separately used to express the linear stage and the non-linear stage. A straight line is used to express the lower load levels (0.2-1.4kN/m^2) and an exponential line is used to express the higher load levels (1.6-2.6kN/m^2).
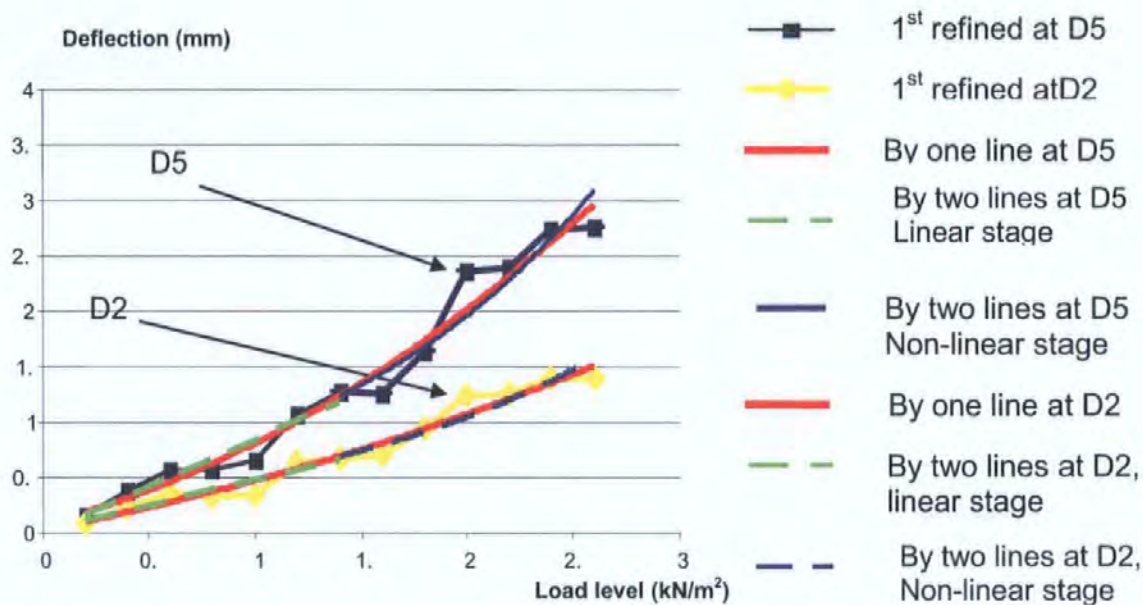
Figure.4.15 the comparison between using one and two formulae in grid D

(Note: the vertical coordinate is deflection)
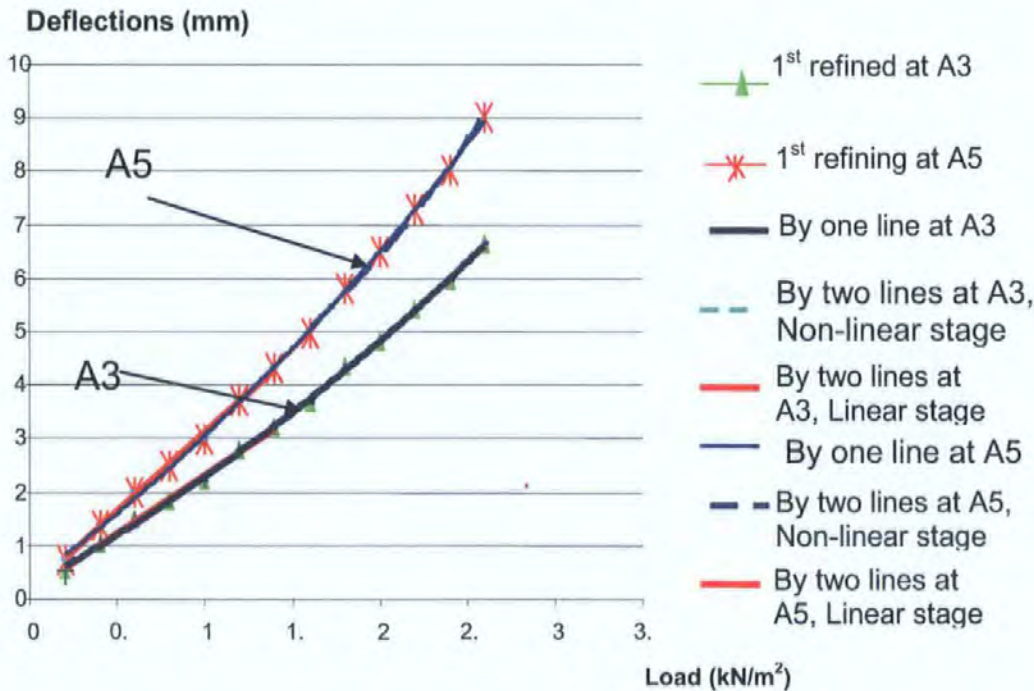
Figure.4.16 the comparison between using one and two formulae in grid A

(Note: 1. the vertical coordinate is deflections, 2. A3 1[st]and A5 1st are deflections of 1st refining)

It is seen that, for all measuring points within the panel, the results of using one formula and two formulae are very similar with differences smaller than 8% (see Figure 4.15, 4.16). Consequently, a single line of second-order polynomial formula is selected for regression, i.e. only one polynomial formula as shown in (4-5) is used for the second refinement.

4.5.3 The effectiveness of load-deflection curve refinement

Those load-deflection relationships by the first and second refinement and the original experimental ones are compared as shown in Figure 4.17. From the figure it can be seen that the first refinement makes the main contribution to the data refinement than the second refinement does. The second refinement is more effective at the location near the supported edges such as C1 and C9, but less effective at positions far from the supported edges such as C5.
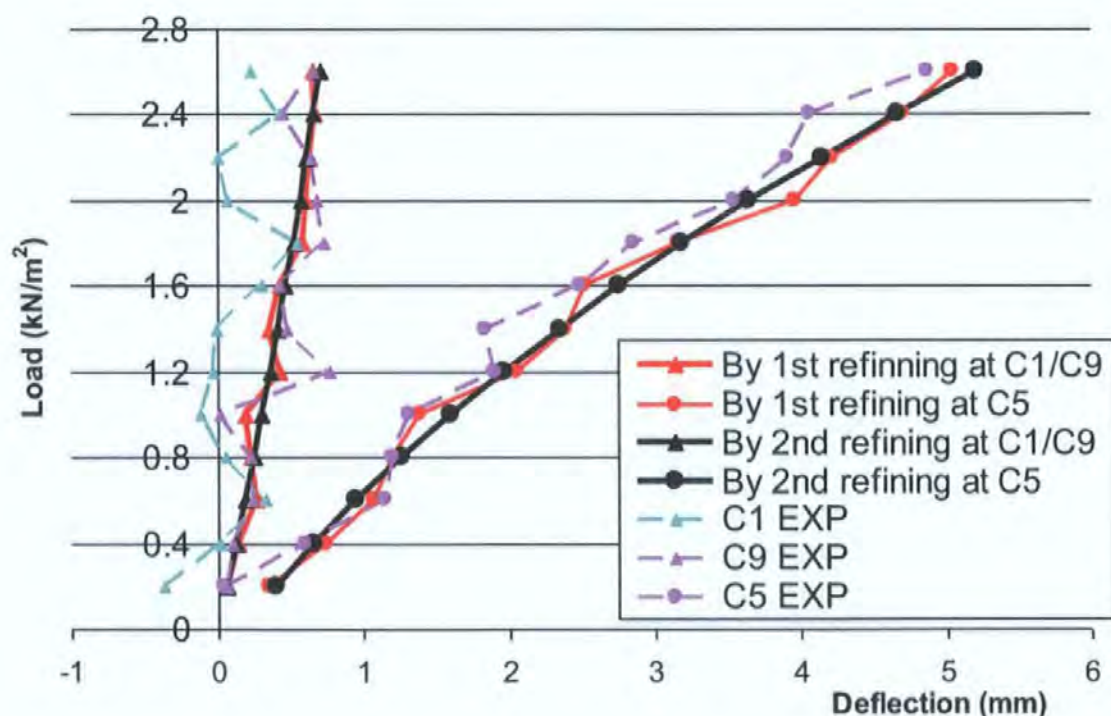
Figure.4.17 the comparison between the 1st and 2nd refining in grid C

(Note: because of symmetry, deflections of C1 and C9 are the same after refining)

4.6 RESULTS OF REFINING AND MATHEMATICAL EXPRESSIONS

After deflection-surface refinement by formula (4-3) and load-deflection curve refinement by formula (4-5), the load deflections and load deflection curves appear more regular as Figure 4.18, 4.19 shows. More refined data at the measuring point can be found in Appendix 2.

Moreover, using mathematical formulae, the continuum expression of the deflections of the lateral deformation at all load levels, and the load deflection relationships at any position of the panel are then obtained.
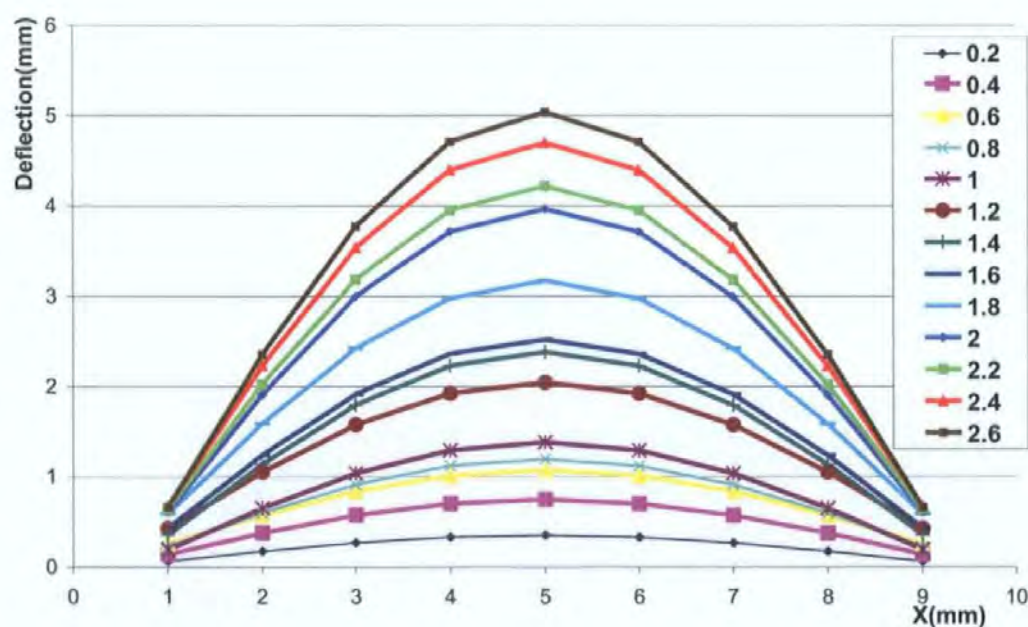
Figure 4.18 The refined deflections at grid C under different load levels (kNm^2)
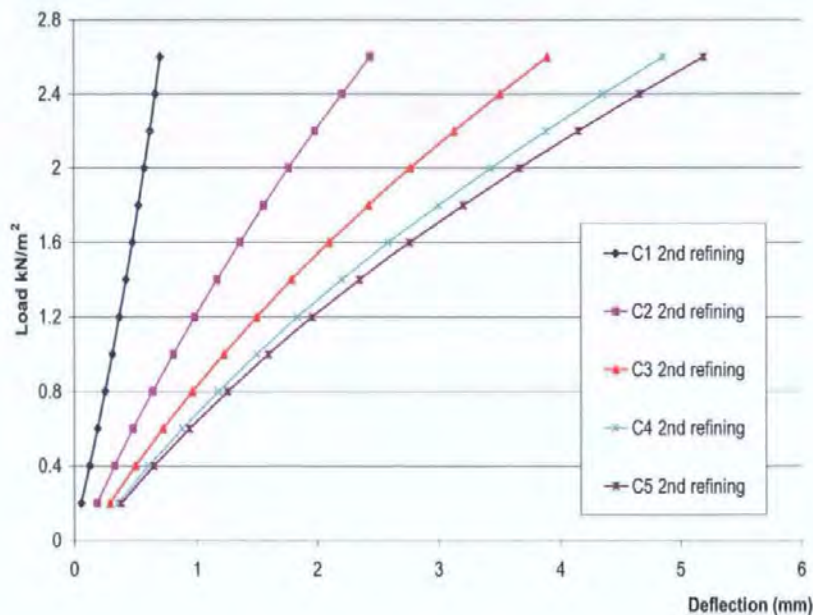
Figure 4.19 The refined load-deflection relationships at grid C

4.6.1 Mathematical expression of deflection surfaces

The mathematical expressions of the deflections surface are obtained by using the equation (4-3) but without weights.

Applying the equation as (4-3) to the refined data without considering the weights, a set of parameters is obtained as shown in Table 4.3. Substituting them back to equation (4-3), the mathematical formulae of expressing the refined deflection surfaces are obtained. To each load level, the discrepancy between refined deflection data and those of mathematical expression are checked; the maximum are smaller than 2%. The mathematical expression is acceptable.

Table 4.3 Parameters in the Formula of Expressing the Deflection Surface

Load(kN/m^2)	0	0.2	0.4	0.6	0.8	1	1.2
A0	10.025	20.757	29.711	36.886	42.284	45.904	47.746
A1	-4.923	-9.856	-13.749	-16.603	-18.416	-19.189	-18.922
A2	-1.765	-2.915	-3.437	-3.331	-2.596	-1.232	0.761
A3	-9.872	-20.516	-29.403	-36.532	-41.903	-45.517	-47.374
A4	-0.023	0.036	0.091	0.142	0.19	0.233	0.272

Load(kN/m^2)	1.4	1.6	1.8	2	2.2	2.4	2.6
A0	47.81	46.096	42.604	37.335	30.287	21.461	10.857
A1	-17.615	-15.268	-11.881	-7.453	-1.986	4.521	12.068
A2	3.382	6.631	10.51	15.017	20.152	25.916	32.309
A3	-47.474	-45.816	-42.4	-37.228	-30.297	-21.61	-11.165
A4	0.308	0.339	0.366	0.39	0.409	0.425	0.436

4.6.2 Mathematical expression of load-deflection relationships

Similarly, the mathematical expressions of the load deflections curves are obtained by using the equation (4-5) but without weights.

Applying equation (4-5) to the refined data without considering the weights, the parameters are achieved as shown in Table 4.4, put them back to equation (4-5), the mathematical formulae of expressing the refined load-deflection curves at different points are obtained. For each measuring point, the residuals between refined values and the mathematical expressions are also checked; all of them are smaller than 1%. Mathematical expression is acceptable.

Table 4.4 Coefficients for expressing the load-deflection curves at measuring points.

Positions / Parameters	D1	D2	D3	D4	D5
A0	-0.019	0.008	0.031	0.047	0.052
A1	0.319	0.403	0.474	0.521	0.537
A2	-0.034	0.066	0.149	0.205	0.224
Positions / Parameters	C1	C2	C3	C4	C5
A0	-0.014	0.044	0.093	0.126	0.137
A1	0.353	0.664	0.924	1.096	1.156
A2	-0.03	0.099	0.207	0.278	0.303
Positions / Parameters	B1	B2	B3	B4	B5
A0	-0.004	0.118	0.22	0.287	0.311
A1	0.415	1.13	1.728	2.125	2.263
A2	-0.028	0.111	0.228	0.306	0.333
Positions / Parameters	A1	A2	A3	A4	A5
A0	-0.002	0.136	0.252	0.329	0.356
A1	0.417	1.141	1.746	2.148	2.288
A2	-0.025	0.136	0.27	0.36	0.391

4.7 VERIFICATIONS

Now the method of refining the experimental deflection data is proposed. Because the method is based on the experimental results of one masonry panel, it is very necessary to check its validity on more general panels. To check the validity of this method, masonry panel SBO2 and SBO5 is used as follows.

4.7.1 The verification by SBO5

Panel SBO5 is another masonry panel tested by Chong (1993), which has the same material properties and dimensions as SBO1 as shown by Figure 4.1. Both panels have the same loading condition and measuring points as well; the only difference is that panel SBO5 has a bituminous d.p.c. (damp proof course) built into the first bed joint. The validity here is carried out by comparing the refined data of SBO1 with the refined data of SBO5, also their refined data with their relevant experimental data.

The findings by the comparison are as follows:

1. Each refined deflection surface matched their experimental deflection surfaces quite well (see Figures 4.20, 4.21, 4.22, 4.23, 4.24).

2. The refined data of SBO1 and SBO5 match each other quite well; although their original experimental deflections are quite different (see Figures 4.25, 4.26, 4.27, 4.28).
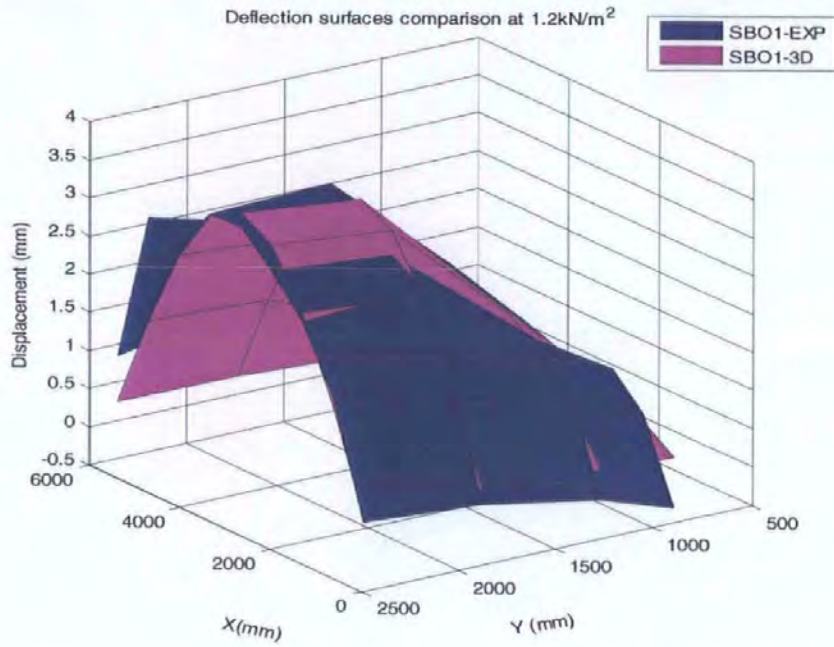
Figure.4.20 Experimental and refined deflection surface of SBO1at 1.2kN/m^2
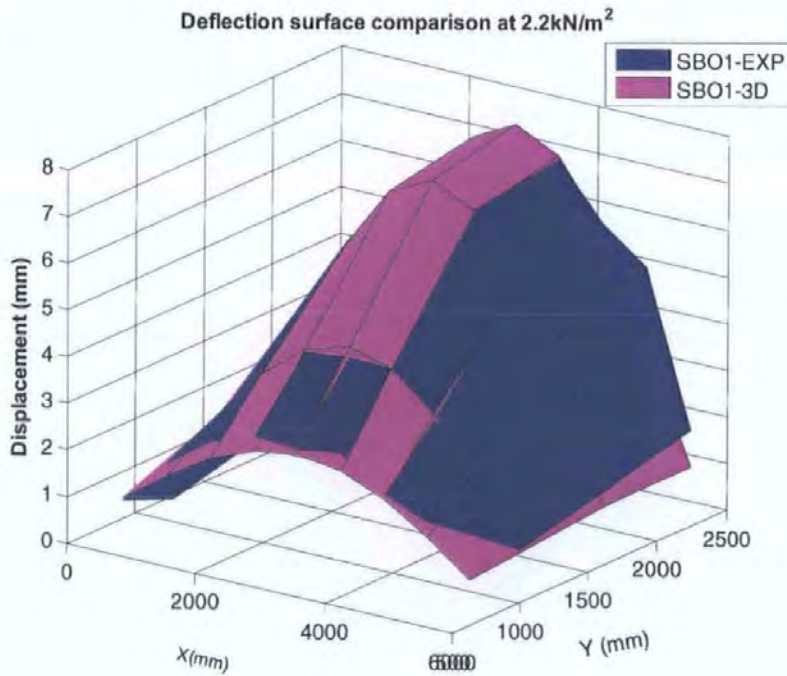
Figure.4.21 Experimental and refined deflection surface of SBO1at 1.6kN/m^2
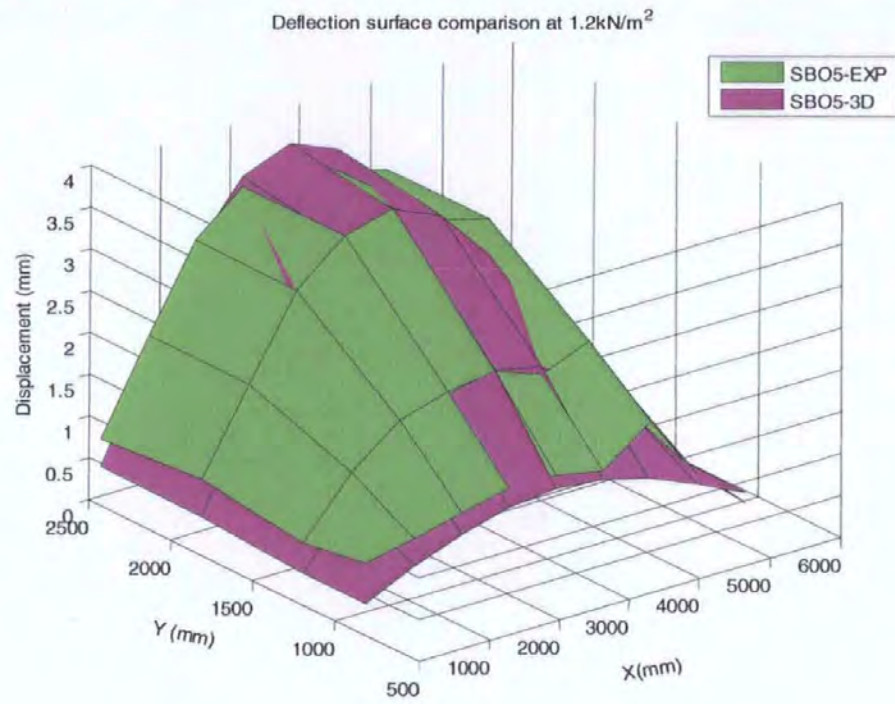
Figure 4.22 Experimental and refined deflections of SBO5 at 1.2kN/m²
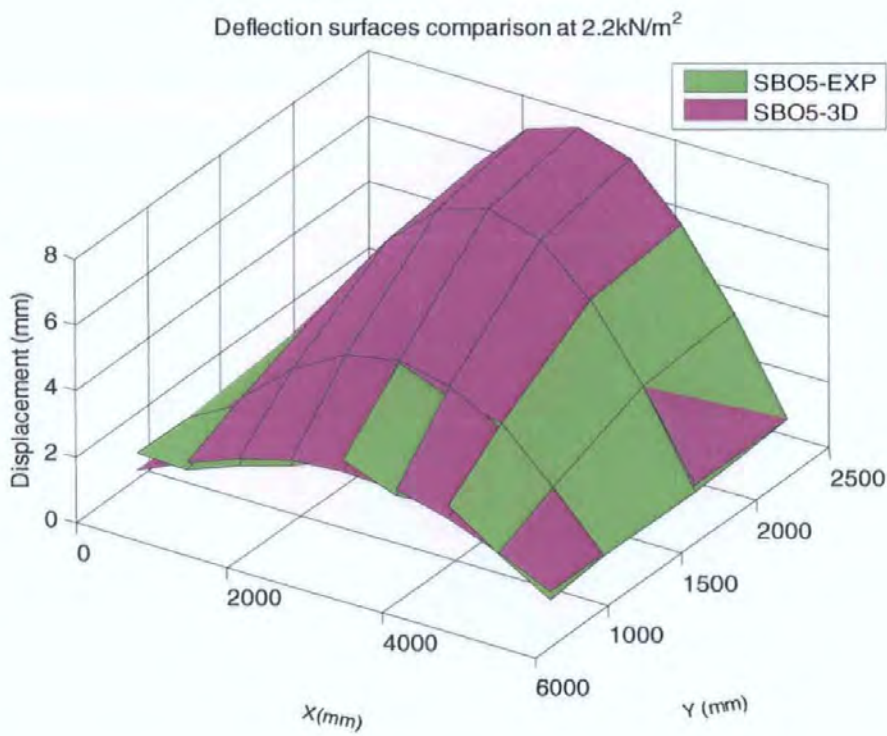
Figure 4.23 Experimental and refined deflections of SBO5 at 2.2kN/m²
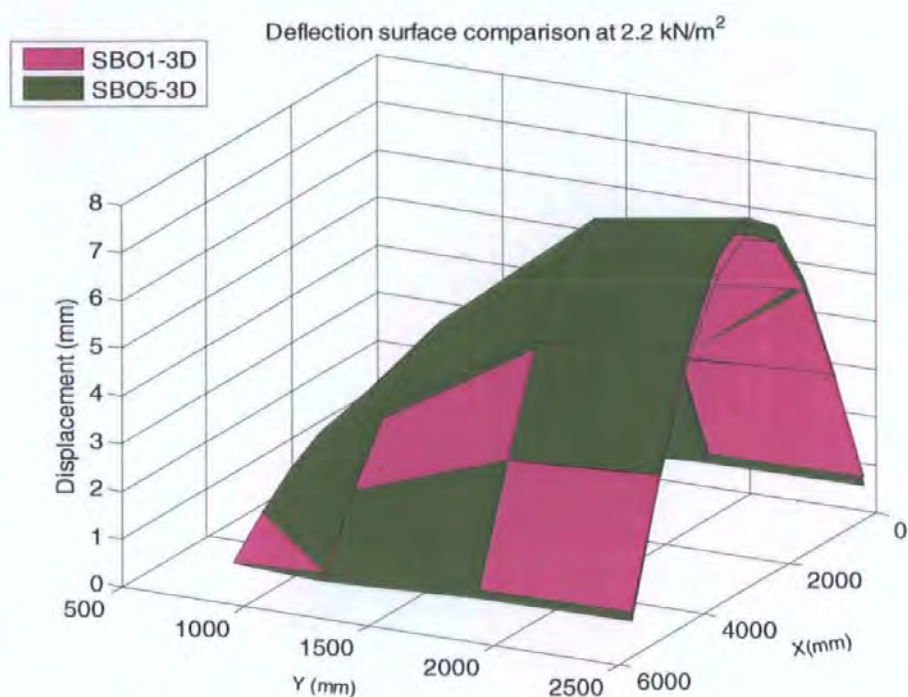
Figure 4.24 Comparison of the refined deflections of SBO1 and SBO5 at 2.2kN/m^2

To further validate the proposed method, load deflection relationships from the two panels on the relevant measuring points are compared and shown in Figures 4.25, 4.26, 4.27 and 4.28. In Figure 4.25, two measuring points A5 and A3 which are far from the supported edges, on both SBO1 and SBO5, are compared. The refined deflection data from the two panels are much closer to their relevant experimental deflections. Looking at the point B8 in Figure 4.26, C8 and D3 in Figures 4.27 and 4.28, even though the experimental load deflection curves of the two panels differs greatly, their refined deflections agree with their relevant experimental deflections very well. This suggests that the proposed method work well and is reliable.
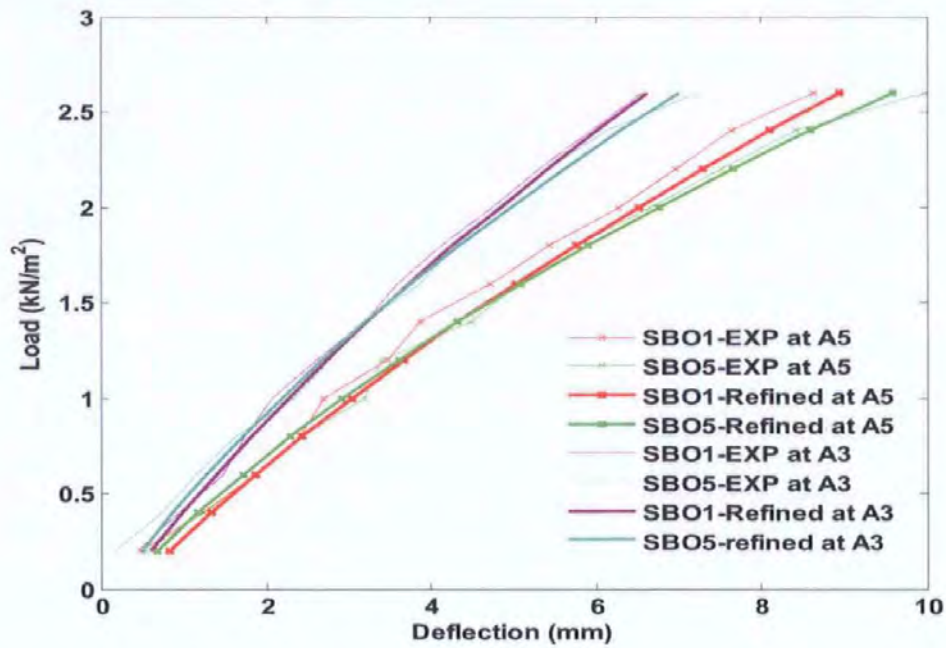
Figure.4.25 Comparison of the refined and experimental deflections of SBO1 & SBO5 at
A5 & A3
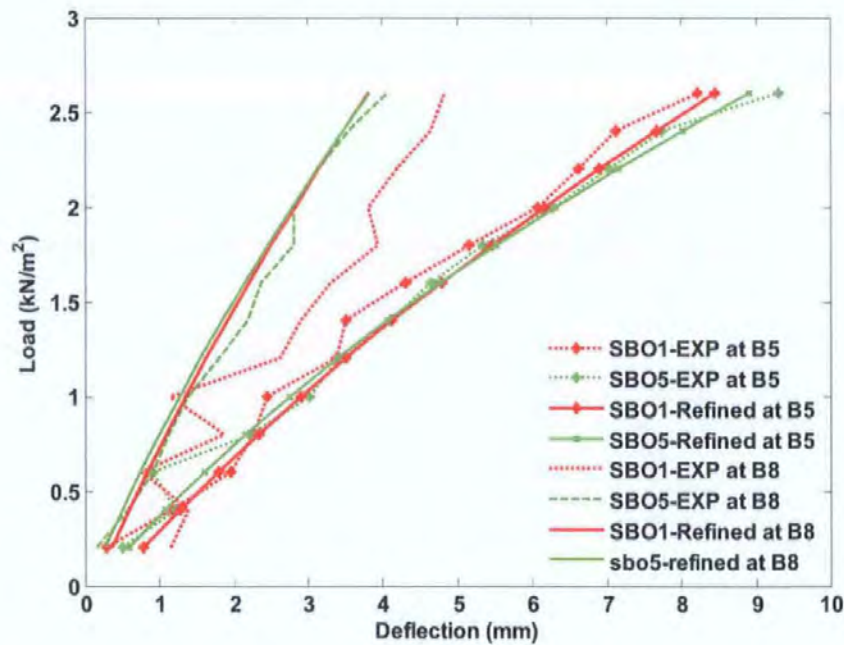
Figure.4.26 Comparison of the refined and experimental deflections of SBO1 & SBO5 at
B8 & B5
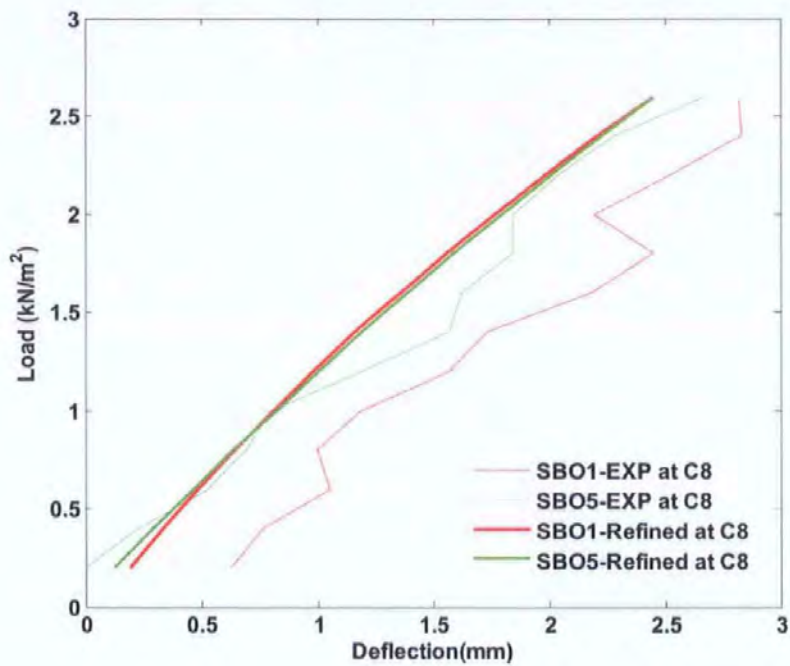
Figure.4.27 Comparison of the refined and experimental deflections of SBO1 & SBO5 at C8
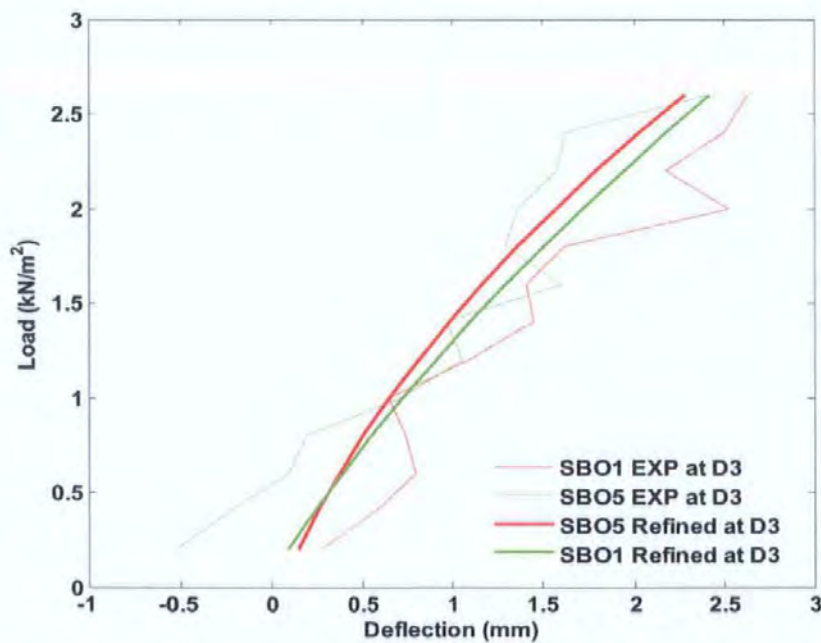
Figure.4.28 Comparison of the refined and experimental deflections of SBO1 & SBO5 at D3

4.7.2 Verification by SBO2 with openings

SBO2 is another masonry panel similar to SBO1 with the same dimension and material

properties, but with a opening. Its configuration is shown as Figure 4.29. The

comparison between the experimental and refined load-deflection curves are shown in

Figure 4.30 and 4.31. Obviously, the irregular load deflection relationships are refined

with some revision such as D1, D9, A3, A8, but the regular ones are refined with little

revision such as D5, A5.
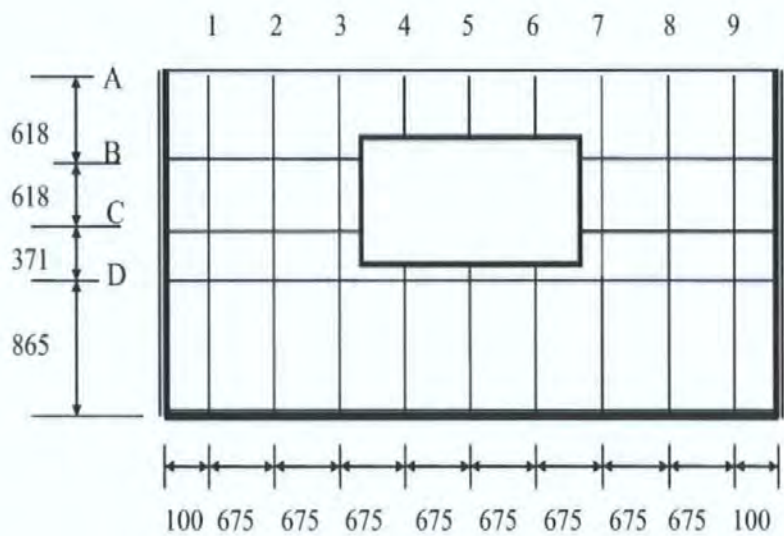
Figure.4.29, The configuration and the measuring points of masonry panel SBO2
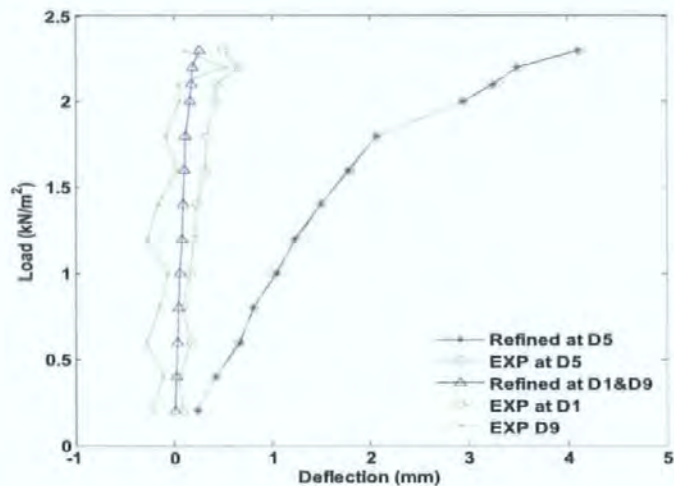
Figure.4.30, Rectified deflections of SBO2 at D1, D5 and D9
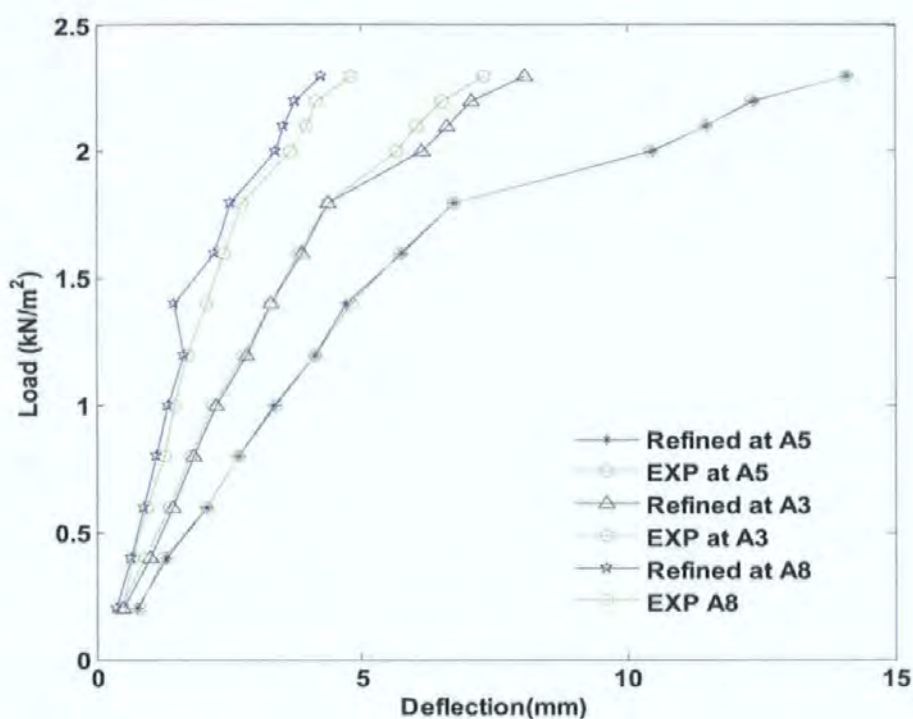
Figure.4.31, Rectified deflections of SBO2at A3, A5, and A8

4.8 SUMMARY

In this chapter, a method of refinement the irregular experimental deflection data of laterally loaded masonry panels is studied. Mathematical regression is used to carry out two kinds of refinement, the first one is the deflection surface refinement and the second one the load deflection curve refinement. The refined deflections are proved to be reliable according to validation of another two masonry panels.

The data refined by the method proposed in this chapter brings such advantages: Firstly, load deflection relationships at any position on the panel can be obtained, which provide sufficient load deflection relationships for further numerical analysis. Secondly, numerical methods, such as finite element analysis (FEA), generate regular lateral deformation of the panel. Since the refined data also represents a regular deformation, it

has become more convenient to compare like with like, especially for a symmetrical wall panel.

The refined deflections are intended to be used as the substitution of the original experimental data for further numerical analyses such as model updating process that will be introduced in the following Chapters.

5. INITIAL STUDY OF CORRECTOR FACTORS

5.1 INTRODUCTION

Based on the refined deflection data of laterally loaded masonry panels derived in Chapter 4, a further study of corrector factors will be carried out in this chapter. The aim of the study in this chapter is to understand the definition and nature of corrector factors developed by Zhou(2002) and Rafiq, *et al.*(2003) so as to get further improved predictions of the response of the laterally loaded masonry wall panels.

In this chapter, the study of corrector factors will be carried out by repeatedly using the definition given by Zhou(2002) and Rafiq, *et al.*(2003).

5.2 ITERATION METHOD

Chapter 3 stated that, Zhou(2002) and Rafiq, *et al.*(2003) defined corrector factors to be the ratio between the two kinds of deflections, i.e. those of FEA and those of experiment at measuring points across the masonry panel, as expressed by equation (5-1), and normally at failure load level. They subsequently work by revising the flexural stiffness matrix or strength matrix as equations (5-2) and (5-3) show,

$$\{\Psi I\} = \left\{ \frac{\omega_{FEA}^{0}}{\omega_{EXP}} \right\} \qquad (5\text{-}1)$$

$$\{D_1\} = \{D_0\} * \{\Psi_1\} \qquad (5\text{-}2)$$

$$\{f_1\} = \{f_0\} * \{\Psi_1\} \qquad (5\text{-}3)$$

Here,

{ΨI}: corrector factors.

$\{D0\}$: the smeared rigidity of masonry panels. In this research $\{D0\}$ =12kN/mm² is used

as Zhou(2002) and Chong(1993) did.

$\{f0\}$: the smeared flexural strength of masonry panels either perpendicular (fx) or

parallel (fy) to the bed joint. In this research $\{fx_0\}$ =2.28N/mm² , $\{fy_0\}$

=0.965N/mm² is used as Zhou(2002) and Chong(1993) did

ω^{0}_{FEA} : deflections of FEA using $\{D0\}$. ω_{EXP} : experimental deflections.

The obtained new flexural stiffness $D1$ is used for improving the analysis; the improved

deflections of the FEA is obtained and denoted as ω^{1}_{FEA} .

This is the definition of corrector factors given by Zhou (2002) and Rafiq, *et al.*(2003)and the way they work.

Now regard ω^{1}_{FEA} as ω^{0}_{FEA} , $\{D_1\}$ as $\{D_0\}$ and $\{f_1\}$ as $\{f_0\}$, then using equations

(5-1) , (5-2) again, new corrector factors can be obtained as shown in (5-4), and make

further revision to flexural stiffness or strength as (5-5) and (5-6) show to get further

improvements:

$$\{\Psi_2\}= \{\frac{\omega^{1}_{FEA}}{\omega_{EXP}}\} \qquad\qquad (5\text{-}4)$$

$$\{D_2\} = \{D_1\}*\{\Psi_2\} \qquad\qquad (5\text{-}5)$$

$$\{f_2\} = \{f_1\}*\{\Psi_2\} \qquad\qquad (5\text{-}6)$$

Where : Ψ_2 is the new corrector factor obtained using the definition of corrector factors

the second time; the corresponding improved deflections are denoted as ω^{2}_{FEA} , which

can be once more used to derive new corrector factors Ψ_3 for further improvement.

More generally, by using the definition of corrector factors as show by equation (5-4) for i times, the obtained corrector factors $\{\Psi i\}$ can be expressed by equation (5-7), which is used to revised flexural stiffness matrix and strength matrix as shown by equation (5-8) and (5-9) to get the much improved ω^i_{FEA}. The whole procedure is an iteration process.

$$\{\Psi_i\} = \{\frac{\omega^{i-1}_{FEA}}{\omega_{EXP}}\} \quad\quad\quad\quad (5\text{-}7)$$

$$\{D_i\}=\{D_{(i-1)}\}*\{\Psi_i\} \quad\quad\quad\quad (5\text{-}8)$$

$$\{f_i\} = \{f_{(i-1)}\}*\{\Psi_i\} \quad\quad\quad\quad (5\text{-}9)$$

$i=1, 2, 3...$ is the number of iterations.

It is intended that with enough iterations, the corrector factors would tend to converge to a set of values, and the difference between analytical and experimental results are minimised.

Moreover, equation (5-2) means that, those corrector factor values bigger than 1 increase the flexural stiffness values and those smaller than 1 decrease the flexural stiffness value. To facilitate the convergence, a power m is introduced in equations (5-8) and (5-9) to make a smaller revision to the flexural stiffness. The equations become as shown in equation (5-10) and (5-11).

$$\{D_i\} = \{D_{(i-1)}\}*\{\Psi_i^{\,m}\} \quad\quad\quad\quad (5\text{-}10)$$

$$\{f_i\} = \{f_{(i-1)}\}*\{\Psi_i^{\,m}\} \quad\quad\quad\quad (5\text{-}11)$$

Obviously, if $m=0$, there would be no revision because all corrector factors would become 1. $m < 1$ is the revision with smaller steps; $m=1$ is the case of simple iteration

using (5-8) and (5-9). If m >1, the revision is in the enlarged steps, which is not helpful for convergence and will not be involved in this study.

5.3 ITERATIONS TO REVISE FLEXURAL STIFFNESS

By keeping the flexural strength *{fx}* and *{fy}* unchanged, but only revising the smeared flexural stiffness *{D}* in iterations using equation (5-7) and equation (5-10), iterations are implemented to find new corrector factors. The failure deflections of FEA and the corresponding experimental deflections are used in the implementation and the results are discussed as follows:

1. When *m=1*, the load deflection relationships under iteration are shown in Figure 5.1. It is seen that, the load deflection relationships almost converge to the experimental one. However, the obtained failure load is far smaller than the experimental one, which means equation (5-7), (5-8), (5-9) are not suitable for deriving corrector factors that comprehensively improve the FEA model, although some improvements could be obtained by some of the iterations

2. While 0<*m*<1, the load deflection relationships by iteration are shown in Figure 5.2. It is seen that, most load deflection relationships obtained by iteration are still very similar to what is presented in Figure 5.1, iteration make the deflections converge to the experimental deflections, but the failure load still decreases. However, there are several iterations which make some improvements simultaneously on both the deflections and the failure load, compared with those using corrector factors proposed by Rafiq, *et al.*(2003). This finding means that, iteration method can derive the corrector factors that make further improvement to the FEA model.
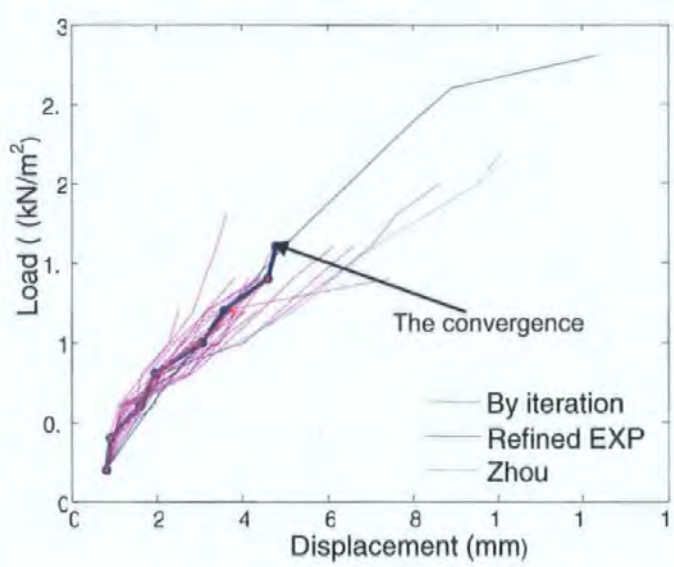
Figure 5.1 Using corrector factors by iterations to revise stiffness (m=1,i=1-50)
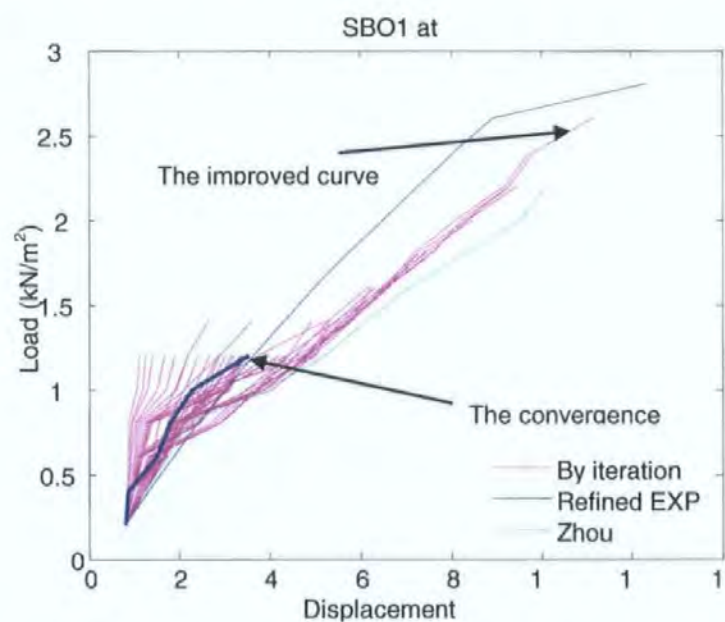
Figure 5.2 Using corrector factors by iterations to revise stiffness (m=0.3,i=1-50)

The derived corrector factors that are able to improve both the analysis to failure load

and deflections are presented in Table 5.1, Figure 5.3, 5.4. From Table 5.1, Figure 5.3

and 5.4, it can be seen that the values and the distributions of all the obtained corrector

factors by different *m* and *i* values are almost the same to each other. Moreover,

comparing Table 5.1 with Table 3.1, or comparing Figure 5.4 with Figure 3.8, it also

can be seen that the obtained corrector factors appear the same distribution to those suggested by Zhou.

The corresponding load deflection relationships presented in Figure 5.5 reveals that both the failure load and deflections by FEA are improved compared to those of using the corrector factors proposed by Zhou in Table 3.1.

However, Figure 5.5 shows that bigger discrepancy still exists between FEA and the experimental ones. Moreover, it has been found that, other corrector factors with similar values but beyond those listed in Table 5.3 are not able to improve the FEA, which means the obtained corrector factors are just scattered in that domain, which means a further investigation to corrector factors should be carried out.

Table 5.1 the improved corrector factors by iteration

m=0.28 i=1	X1	X2	X3	X4	X5	X6	X7	X8	X9
Y4	0.88	1.04	1.05	1.05	1.05	1.05	1.05	1.04	0.88
Y3	0.82	0.97	0.98	0.99	0.99	0.99	0.98	0.97	0.82
Y2	0.77	0.99	1.01	1.01	1.01	1.01	1.01	0.99	0.77
Y1	0.73	1.02	1.05	1.06	1.06	1.06	1.05	1.02	0.73
m=0.26,i=1	X1	X2	X3	X4	X5	X6	X7	X8	X9
Y4	0.89	1.04	1.05	1.05	1.05	1.05	1.05	1.04	0.89
Y3	0.84	0.98	0.99	0.99	0.99	0.99	0.99	0.98	0.84
Y2	0.8	0.99	1.01	1.01	1.01	1.01	1.01	0.99	0.8
Y1	0.75	1.02	1.05	1.06	1.06	1.06	1.05	1.02	0.75
m=0.23,i=1	X1	X2	X3	X4	X5	X6	X7	X8	X9
Y4	0.9	1.03	1.04	1.04	1.04	1.04	1.04	1.03	0.9
Y3	0.84	0.98	0.99	0.99	0.99	0.99	0.99	0.98	0.84
Y2	0.82	0.99	1.01	1.01	1.01	1.01	1.01	0.99	0.82
Y1	0.77	1.01	1.04	1.05	1.05	1.05	1.04	1.01	0.77
m=0.06,i=3	X1	X2	X3	X4	X5	X6	X7	X8	X9
Y4	0.91	1.02	1.03	1.03	1.03	1.03	1.03	1.02	0.91
Y3	0.88	0.97	0.97	0.97	0.97	0.97	0.97	0.97	0.88
Y2	0.84	0.98	1.0	1.0	1.0	1.0	1.0	0.98	0.84
Y1	0.79	1.0	1.03	1.03	1.03	1.03	1.03	1.0	0.79

Note: X1... X5 and Y1... Y4 are zone divisions (see Figure 3.7)
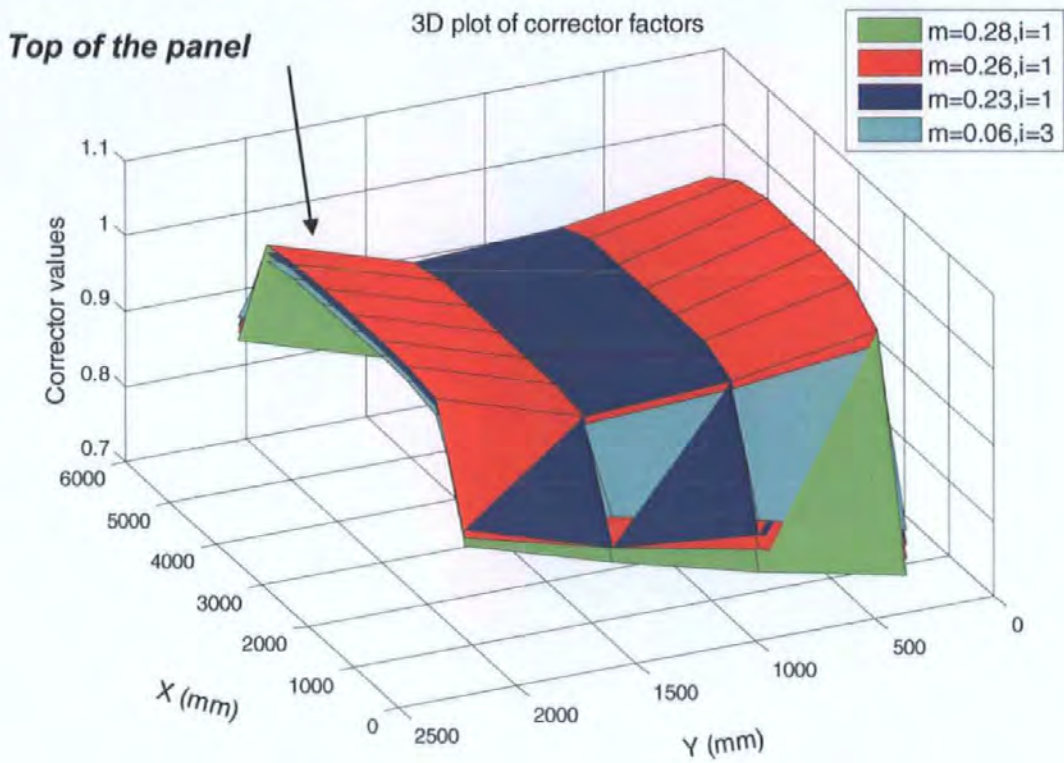
Figure 5.3 the improved corrector factors by iteration
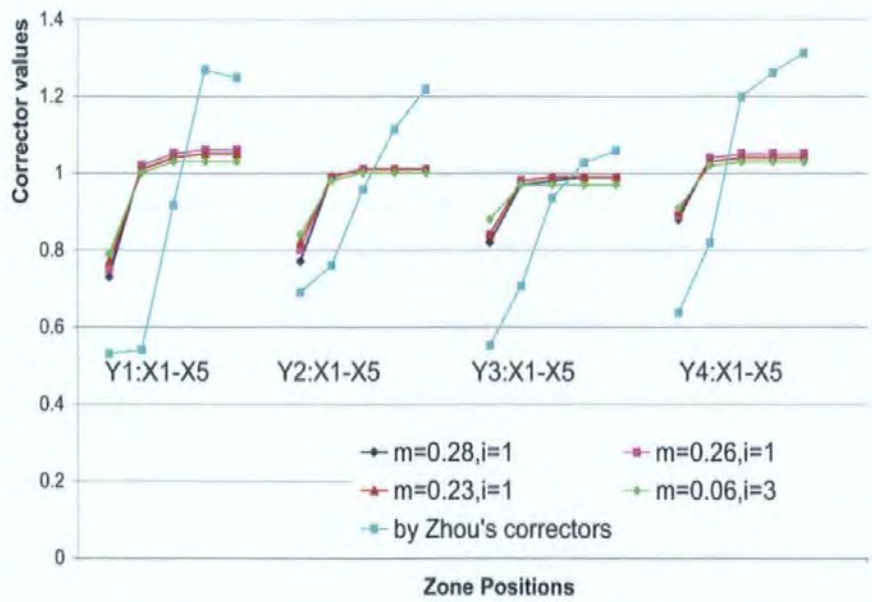
Figure 5.4 Comparing the improved corrector factor with those of Zhou (Left Half Panel)
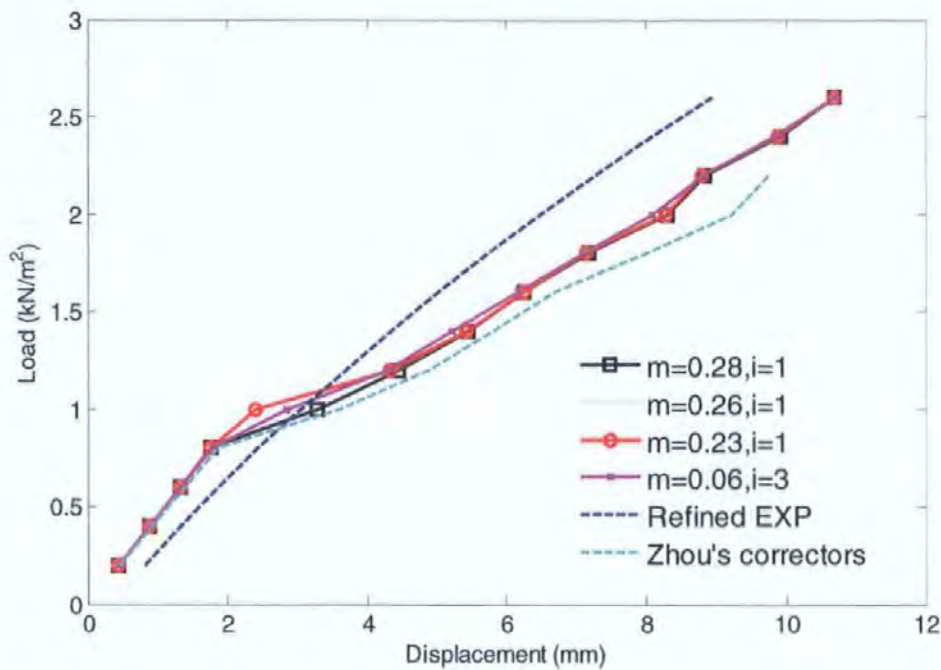
Figure 5.5 The effect of using the improved corrector factors (revising stiffness E)

5.4 ITERATIONS TO REVISE STRENGTH

5.4.1 Revising flexural strength parallel to the bed joints fx

Similar to the study in section 5.3, iterations are used again to find the new corrector factors for revising the smeared flexural stiffness $\{fx\}$. The equation (5-7) and equation (5-11) are used and the flexural stiffness D and flexural strength $\{fy\}$ are kept unchanged. The implementation of the iteration is presented in Figure 5.6.

Figure 5.6 reveals that, using the correctors obtained by iteration to revise the flexural strength parallel to bed joints of masonry panel (fx) cannot improve the deflections and failure load.
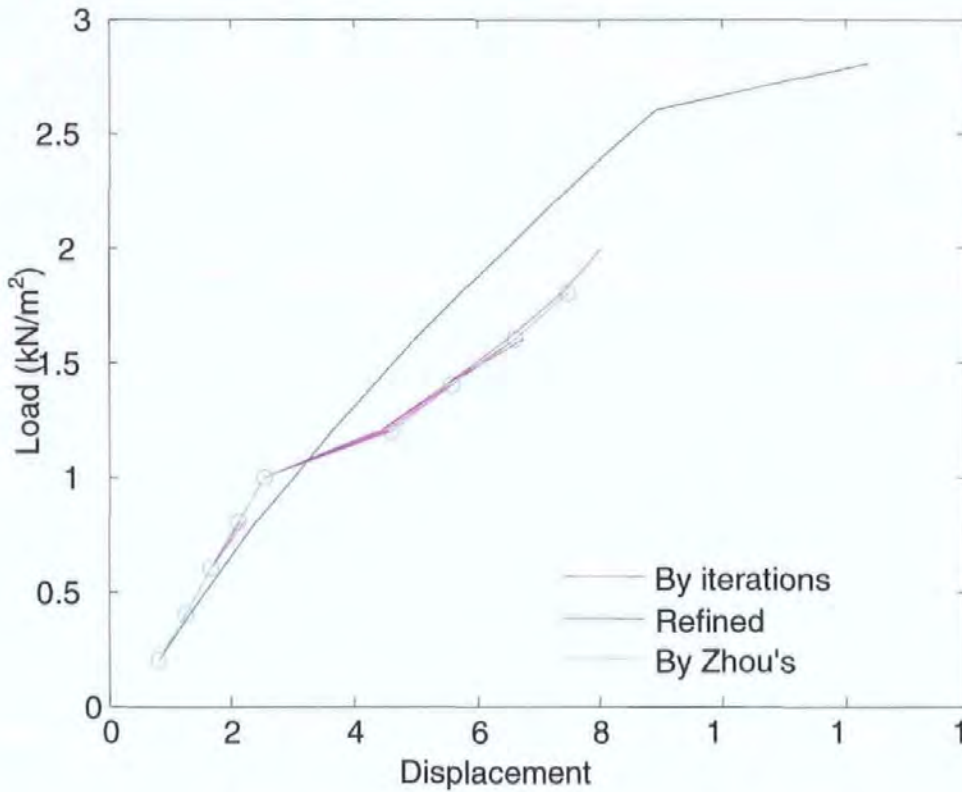
Figure 5.6 Using corrector factors by iteration to revise strength fx

5.4.2 Revising flexural strength perpendicular to the bed joints fy

By keeping the flexural stiffness **D** and flexural strength *{fx}* unchanged and changing smeared flexural strength *{fy}* and using equation (5-7) and equation (5-11), a number of iterations are implemented again to find new corrector factors. It has been found that, when $0<m\leq1$, the failure deflections and the failure load are almost not changed (see Figure 5.7).

5.4.3 Revising flexural strength both perpendicular and parallel to the bed joints

By keeping the flexural stiffness **D** unchanged, changing smeared flexural stiffness *{fx}* and *{fy}* simultaneously and using equation (5-7) and equation (5-11), a number of iterations are used again to investigate the new corrector factors. The failure deflections

from FEA and those of experiment at the corresponding failure load level of FEA are used in the implementation. Typical results are shown in Figure 5.8.

It could be seen that, when revising fx and fy and keeping $0<m\leq1$, all corrector factors derived by iteration are not able to improve the deflections and the failure load, they appear more irregular.
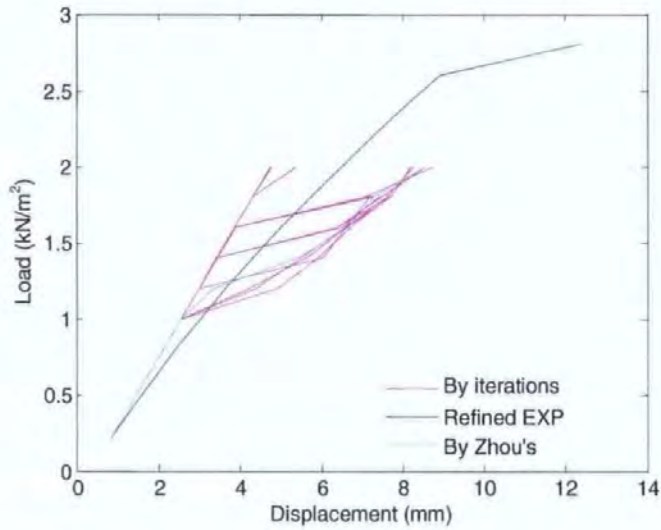
Figure 5.7 Using corrector factors by iteration to revise strength fx
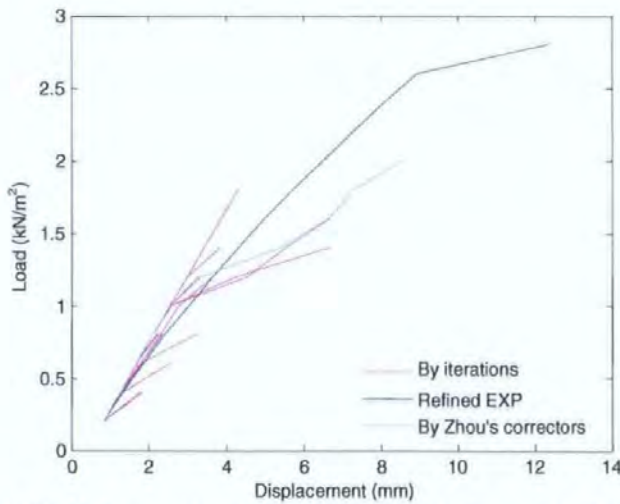
Figure 5.8 Using corrector factors by iteration to revise strength fy

5.5 SUMMARY

From the investigations in this chapter, it can be concluded that, repeating the definition of corrector factors suggested by Zhou(2002) and revising the flexural stiffness E in zones, both failure load and failure deflections can be improved compare with using those corrector factors suggested by Zhou. However, further improvements are not available by revising flexural strength. This conclusion means that the definition of corrector factors is only a revision based on the summary of experiments but not based on numerical computations in a theoretical way.

Corrector factors work in the way that, they revise the input data of FEA to make the load deflection relationships to approach to those of experiments, therefore, the way of obtaining corrector factors becomes how to decrease the discrepancy between FEA and experiment, which is the process of model updating, which will be introduced in the following chapters.

6. PARAMETER ANALYSES ON THE FEA MODEL

6.1 INTRODUCTION

In Chapter 5, it was concluded that, simply repeating the definition of corrector factors given by Zhou(2002)and Rafiq, *et al.*(2003) could not dramatically improve the FEA model. Therefore, further study should be carried out as will be introduced in this chapter.

The concept of corrector factors proposed by Zhou(2002) and Rafiq, *et al.*(2003) is to revise parameter values for the purpose of improving the FEA model, which in fact is a kind of model updating procedure (Brownjohn 2001). Therefore, from this chapter, the study to corrector factors will be carried out in the way of model updating.

As have been reviewed in Chapter 2, model updating techniques arisen in 1990s (Dascotte 1991, Friswell and Mottershead 1995) are widely used for model calibration, parameterization and damage detection and diagnosis. It becomes an effective way to analyse and revise the error of the model (Atalla 1996); model updating process aims to minimise the discrepancy between experiment and FEA by changing the values of model parameters, this procedure is normally completed through optimisation. Although most cases of model updating are applied to vibration frequencies in dynamic test, there are cases of using static deflections (Sanayei and Onipede 1991, Hjelmsad and Shin 1997, Sanayei,et.al. 1997, Chen 2005).

When carrying out a finite element analysis, it is important to consider three kinds of modelling errors (Friswell and Mottershead 1995): (a) model parameter errors, which would typically include the application of improper boundary conditions and inaccurate assumptions used in order to simplify the model. (b) Model order errors, which arise in the discretization of complex system and can result in a model of insufficient order. (c)

Model structural errors are liable when there is an uncertainty concerning the governing equations—such error might occur typically in the modelling of neurophysiologic process and strongly non-linear behaviour in certain engineering systems. What is concerned in this paper is dealing with model parameter errors.

Model updating is processed by optimisation but it is more than optimisation itself, it requires a understanding of the exiting model so as to choose proper parameters for updating and to minimise the underlying modelling errors (Sinha and Freswell 2002). Once the model is fully understood, the objective function needs to be formulated aiming to express the errors between the experimental and the analytical results, and then minimise it using optimisation techniques.

In this chapter, the FEA model is analysed to clarify how the FEA model is influenced by changing the parameters, and thereby to determine which parameters should be revised by corrector factors, this is the parameter analysis. In the study, parameters such as flexural stiffness E, flexural strength fx and fy, Poisson's ratio v in the FEA are involved.

6.2 METHOD OF PARAMETER ANALYSIS

To make model updating, first of all, it is necessary to know which parameter is suitable for the revision because revising different parameters have different effect on the FEA model, such as shown in Figure 6.1 which represents the different load deflection relationships by revising flexural stiffness and strength respectively using the same corrector factors.
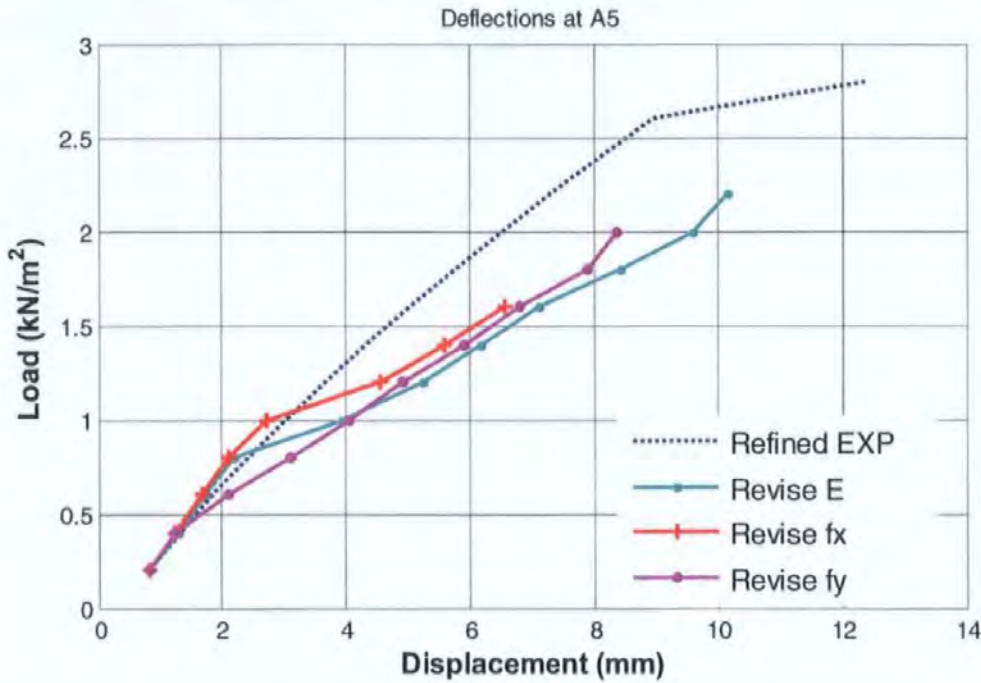
Figure 6.1, comparison of using the same corrector factors to revise different parameters

In this Chapter, parameter analyses, or say sensitivity analyses, are studied using the masonry panel SBO1. This panel is divided into 18 x 8=144 elements, each 4 elements neighboured to each other are combined to one zone, which means there are in total 36 zones on the panel. The following parameters are involved: flexural stiffness E, flexural strength perpendicular and parallel to the bed joints (denoted as fx and fy respectively) and the Poisson ratio v. Therefore, these parameters are investigated for their sensitivity. Since the output of the model includes deflections and failure load, load deflection relationships as shown in Figure. 6.1 are used to express the responses of the model.

In the parameter analyses, elements in a same zone are assigned with the same parameter value. The parameter values are changed around those global smeared values used by Chong which were obtained by Monte Carlo simulation based on experiments; these values are:

E=12kN/mm^2, fx =2.28N/mm^2,

fy =0.965N/mm^2, v =0.2.

When changing one parameter value, all other parameter values are kept unchanged. In this study, two ways of changing the parameter value are used; i.e. two kinds of models are used for parametric study:

- Smear model: Smear model mean that, whilst changing one parameter, the changed parameter values in all zones are the same, i.e. zones are always assigned with a equally revised parameter values.

- Updating model: updating model means that, whilst changing one parameter, the changed parameter values in all zones are different; i.e. parameter are changed in this way: a number of random parameter values are generated by computer and assigned to all zones, the assigned parameter values in zones are different.

6.3 PARAMETER ANALYSIS WITH SMEARED MODEL

In the smeared model, the same parameter value is assigned to all zones. Stiffness E, flexural strength fx and fy, Poisson's ratio v are investigated.

6.3.1 Changing the stiffness E

To investigate the influence of stiffness E on failure loads and deflections, other parameters are kept to be unchanged (fx = 2.28N/mm^2, fy=0.965N/mm^2, v=0.2), the changed stiffness E value is assigned to all zones of the panel in each case. The change of stiffness E is from 6kN/mm^2 to 18kN/mm^2. Result of this investigation is presented in Figure 6.2. From Figure 6.2, it is clear that, in the smeared model, changing stiffness E affects deflections but has little influence on failure load.
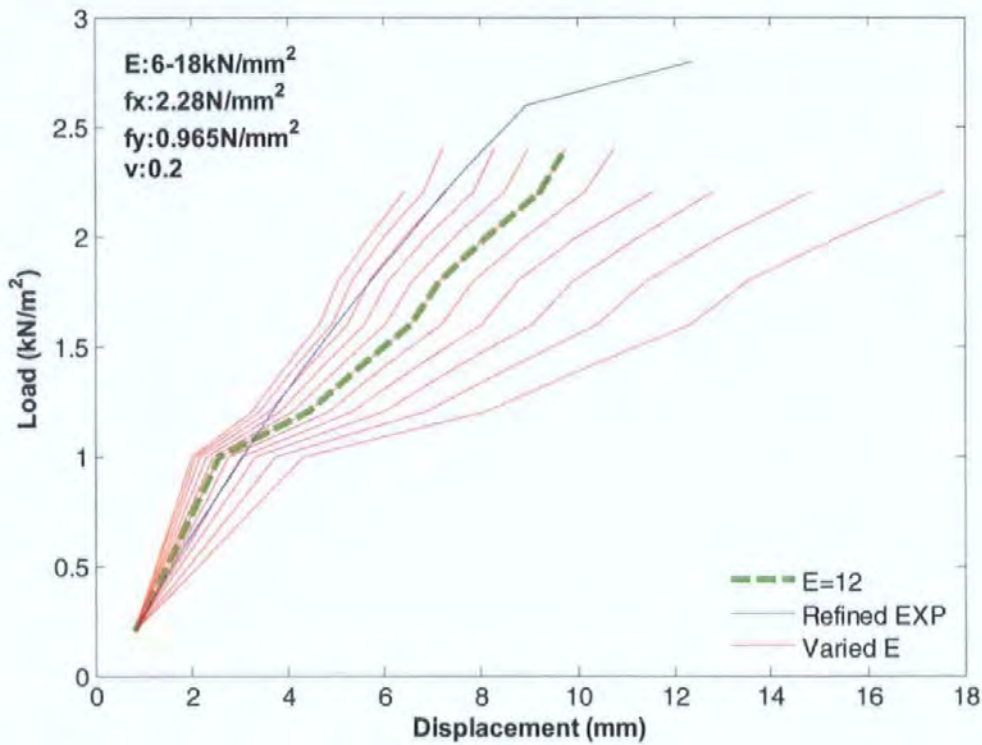
Figure 6.2 Failure load and deflections by changing smeared stiffness *E*

6.3.2 Changing the strength parallel to the bed joints *fx*

The flexural strength parallel to the bed joints fx is another main parameter of the model, fx is changed in the range from 1.14 N/mm^2 to 5.70 N/mm^2 and other parameters are kept unchanged (E=12kN/mm^2, fy=0.965N/mm^2, v=0.2). The result of this investigation is presented in Figure 6.3. Figure 6.3 clearly shows that fx only affects the failure load but has not influence on deflections.
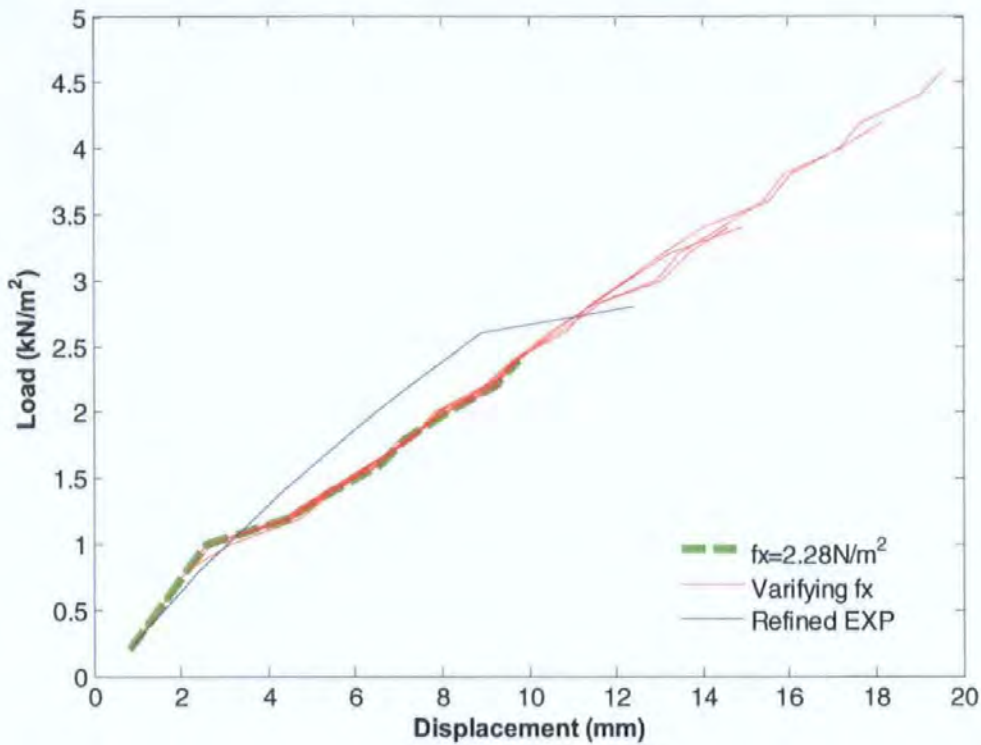
Figure 6.3 Failure load and deflections by changing smeared fx

6.3.3 Changing the flexural strength perpendicular to the bed joints fy

When fy is changed in the range from 0.483 N/mm^2 to 2.413 N/mm^2 and other parameters are kept unchanged (E=12kN/mm^2, fx=2.28kN/mm^2, v=0.2). The corresponding failure load and deflections are shown in Figure 6.4.

It can be seen that, the length of the straight-line of the load deflection relationships changes, but the slope of the straight-line is still the same and the failure deflections are similar. Figure 6.4 reveals that fy affects the position of the 'kink', but has little influence on failure load. The physical meaning of the 'kink' will be investigated in section 6.5.
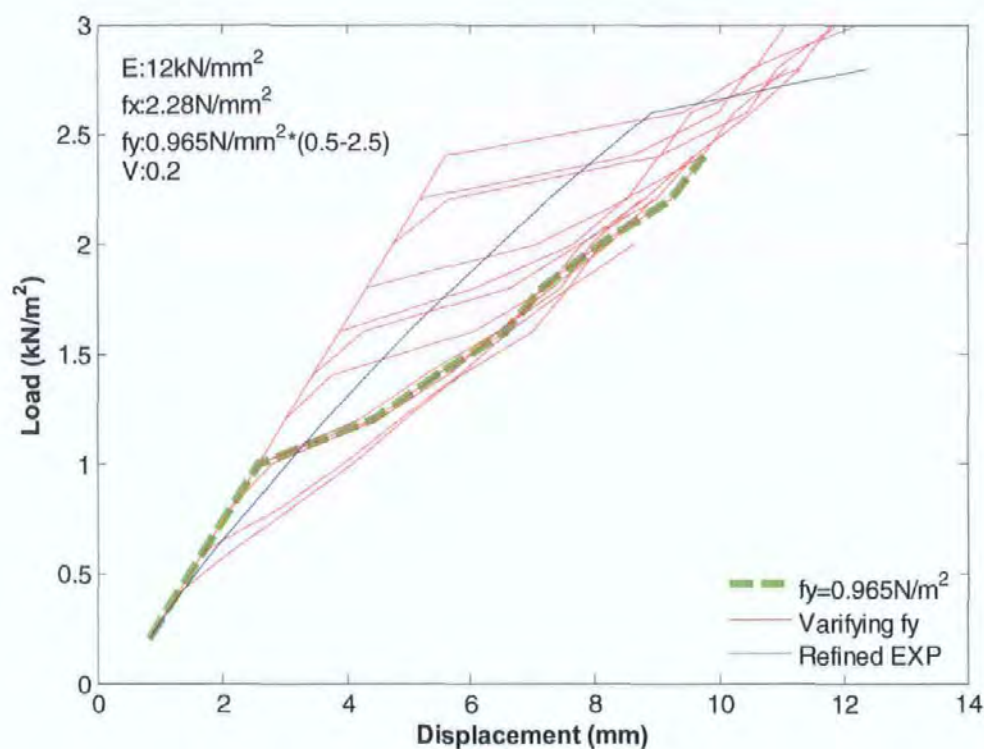
Figure 6.4 The failure load and deflections by changing smeared fy

6.3.4 Changing the Poisson's ratio v

Poisson's ratio v is changed from 0.1 to 0.4 while keeping other parameters unchanged (E=12kN/mm^2, fx=2.28N/mm^2,fy=0.965N/mm^2). The result of this investigation is presented in Figure 6.5. It is clear that load deflection relationships are almost unchanged, which means changing v has a little influence on the load deflection relationships.

From the investigation in this section, it can be argued that, changing the stiffness E mainly affects the deflections as expected but makes little influence on failure load. Changing the flexural strength fx is more affects failure load as expected but has less influence on deflections. Changing the flexural strength fy mainly changes the position of the 'kink' point. Poisson's ratio v has little influence on both failure load and the deflections.
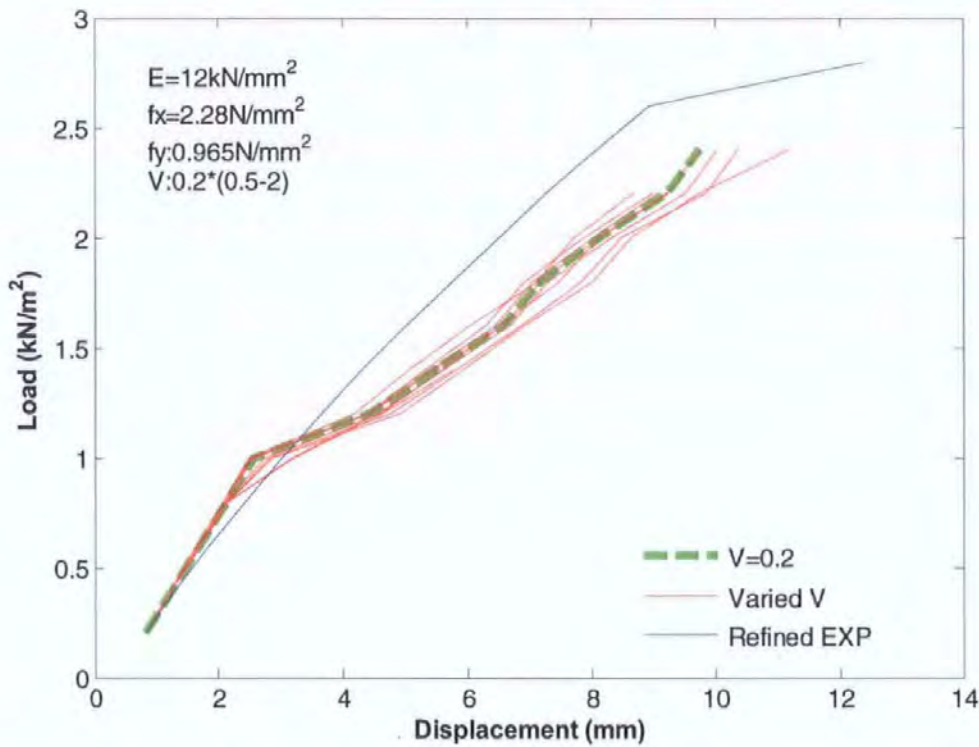
Figure 6.5 The failure load and deflections by changing smeared v

6.4 PARAMETER ANALYSIS WITH UPDATING MODEL

In this section, parameter values that randomly scattered in a specific range are assigned to different zones. Cases of changing the stiffness E, the flexural strength fx and fy and Poisson's ratio v are investigated separately.

6.4.1 Randomly assign stiffness E to different zones

Here parameter values are changed in a way that, a group of randomly generated stiffness E values ranging from 6 kN/mm^2 to 18 kN/mm^2 are assigned to different zones of the panel while other parameters are kept unchanged ($fx = 2.28$N/mm^2, $fy = 0.965$N/mm^2, v=0.2). Totally 30 groups of random E values are investigated and the results are summarised in Figure 6.6.
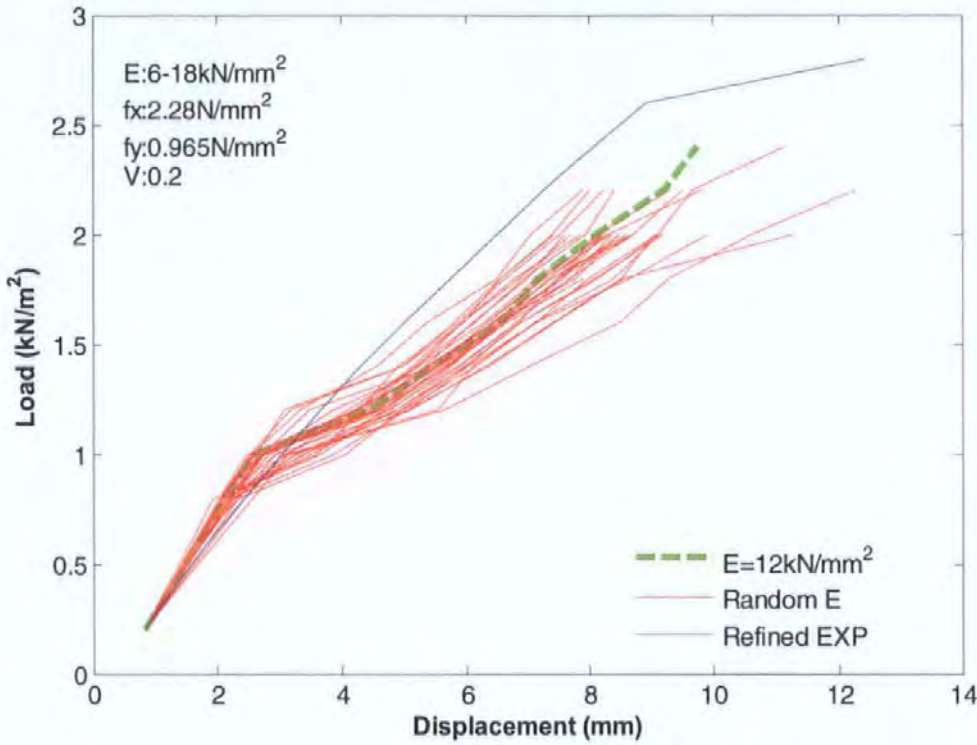
Figure 6.6 The failure load and deflections by assigning random E

From Figure 6.6, it can be concluded that stiffness E has a little influence on failure load but much effects on deflections; this conclusion is the same as what had been drawn from Figure 6.2. However, if carefully compare Figure 6.6 with 6.2, two differences are found. Firstly, in Figure 6.2, deflections vary in a larger range, but in Figure 6.6, deflections are scattered in a comparatively smaller range; secondly, the position of the "kink" in Figure 6.6 have changed but those in Figure 6.2 do not change. This difference indicates that the updating model is flexible and more suitable for analysing masonry.

6.4.2 Randomly assigned flexural strength *fx* to different zones

In this investigation, a group of randomly generated fx values scattered in the range from 1.14N/mm^2 to 5.7 kN/mm^2 are assigned to zones while other parameters are kept unchanged (E=12kN/mm^2, fy=0.965N/mm^2, v=0.2). In total 30 groups of such random fx values are investigated, the results are summarised in Figure 6.7.

From Figure 6.7, it is very clear that assigning *fx* randomly strongly affect the failure

load but have a little influence on deflection, which is quite similar to what can be seen

in Figure 6.3 using a smeared model. However, if carefully compared with Figure 6.3, it

can be seen that in Figure 6.7 some lines change their trace at the higher load level, but

those lines in Figure 6.3 keep unchanged. This difference indicates that the updating

model might be more flexible and suitable to analyse masonry.
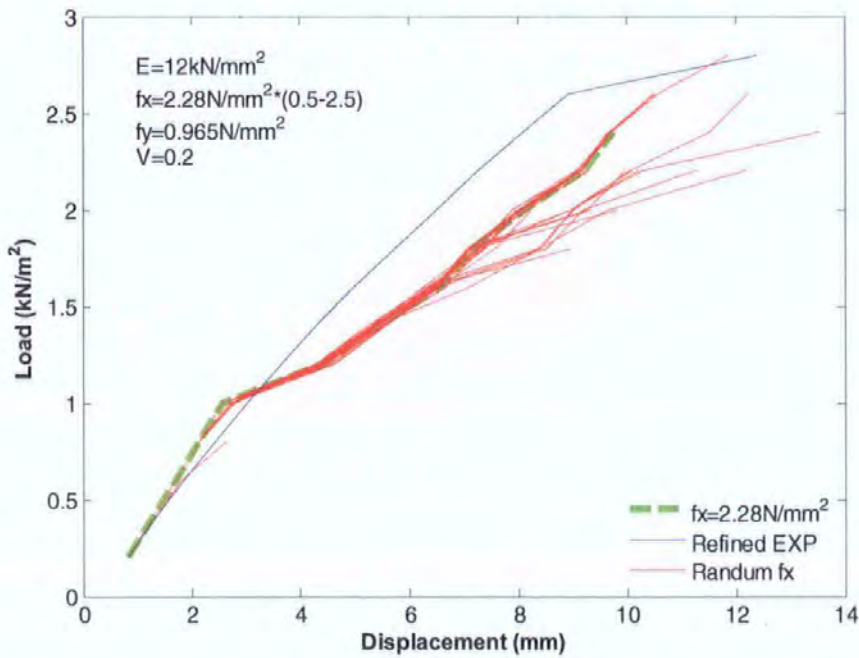
Figure 6.7 the failure load and deflections by assigning random fx

6.4.3 Randomly assigned flexural strength *fy* to different zones

Similarly to the investigation on flexural strength *fx*, here a group of random *fy* values

scattered in the range from 0.483 N/mm^2 to 2.41 N/mm^2 are assigned to the different

zones while other parameters are kept unchanged (E=12kN/mm^2, fx=2.28N/mm^2,

v=0.2). In total 30 groups of these random values are investigated; their results are as

shown in Figure 6.8.

From figure 6.8 it can be seen that, the position of the "kink" is changed, but the slope of the straight line of the load deflection relationships is still the same and the failure deflections are similar. They are quite similar to those in Figure 6.4. However, in Figure 6.8, the kink position has not changed as much as that in Figure 6.4,
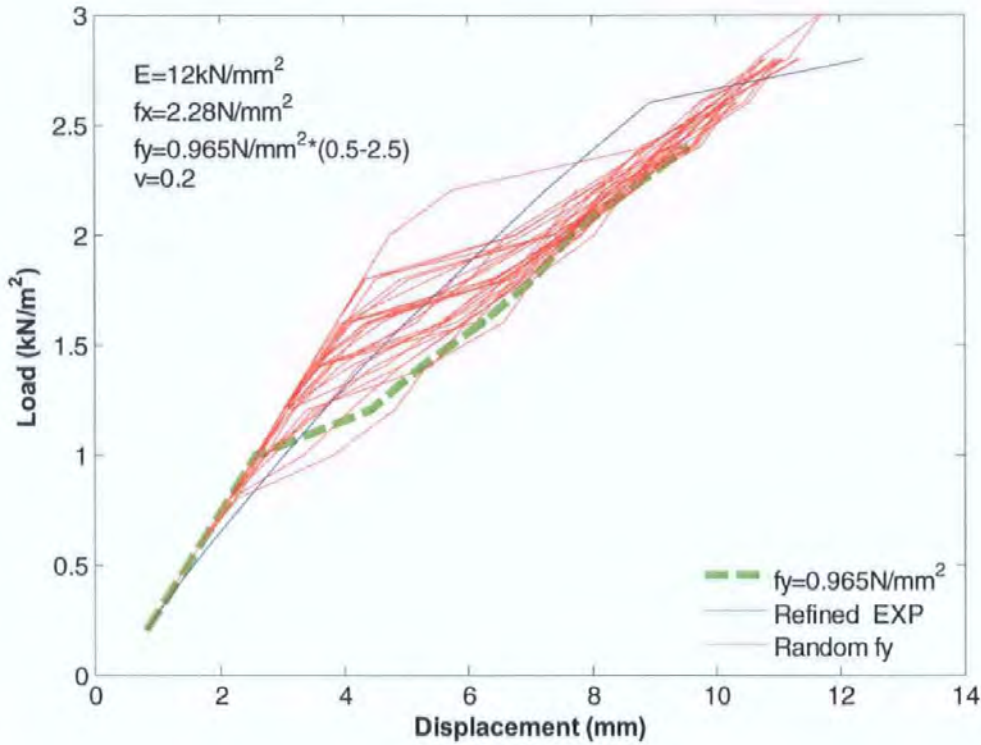
Figure 6.8 The failure load and deflections by assigning random fy

6.4.4 Randomly assigned Poisson's ratio v to different zones

Here again, values of Poisson's ratio scattered between 0.1-0.4 are randomly assigned to the different zones of the panel and in total 30 groups of random values are investigated as shown in Figure 6.9.

Compared to Figure 6.5, it can be seen that the deflection relationships in Figure 6.9 are quite similar to those of Figure 6.5. The deflections and failure load, the positions of the "kink" are almost unchanged. Therefore, it can be concluded that Poisson's ratio has little influence on failure load and deflections.

The conclusions can be drawn from this section are that stiffness E mainly affects deflections and flexural strength fx mainly affects failure load, fy mainly affects the position of the kink and Poisson's ratio v has little influence on both failure load and the deflections. This conclusion is quite similar to what was obtained in section 5.2.
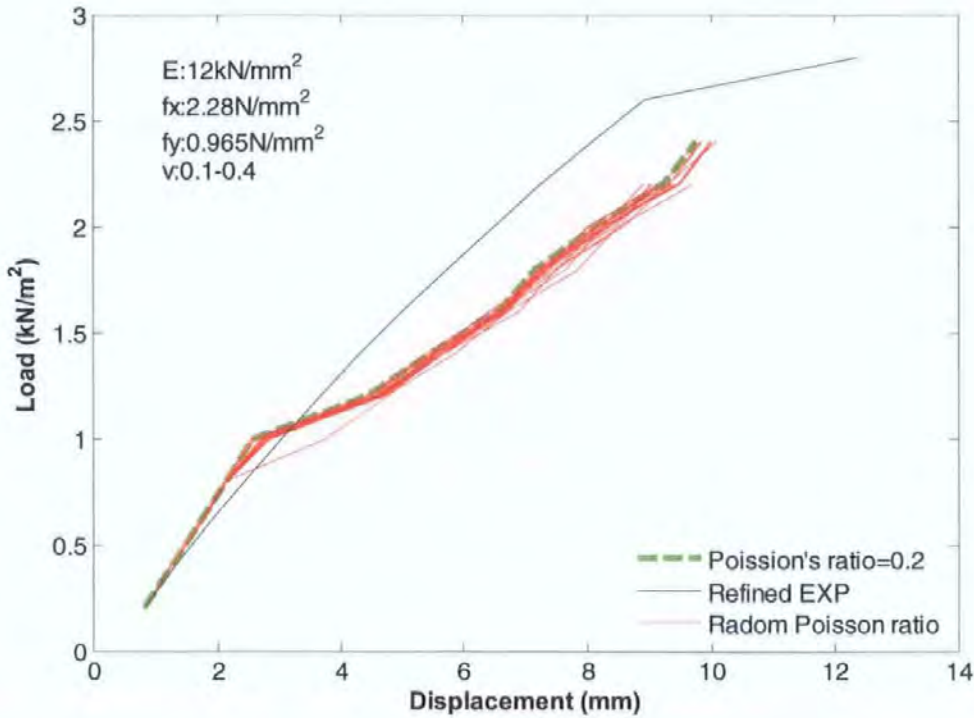
Figure 6.9 the failure load and deflections by assigning random v

6.5 INVESTIGATION OF THE "KINK" ON THE LOAD DEFLECTION RELATIONSHIPS

In Figures 6.2 to 6.9, it can be seen that, at a specific load level, a "kink" appears on the load deflection curves of FEA which represents a sudden decrease in the flexural stiffness of the plate (see also Figure 3.9 for the clear show). However, in the actual experiment, the flexural stiffness changes gradually without a sudden decrease, i.e. there is no an obvious "kink" on the experimental curve. From Figures 6.4 and 6.8, it can be seen that, fy influences the position of 'kink', therefore, it is necessary to clarify what the 'kink' represents and what is the cause of the kink so as to understand the model.

To further clarify the physical meaning of the "kink", fy is changed over a larger range (from 0.965N/m^2 to 3.957 N/m^2), the change of the position of "kink" is shown in Figure 6.10.

From Figure 6.10, it is clear that when fy is very small, the load deflection relationship appears as a strait line of smaller slope with no kink. When fy is increased, the kink appears and it moves upwards on the load deflection curves.

To clarify the physical meaning of the 'kink', the contour plot of stress on the face of panel is explained. It is found that the 'kink' is always accompanied with the first crack on the panel which in this case is due to the hogging moment near the built-in support and on the loaded face of the panel.

Figure 6.11 is the load deflection relationships of SBO1. A 'kink' appears at a load of 1.0kN/m^2. The contour plot of stress in the inner and outer faces at 1.0kN/m^2 and 1.2 kN/m^2 are shown in Figures 6.12, 6.13, 6.14, and 6.15. It is seen that when the load reaches 1.2kN/m^2, the crack appears clearly at the inner bottom face of the panel as expected.

To better show this finding, fy is purposely increased to 3 times and 10 times, and the corresponding load deflection relationships is presented in Figure 6.16. From Figure 6.16 it can be seen that when increasing fy by 3 times, there is a kink at 2.8kN/m^2 and the panel failed at 3.4 kN/m^2; the failure patterns around 2.8kN/m^2 and at 3.4kN/m^2 are shown in Figure 6.17 to Figure 6.22. From Figure 6.18 and 6.20, it can be seen that the inner bottom support is cracking, and at 3.4 kN/m^2, the outer face cracked at 3.4 kN/m^2 as Figure 6.21 shows.
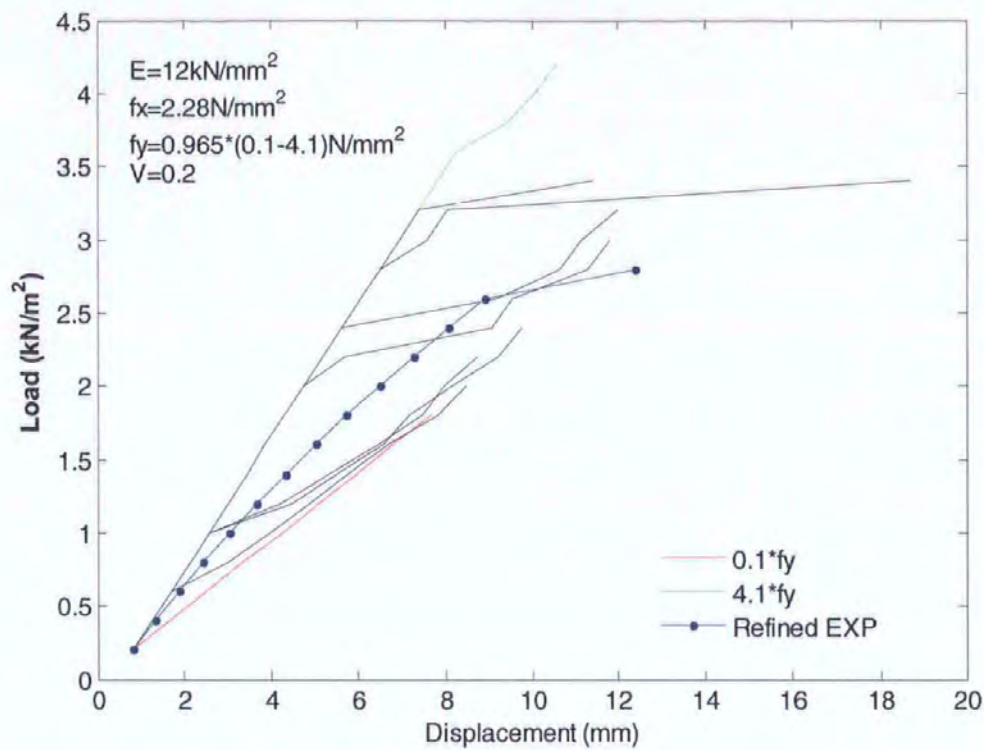
Figure 6.10 "kink" moves with the change of fy
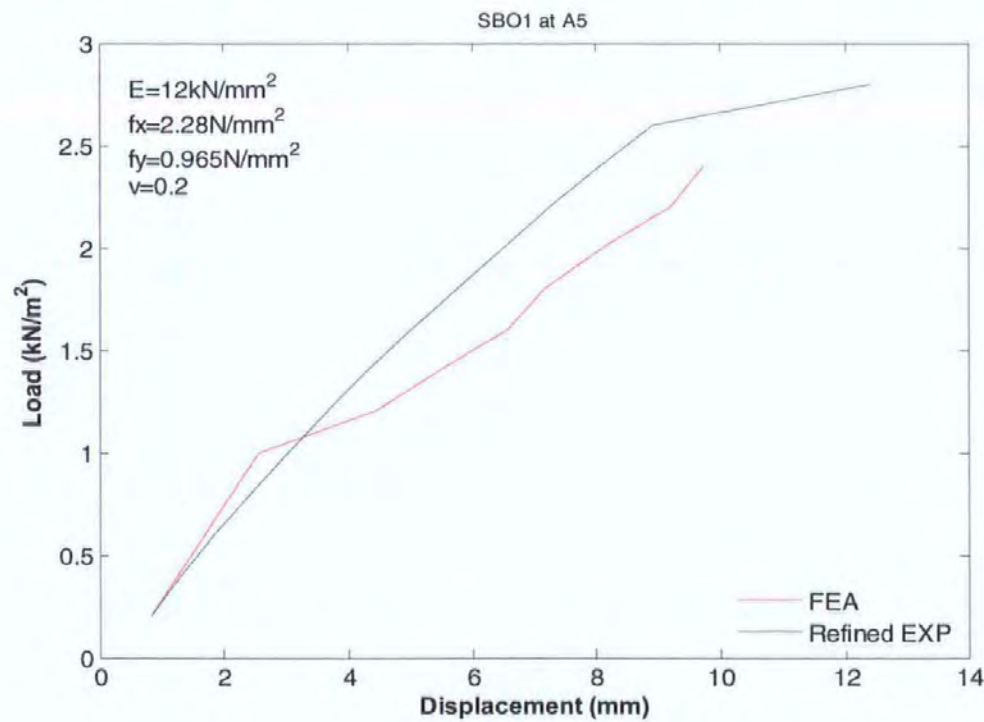
Figure 6.11 load-deflection relationships of FEA

Principal stress contour plot at the outer surface at laterally loading of 1.0 KN/m^2

Tends to Crack
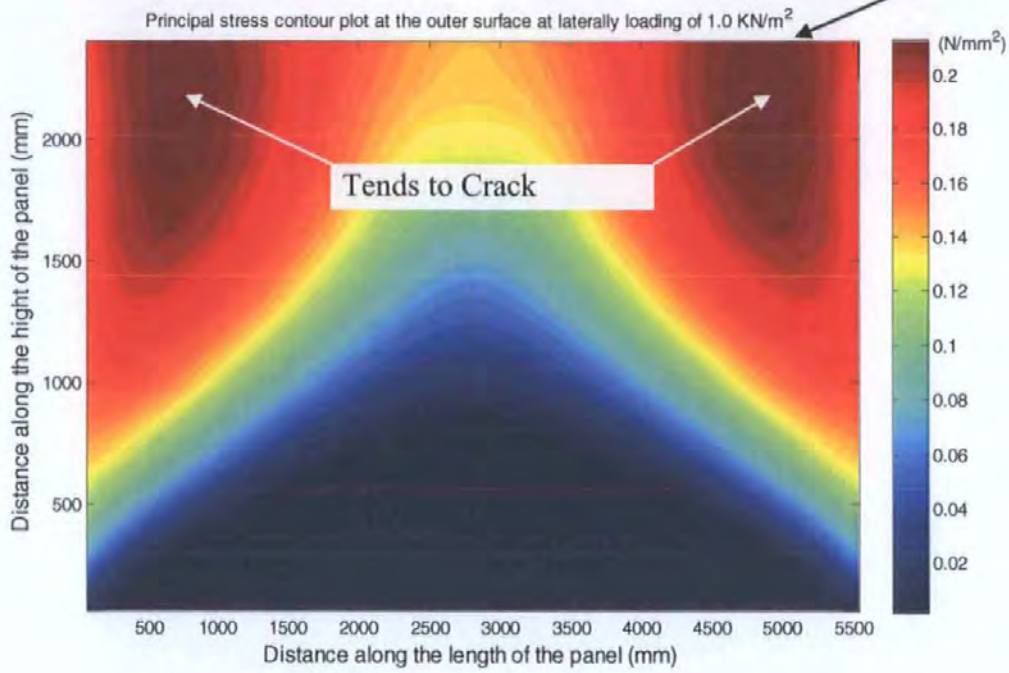
Figure 6.12, Failure pattern of outer face at 1.0kN/m^2

The top of the panel

Principal stress contour on the inner surface at laterally loading of 1.0 KN/m^2

About to Crack
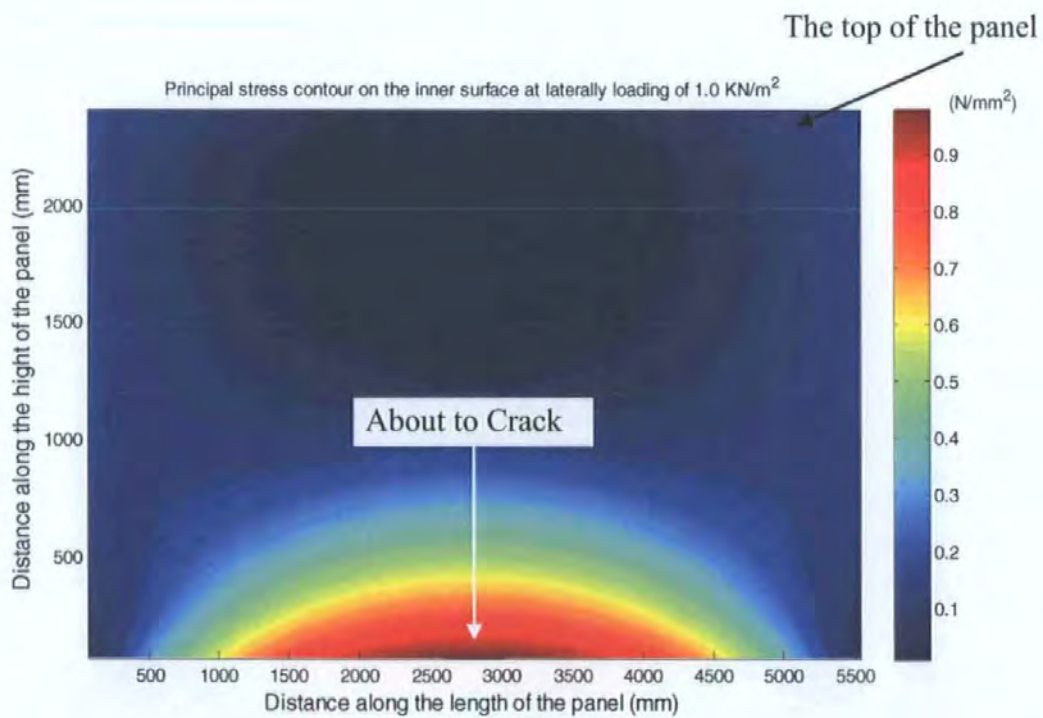
Figure 6.13, Failure pattern of inner face at 1.0kN/m2

The top of the panel
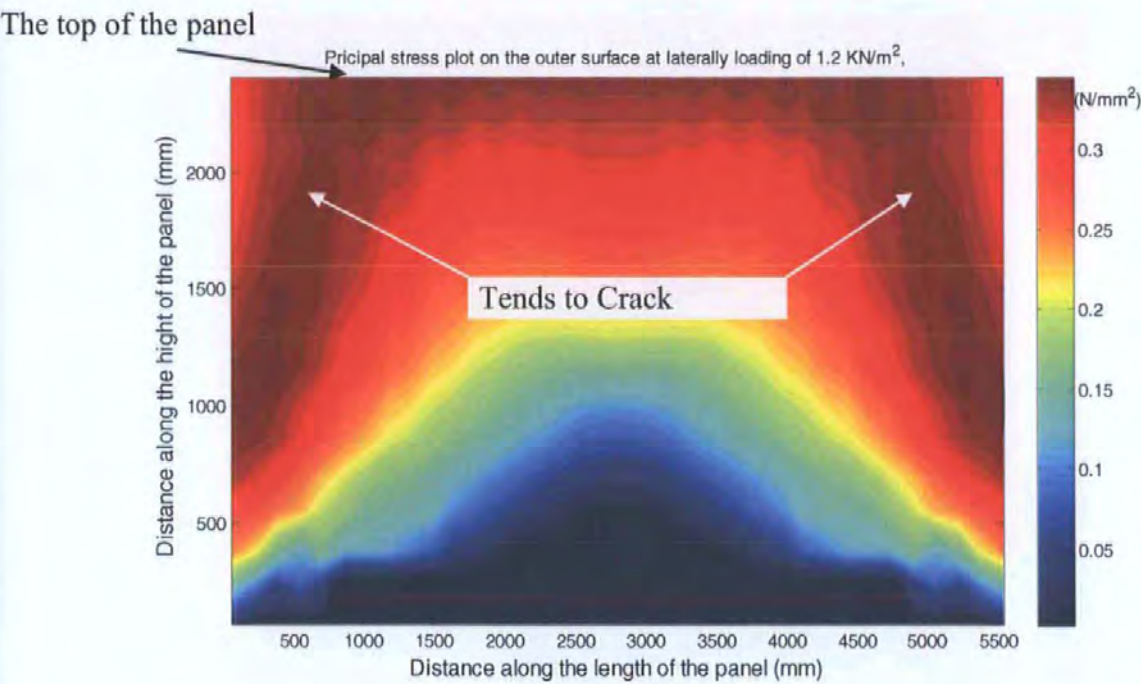
Figure 6.14, Failure pattern of outer face at 1.2kN/m^2

The top of the panel
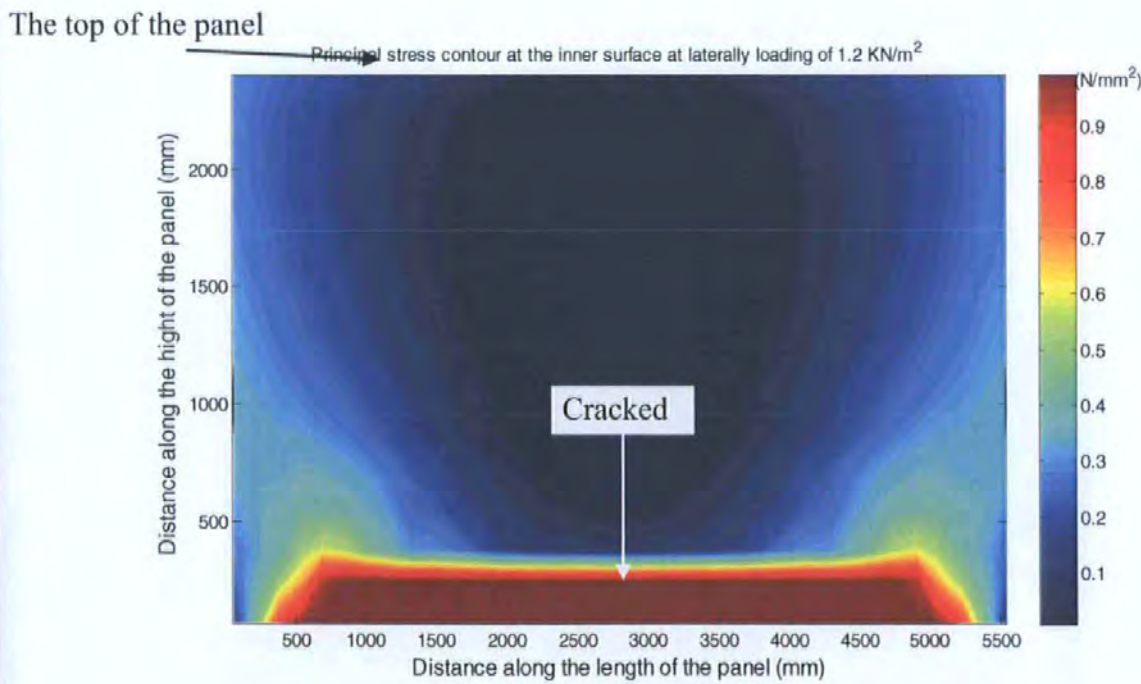
Figure 6.15, Failure pattern of inner face at 1.2kN/m^2

When fy is increased 10 times, the kink occurs and appears at 7.2kN/m^2 and failed at 8.0kN/m^2 as shown in Figure 6.16. The contour plots of the stress on its inner and outer

faces are shown in Figure 6.23 to Figure 6.28. It can be seen that, the outer surface is about to crack at $7.0kN/m^2$ and cracks at $7.2kN/m^2$ as shown in Figure 6.23 and 6.25 respectively and the outer face cracks first rather than the inner face. The inner surface cracks first rather than the out surface only happens when fy is comparatively quite small such as shown in Figures 6.19, 6.20. This is because the boundary conditions of SBO1 are that the two vertical edges are simply supported and the bottom edge is built-in and the top edge is free. When fy is small, the panel first cracks along the direction parallel to the bed joints at the bottom of the inner side due to hogging moments at this region. However, when fy is bigger, say 10 times larger, the panel would first crack along the vertical direction (perpendicular to bed joint) at the outer face.
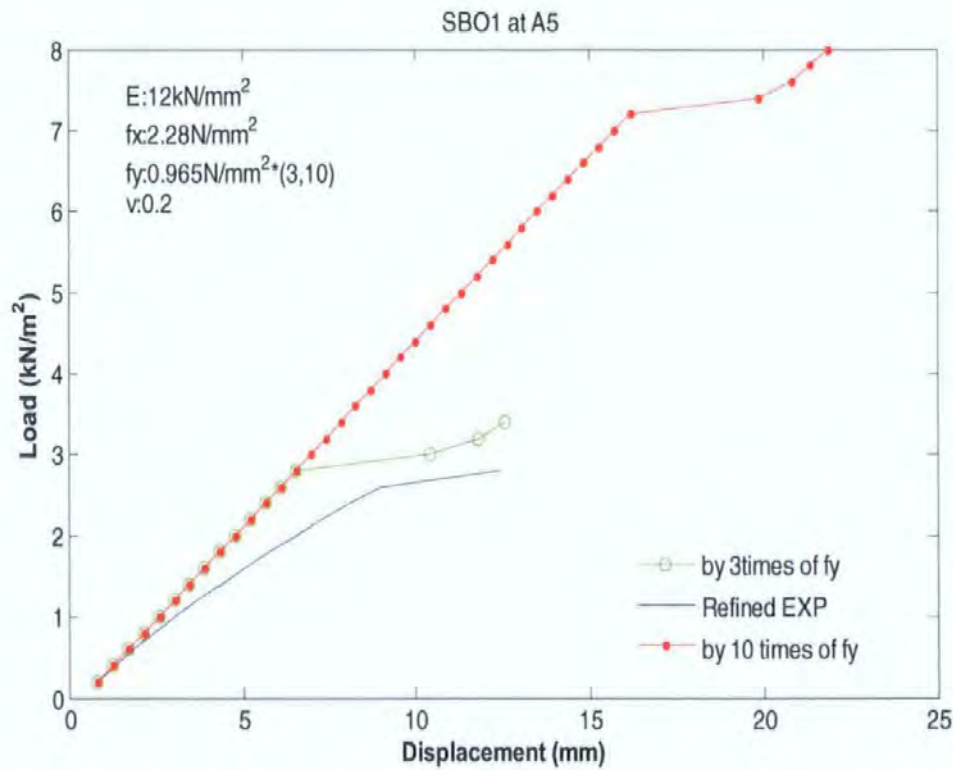
Figure 6.16 Load deflection relationships by increasing fy

Principal stress contour on the outer surface at laterally loading of 2.8 KN/m²,   (N/mm²)

Tends to Crack

Distance along the hight of the panel (mm)

Distance along the length of the panel (mm)
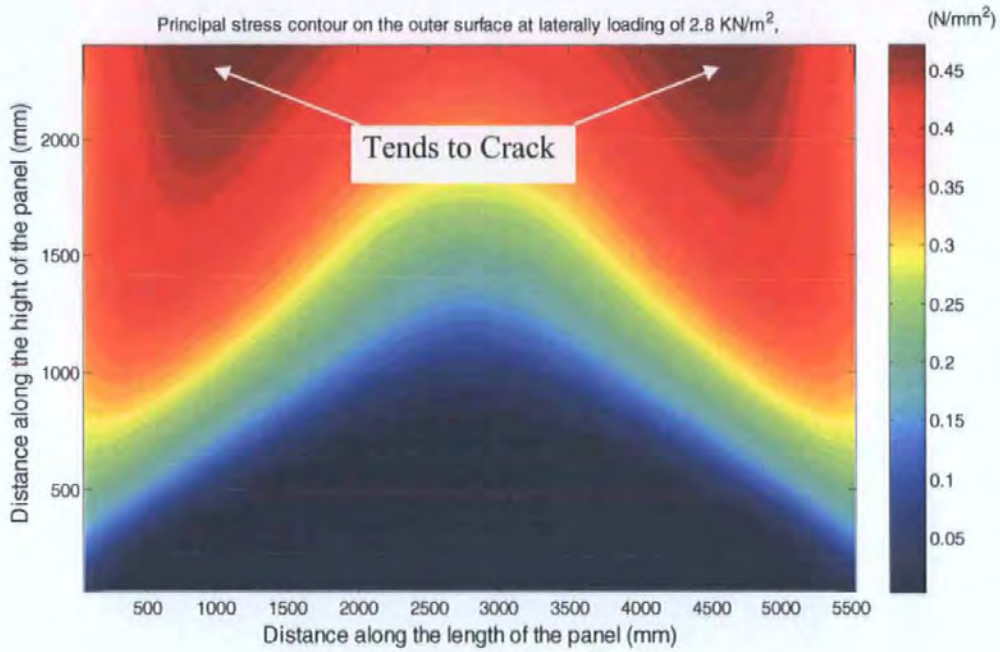
Figure 6.17 Failure pattern of the outer face at 2.8kN/m²

Principal stress contour on the inner surface at laterally loading of 2.8 KN/M²   (N/mm²)

About to Crack

Distance along the hight of the panel (mm)

Distance along the length of the panel (mm)
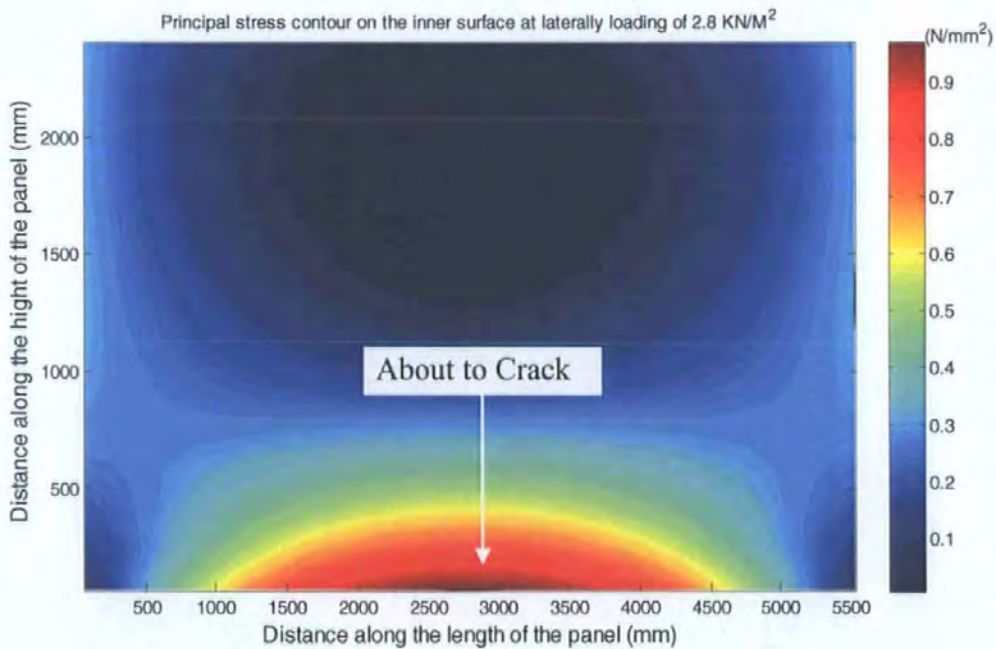
Figure 6.18 Failure pattern of the inner face at 2.8kN/m²

Principal stress contour on the outer surface at laterally loading of 3.0 KN/m², (N/mm²)
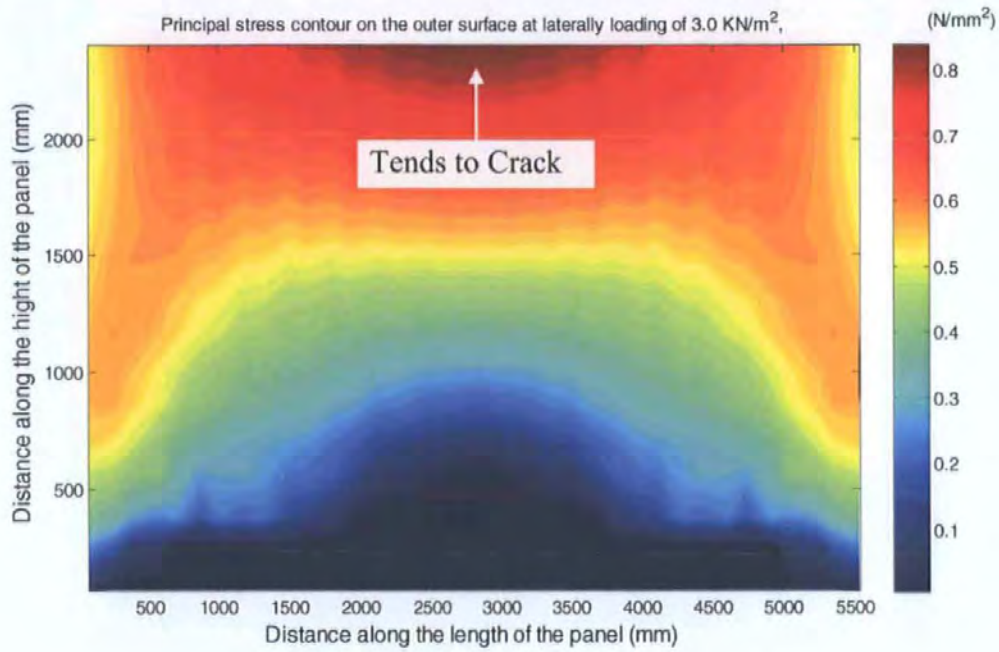
Figure 6.19 Failure pattern of the outer face at 3.0kN/m²

Principal stress contour on the inner surface at laterally loading of 3.0 KN/M² (N/mm²)
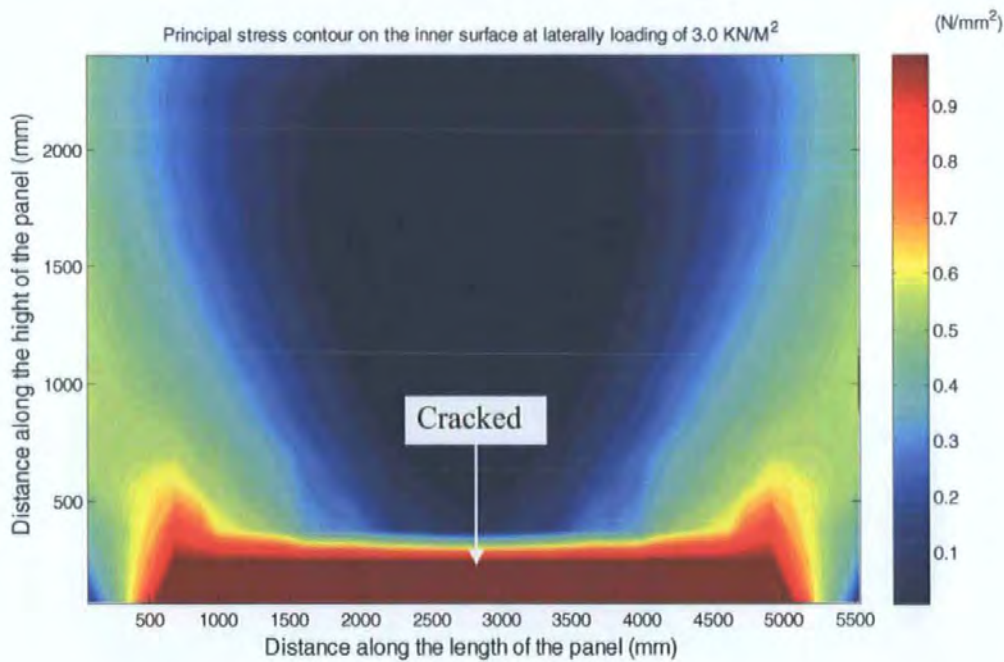
Figure 6.20 Failure pattern of the Inner Face at 3.0 kN/m^2

Principal stress contour on the outer surface at laterally loading of 3.4 KN/m^2,
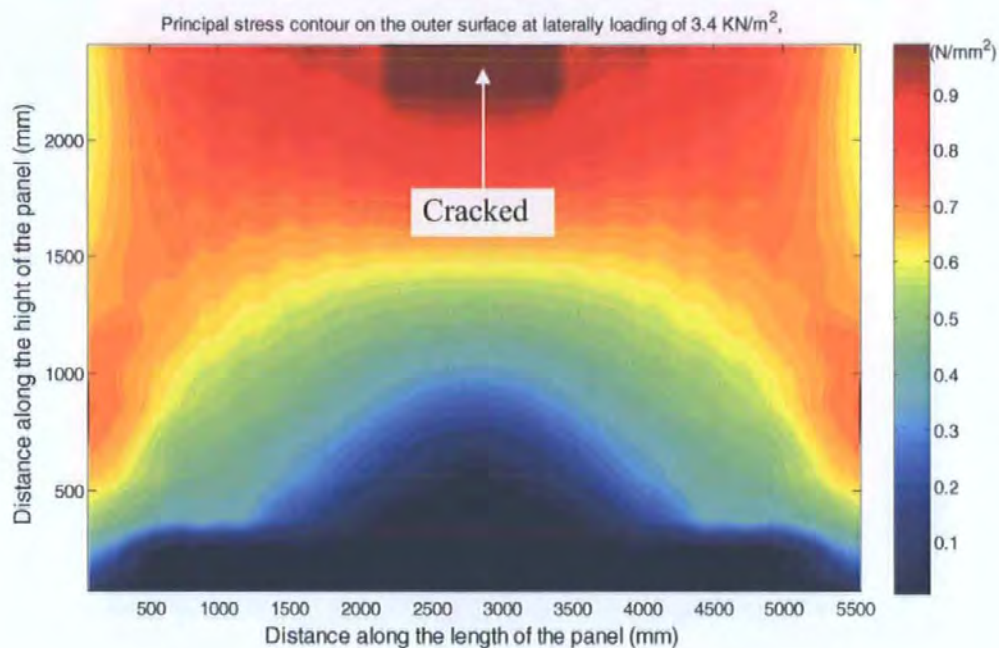
Figure 6.21 Failure pattern of the outer face at 3.4 kN/m^2

Principal stress countour on the inner surface at lateral loading of 3.4 KN/m^2
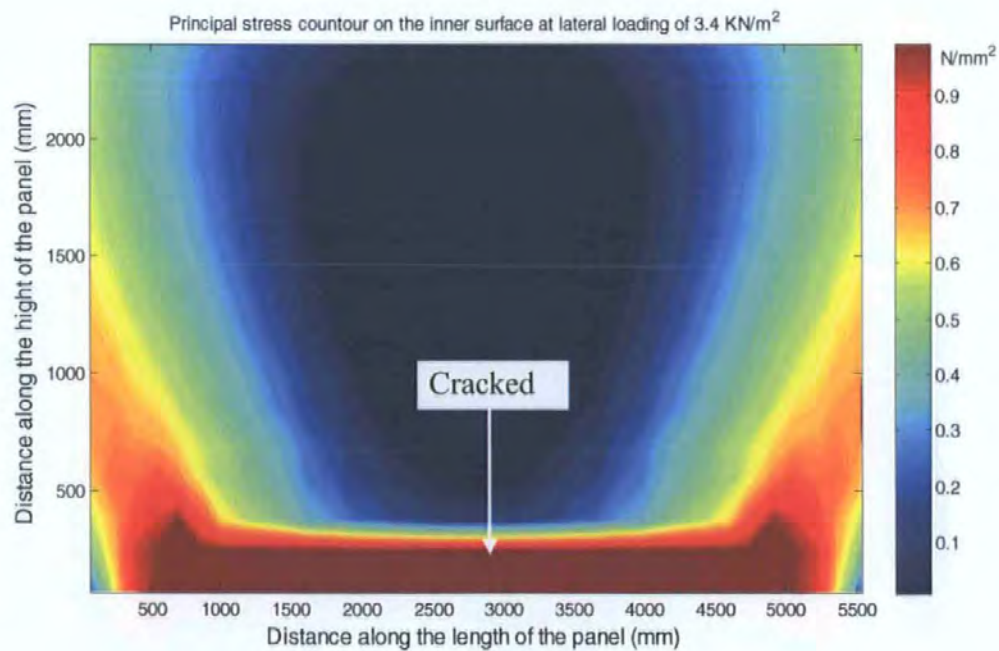
Figure 6.22 Failure pattern of the inner face at 3.4 kN/m^2

Principal stress on the outer surface at laterally loading of 7.2 KN/m^2,

Distance along the length of the panel (mm)
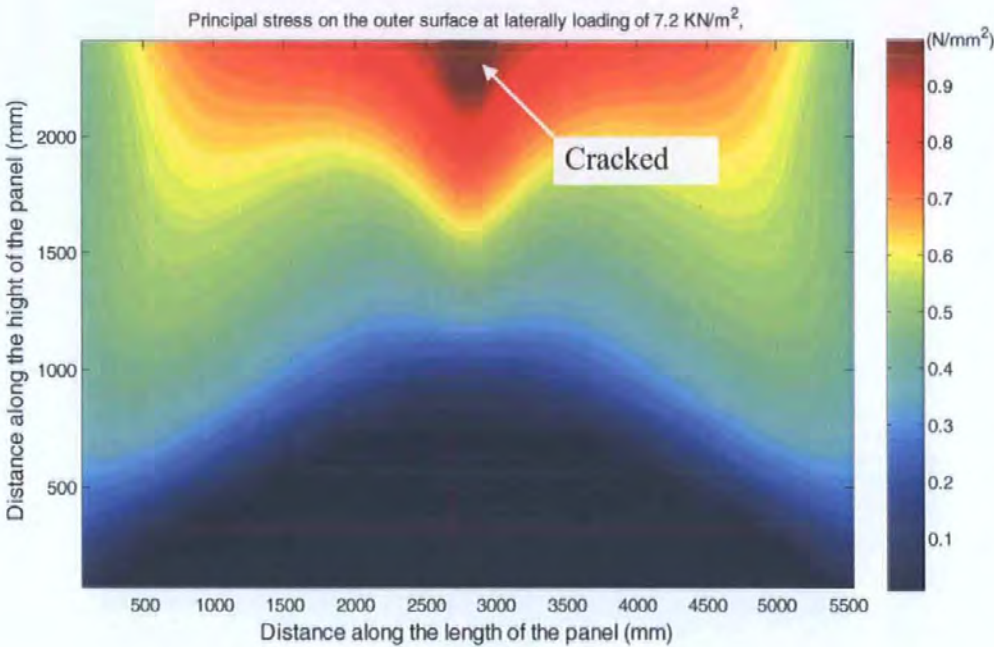
Figure 6.23 Failure pattern of the outer face at 7.2 kN/m^2

Principal stress contour on the inner surface at laterally loading of 7.2 KN/m^2

Distance along the length of the panel (mm)
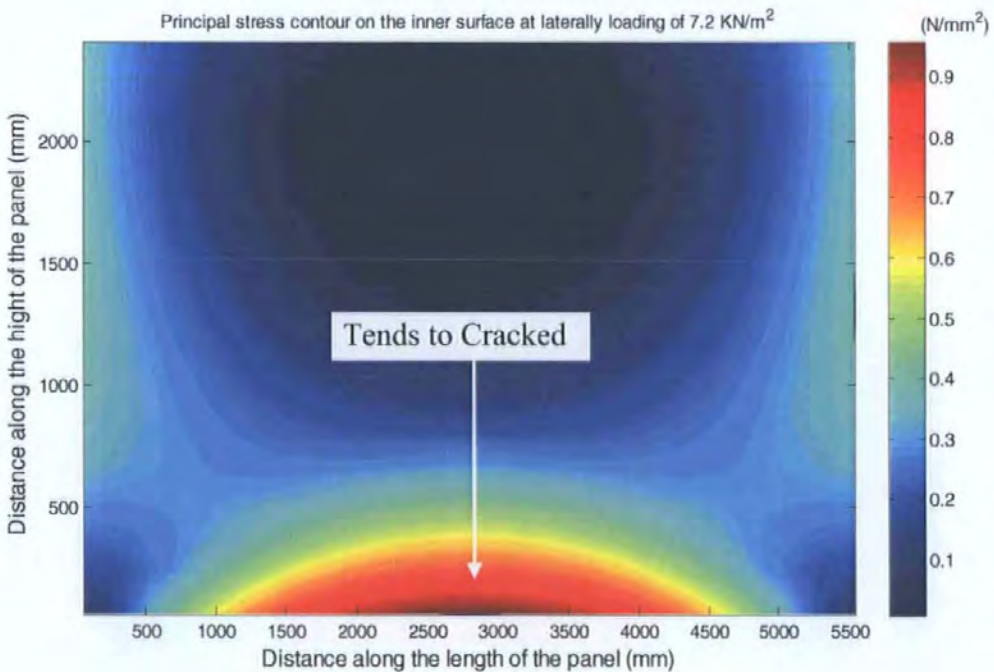
Figure 6.24 Failure pattern of the Inner face at 7.2 kN/m²

Principal stress contour on the outer surface at laterally loading of 7.4 KN/m²,
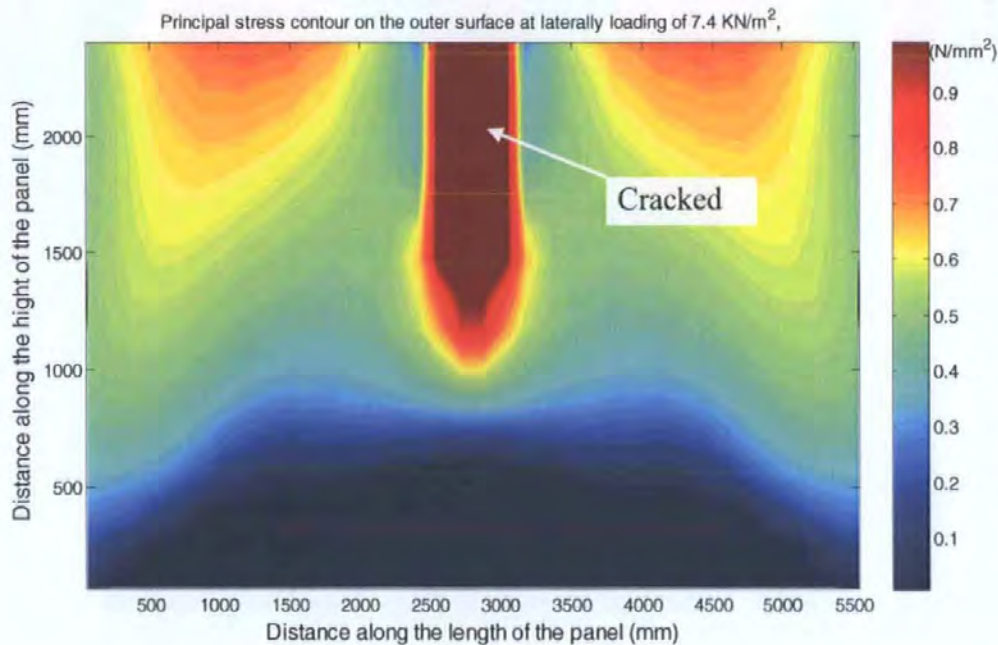
Figure 6.25 Failure pattern of the outer face at 7.4 kN/m²

Principal stress contour on the inner surface at laterally loading of 7.4 KN/m²
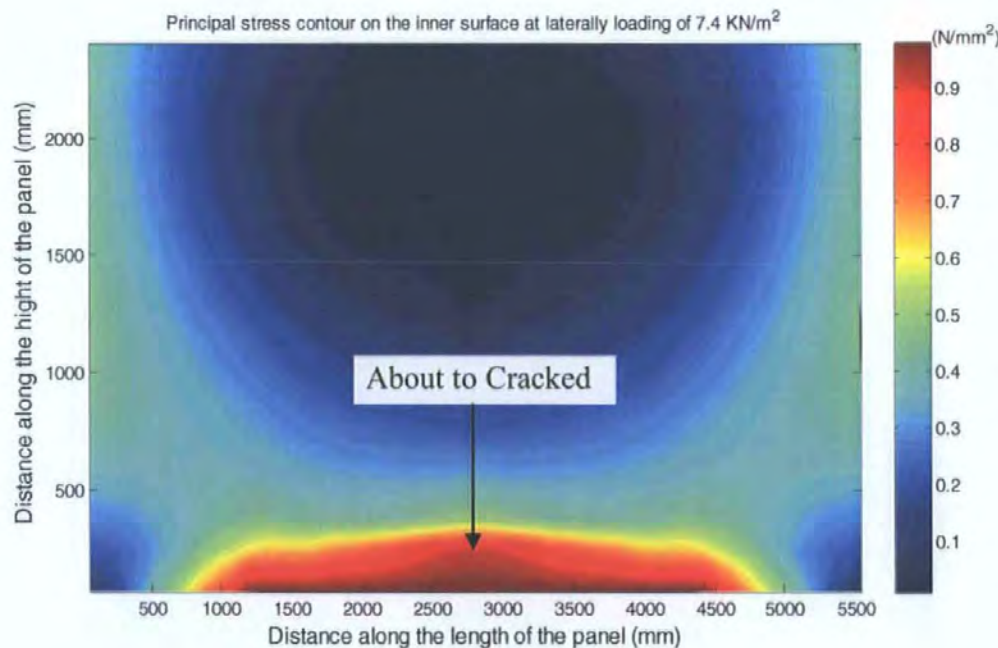
Figure 6.26 Failure pattern of the inner face at 7.4 kN/m²
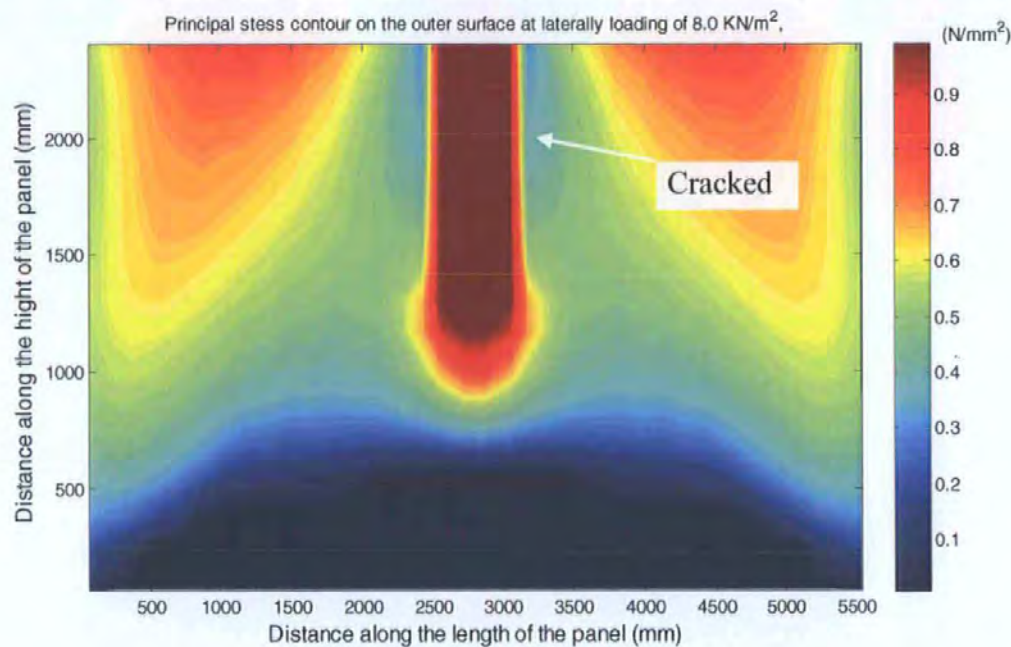
Figure 6.27 Failure pattern of the outer face at 8.0 kN/m^2
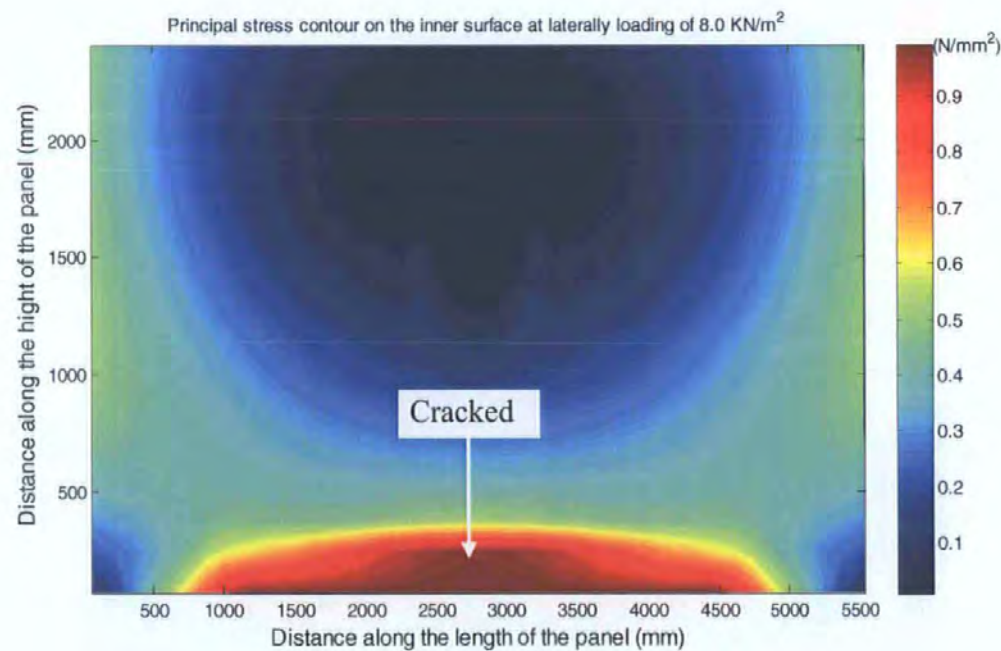
Figure 6.28 Failure pattern of the inner face at 8.0 kN/m^2

For the actual masonry panel, it is impossible that fy is so large, therefore, it could be

concluded that, for panel SBO1, the kink is always due to the failure along the direction

parallel to the bed joint (fy) at the bottom of inner face of the panel. This crack could

not be observed and recorded due to the air bag covered the whole inner face of the panel and any crack would be hidden under the air bag.

However, the experimental load deflection relationship is approximately a smooth curve on which there is no "kink" that indicating the first crack; the reason will be investigated in the following chapters.

6.6 SUMMARY

In this Chapter, parameter analyses are carried out on the FEA model used for laterally loaded masonry wall panel. It has been found that, the elastic stiffness E mainly affects the deflection of the model but has less influence on the first cracking or failure load. Flexural strength fx mainly affects the failure load and flexural strength fy mainly affects the first cracking load. Poisson's ratio has little influence on the first cracking load, failure load and deflections. Subsequently, it can be concluded that when using corrector factors to revise parameters in the FEA model, it is advisable to involve the flexural stiffness E, flexural strength fx and fy. Poisson's ratio v is not necessary to be involved.

It is also found that, the "kink" is caused by the first crack due to the failure at the bottom in the inner surface of the panel.

Based on the find in this chapter, the process of obtaining corrector factors could be divided into two steps: 1. Revise flexural stiffness in each zone (using corrector factors) first, 2. Revise smeared flexural strength secondly. The detail will be introduced in Chapter 7.

7. DERIVING CORRECTOR FACTORS BY MODEL UPDATING TECHNIQUES

7.1 INTRODUCTION

The findings of model analysis in Chapter 6 is that, flexural stiffness E has more effect on deflections but less effect on failure load; flexural strength fx has more effect on the failure load but fy has more effect on the first crack load; Poisson's ratio has little effect on both the failure load and deflections. Therefore, flexural stiffness E, flexural strengths fx and fy are eligible to be revised to improved the FEA model and accordingly two kinds of revision to these parameters will be concerned in this chapter:

1. Firstly revise flexural stiffness in each zone (using corrector factors), i.e. to get stiffness corrector factors, as will be shown in section from 7.2 to 7.4.

2. Secondly revise smeared flexural strength, i.e. to get strength correctors, as will be shown in section 7.5.

Consequently, a detailed model updating procedure will be studied in the following study to get corrector values. Since the nature of model updating is an optimisation procedure, model updating process is much related to optimization computations. Generally, model updating process is implemented using traditional optimizations. However, it is found that to the problem studied in this Chapter, the solution space of the problem is not continuous, which means the traditional optimisation methods are not able to get the solution. Consequently, the genetic algorithms (GAs) are used in this study, to implement the model updating and to get corrector factors. Because the objective function has a decisive effect on model updating process, study of the objective function of the GA is also studied.

Two kinds of models will investigated in this chapter: (1), using a smear model, i.e. during the model updating process, the same parameter value is always assigned to all

elements; (2) using a updating model, i.e. during the model updating process, zones are always assigned with different parameter values.

7.2 THE GENETIC ALGORITHM AND THE OBJECTIVE FUNCTION

The genetic algorithm (GA) is a stochastic search technique based on the mechanism of natural selection and natural genetics. The genetic algorithm works in the following way (Gen and Cheng 1997)it starts with an initial set of random solutions called population. Each individual in the population is called chromosome which represents a solution of the problem. A chromosome generally is a binary bit string which evolves through successive iterations, called generations. During each generation, the chromosomes are evaluated using some measures of fitness. To create the next generation, new chromosome (also called offspring) are formed by either two ways: (a) merging a chromosome from current generation using a crossover operator; (b) modifying a chromosome using a mutation operator. A new generation is evaluated by the fitness function and those of higher fitness values are kept for the next generation. After several generations, the algorithms converge to the best chromosome, which represents the optimum or suboptimal solution to the problem.

When running the genetic algorithm, adequate control parameters are necessary to get a quick convergence. In this study, the control parameters are defined in Table 7.1 according to some trial search.

Table 7.1 Control parameters in GA

Parameters kinds	Population (Npop)	Probability of crossover (Pc)	Probability of mutation (Pm)	No. of generations (Ngen)
Range	20-200	0.25-1.0	0.001-0.75	10-3000
Mostly used	80-200	0.5-0.8	0.01-0.03	50-300
This research	**200**	**0.6**	**0.03**	**100**

Model updating process is to minimise the discrepancies between the FEA and the experimental results, this discrepancies is defined as the objective function of the GA. The behaviour of laterally loaded masonry panels includes two parts: failure load and deflections; therefore the associated discrepancies can be defined in equations (7-1), (7-2), which can be integrated into one criterion of weighted sum as shown in equation (7-3). When considering all measuring points on the entire panel, equation (7-1) is integrated to give equation (7-4).

$$\delta d = [(\frac{Df - De}{De})^2]^{0.5} \qquad (7\text{-}1)$$

$$\delta l = [(\frac{Ff - Fe}{Fe})^2]^{0.5} \qquad (7\text{-}2)$$

$$\delta t = wl * \delta l + wd * \delta d \qquad (7\text{-}3)$$

$$\delta d = \{\frac{1}{mn} \sum_{k=1}^{m} [\sum_{j}^{n} (\frac{Dfj - Dej)}{Dej})^2]_k\}^{0.5} \qquad (7\text{-}4)$$

Where

δd: error resulted from comparison of deflections between the FEA and the refined experimental results (see appendix 1).

δl: error due to failure load between the FEA and the experimental results.

δt: total error consisted of the combination of failure load and deflections error between FEA and experimental results.

n: number of points on the panel for which the deflections are considered. In this study, all of the 36 measuring points are selected.

m: total number of load levels determined from non-linear FEA.

Dfj: the deflection by FEA at jth row of measured points.

Dej: the experimental deflection at jth row of measuring points. Here the refined experimental deflections obtained using the method introduced in Chapter 4 are used.

j: jth measuring point,   *k*: kth load level,   *Fl*: failure load obtained by FEA

Fe: failure load by the experiment. In this research, *Fe*=2.8kN/m^2 for the base panel SBO1. *Fl*: failure load by the FEA

wd, wl: weights of deflection and failure load respectively, used for a weighted sum of failure load and deflections objectives calculated to define the fitness for each solution of the GA. After the detailed investigation, it has been found that *wd* = 0.4 and *wl* = 0.6 are suitable values.

7.3 MODEL UPDATING PROCESS WITH SMEAR MODEL

Because the smear model is simpler than the updating model, investigations of model updating are firstly carried out on the smear model. Using the objective functions defined in equations (7-2), (7-3), (7-4), a model-updating algorithm is implemented using the GA. The material properties of the smeared model, both before and after the model updating, are summarised in Table 7.2. The corresponding load deflection relationship of using the updated material properties is shown in Figure 7.1. From Figure 7.1, it can be seen that, model updating make the FEA have a good correlation with the experimental results of panel SBO1.

To examine the suitability of the updated results, the updated material properties are used to analyse another masonry panel SBO2 (see Figure 9.4) which has the same dimensions and boundary conditions to SBO1 but with central opening. The result is shown in Figure 7.2. From Figure 7.2, it can be seen that some improved prediction to

SBO2 is achieved. This means the FEA models has been improved by model updating, or say using corrector factors obtained.

Table 7.2, Parameters after updating (corrector factors)

	$E(kN/m^2)$	$fx(kN/m^2)$	$fy(kN/m^2)$
Smeared material properties	12.00	0.002280	0.000965
Material properties after updating	6.00	0.001870	0.002730
corrector factors	0.50	0.820	2.829

Note: * Smeared material properties were from Chong (1993) which were obtained by Monte Carlo simulation based on the experimental results.
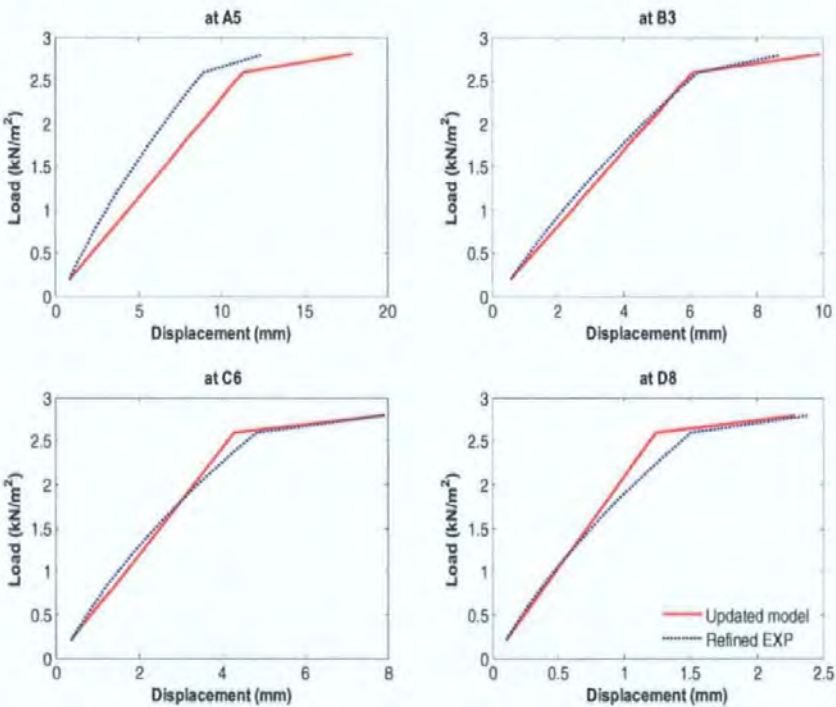
Figure 7.1 The "improved" load deflection relationships of SBO1 at A5

However, from Table 7.2 it can be seen that, the flexural strength perpendicular to the bed joints fy is much larger than that parallel to bed joints fx. This is contradictory to the common knowledge and is not acceptable though it "improves" the analyses.

Consequently, it can be concluded that, smeared masonry model is not suitable for model updating to achieve the improved analyses.

Subsequently, updating model is investigated will be introduced in the following section.
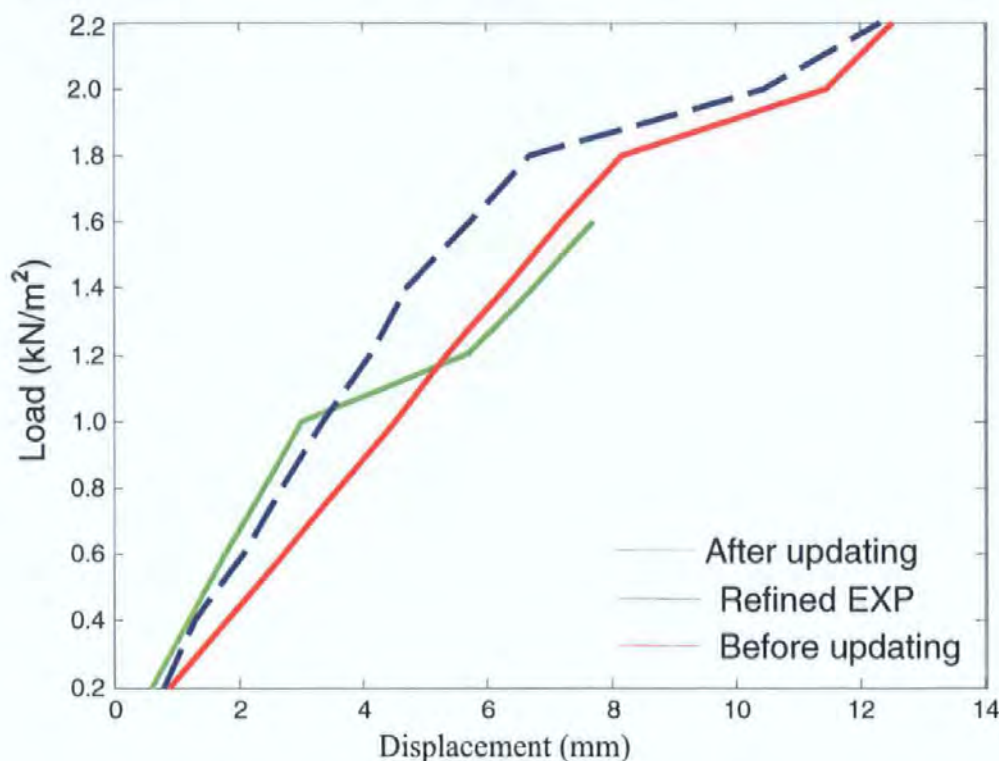
Figure 7.2, The "improved" load deflection relationships of SBO2

7.4 MODEL UPDATING PROCESS WITH UPDATING MODEL

As seen in the previous section, the updated smeared model could not be used to analyse masonry panels because the parameter values lost their physical meaning after model updating. Therefore, it is necessary to assign different parameter values to each element, i.e. using the updating model in which different parameter values are assigned to the zones. Because it is also found that, using the updating model, the model updating process is likely to get the local optima due to the number of variables are increased, the model updating procedure is carried out by two steps in this study based on the findings in Chapter 6: (a) keeping flexural strength unchanged but only revising flexural stiffness

E values, to make the deflections of the FEA model match the experimental ones well; (b) keeping the flexural stiffness E values that obtained in the first step unchanged but revising flexural strength fx and fy, to make the failure load match the experimental one well whilst still keeping the smaller discrepancies of the deflections between FEA and those of experiment.

7.4.1 Direct model updating process by the GA

In this study, modified values of stiffness E is randomly assigned to each element by the GA, but value of flexural strengths fx and fy are kept constant (fx=2.28 N/mm^2 and fy=0.965N/m^2). Because the solutions obtained by different runs of GA search can not be exactly the same, a number of runs of the GA are performed. A summary of 5 different runs of the GA ,which are denoted as GA1, GA2, ...GA5, are given in Table 7.2, the corresponding 3D plot is shown in Figure 7.3 (only GA1 is presented) and their corresponding load-deflection relationships are shown in Figure 7.4.

From Figure 7.4, it can be seen that the load deflection relationships are effectively improved by using the updated stiffness values (corrector factors). However, the correctors as shown in Table 7.3 are not regular; they don't indicate any physical meaning. To reveal the feature of these corrector factors, regression is conducted which will be discussed in the next section.

Table 7.3 Corrector values obtained using the direct GA search

GA1	X1	X2	X3	X4	X5	X6	X7	X8	X9
Y4	0.984	0.855	0.855	1.242	1.468	1.242	0.855	0.855	0.984
Y3	0.758	0.952	1.048	1.403	1.436	1.403	1.048	0.952	0.758
Y2	0.758	0.919	1.436	1.436	1.21	1.436	1.436	0.919	0.758
Y1	0.565	1.468	1.5	1.5	1.371	1.5	1.5	1.468	0.565
GA2	X1	X2	X3	X4	X5	X6	X7	X8	X9
Y4	0.758	0.758	1.016	1.242	1.5	1.242	1.016	0.758	0.758
Y3	0.887	0.919	1.177	1.113	0.726	1.113	1.177	0.919	0.887
Y2	0.758	0.952	1.436	1.5	1.5	1.5	1.436	0.952	0.758
Y1	0.532	1.5	1.5	1.468	1.339	1.468	1.5	1.5	0.532
GA3	X1	X2	X3	X4	X5	X6	X7	X8	X9

Y4	0.5	1.016	1.145	1.177	0.952	1.177	1.145	1.016	0.5
Y3	0.887	1.016	1.21	1.403	1.371	1.403	1.21	1.016	0.887
Y2	0.919	0.984	1.468	1.371	1.306	1.371	1.468	0.984	0.919
Y1	0.758	1.21	1.468	1.21	1.436	1.21	1.468	1.21	0.758
GA4	X1	X2	X3	X4	X5	X6	X7	X8	X9
Y4	0.597	0.984	1.048	1.177	1.177	1.177	1.048	0.984	0.597
Y3	0.919	1.016	1.145	1.468	1.274	1.468	1.145	1.016	0.919
Y2	0.855	0.952	1.371	1.436	0.887	1.436	1.371	0.952	0.855
Y1	0.694	1.403	1.468	1.5	1.403	1.5	1.468	1.403	0.694
GA5	X1	X2	X3	X4	X5	X6	X7	X8	X9
Y4	0.5	0.897	1.167	1.135	1.405	1.135	1.167	0.897	0.5
Y3	0.77	1.04	1.341	0.77	1.119	0.77	1.341	1.04	0.77
Y2	0.849	1.008	1.341	1.421	1.5	1.421	1.341	1.008	0.849
Y1	0.675	1.5	1.468	1.246	1.405	1.246	1.468	1.5	0.675

Note: D1-D9,C1-C9,B1-B9,A1-A9 are the measured points. GA1… GA5 are 5 groups of GA results
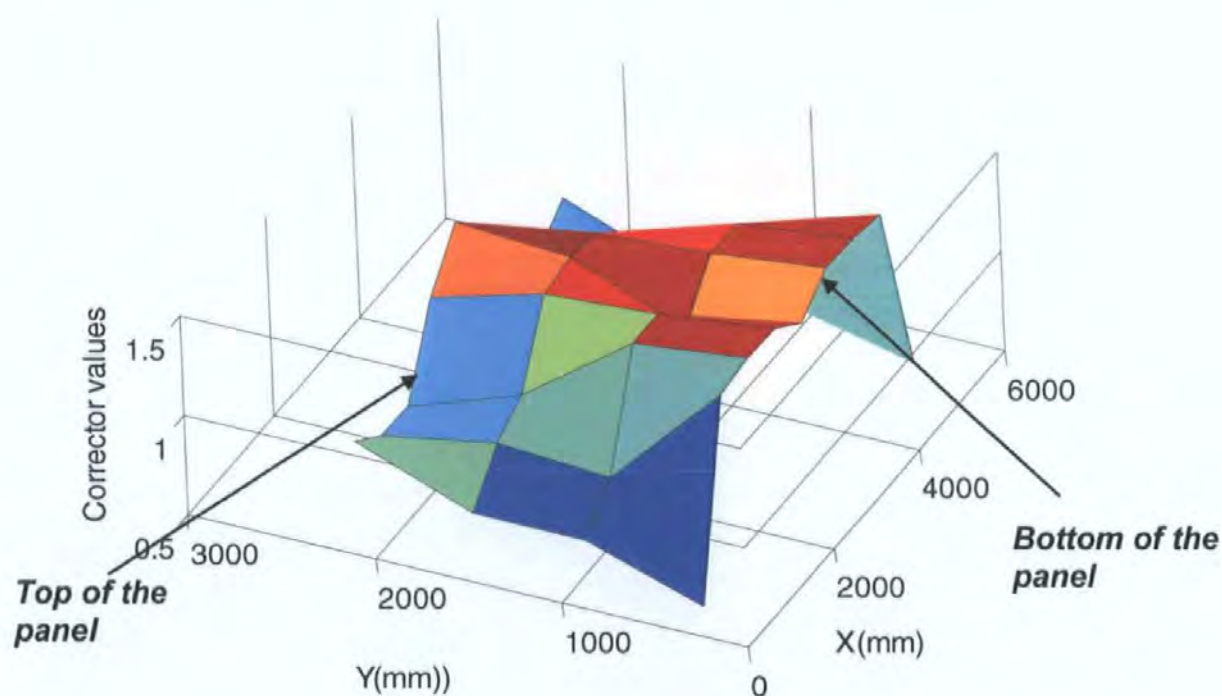
Figure.7.3, 3D plot of corrector factors obtained by search (GA1)
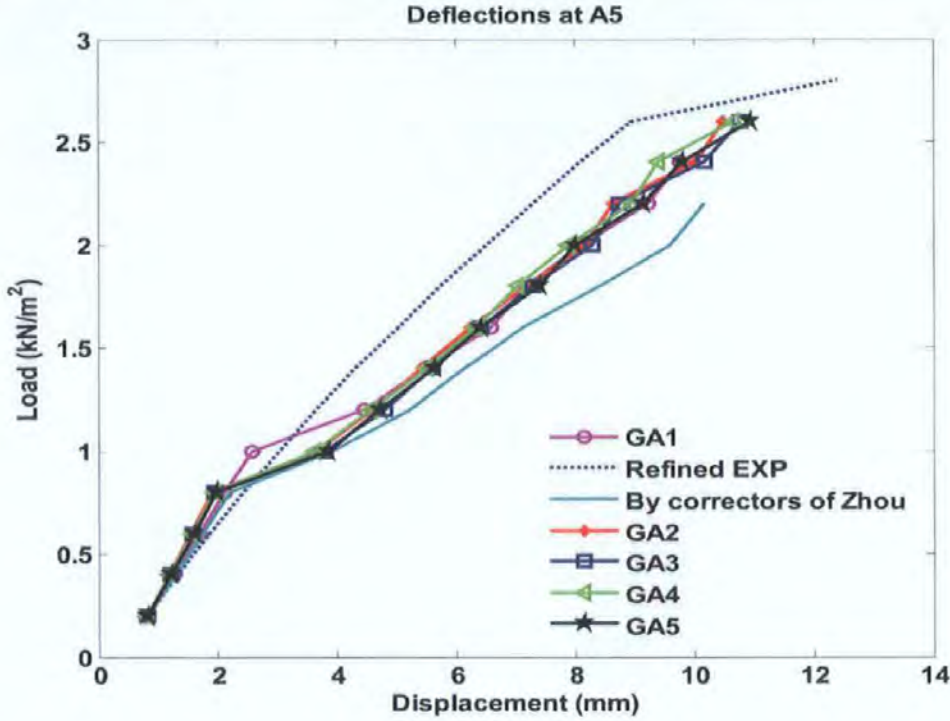
Figure 7.4 Load deflection relationships of using corrector factors by GA search

7.4.2 Regression analysis to the corrector factors derived by the GA

To further reveal the characteristics of correctors as shown in Table 7.3, regression study is carried out in this section.

7.4.2.1 Formulae for regression and their reliability

When constructing the formula used for regression, the errors of FEA are compared between using corrector factors with and without regression, only those formulae that would not deteriorate the corrector factors would be selected. Based on this principle and referring to the formulae style presented by Wahab(1999) and considering the feature of 3D plot in Figure7.3, extensive studies are carried out and the following three formulae are selected for regression. They are shown as below.

Formula 1 (denote as FML1)

Let

$F1 = Y/Ly$

$F2 = COS (\pi * X/Lx) A1$

Then

$$\Psi = (A2*F12 + A3*F1 + A4)*F2\ 2 + A0 \qquad (7\text{-}5)$$

Formula 2 (denote as FML2)

Let

$$F1 = Y/Ly$$

$$F2 = COS\ [\pi\ *(X/Lx)\ A1]$$

Then

$$\Psi = A2*F1A3*F22 + A0 \qquad (7\text{-}6)$$

Formula 3 (denote as FML3):

Let

$$F1 = SIN\ c$$

$$F2 = \{COS\ [\pi\ *X/\ Lx)\ A5]\}\ 2$$

Then

$$\Psi = F2*\ A2*F12 + A3*F1 + A4) + A0 \qquad (7\text{-}7)$$

Where,

Lx: length of the panel.

Ly: height of the panel.

A0, A1... An: constants to be determined by GA

It should be mentioned that these constructed formulae are only suitable to make regression to corrector factors of the right half panel; correctors of the left panel are obtained due to the symmetry of the masonry panel. The reliability of these formulae is checked in the next section.

7.4.2.2 reliability of formulae for regression

Using formulae (7-5), (7-6), (7-7) to make regression to corrector factors in Table 7.3 respectively, the correctors after regression are summarised in Table 7.4, 7.5, 7.6.

To check the reliability of formulae for regression, the load deflection relationships of using corrector factors with and without regression are compared as shown in Figure 7.5. From Figure 7.5 it can be seen that, regression don't change the, the load deflection relationships. This means that the character of the corrector factors is not affected by regression. Subsequently, it can be concluded that the formulae are safe enough here.
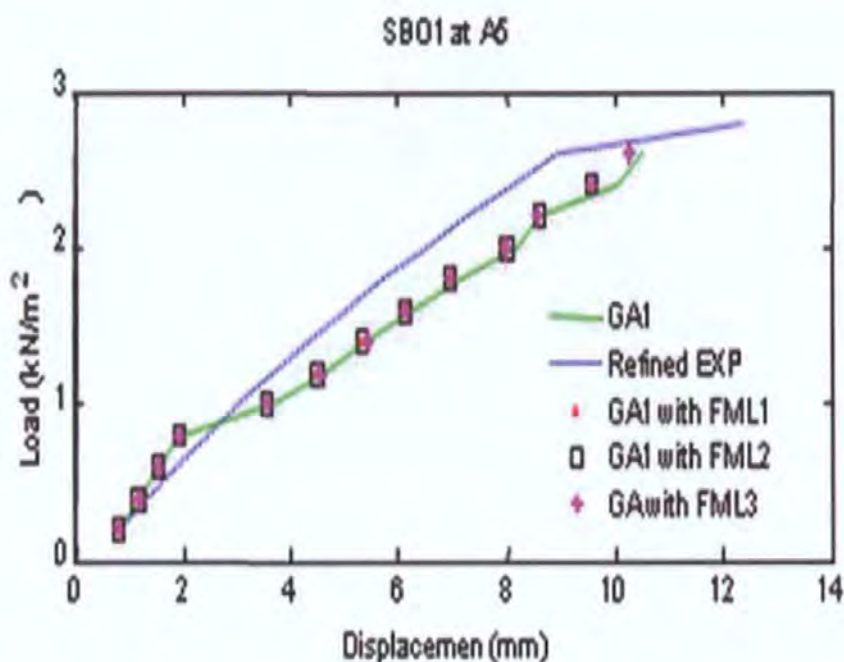
Figure 7.5 Comparison of using corrector factors (GA1) with and without regression

7.4.2.3 The Feature of Corrector Factors by Regressions

From Table 7.4, 7.5, 7.6, it can be seen that after regression by these formulae, the data becomes more regular. To clearly view the distribution of the data in Table 7.4, 7.5, 7.6, their typical 2D and 3D plot are shown in Figure 7.7, 7.8 and 7.9 respectively. From Figure 7.7, it can be seen that all the regression results for those 5 groups of corrector factors obtained by the GA are quite similar when using the same formula. Figure 7.8 reveals that there are some differences between using different formulae, but their distribution tendencies are similar. From Figure 7.9 it could be concluded that corrector

factors along the simply supported edges are smaller and those close to the built-in edge are larger compared with the central parts of the panel. This tendency is quite the same as those presented by Zhou(2002) as shown in Chapter 3 (Figure 3.8) except with better regularity. The big changes near the supported boundaries edges indicate that the boundary conditions significantly affect the behaviour of the masonry panel.

Because some discrepancy along with "kink" still exist using the obtained corrector factors, objective function is studied in the next section.

Table 7.4, the regression by Formula 1

Zones	X	Y	FML1_GA1	FML1_GA2	FML1_GA3	FML1_GA4	FML1_GA5
D9 (D1)	2488.89	309	0.773	0.754	0.77	0.79	0.736
D8 (D2)	1866.67	309	1.152	1.247	1.144	1.24	1.305
D7 (D3)	1244.44	309	1.443	1.502	1.344	1.44	1.45
D6 (D4)	622.22	309	1.539	1.552	1.386	1.47	1.462
D5	0	309	1.547	1.554	1.387	1.47	1.462
C9 (C1)	2488.89	927	0.756	0.719	0.771	0.76	0.696
C8 (C2)	1866.67	927	1.051	1.077	1.149	1.12	1.159
C7 (C3)	1244.44	927	1.276	1.262	1.351	1.28	1.278
C6 (C4)	622.22	927	1.35	1.298	1.393	1.3	1.287
C5	0	927	1.357	1.3	1.394	1.3	1.287
B9 (B1)	2488.89	1545	0.75	0.702	0.759	0.75	0.672
B8 (B2)	1866.67	1545	1.011	0.99	1.088	1.05	1.073
B7 (B3)	1244.44	1545	1.212	1.139	1.264	1.18	1.175
B6 (B4)	622.22	1545	1.278	1.168	1.301	1.2	1.183
B5	0	1545	1.284	1.17	1.302	1.2	1.183
A9 (A1)	2488.89	2163	0.746	0.701	0.734	0.74	0.664
A8 (A2)	1866.67	2163	0.988	0.986	0.963	1.02	1.044
A7 (A3)	1244.44	2163	1.173	1.133	1.084	1.14	1.141
A6 (A4)	622.22	2163	1.235	1.162	1.11	1.16	1.149
A5	0	2163	1.24	1.163	1.111	1.16	1.149

Table 7.5, the regression by Formula 2

Zones	X	Y	FML2_GA1	FML2_GA2	FML2_GA3	FML2_GA4	FML2_GA5
D9 (D1)	2488.89	309	0.773	0.749	0.773	0.792	0.734
D8 (D2)	1866.67	309	1.152	1.237	1.178	1.252	1.302
D7 (D3)	1244.44	309	1.443	1.484	1.387	1.452	1.444
D6 (D4)	622.22	309	1.539	1.531	1.427	1.484	1.455
D5	0	309	1.547	1.533	1.429	1.485	1.455

C9 (C1)	2488.89	927	0.756	0.716	0.756	0.76	0.691
C8 (C2)	1866.67	927	1.051	1.076	1.092	1.107	1.148
C7 (C3)	1244.44	927	1.276	1.258	1.264	1.258	1.262
C6 (C4)	622.22	927	1.35	1.292	1.298	1.282	1.271
C5	0	927	1.357	1.294	1.299	1.282	1.272
B9 (B1)	2488.89	1545	0.75	0.704	0.749	0.749	0.674
B8 (B2)	1866.67	1545	1.011	1.016	1.056	1.052	1.087
B7 (B3)	1244.44	1545	1.212	1.174	1.214	1.184	1.191
B6 (B4)	622.22	1545	1.278	1.204	1.245	1.205	1.199
B5	0	1545	1.284	1.205	1.247	1.206	1.199
A9 (A1)	2488.89	2163	0.746	0.697	0.744	0.742	0.664
A8 (A2)	1866.67	2163	0.988	0.981	1.035	1.02	1.05
A7 (A3)	1244.44	2163	1.173	1.125	1.184	1.141	1.147
A6 (A4)	622.22	2163	1.235	1.152	1.213	1.16	1.155
A5	0	2163	1.24	1.153	1.215	1.161	1.155

Table 7.6, the regression by Formula 3

Zones	X	Y	FML3_GA1	FML3_GA2	FML3_GA3	FML3_GA4	FML3_GA5
D9 (D1)	2488.89	309	0.773	0.752	0.771	0.728	0.728
D8 (D2)	1866.67	309	1.148	1.176	1.145	1.263	1.263
D7 (D3)	1244.44	309	1.436	1.444	1.345	1.422	1.422
D6 (D4)	622.22	309	1.531	1.513	1.387	1.438	1.438
D5	0	309	1.54	1.517	1.389	1.438	1.438
C9 (C1)	2488.89	927	0.758	0.746	0.769	0.716	0.716
C8 (C2)	1866.67	927	1.062	1.144	1.138	1.216	1.216
C7 (C3)	1244.44	927	1.294	1.395	1.336	1.364	1.364
C6 (C4)	622.22	927	1.371	1.459	1.377	1.379	1.379
C5	0	927	1.377	1.463	1.378	1.379	1.379
B9 (B1)	2488.89	1545	0.75	0.698	0.762	0.658	0.658
B8 (B2)	1866.67	1545	1.014	0.88	1.104	0.991	0.991
B7 (B3)	1244.44	1545	1.215	0.995	1.287	1.09	1.09
B6 (B4)	622.22	1545	1.282	1.024	1.324	1.099	1.099
B5	0	1545	1.288	1.026	1.326	1.099	1.099
A9 (A1)	2488.89	2163	0.745	0.72	0.733	0.676	0.676
A8 (A2)	1866.67	2163	0.979	1.001	0.957	1.058	1.058
A7 (A3)	1244.44	2163	1.158	1.179	1.076	1.173	1.173
A6 (A4)	622.22	2163	1.218	1.224	1.101	1.184	1.184
A5	0	2163	1.223	1.227	1.102	1.184	1.184
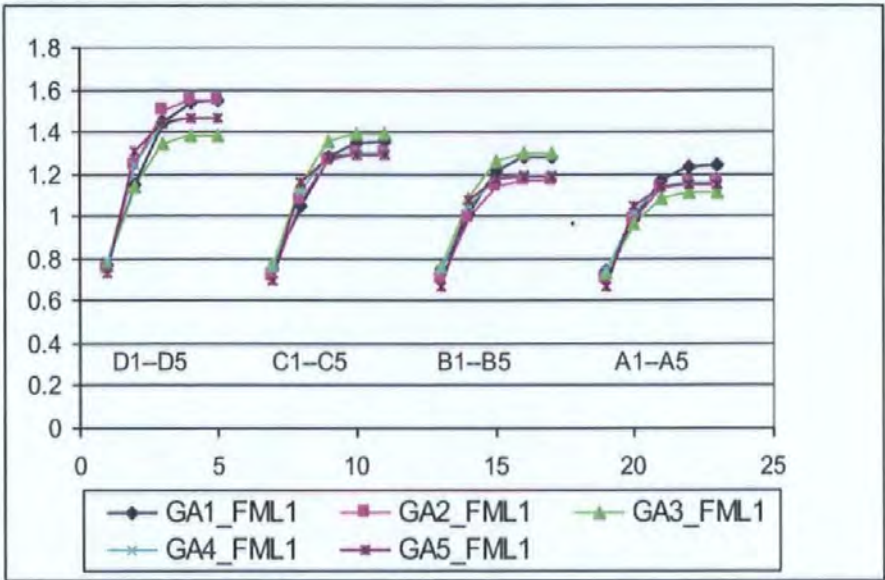
Figure.7.6 The corrector factors derived by different GA search, after regression (for the left half panel)

(Note: GA1-FML1, GA1-FML2… represents the regression to GA1 by formulae 1, 2… respectively)
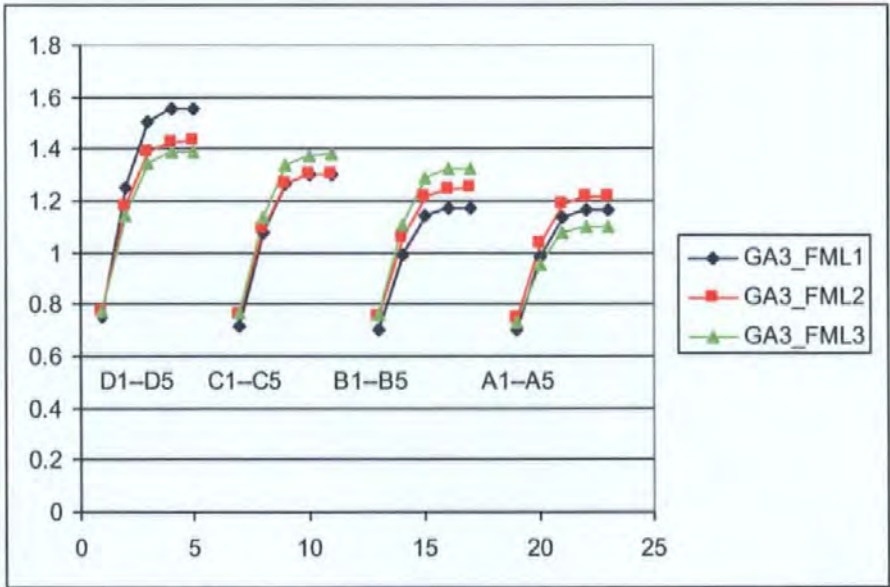
Figure.7.7 The corrector factors derived by GA, after regression using different formulae (for the left half panel)
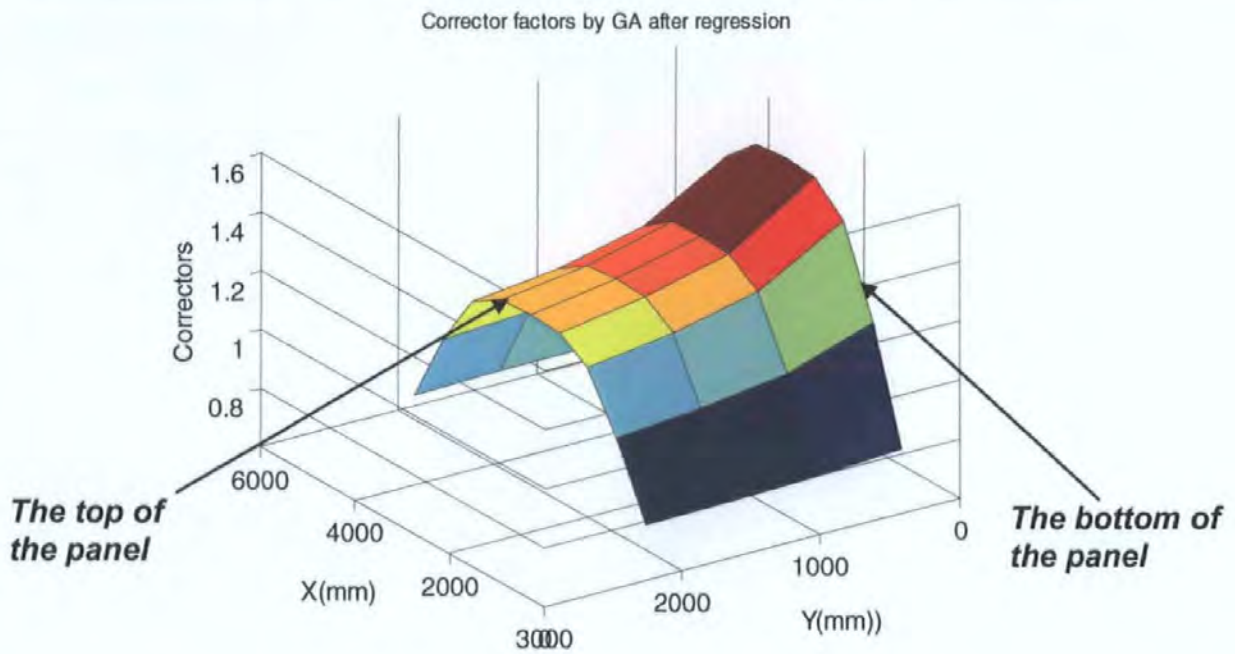
Figure.7.8 Typical 3D plot of corrector factors obtained by GA and with regression (for the whole panel)

7.4.3 Adding gradients to the objective function

Figure 7.9 demonstrates the existence of "kink" on load deflection curves when using corrector factors. On the contrast, the kink does not appear on the experimental load deflection curves. Since the gradient is another important parameter to express the differences between two load deflection curves besides the failure load and deflections, the gradients of the load deflection curves are added to the objective function in this study.
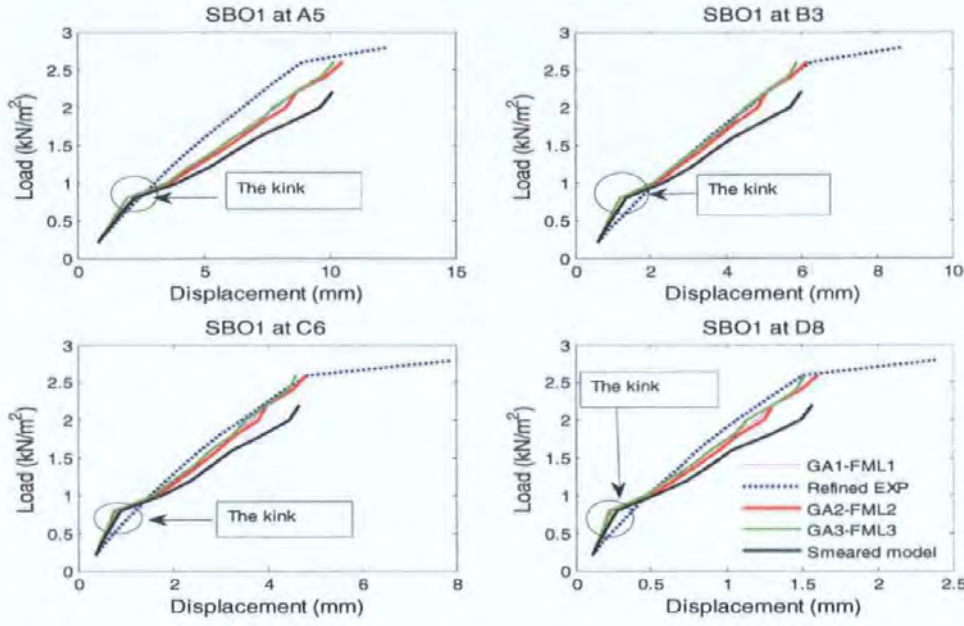
Figure 7.9 The "kink" on the load deflection curves

7.4.3.1 Gradient added to the objective function

The gradients of load deflection curves at two adjacent load levels are defined by equation (7-8). When considering the combined effect of all load levels at all measuring points on the panel, the discrepancy of gradients between FEA and the refined experimental load deflection curves can be expressed in equation (7-9). The weight sum of the objective function is given in equation (7-10).

$$G_j = \frac{F_{j+1} - F_j}{D_{j+1} - D_j} \tag{7-8}$$

$$\delta g = \{\frac{1}{m(n-1)} \sum_k^m [\sum_{j=1}^{n-1} (\frac{Gfj - Gej}{Gej})^2]_k\}^{0.5} \tag{7-9}$$

$$\delta = wl * \delta l + wd * \delta d + wg * \delta g \tag{7-10}$$

Where

F, D are respectively the load and corresponding deflections.

j: j^{th} the load level.

G is the gradient of load deflection curves in-between two neighboured load levels.

δg is the total discrepancy of gradient between the load deflection curve of FEA and the refined experimental ones, which has covered in-between every neighbour load level and the entire panel.

G_{fj}, G_{ej}: gradient of FEA and experimental one in between j[th] load level.

k :k[th] measuring points

n: total load levels of FEA results

m: total number of measuring points

δ: total discrepancy between load deflection curves of FEA and the refined experimental ones.

δl, δd : as defined in equation (7-3)

wl, wd, wg: weight for failure load, deflections and gradient respectively, which are used to express the contribution of the each part in objective function.

A detailed investigation of minimising the error between experimental & analytical model proved that $wl=0.5$, $wd=0.2$, $wg=0.3$ lead to the GA converge to the smaller error and with a smooth load deflection relationships and the kink was eliminated (see Figure 7.11). These weights values are used in the subsequent study of corrector factors using the GA.

7.4.3.2 Corrector factors obtained by GA using the objective function the with gradient introduced

Using the objective function (7-10) with gradient introduced, the corrector factors obtained by GA are shown in Table 7.7, the 3D plot of these corrector factors is shown in Figure 7.10, and the load deflection relationship is shown in Figure 7.11.

Figure 7.10 shows that, the obtained corrector factors almost results in a perfect match between the FEA and the experimental results. However, the corrector factors obtained as shown in Table 7.7 and Figure 7.10 still appears irregular in places. Therefore, the similar regression as described in section 7.4.2 is carried out once again using equation

(7-5), (7-6) and (7-7). The corrector factors after regression are shown in Table 7.8 and their 3D plot are shown in Figure 7.12, the corresponding load deflection relationships are shown in Figure 7.13.

From Figure 7.13, it can be seen that, the corrector factors after regression (as shown in Table 7.8) make the load deflection relationships worse compared with those in Table 7.7 that without regression, but they still make better improvements compared with those without adding gradient such as in Table 7.4, 7.5 and 7.6. Comparing Figure 7.12 with Figure 7.8, it can be seen that the corrector factors along the bottom side of the panel appear drastically different. In Figure 7.12 these corrector factors decreased dramatically whereas those in Figure 7.8 increase.

Table 7.7 corrector factors by GA with gradient objective function (left half panel)

	1	2	3	4	5
a	0.826	1.329	1.368	1.29	1.174
b	1.135	1.252	1.252	1.368	1.252
c	1.174	1.29	1.445	1.484	0.71
d	0.865	0.4	0.4	0.477	1.484
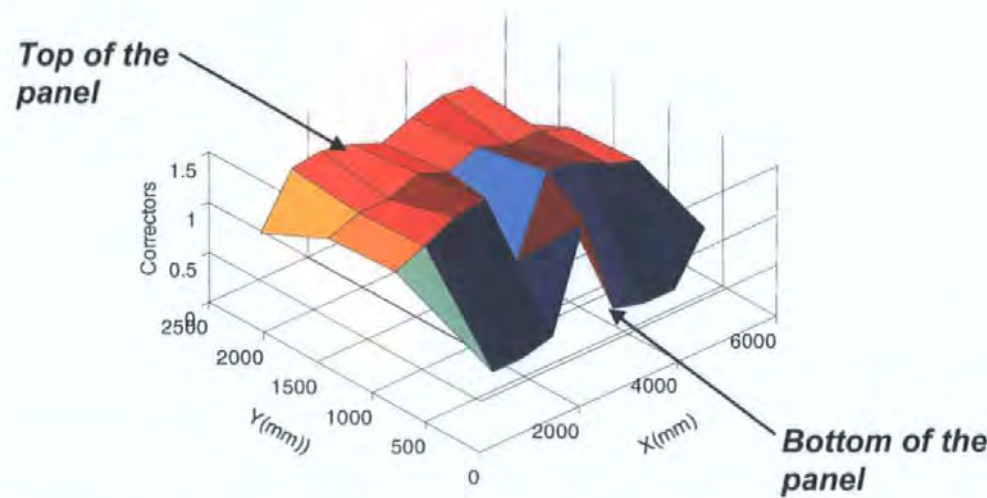
Figure 7.10, 3D plot of corrector factors derived by GA with gradient objective function
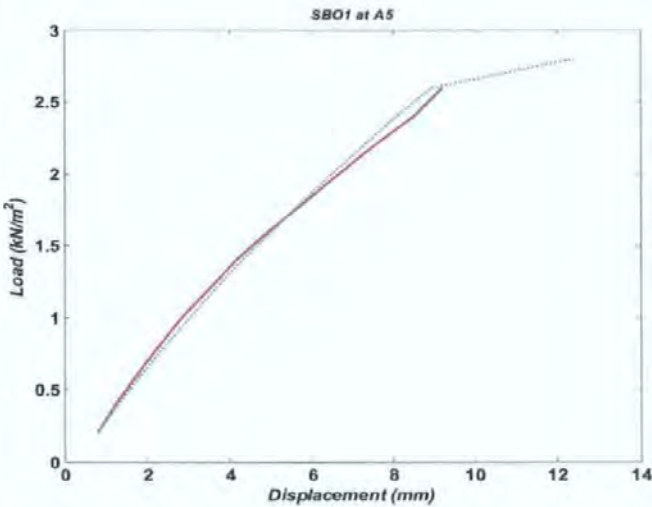
Figure 7.11 Load deflection relationships of SBO1 using corrector factors in Table 7.7

Table 7.8 corrector factors after regression

BY FML1	1	2	3	4	5
A	1.049	1.233	1.245	1.246	1.246
B	1.098	1.342	1.358	1.358	1.358
C	1.021	1.172	1.182	1.182	1.182
D	0.819	0.725	0.719	0.719	0.719
BY FML2	1	2	3	4	5
A	1.206	1.330	1.330	1.330	1.330
B	1.118	1.241	1.241	1.241	1.241
C	0.983	1.106	1.106	1.106	1.106
D	0.694	0.817	0.817	0.817	0.817
BY FML3	1	2	3	4	5
A	1.086	1.187	1.230	1.251	1.258
B	1.130	1.235	1.280	1.303	1.310
C	1.098	1.200	1.244	1.266	1.273
D	0.656	0.716	0.741	0.754	0.758
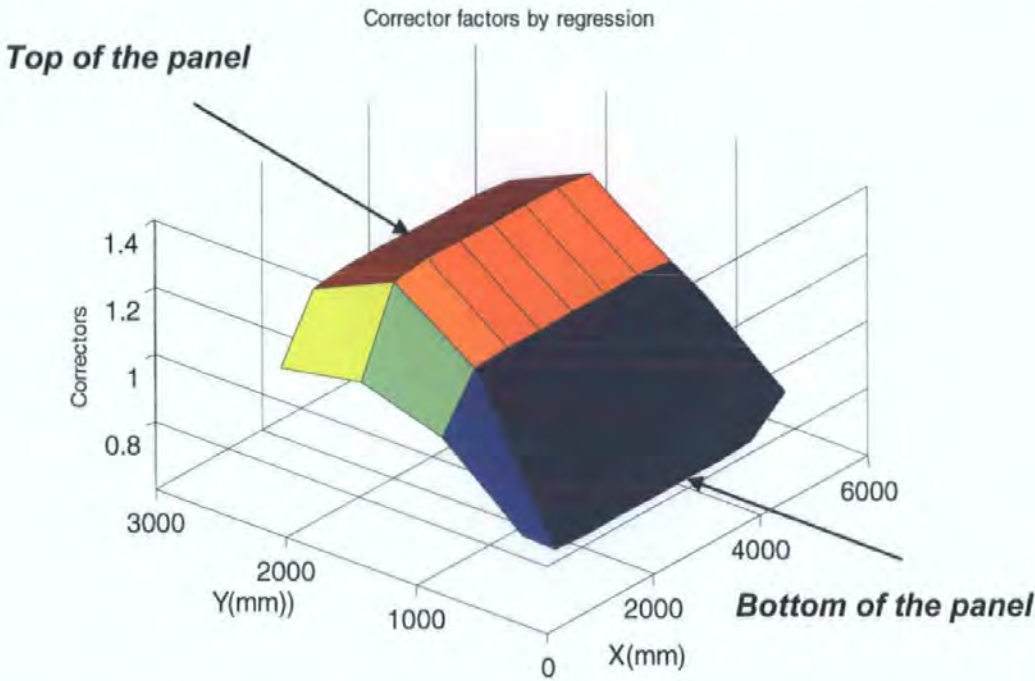
Figure 7.12, 3D plot of corrector factors derived by GA after regression
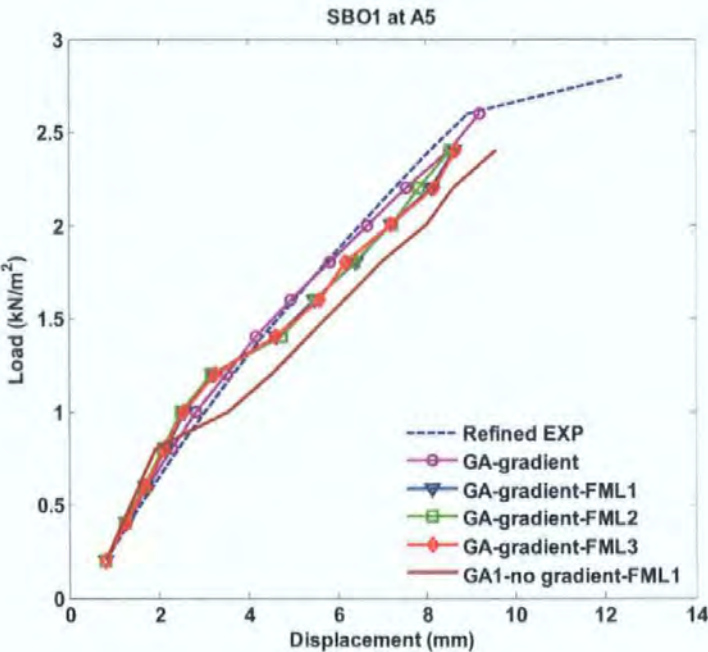
Figure 7.13 The load deflection relationships by different correctors

Corrector factors are multiple coefficients to revise to the flexural stiffness of zones on the panel, the flexural stiffness is increased when corrector factor values are bigger than 1 and are decreased when corrector factor values are smaller than 1. Therefore,

corrector factors in Table 7.8 (after regression) assigned smaller flexural stiffness to zones close to the fixed bottom edge to match the experimental results. However, to the actual panel in the experiment, materials properties on each zone should be approximately the same. Therefore, it can be deduced that, the bottom edge is not totally fixed during the actual experiment. This is one of the main findings of this research. Generally in practice the base of the panel constructed in a manner shown in Fig 3.4 is considered to be fully fixed. The findings of this investigation proved that this is not the case and there is a certain degree of rotation at the base of the panel. Therefore, this has been resulted by the low values of corrector factors at zones adjacent to the bottom support to soften these regions to allow rotation. Validation of this point is carried out in section 9.3 of this thesis using cases studies from various sources.

Because the corrector factors after regression in Table 7.8 results in a increased error compare to the corrector factors without regression in Table 7.7 as shown in Figure 7.8, further studies are needed using the constraint function in the GA. This process will be discussed in the following section.

7.4.4 Using constraint functions

As mentioned in the last section, using the objective function with gradient can result in corrector factors with a better match to the experiment, but the results becomes worse after applying regression to the corrector factors. Because Figures 7.8 and 7.12 disclosed that a larger change of corrector factors occurs near the supported boundaries than in the central parts of the panel where appears to be a smaller change. This means that corrector factors near the supported boundaries are more influenced by the boundary effects. Consequently the constraint function is introduced to directly express the effects of boundary conditions.

7.4.4.1 Using single constraint function

As discussed in previous section, the corrector factors appear a bigger change near the supported boundaries and a smaller change far from the boundaries. Therefore the distribution of corrector factors should be of two kinds: From the boundary to the centre of the panel, corrector values would either monotonously decrease or monotonously increase, as presented in Figure 7.14. Based on this assumption, the constraint functions that represent these two kinds of boundary effects are used.
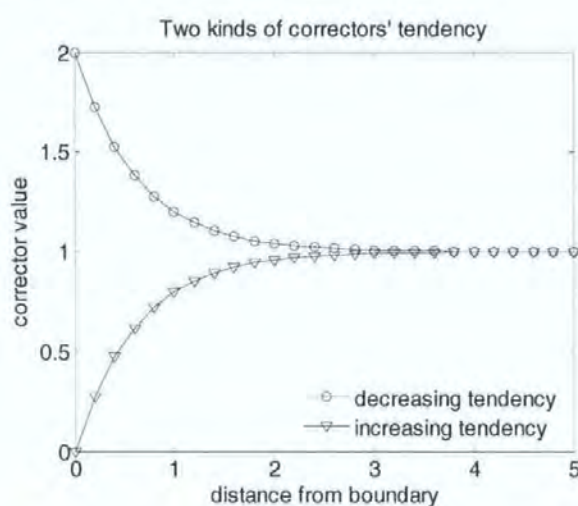
Figure 7.14 Two kinds of boundary effects (tendencies of corrector factors)

After studies on different equation styles, a single constraint function as shown in equation (7-11) is found suitable to express the two kinds of boundary effects.

$$CR=A*exp\,(B/x)\,+C*exp\,(D/x)\,+F; \tag{7-11}$$

Where CR is the boundary effect, A, B, C, D, F are coefficients that assigned by the GA (GA variables), and x is the distance from the centre of a zone to the corresponding boundary.

Masonry panel SBO1 has three distinct supported boundaries, two vertical edges simply supported and a bottom edge built-in. The boundary effect corresponding to each boundary can be separately expressed using equation (7-11) with different coefficients, as shown in equations (7-12), (7-13), and (7-14). The corrector factors (or say the total boundary effects) is assumed to be the means of the three individual boundary effects and is shown in the equation (7-15).

$$CR_l = A_l * exp\ (B_l/X_l) + C_l * exp\ (D_l/X_l) + F_l \qquad (7\text{-}12)$$

$$CR_r = A_r * exp\ (B_r/X_r) + C_r * exp\ (D_r/X_r) + F_r \qquad (7\text{-}13)$$

$$CR_b = A_b * exp\ (B_b/X_b) + C_b * exp\ (D_b/X_b) + F_b \qquad (7\text{-}14)$$

$$CR = (CR_l + CR_r + CR_b)/3 \qquad (7\text{-}15)$$

Where, the subscript *l, r b* denote the left, right and bottom boundaries.

Because both left and right edges are simply supported and the panel is symmetrical, boundary effects of the left edge and right edge are same, therefore the constants in (7-12) and (7-13) are the same one. Subsequently, only 10 independent coefficients are needed to be assigned by the GA and corrector factors at all points on the panel are thereby derived.

The corrector factors obtained using the constraint functions as shown in equation (7-12), (7.13), (7.14), (7-15) are presented in Table 7.9. The 3D plot of the obtained corrector factors is shown in Figure 7.15, and the load deflection relationships using these corrector factors are shown in Figure 7.16.

From Figure 7.16, it is clear that the load deflection relationships agree well with the experimental results. Comparing Figure 7.15 with Figure 7.12, it can be seen that using a constraint function, the corrector factors along the bottom edge still decrease, but those along the two vertical edges slightly increase, and the central parts of the panel appear much flatter.

The physical meanings of these corrector factors are becoming clearer. They reveals that: for a masonry panels with boundary conditions like two vertical edges simply supported, the bottom edge built-in and the top edge free, they are only the ideal assumptions. The real boundary condition in the experiments is that the built-in side tends to be less constrained and some rotation has occurred where the simply supported sides tends to be slightly constrained against rotation.

Table 7.9, Corrector factors derived by GA with constraint function (symmetrical left half)

err=0.2461	1	2	3	4	5
a	1.6073	1.1063	1.1320	1.1383	1.1397
b	1.5870	1.0860	1.1117	1.1180	1.1193
c	1.5263	1.0253	1.0510	1.0573	1.0587
d	0.7173	0.2163	0.2420	0.2483	0.2497
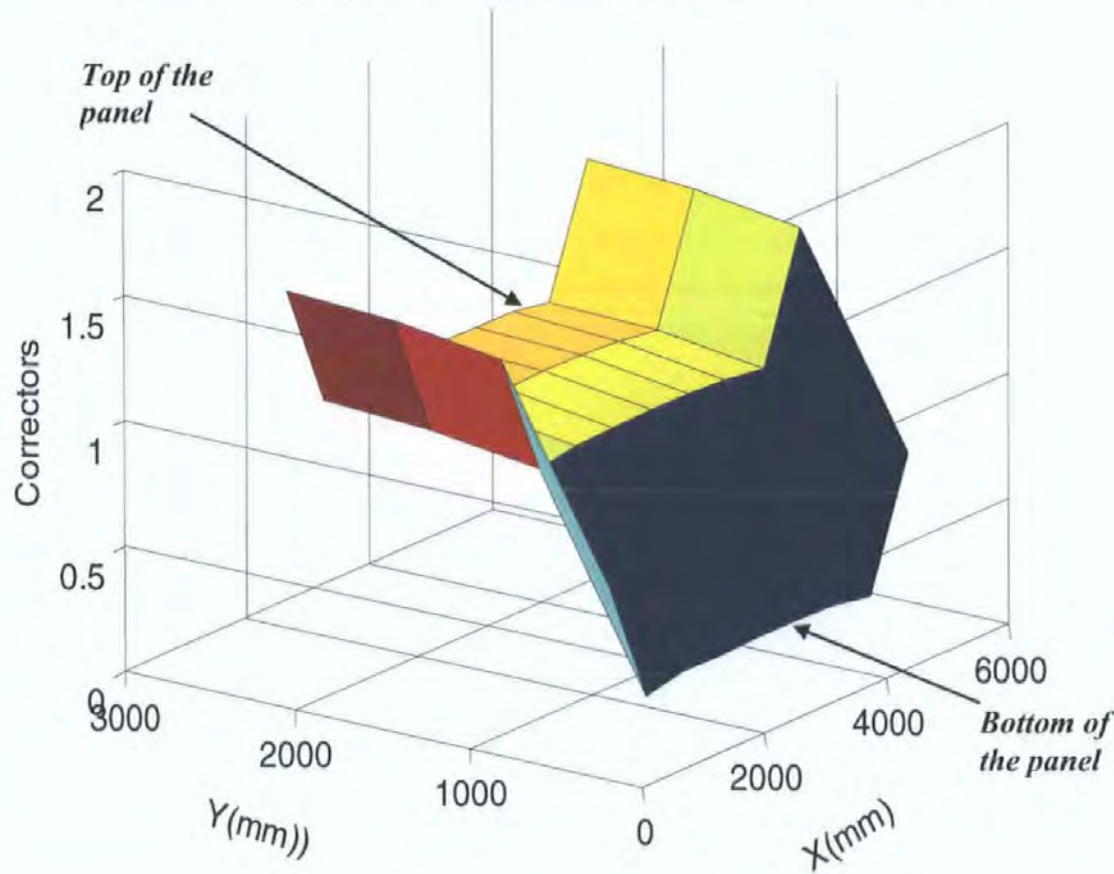
Figure 7.15, 3D plot of corrector factors derived by GA using a constraint functions
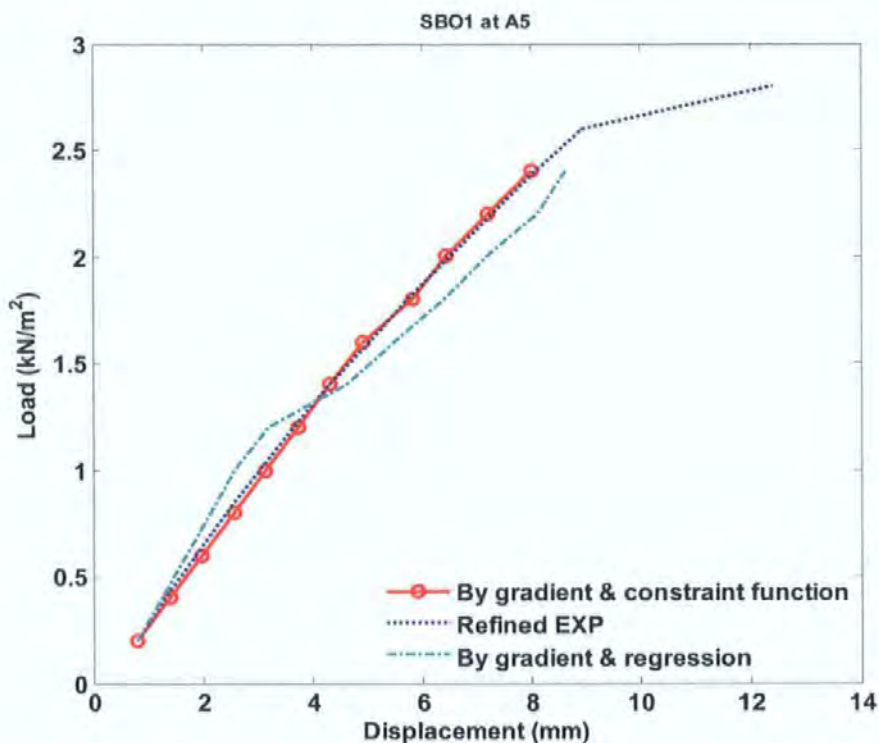
Figure 7.16, Load deflection relationships using the corrector factors obtained with a constraint function

However, it has been found that, using equation (7-12) to (7-15) as the constraint function is difficult to get convergence. Because expressing both the increasing and decreasing boundary effects simultaneously using equation (7-11), the coefficient in the equation must be defined in a relatively larger range, which is very likely to get to the local optima. Therefore, the GA search using two equations as the constraint function is studied in the next section.

7.4.4.2 Using separate constraint function for each boundary type

Two kinds of boundary effects in SBO1 in Figure 7.15 could be expressed separately using equations (7-16), (7-17).

$$CR_i = A_i (1 - B_i C_i^{Xi}) \qquad (7-16)$$

$$CR_d = A_d (1 + B_d C_d^{Xd}) \qquad (7-17)$$

Where the subscript i, d denotes the constraint function of increasing and decreasing tendency respectively, A, B, C are the coefficients, X is the distance from the zone centre to the relevant boundary. When $A \geq 0$, $B \geq 0$, $0 < C < 1$, the term C^x will be monotonously decreasing with increasing values of x, therefore, CR_i represents the boundary effects of deceasing tendency. CR_d represents the boundary effects of increasing-tendency (from the boundary to the centre on the panel).

Therefore, the boundary effects from the bottom built-in boundary and the two vertical simply supported boundaries can be expressed using equation (7-16) and equation (7-17) respectively as shown in equations (7-18), (7-19),(7-20).

$$CR_l = A_l(1 + B_l \, C_l^{Xl}) \tag{7-18}$$

$$CR_r = A_r(1 + B_r \, C_r^{Xr}) \tag{7-19}$$

$$CR_b = A_b(1 - B_b \, C_b^{Xbi}) \tag{7-20}$$

Where, the subscript l, r b denote the left, right and bottom boundaries. Similar to section 7.4.4.1, the corrector factors (or say the total boundary effects) is still assumed to be the means of the three individual boundary effects and is shown in the equation (7-21).

$$CR = (CR_l + CR_r + CR_b)/3 \tag{7-21}$$

Where, CR is the total boundary effect.

Using equation (7-18) ,(7-19) and (7-20) to express the boundary effects from the bottom edge and the two vertical edges of SBO1, the corrector factors obtained are shown in Table 7.10, the 3D plot and the load deflection relationships are shown in Figure 7.17, 7.18 respectively.

Comparing Table 7.10 with Table 7.9, or Figure 7.17 with Figure 7.15, it can be seen that corrector factors obtained using two constraint functions are similar to those of using single constraint function. The difference is that, corrector factors appear a little

different along the horizontal direction, which means the boundary effects from the vertical simply supported edges are not as big as those from the built-in edge at bottom. Figure 7.18 show that, using the correctors derived by the two constraint function, the load deflection relationships are further improved. Moreover, the "kink" remains not present although some small turns still occur on the curve but it is acceptable, because trying to acquire a smooth curve is not necessary considering the errors in real experimental data.

Table 7.10 corrector factors by GA using two constraint functions

err=0.1466	1	2	3	4	5
a	1.283	1.278	1.277	1.277	1.277
b	1.187	1.181	1.181	1.181	1.181
c	0.926	0.921	0.920	0.920	0.920
d	0.223	0.218	0.217	0.217	0.217

Comparing Table 7.10 with Table 7.9, or Figure 7.17 with Figure 7.15, it can be seen that corrector factors obtained using single constraint functions are similar to those of using two constraint functions. The corrector factor values appear a little different along the horizontal direction, even for those near the vertical simply supported edges, which means the boundary effects from the vertical simply supported edges are limited. Figure 7.18 show that load deflection relationships are further improved. Moreover, the "kink" has disappeared although some small turns still occur on the curve but it is acceptable, because trying to acquire a smooth curve is not necessary considering the errors in real experimental data.

Corrector factors by GA with two constraint function

Top of the panel

Bottom of the panel
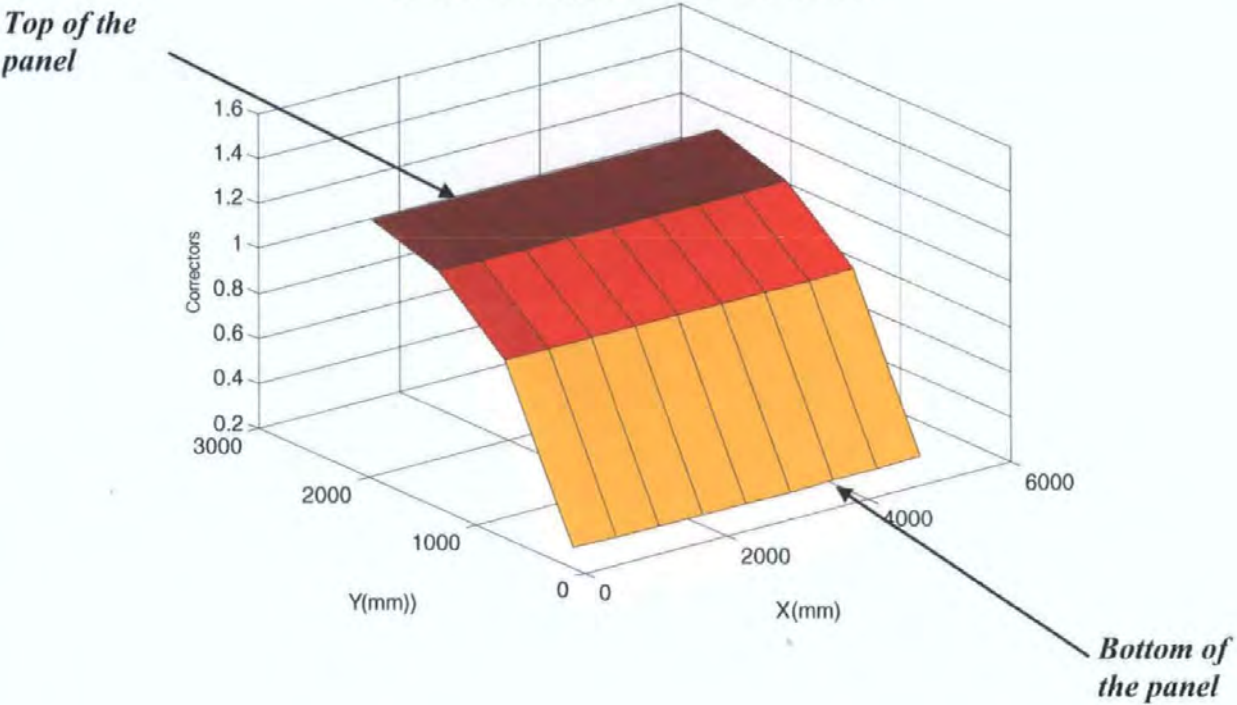
Figure 7.17 3D plot of the corrector factors derived using two constraint functions
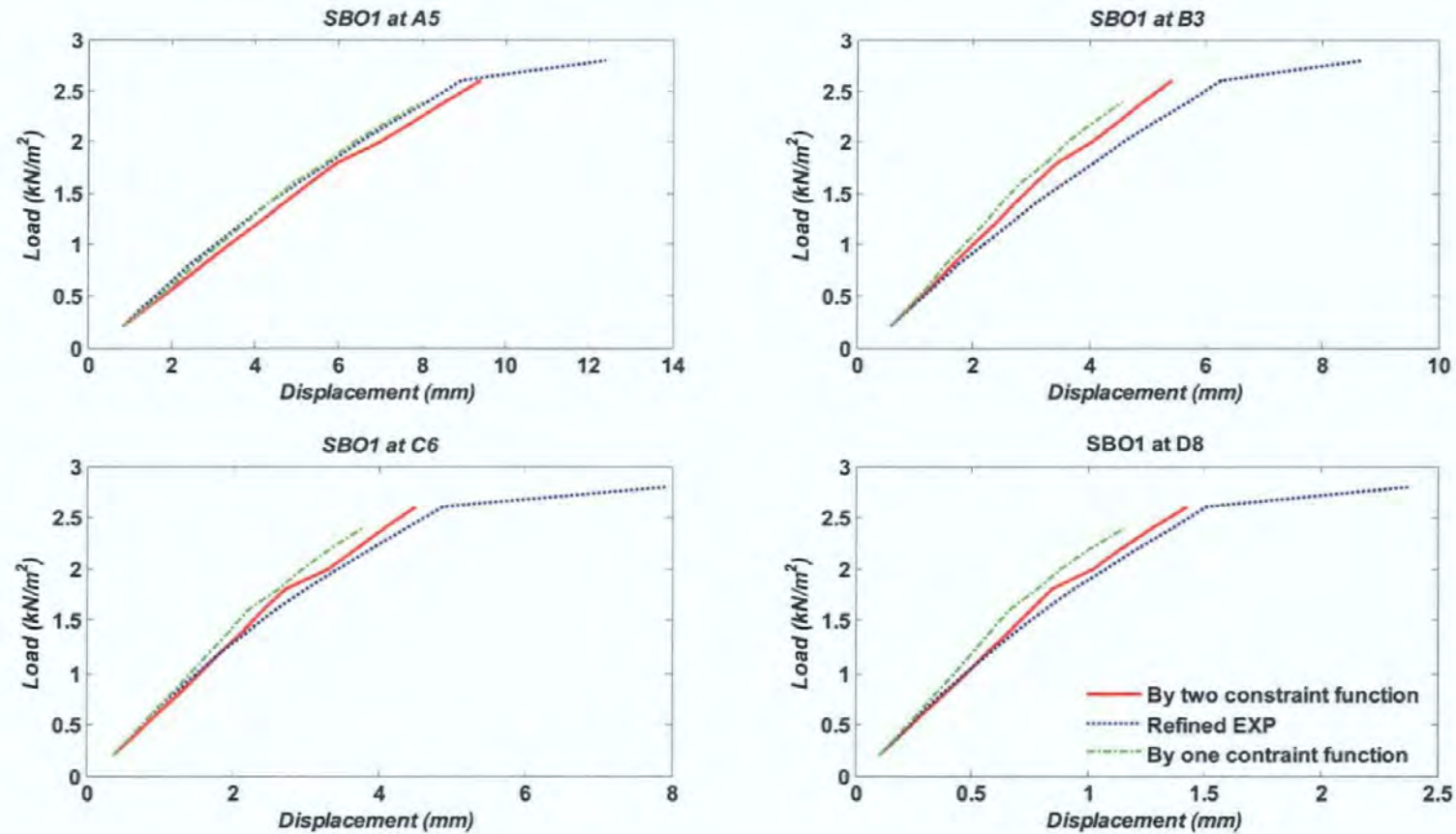
Figure 7.18 Comparison of using corrector factors derived by one and two constraint function

7.5 Derive the strength-corrector factors

Looking again at Figure 7.18, it can be seen that although the deflections from FEA using corrector factors match the experimental deflections well, there is still an error in matching the failure load. From Chapter 6 it is clear that failure load is mainly affected by flexural strength but less affected by the flexural stiffness. Therefore, in this section flexural strength will be selected as the parameter for model updating, whereas the flexural stiffness-corrector factors in Table 7.9, 7.10 are kept unchanged. Here it is not necessary to assign different strength values to different zones, because the objective to update the strength is to improve the response of the FEA model on failure load, the smeared model can meet this demand, i.e. strengths values in all zones are equal.

The GA is used to derive strength-corrector factors and the objective function as shown in equation (7-10) is once again used. The strength-corrector factors in Table 7.9 and Table 7.10 are derived as shown in Table 7.11, the improved load-deflection relationships are shown in Figure 7.19.

Table 7.11, strength correctors derived by GA based on strength by Mote Carole analysis

	Table 7.10	Table 7.11
Cfx	1.489	1.473
Cfy	1.04	1.04

It should be noted that the strength corrector factors in Table 7.11 are used to revise strength values fx=2.28 N/mm^2, fy=0.965N/mm^2, they are the values obtained by Monte Carlo simulation but not the actual experimental strengths of wallette test (Chong 1993). Therefore, when using the actual experimental strengths of wallette test, the ratio between these Monte Carlo values and the actual experimental values should be considered. For the docked bricks (i.e. sunk into water before construction), the

corresponding wallette experimental flexural strength perpendicular and parallel to the bed joints is 2.09N/mm^2 and 0.740N/mm^2 respectively, for the undocked bricks; the corresponding wallette experimental flexural strength perpendicular and parallel to the bed joints is 1.67N/m^2 and 0.474N/m^2 respectively (Chong 1993). Therefore, the strength corrector factors in Table 7.11 become those in Table 7.12 and Table 7.13.

Table 7.12, strength correctors derived by GA based on experimental strengths (docked)

docked	Table 7.9	Table 7.10
Cfx	1.624	1.607
Cfy	1.356	1.356

Table 7.13, strength correctors derived by GA based on experimental strengths (undocked)

undocked	Table 7.9	Table 7.10
Cfx	2.033	2.011
Cfy	2.117	2.117

Figure 7.19 shows that using the strength-corrector factors together with stiffness-corrector factors, both the deflections and the failure load of FEA match the experimental ones well. Table 7.10 to Table 7.13 shows that the derived strength-corrector factors based on the two groups of stiffness-corrector factors are quite similar, which once again proves that the strength is less affected by the flexural stiffness.
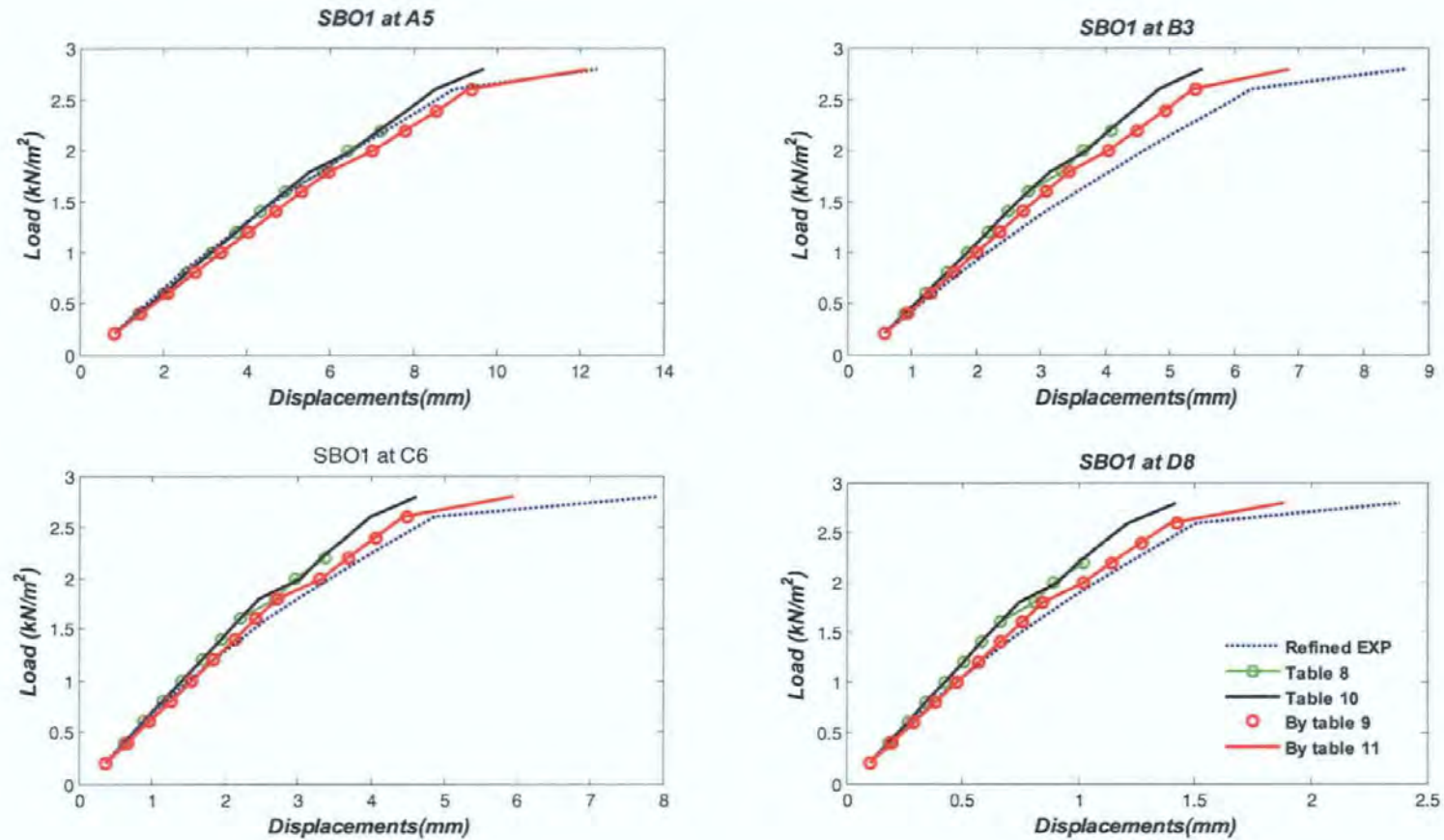
Figure 7.19 comparisons of using different strength corrector factors

7.6 Check the failure pattern using stiffness and strength corrector factors

Figure 7.20, 7.21 are the experimental failure pattern of masonry panel SBO1 & 5, which have the same dimension and configuration (see section 4.7.1 in chapter 4).Figure 7.22 are the principal stress contour plot at the failure load level $(2.6KN/m^2)$.Obviously that the failure pattern using corrector factors are quite similar to the experimental ones.

Figure 7.19 the experimental failure pattern of masonry panel SBO1
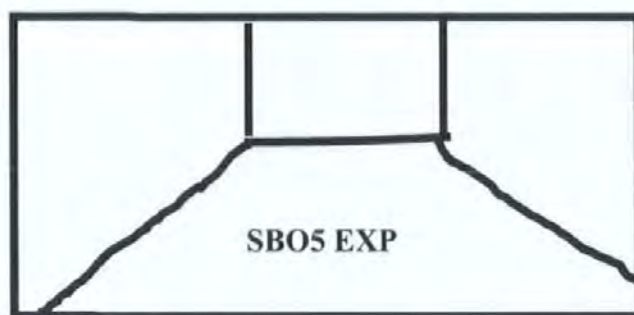
Figure 7.20 the experimental failure pattern of masonry panel SBO6

Principal stress contour of SBO1 using correctors on the outer surface at 2.6 kN/m^2,
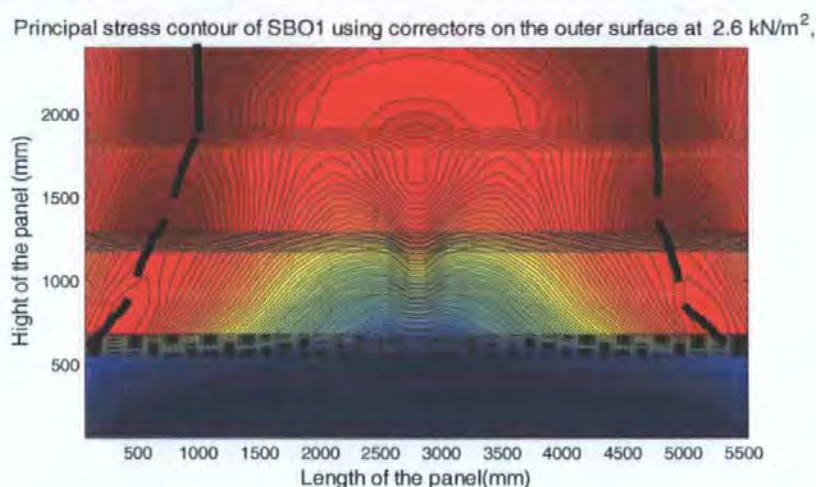
Figure 7.21 the experimental failure pattern of masonry panel SBO1

7.7 SUMMARY

Based on model updating process used in this chapter, the following findings are achieved:

- The smear model can not model the real behaviour of the masonry panels; it needs to be modified to become an updating model, i.e. using corrector factors, to assign different flexural stiffness to different parts of the panel.

- The genetic algorithm is an effective tool for model updating process. With the gradient added to the objective function and along with using constraint function to represent the boundary effects, the GA is more likely to converge to smaller error and thereby the corrector factors is obtained.

- The derived corrector factor indicated that, in the FEA model, defining the built-in edge to be totally fixed is not adequate, some rotation occurred at the built-in laboratory edge. Similarly, defining the simply supported edge to be totally free against rotation is not suitable, because the simply supported edge in laboratory might be restrained in rotation to some extent.

- Strength-corrector factors are independent to stiffness corrector factors. Strength corrector factors mainly modify the flexural strength perpendicular to the bed joints rather than parallel ones and thereby improve the failure load.

Because model updating process solves a reverse problem, which means the obtained solutions might not be the unique one. Therefore, uniqueness of the model updating is further studied in next chapter.

8. THE EXTENDED STUDY OF CORRECTOR FACTORS

8.1 INTRODUCTIONS

The stiffness-corrector factors derived using model updating techniques in Chapter 7 indicated that, the real boundary conditions of masonry panels (such as SBO1) are different from those defined in the FEA model, the actual built-in edge tends to be less constrained, and the actual simply supported edges tend to have some resistance to rotation in the experiment.

However, deriving corrector factors by model updating techniques in fact is solving a reverse problem. From the mathematical point of view, the solution of such reverse problem could be many rather than a single one (unique solution); particularly when using the genetic algorithm, the obtained solution might be the local optima which results in the illogical solution such as discussed in section 7.3 or the local optima such as discussed in section 7.4.1 and 7.4.2.

Using two constraint functions is helpful to avoid the local optima for model updating process as introduced in section 7.4.4 in Chapter 7. Nevertheless, using the defined constraint function forcefully limit the solution space (i.e. the corrector factors were compulsorily restricted to be decreasing-tendency from simply supported edge to the centre of the panel, and increasing-tendency from the built-in edge to the centre of the panel). Therefore, there is such possibility that the global optima might locate outside of the solution space formed by the constraint function. Subsequently, more study should be carried out, to check whether the result obtained in Table 7.9 and 7.10 in Chapter 7 is the global optima, and the physical meaning they indicated is unique; this is termed a uniqueness study in the area of model updating.

In this chapter, the studies on uniqueness of corrector factors are carried out by investigating the entire solution space that is formed by all the combinations (permutation) of two constraint functions (7-16) and (7-17) and all the combinations (permutation) of the boundary types defined in the FEA model.

The uniqueness will be checked in two ways: (a) to compare the error in each possible case, (b) to check the physical meaning of the corrector factors obtained and compare the physical meaning with that indicated in Chapter 7.

8.2 THE PERMUTATION OF CONSTRAINT FUNCTIONS AND BOUNDARY TYPES

8.2.1 Permutation of the constraint function

In Chapter 7, because using a single constraint function to express boundary effects is more likely to get the local optima, then two independent constraint functions with increasing and decreasing tendency respectively were used (see Figure 7.14 in Chapter 7).

In section 7.4.4.2, equation (7-16) was used to express the boundary effects of built-in edge, and equation (7-17) was used to express the boundary effect of simply supported edges. This was based on the information discovered from Figure 7.15 which implied that the obtained corrector factors decreased from the simply supported edge to the centre of the panel, and increased from the built-in edge to the centre of the panel. In theory, each supported boundary has possibly two kinds of boundary effects, increasing tendency or decreasing tendency. To cater for all possible cases of boundary effects, it would be reasonable to study the permutation of this two kinds of boundary effects on all panel boundaries by applying equations (7-16) and (7-17) to each supporting edge separately. Because one supporting edge has two possible boundary effects, there would

be in total $2^3 = 8$ kinds of boundary effects for 3 supporting boundaries. However, the two vertical edges of SBO1 have the same boundary condition, therefore its 3 supporting boundaries could be regarded as the two kinds of boundaries (simply supported and built-in) and the total cases of applying the constraint functions to the two kinds of supporting edges would be $2^2 = 4$. Denote the constraint functions of increasing and decreasing tendency as **i** and **d** respectively, and **o** for no constraint function at the top free edge, the whole cases can be denoted as **ddio, iido, dddo, iiio** (in the order from left, right, bottom to top edge) as listed as below which is presented in Figure 8.1
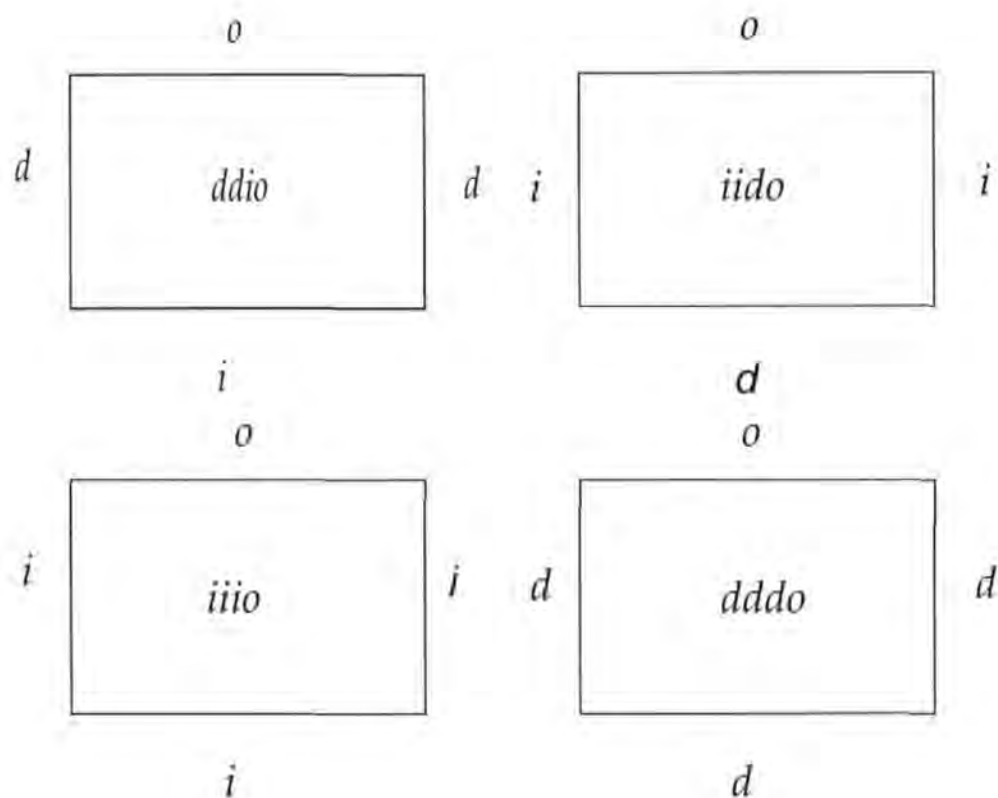
Figure.8.1 permutation of the constraint functions

1. The constraint function of decreasing-tendency is applied to the simply supported vertical edges and that of the increasing-tendency is applied to the built-in bottom edge (***ddio***).

2. The constraint function of increasing-tendency is applied to the vertical edges and that of the decreasing-tendency is applied to the bottom edge (***iido***).

3. The constraint function of decreasing-tendency is applied to both the vertical edges and bottom edge (***dddo***).

4. The constraint function of increasing-tendency is applied to both the vertical edges and bottom edge (***iiio***).

8.2.2 Permutation of the defined boundary types

In the previous studies, the boundary types of the panel SBO1 in the FEA model were defined as two vertical edges simply supported, the bottom edge built-in and the top edge free, to correspond to the experimental tests. However, since the corrector factors obtained in Table 7.9 & 7.10 indicated that the simply supported edges appeared to have some constraint against rotation and the built-in edge appears to allow some degree of rotation. This means that the real boundary conditions in the actual experiments is neither simply supported nor built-in but are in between the two ideal boundary conditions. Therefore, it is reasonable to define any actual supporting boundaries to be either "simply supported" or "built-in" in the FEA model. Subsequently, forcefully defining the vertical edges to be simply supported and bottom edge to be built-in in the might be at the risk of constructing a "wrong" model. This kind of "wrong" model is more likely to result in the local optima. Therefore, further investigation to corrector factors based on the alternative definition of the boundary conditions in the FEA should be carried out as illustrated bellow.

Similar to section 8.2, because each supporting edge can be either defined to be simply supported or built-in, and there are in fact two kinds of the supported boundary edges due to the symmetry of the masonry panel SBO1, the total kinds of the defined boundary conditions are the permutation of the two boundary conditions, i.e. in total 2 x 2 = 4 kinds of defined boundary conditions, they are:

(1) The vertical edges are simply supported and the bottom edge is built-in.

(2) The vertical edges are built-in and the bottom edge is simply supported.

(3) All the vertical edges and bottom edge are simply supported.

(4) All the vertical edges and bottom edge are built-in.
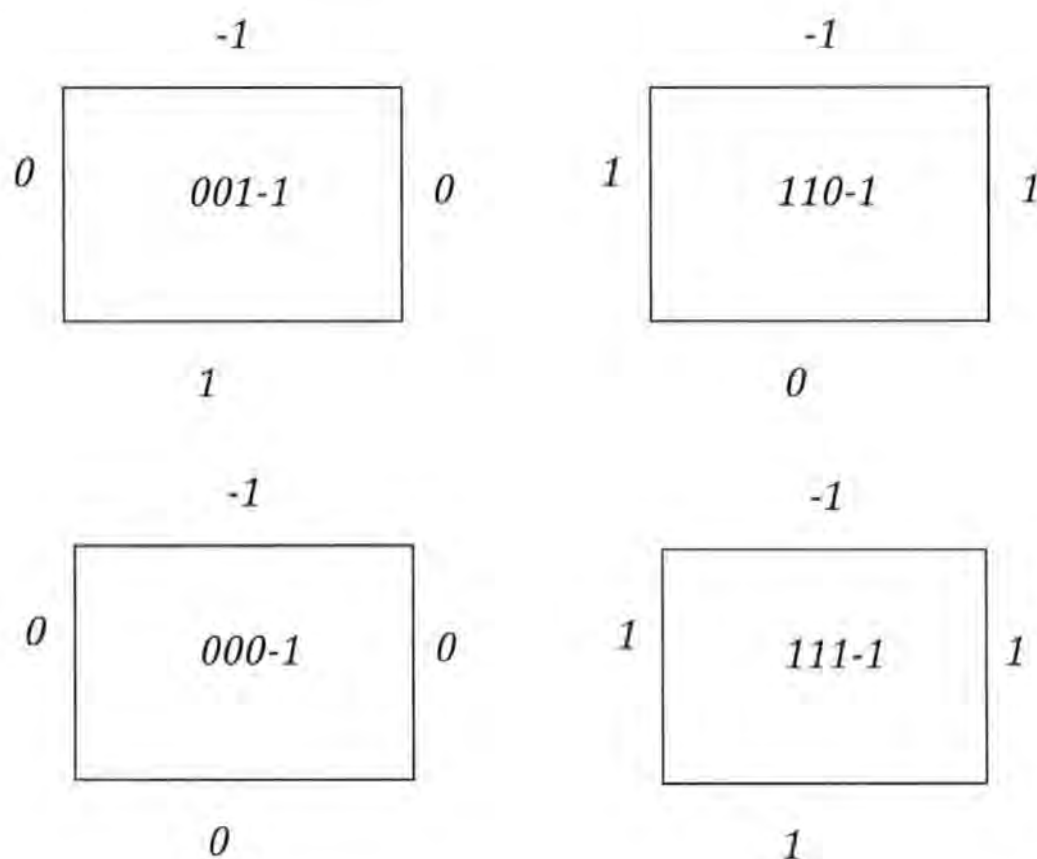
Figure 8.2, the permutation of the boundary conditions

In BS 5628, simply supported edge is denoted as 0, built-in edge is denoted as 1 and free edge is denoted as -1, then the permutation of the defined boundary conditions in the FEA model of SBO1 would be: **001-1, 110-1,111-1,000-1,** (in the order of left, right, bottom and top edge, see Figure 8.2).

Consequently, considering all cases as introduced in section 8.1 and this section, the extended investigation to corrector factors are involve in total of 16 cases as listed as in Table 8.1:

Table 8.1, Total cases need to be investigated to avoid local optima (uniqueness study)

Constraint function / Defined boundary conditions	ddio	iido	iiio	dddo
001-1	Section 7.4.4.2	yes	yes	yes
110-1	yes	yes	yes	yes
111-1	yes	yes	yes	yes
000-1	yes	yes	yes	yes

8.3 CORRECTOR FACTORS BY CHANGING THE DEFINITION OF BOUNDARY CONDITIONS AND THE ASSIGNMENT OF CONSTRAINT FUNCTIONS

8.3.1 Comparing the errors resulted from all sixteen cases

Using equation (7-10) as the objective function of the GA, the error resulted from each case is summarised in Table 8.2. It should be mentioned that, the solution from each round of the GA search is not exactly the same but they are similar. The values in Table 8.2 are only one of those solutions, the results of other repeated searches would be

slightly different but the values in Table 8.2 still have the same feature. In Table 8.2, for

each defined boundary conditions in the FEA model, there is a set of constraint function

which make the smallest error; they are 001-1/ddio, 110-1/iido, 111-1/iiio,000-1/dddo

(the diagonal values in the table).

Table 8.2 Discrepancies between FEA and EXP

Constraint functions Defined Boundary conditions	ddio	iido	iiio	dddo
001-1	0.135	0.217	0.136	0.281
110-1	0.265	0.133	0.176	0.278
111-1	0.221	0.193	0.176	0.261
000-1	0.225	0.223	0.199	0.180

Table 8.2 reveals that, applying the constraint function of increasing-tendency to the

defined built-in edge and that of decreasing-tendency to built-in edges, the FEA give

smallest error. Because the constraint functions of increasing and decreasing tendency

make the zone near the simply supported boundary stiffer but make the zones near the

built-in edge less stiff, it is indicated that the actual built-in edge is not totally fixed and

the simply supported edges are not totally free for rotation. This conclusion is the same

to those obtained in Chapter 7.4.4.2.

8.3.2 Detailed analysis of corrector factors under different defined boundary conditions.

As mentioned in section 8.1, there are in total of 4 kinds of possibly defined boundary

conditions, the corrector factors for each boundary conditions are studied as follows.

8.3.2.1 Defining the boundary conditions as the vertical edges simply supported and the bottom edge built-in (001-1) in FEA

Defining the bottom edge built-in and two vertical edges simply supported and the top edge free (110-1), considering all the permutation of the two constraint function with increasing and decreasing tendency and apply them to the supported boundaries, the derived corrector factors are shown in Table 8.3, 8.4, 8.5, 8.6 and their 3D plot are presented in Figure 8.1, 8.2, 8.3, 8.4.

From Figure 8.5 and Table 8.2, it can be seen that, beside 001-/ddio which results in the smallest error, the error of 001-1/iiio is also far smaller than other two cases 001-1/iido and 001-1/dddo, they give larger errors.

Comparing Tables 8.3 and Table 8.5, or compare Figure 8.3 and Figure 8.5, it can be seen that, the values and distribution of two groups of corrector factors are quite similar. The corrector factors near the defined built-in bottom edge are much smaller than the rest, which means the actual boundary condition is not as fully fixed as defined in the FEA model. Therefore, smaller stiffness is assigned to these zones to represent the reduced fixity of the boundary. Also it can be seen that, the derived corrector factors have the quite smaller variation along the horizontal direction, which means the boundary effects from the vertical edges are small.

However, for the other two cases 001-1/iido and 001-1/dddo, the higher corrector factors are compulsorily assigned to zones near the fixed edge at bottom of the panel. This means to illogically further constrain the absolutely fixed boundary. Subsequently, Figures 8.4 and Figure 8.6 (or Tables 8.4 and Table 8.6) show an opposite effect to that pattern of corrector factors shown in Figures 8.4 and Figure 8.6 respectively, and appear totally flat from the base to the top of the panel, to assign the values as smaller as possible.

Table 8.3 The corrector factors of SBO1 under 001-1/ddio

001-1/ddio	1	2	3	4	5
A	1.184	1.167	1.161	1.159	1.159
B	1.128	1.111	1.105	1.104	1.103
C	0.931	0.914	0.908	0.907	0.906
D	0.234	0.216	0.211	0.209	0.208
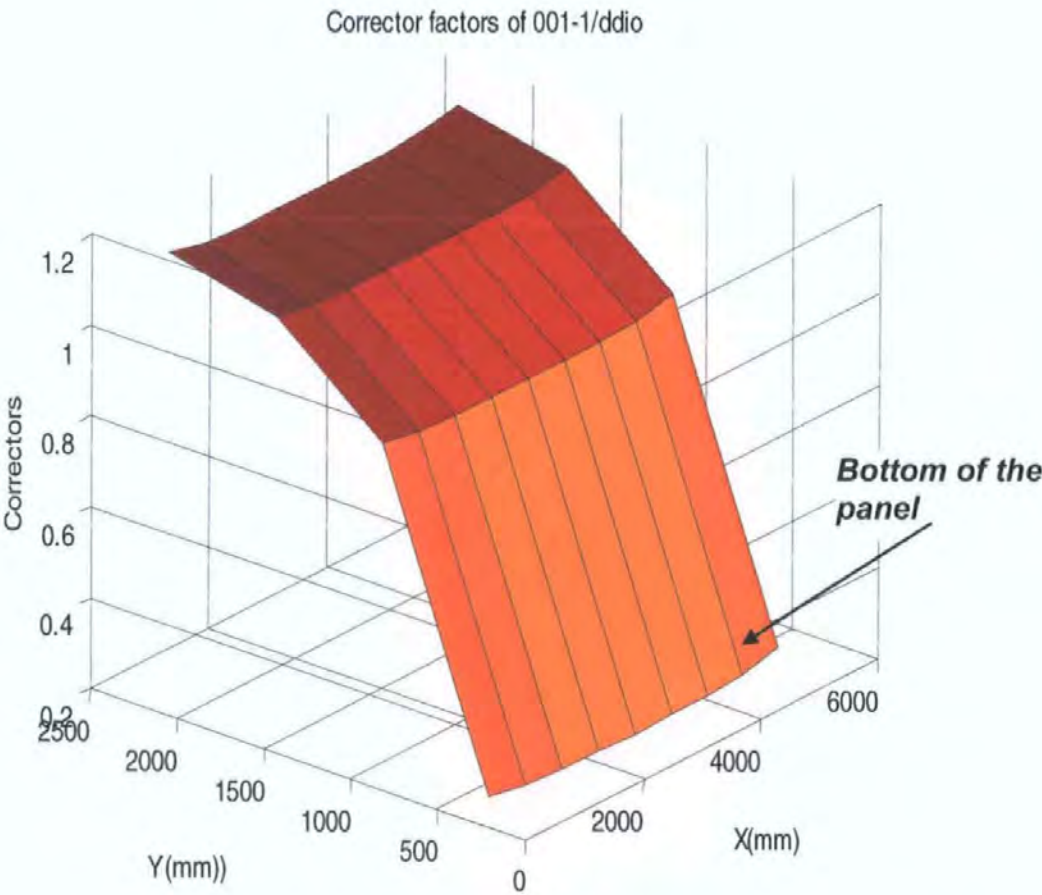
Figure 8.3, 3D-Plot of the corrector factors of SBO1 under 001-1/ddio

Table 8.4 the corrector factors of SBO1 under 001-1/Iido

001-1/iido	1	2	3	4	5
A	0.739	0.913	1.014	1.067	1.083
B	0.74	0.913	1.015	1.068	1.084
C	0.741	0.914	1.016	1.069	1.085
D	0.742	0.915	1.017	1.069	1.085
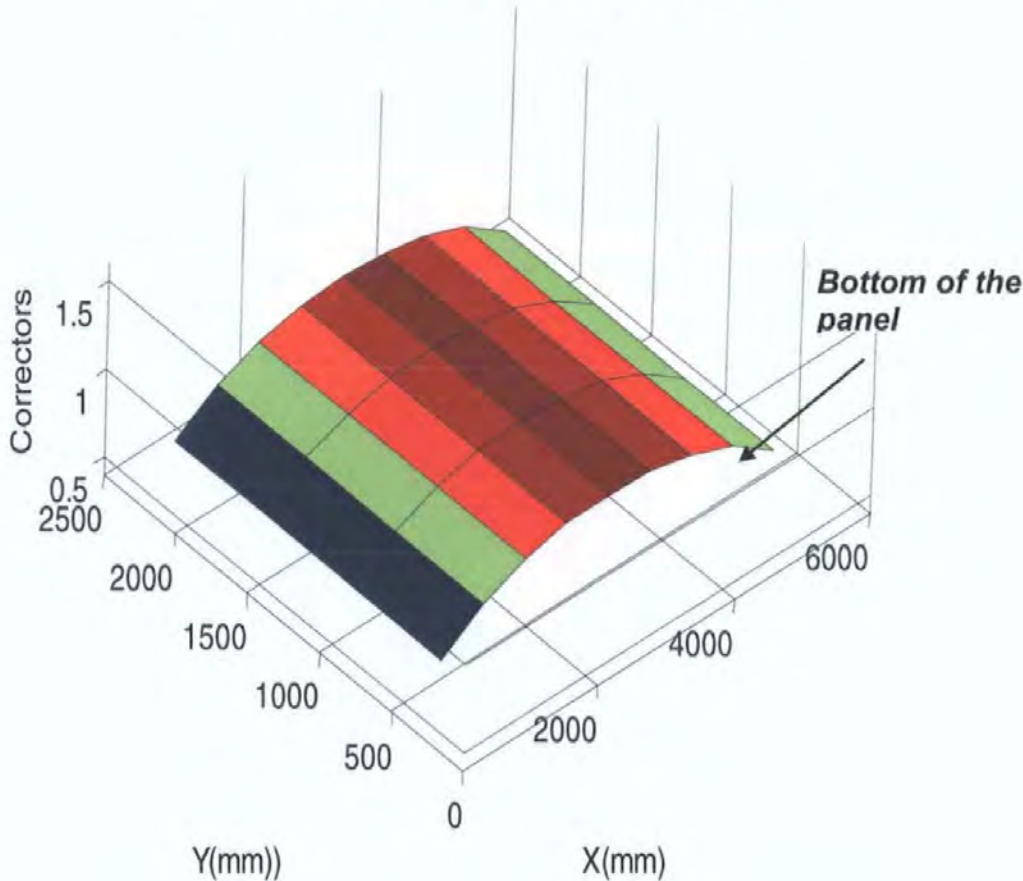
Figure 8.4 3D-plot of corrector factors of SBO1 under 001-1/iido

Table 8.5 Corrector Factors of SBO1 under 001-1/iiio

001-1/iiio	1	2	3	4	5
A	1.303	1.361	1.402	1.427	1.435
B	1.235	1.293	1.334	1.359	1.367
C	0.989	1.047	1.088	1.113	1.121
D	0.1	0.158	0.2	0.224	0.232
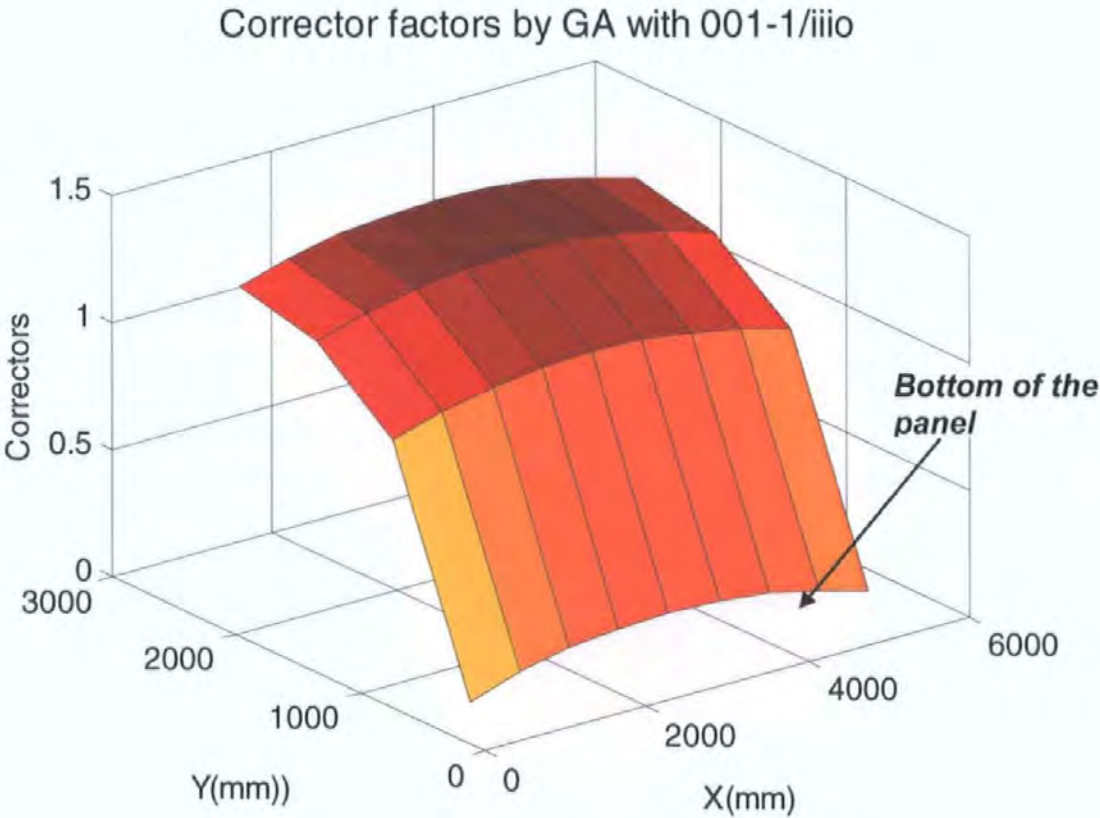
Figure 8.5 3D-Plot of the corrector factors of SBO1 under 001-1/iiio

Table 8.6 Corrector factors of SBO1 under 001/dddo

001-1/dddo	1	2	3	4	5
A	0.824	0.824	0.824	0.824	0.824
B	0.828	0.828	0.828	0.828	0.828
C	0.833	0.833	0.833	0.833	0.833
D	0.839	0.838	0.838	0.838	0.838

Corrector factors by GA with 001-1/dddo
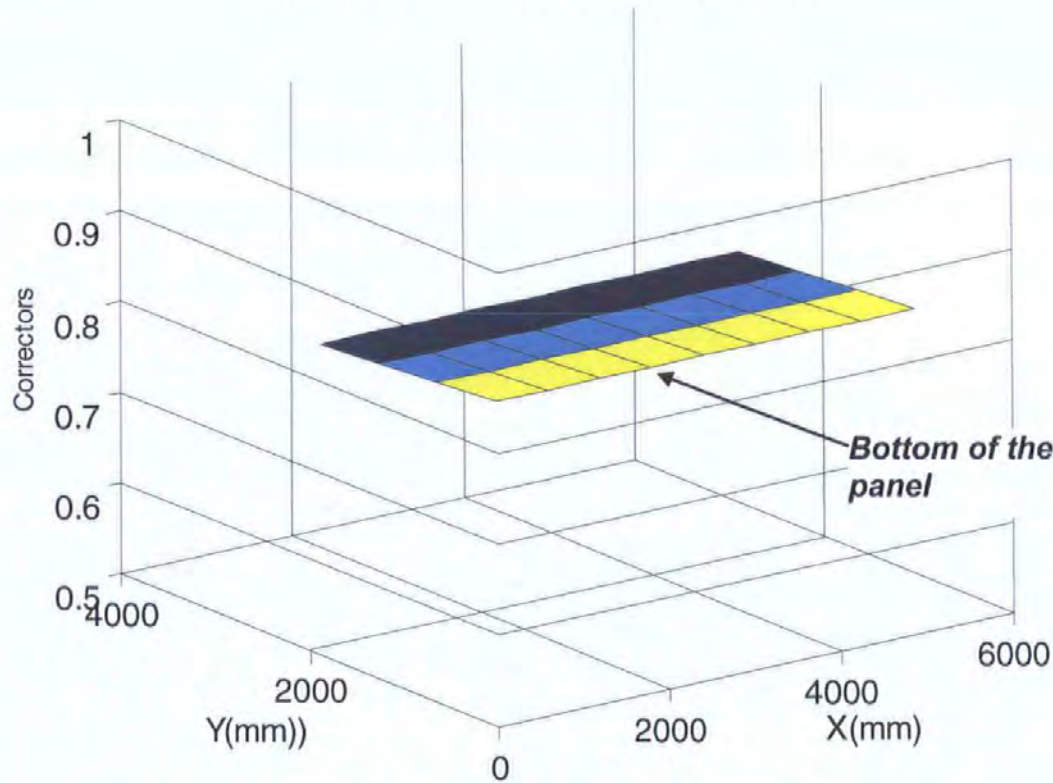
Figure 8.6 3D-Plot of corrector factors of SBO1 under 001-1/dddo
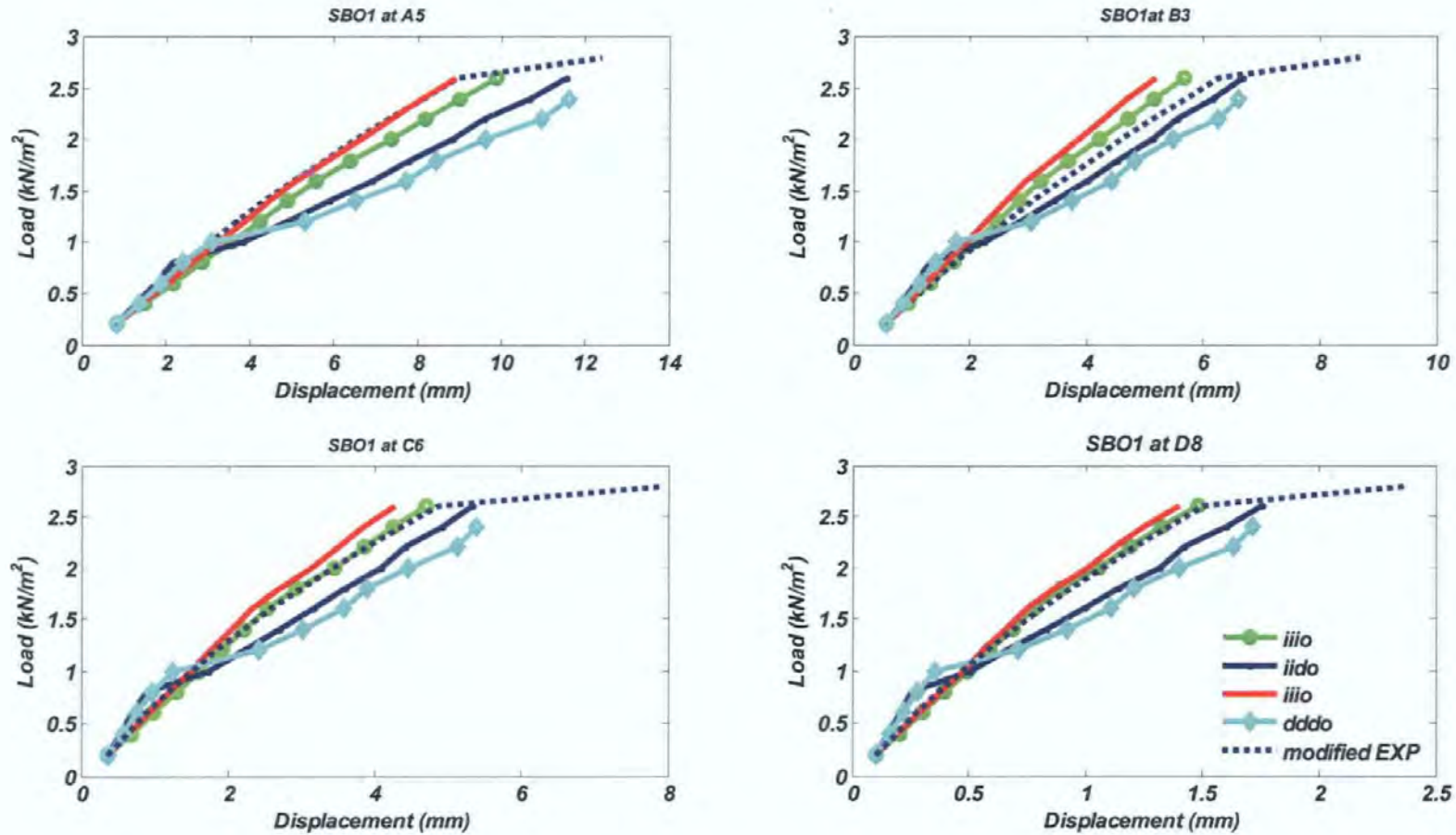
Figure 8.7 Load deflection relationships by corrector factors under 001-1

8.3.2.2 Defining the vertical edges as built-in and the bottom edge as simply supported (110-1) in FEA

Defining the bottom edge simply supported and two vertical edges built-in and the top edge free (110-1), considering the permutation of the two constraint function are applied to each supported boundaries, the corrector factors are derived and shown in Table 8.7, 8.8, 8.9, 8.10 and their 3D plot are presented in Figure 8.8, 8.9, 8.10, 8.11.

Table 8.7 Corrector factors under different constrain function with defining different boundary conditions

110-1/ddio	1	2	3	4	5
A	0.740	0.739	0.738	0.737	0.737
B	0.742	0.740	0.739	0.739	0.739
C	0.745	0.743	0.742	0.742	0.742
D	0.751	0.750	0.749	0.748	0.748
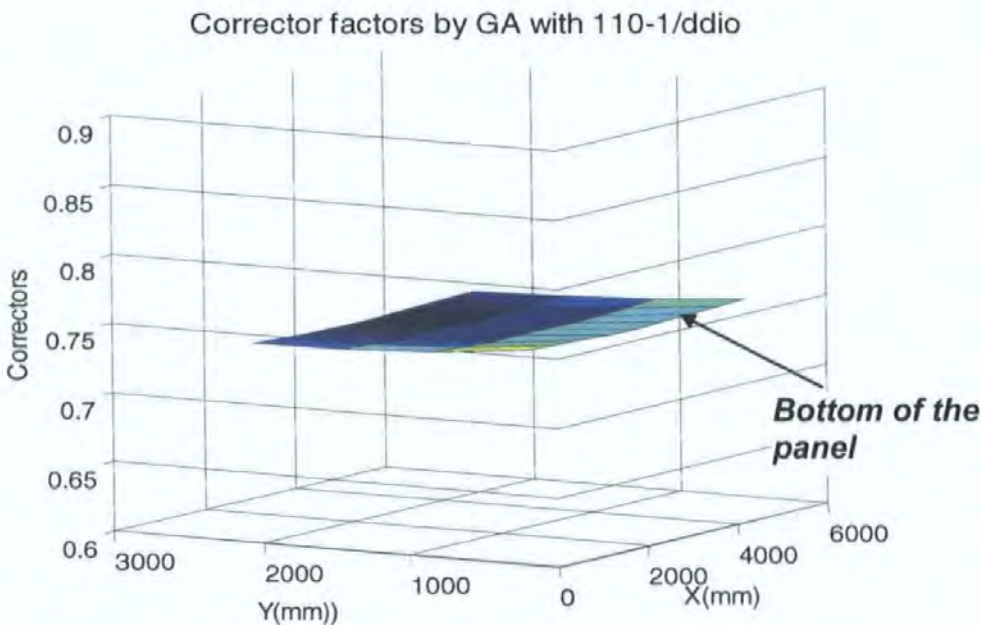
Figure 8.8 3D-Plot of corrector factors of SBO1 under 110-1/ddio

Table 8.8 Corrector factors under *110-1/iido*

110-1/iido	1	2	3	4	5
A	0.063	0.973	1.480	1.735	1.812
B	0.100	1.010	1.517	1.772	1.849
C	0.179	1.088	1.595	1.850	1.927
D	0.345	1.255	1.762	2.017	2.094

Corrector factors by GA with 110-1/iido
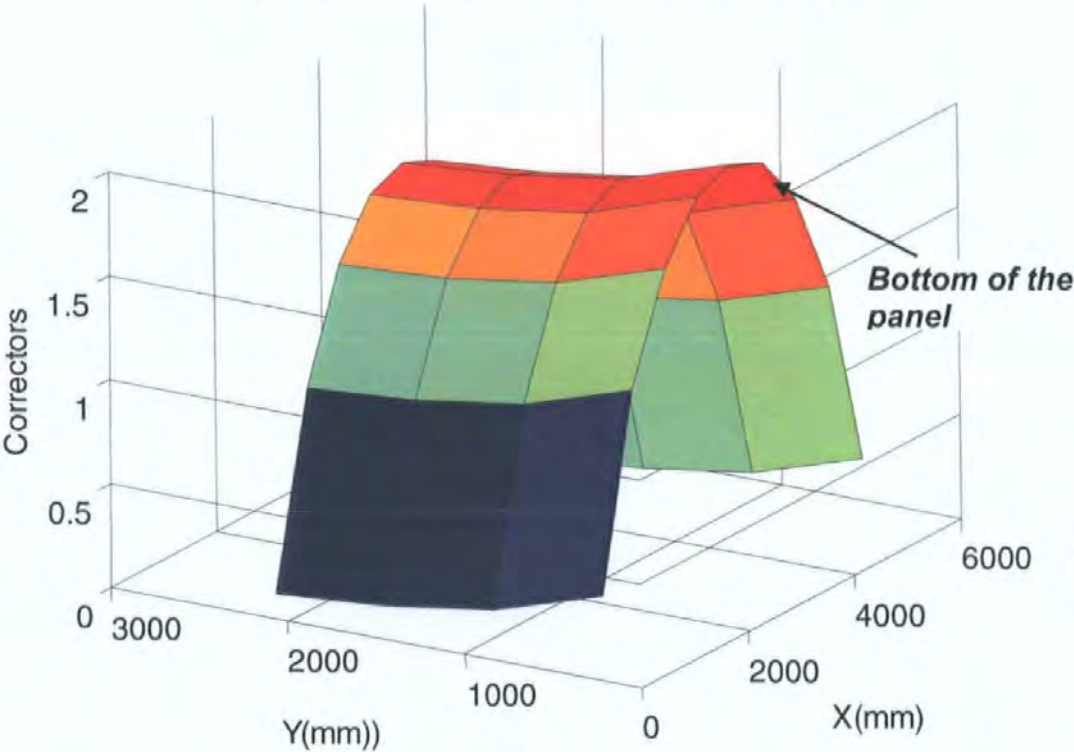
Figure 8.9 3D-plot of corrector factors of sbo1 under 110-1/iido

Table 8.9 Corrector factors under 110-1/iiio

110-1/iiio	1	2	3	4	5
A	0.364	0.692	0.884	0.984	1.015
B	0.363	0.692	0.884	0.984	1.015
C	0.363	0.692	0.884	0.983	1.015
D	0.362	0.691	0.883	0.983	1.014
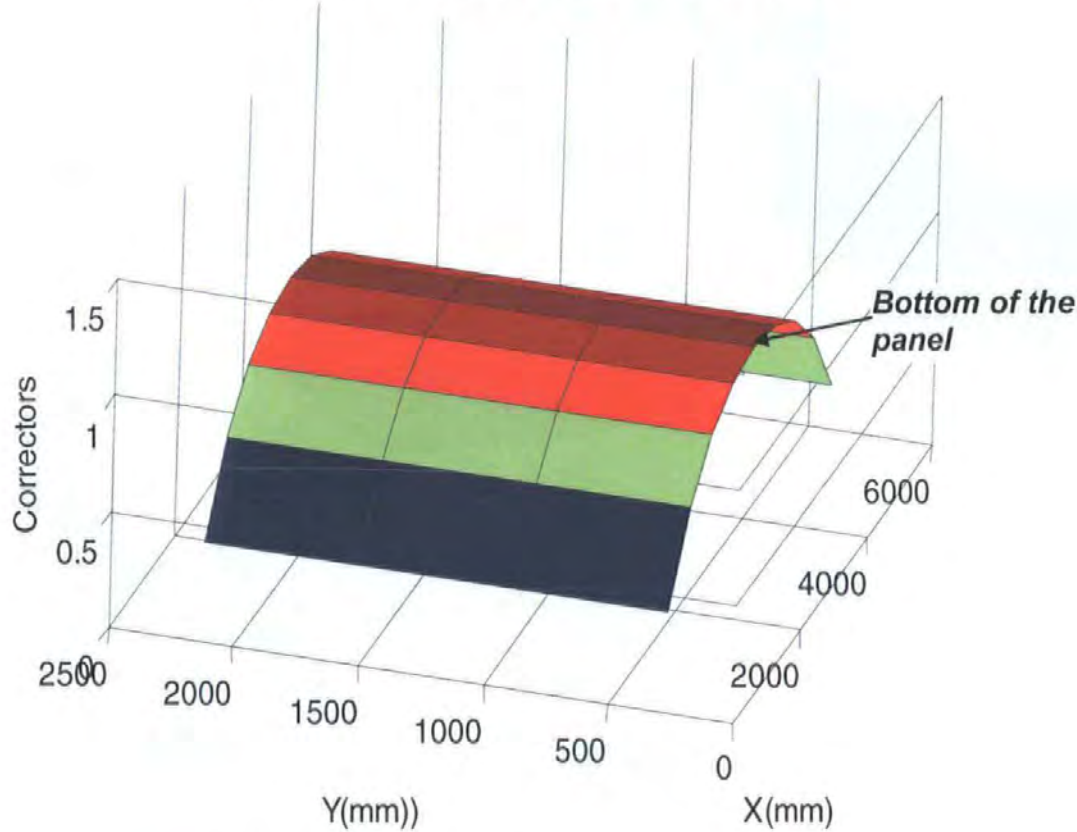
Figure 8.10 3D-plot of corrector factors of sbo1 under 110-1/iiio

Table 8.10 Corrector factors under 110-1/dddo

110-1/dddo	1	2	3	4	5
A	0.734	0.734	0.733	0.734	0.734
B	0.734	0.734	0.733	0.734	0.734
C	0.734	0.734	0.733	0.734	0.734
D	0.734	0.734	0.733	0.734	0.734

Corrector factors by GA with 110-1/dddo
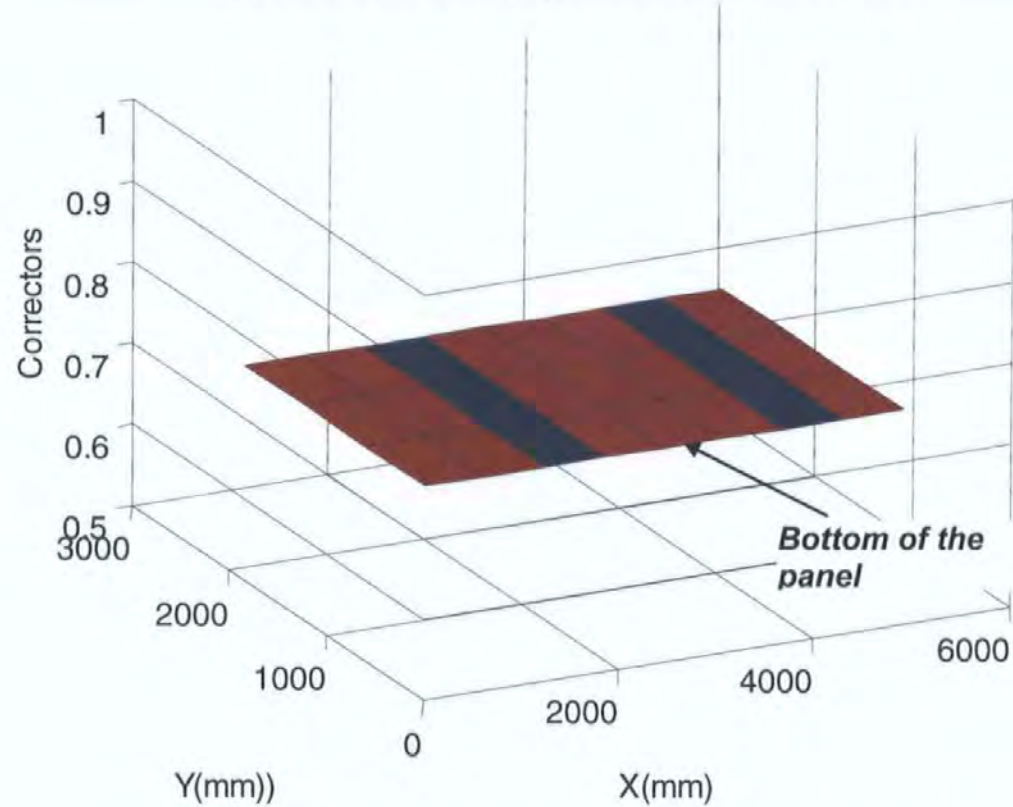
Figure 8.11 3D-Plot of corrector factors of sbo1 under 110-1/dddo

From Figure 8.12, it can be seen that the derived corrector factors can be divided to two sorts. One is the 110-1/iido and 110-1/iiio which give the better agreements to

the experiment. Another sort is 110-1/ddio and 110-1/dddo which make the poor agreements to experiment.

From Figure 8.9 and 8.10, which derived from the two cases 110-1/iido and 110-1/iiio which make the good agreements to experiments, it can be seen that their corrector factors are quite similar. Corrector factors are smaller along the two vertical edges due to using increasing tendency constraint function, which can free the defined built-in edge to better model the actual boundary conditions.

Moreover, for 110-1/iido, the decreasing-tendency constraint function assign larger corrector factors to the defined simply supported edge at the bottom, to match the actual boundary conditions. For 110-1/iiio, it intends to illogically further free the defined simply supported edge at the bottom of the panel. Therefore, 110-1/iido makes a better agreement than 110-1/iiio.

For another two cases, 110-1/ddio and 110-1/dddo, they make a poor match because corrector factors assigned by the constraint function illogically stiffen the defined built-in edge at two vertical side of the panel. Consequently, the corrector factors appear to be flat to weaken the stiffening effects (see Figure 8.8 and 8.11).
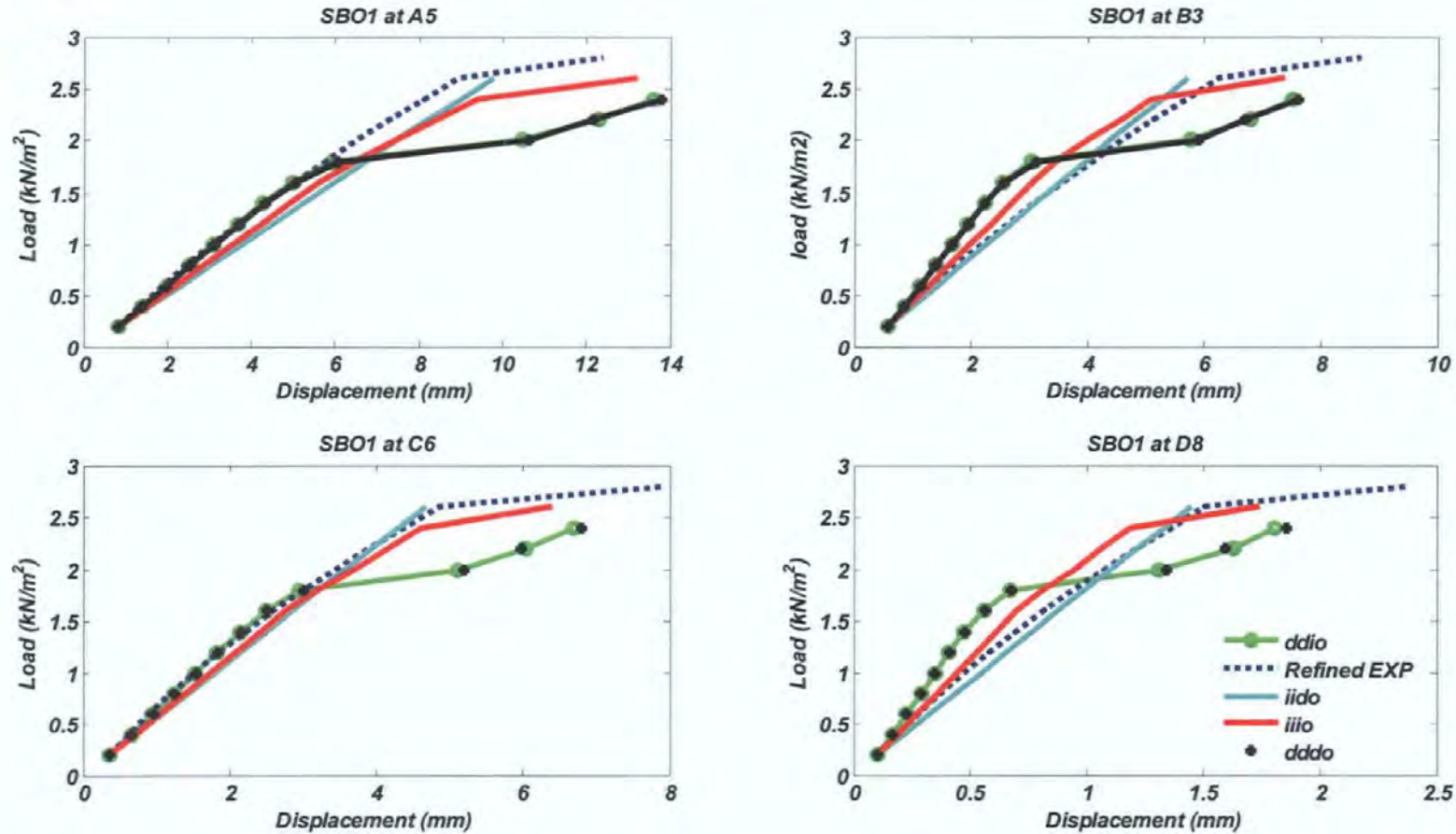
Figure 8.12, Load deflection relationships using corrector factors under 110-1

8.3.2.3. Defining all the supporting edges to be built-in (111-1) in FEA

Defining all the supporting edges to be built-in (110-1), and considering all the permutation of the two constraint functions to be applied to each supporting edges, the derived corrector factors are shown in Table 8.11, 8.12, 8.13, 8.14 and Figure 8.13, 8.14, 8.15, 8.16.

Table 8.11 Corrector factors under 111-1/ddi

111-1/ddi	1	2	3	4	5
A	0.509	0.504	0.501	0.499	0.498
B	0.436	0.431	0.428	0.426	0.425
C	0.319	0.314	0.311	0.309	0.308
D	0.13	0.125	0.122	0.12	0.119

Corrector factors with 111-1/ddio
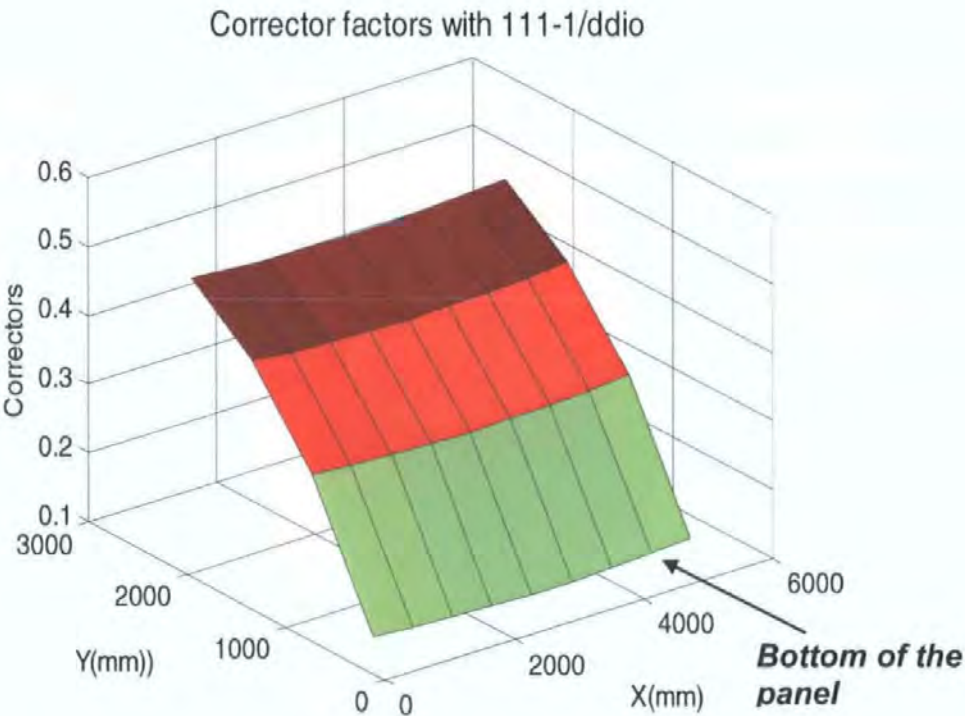
Figure 8.13 3D-Plot of corrector factors of SBO1 under 111-1/ddio

Table 8.12 Corrector factors under 111-1/iido

111-1/iido	1	2	3	4	5
A	0.224	0.398	0.495	0.544	0.559
B	0.225	0.398	0.496	0.545	0.56
C	0.227	0.401	0.498	0.547	0.562
D	0.239	0.413	0.51	0.559	0.574
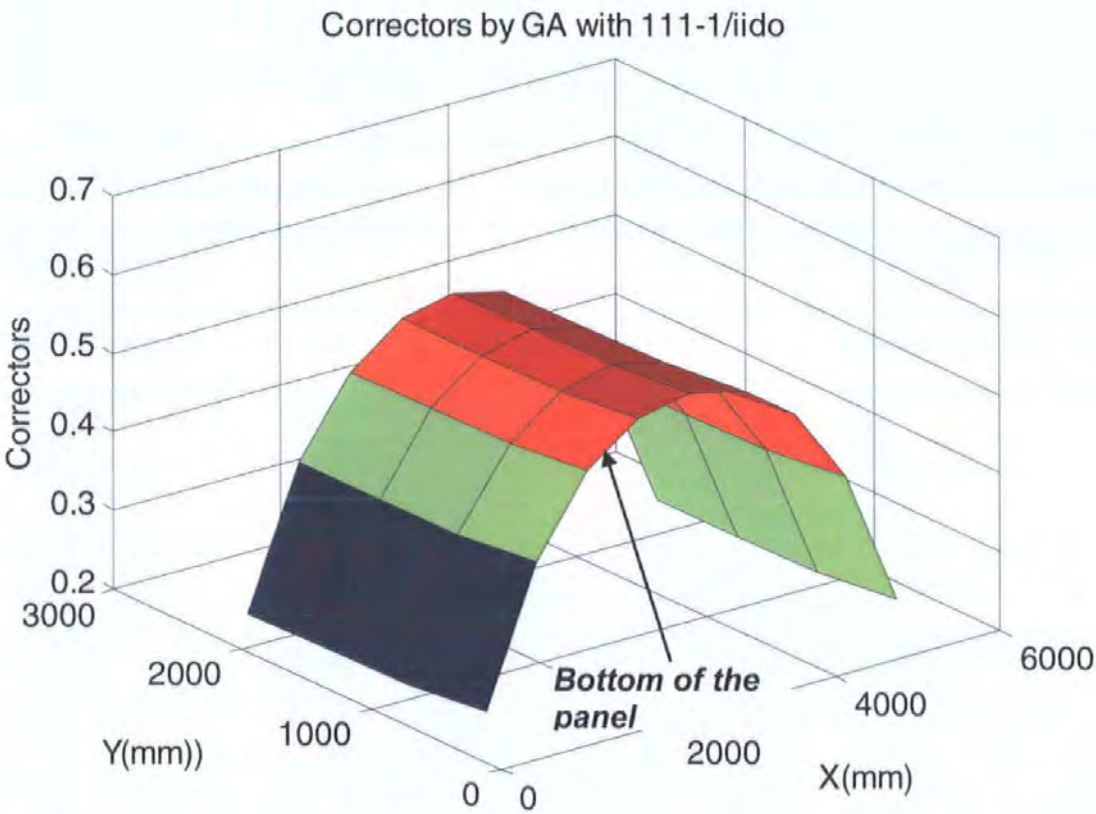
Figure 8.14 3D-Plot of corrector factors of SBO1 under 111-1/lido

Table 8.13 Corrector factors under *111-1/iiio*

111-1/iiio	1	2	3	4	5
A	0.245	0.431	0.559	0.634	0.659
B	0.243	0.429	0.557	0.632	0.657
C	0.225	0.411	0.538	0.613	0.638
D	0.065	0.251	0.379	0.454	0.479

Corrector factors by GA with 111-1/iiio
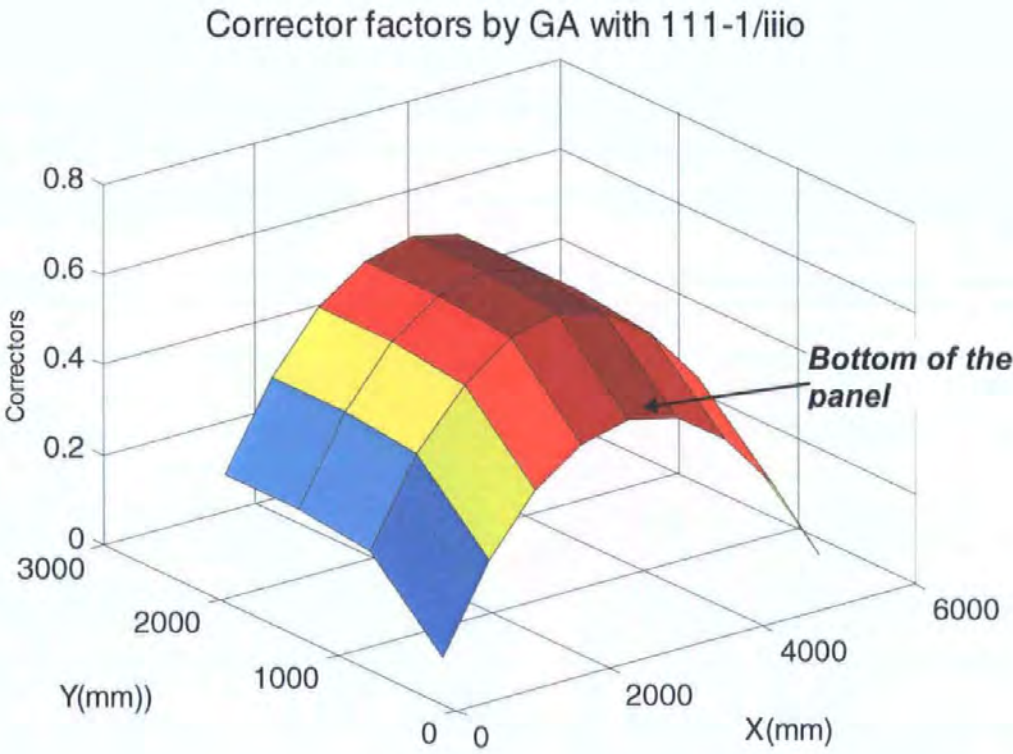
Figure 8.15 3D-Plot of corrector factors of SBO1 under 111-1/iiio

Table 8.14 Corrector factors under *111-1/dddo*

111-1/dddo	1	2	3	4	5
A	0.29	0.29	0.29	0.29	0.29
B	0.33	0.32	0.32	0.32	0.32
C	0.40	0.40	0.40	0.40	0.40
D	0.57	0.57	0.57	0.57	0.57

Corrector factors by GA with 111-1/dddo
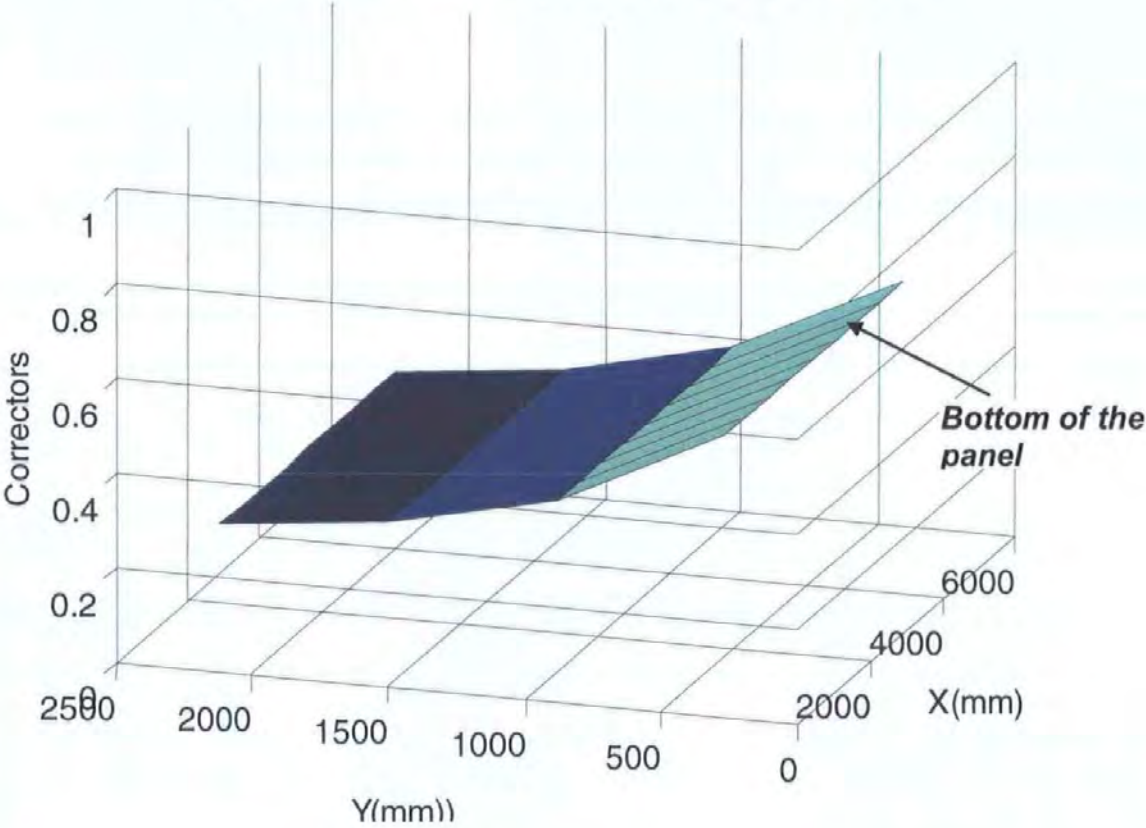
Figure 8.16 3D-Plot of Corrector Factors of SBO1 under 111-1/dddo

From Figure 8.17, it is slightly difficult to identify the best agreement, but with the help of Table 8.2, it can be seen that 111-1/iiio and 111-1/iido are better than the other two cases (111-1/ddio and 111-1/dddo).

From Figure 8.14 and 8.15, it can be seen that the corrector factors under 111-1/iido and 111-1/iiio appear smaller values at the area adjacent to the two defined built-in edges at two vertical sides of the panel, to match the actual boundary condition of these two edges. The difference between 111-1/iiio and 111-1/iido is that, in 111-1/iiio, the bottom of the panel is also softened by smaller corrector factors in the area adjacent to this defined built-in edge. Therefore smaller error acquired. 111-1/iido intends to illogically stiffen the defined built-in edge at the bottom edge of the panel and subsequently result in larger errors than 111-1/iiio.

For the other two cases, 111-1/dddo and 111-1/ddio (See Figure 8.13 and Figure 8.16), they make a poor results because they illogically stiffen the defined built-in edges at two sides of the panel. Meanwhile, 111-1/ddio assign smaller corrector values to the area adjacent to the defined edge at the bottom of the panel, which soften this edge, 111-1/ddio make smaller error than 111-1/dddo.
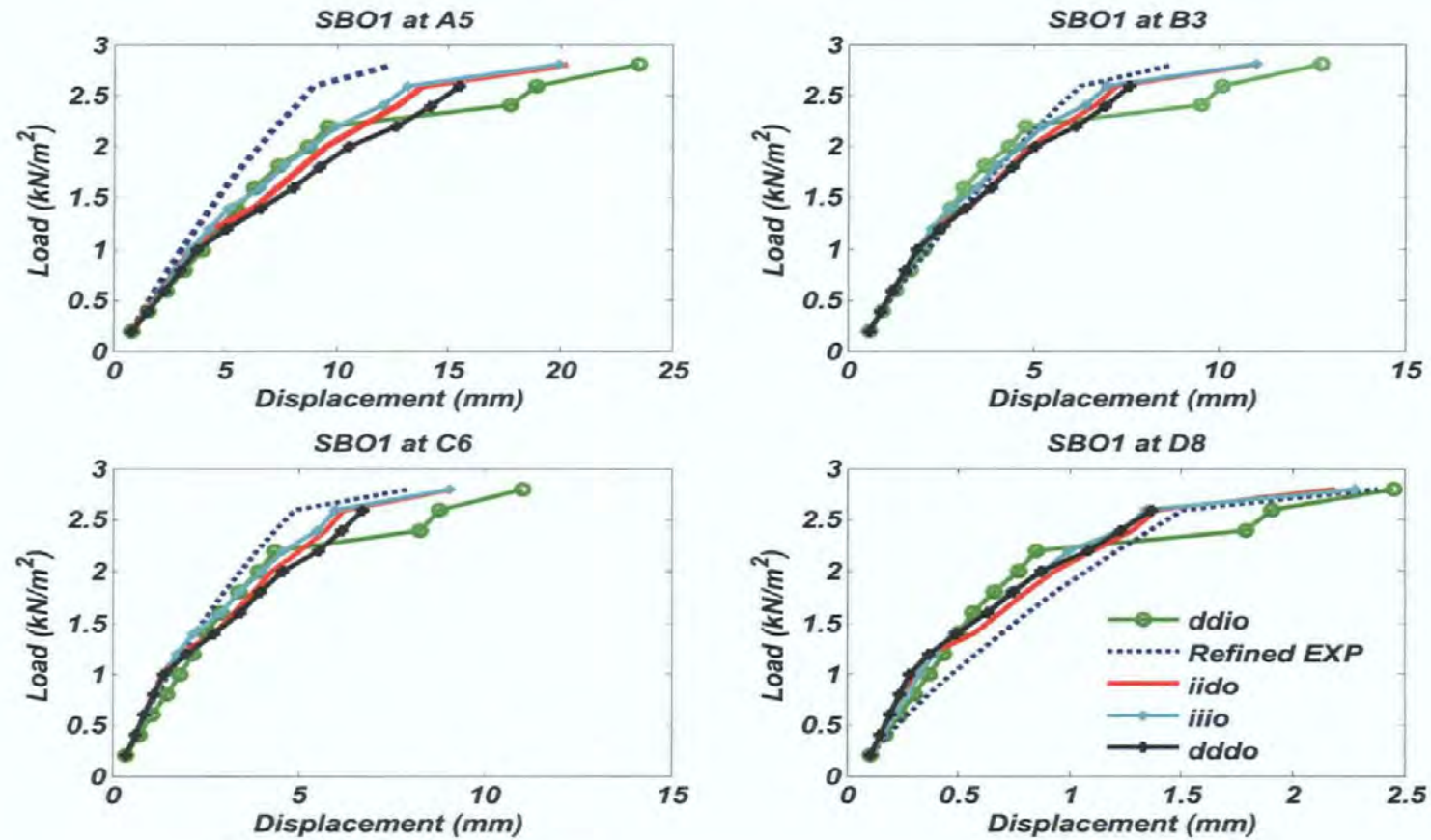
Figure 8.17 Load deflection relationships using correctors under 111-1

8.3.2.4 Defining all the supported edges to be simply supported (000-1) in FEA

Defining all the supporting edges to be simply supported (000-1), considering all

the permutation of the two constraint function to be applied to each supporting

edges, the corrector factors are derived and shown in Table 8.15, 8.16, 8.17, 8.18

and Figure 8.18, 8.19, 8.20, 8.21.

Table 8.15 Corrector factors under 000-1/ddi

000-1/ddi	1	2	3	4	5
A	2.834	2.223	2.056	2.011	2.001
B	2.524	1.913	1.746	1.701	1.692
C	2.058	1.447	1.28	1.235	1.226
D	1.357	0.746	0.579	0.534	0.525
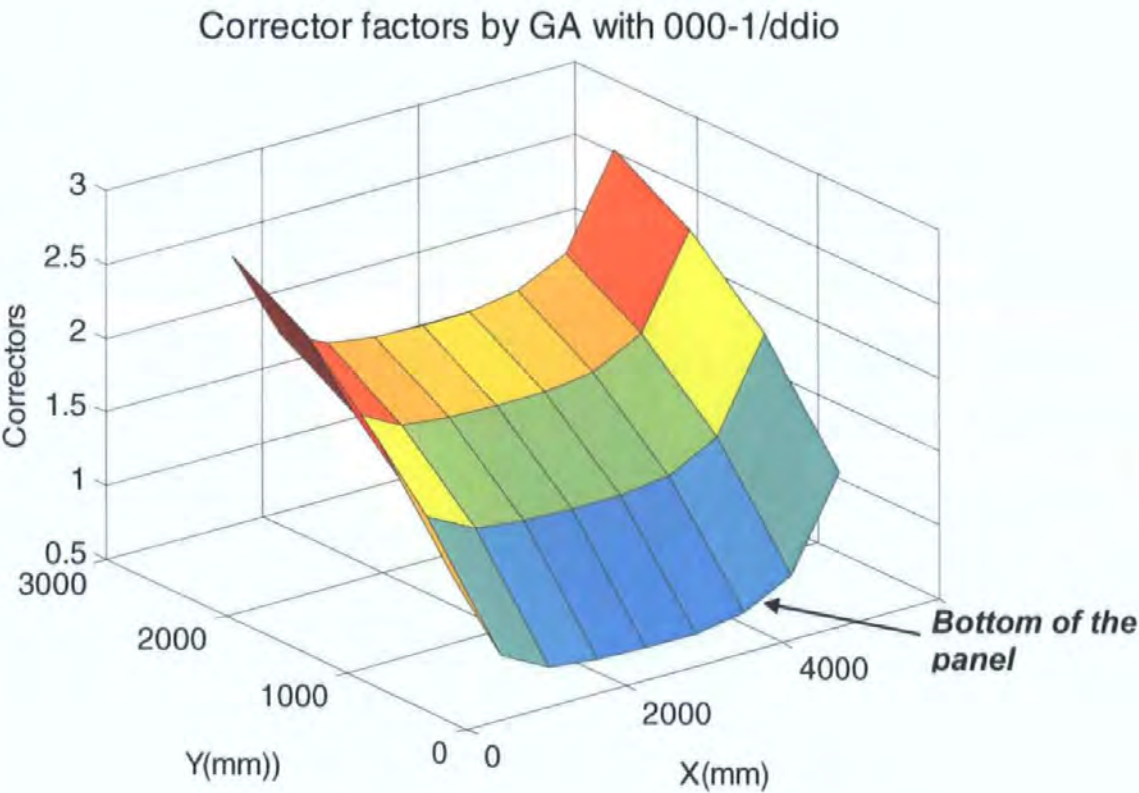
Figure 8.18 3D-plot of corrector factors of SBO1 under 000-1/ddio

Table 8.16 Corrector factors under 000-1/iido

000-1/iido	1	2	3	4	5
A	1.131	1.303	1.409	1.468	1.486
B	1.157	1.329	1.435	1.494	1.512
C	1.267	1.439	1.546	1.604	1.622
D	1.735	1.907	2.014	2.072	2.090

Corrector factors by GA with 000-1/iido
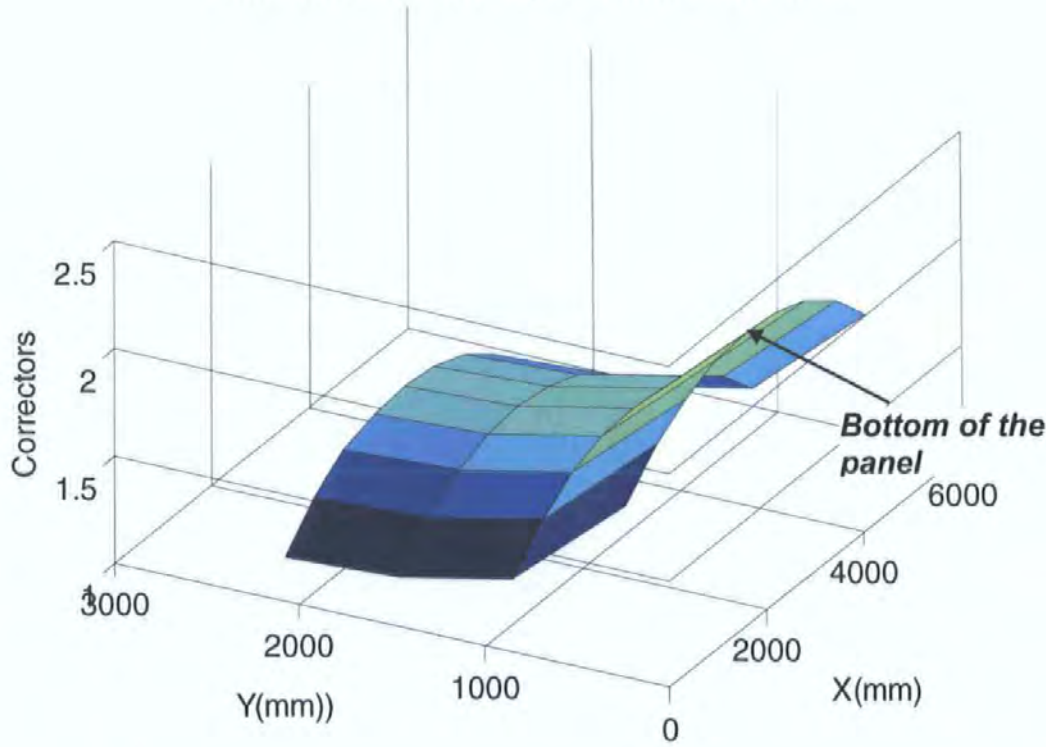
Figure 8.19 3D-plot of corrector factors of SBO1 under 000-1/lido

Table 8.17, Corrector factors under 000-1/iiio

000-1/iiio	1	2	3	4	5
A	1.653	1.673	1.687	1.695	1.698
B	1.626	1.646	1.659	1.667	1.67
C	1.581	1.601	1.615	1.623	1.626
D	1.509	1.529	1.543	1.551	1.554

Corrector factors by GA with 000-1/iiio
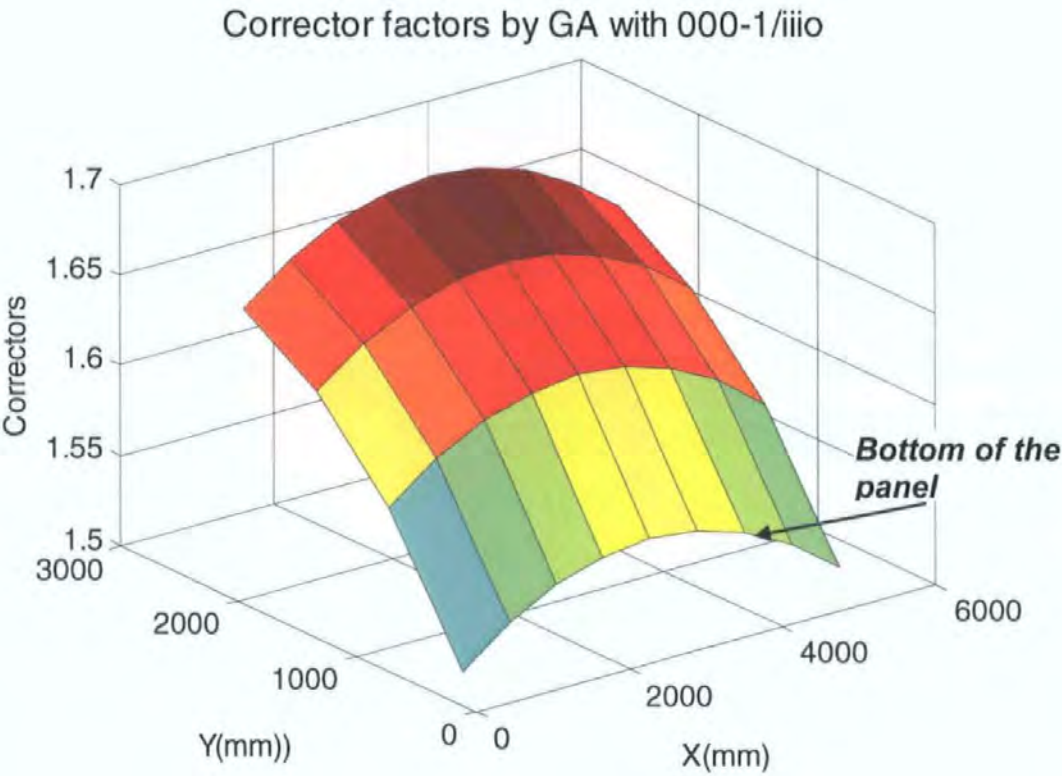
Figure 8.20 3D-plot of corrector factors of SBO1 under 000-1/liio

Table 8.18 Corrector factors under 000-1/dddo

000-1/dddo	1	2	3	4	5
A	1.49	1.483	1.48	1.479	1.479
B	1.495	1.488	1.484	1.483	1.483
C	1.499	1.492	1.489	1.488	1.488
D	1.504	1.497	1.494	1.493	1.493
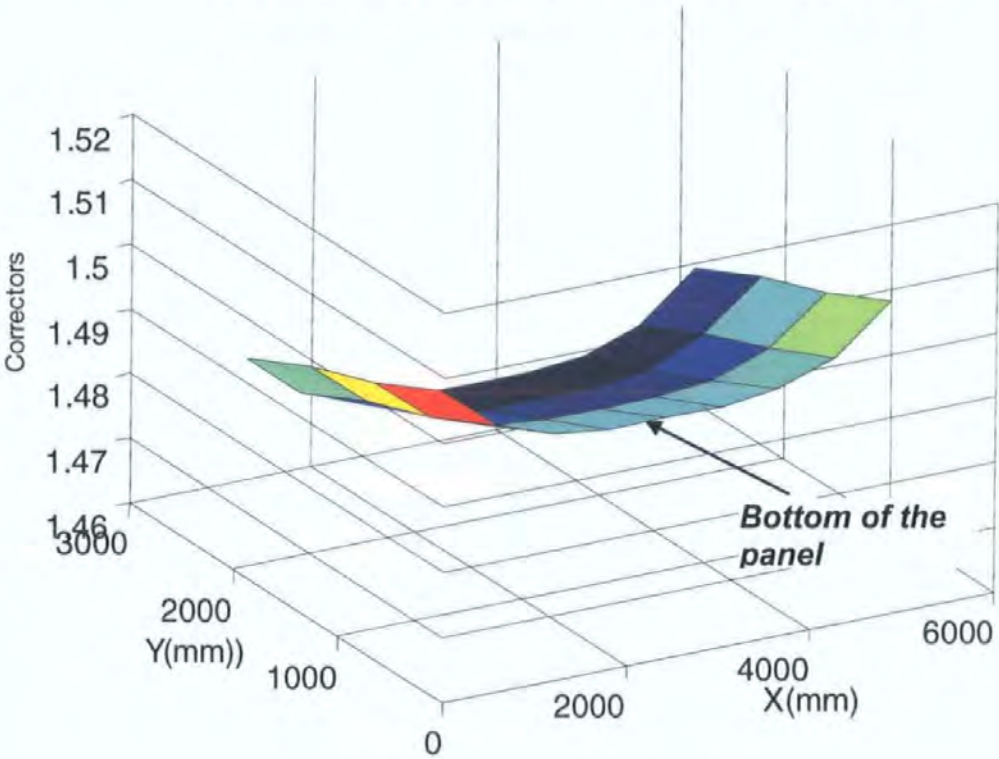
Figure 8.21 3D-plot of corrector factors of SBO1 under 000-1/dddo

In Figure 8.22, the load deflection relationships of the 4 cases are quite similar, but with the help of Table 8.2, it can be seen that the 000-1/dddo results in a smallest error, which means corrector factors still follow the rules that using the decreasing-

tendency constraint function to stiffen the defined simply supported edge would better model the actual boundary conditions and match the experiments well.

In this section, corrector factors are studied by changing the definition of supporting boundaries in FEA model. Two kinds of constraint function are used to compulsorily assign corrector factor values to the defined boundary conditions. It has been found that applying the increasing and decreasing equation to the defined built-in edge and simply supported edge respectively always make the best results, which means that the physical meaning indicated in Chapter 7 are reliable, and it is also indicated that the boundary effects do have influence on the FEA analysis, or say the behaviour of masonry panel is much influenced by the boundary effects..
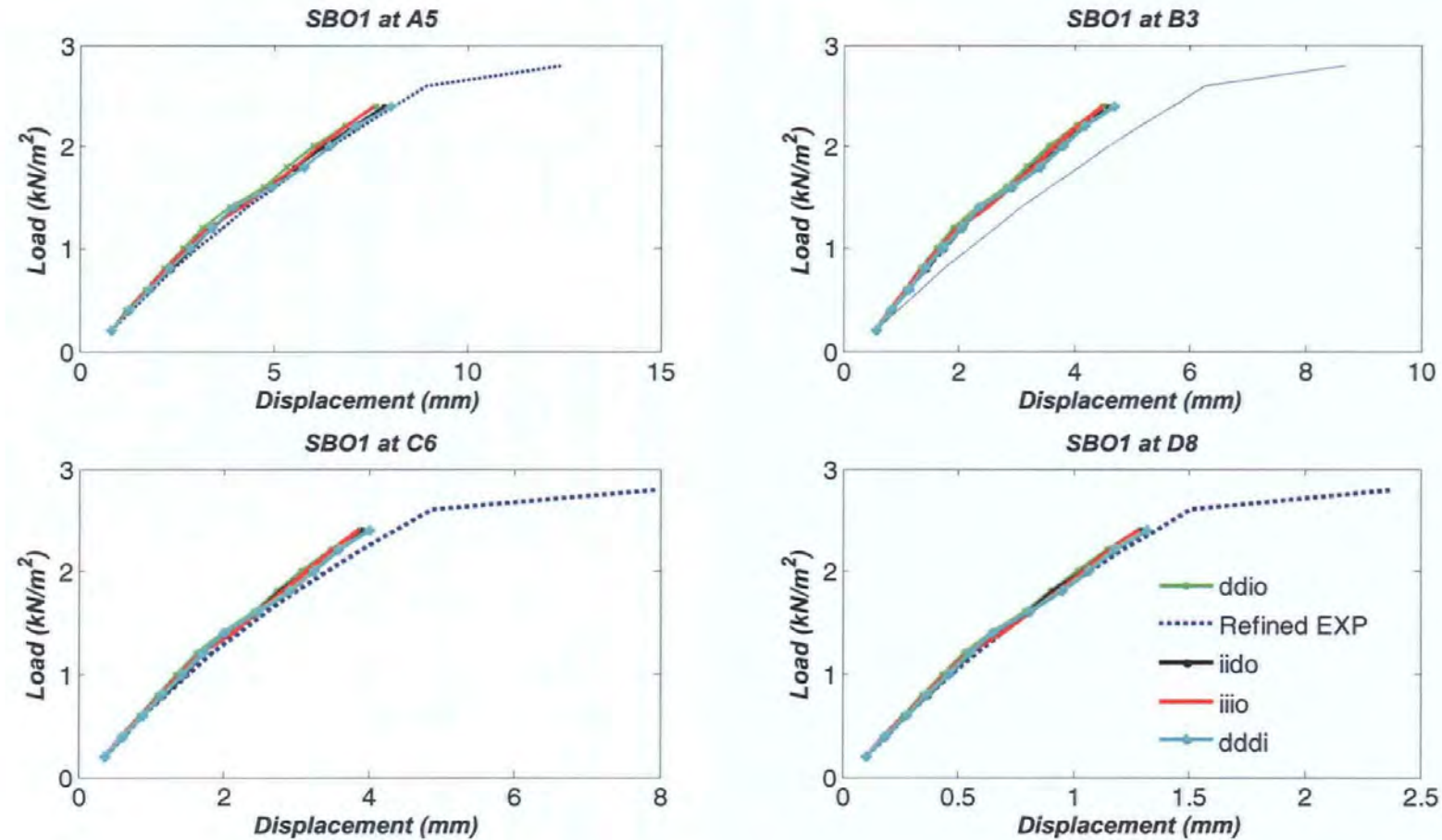
Figure 8.22, Load deflection relationships using corrector factors under 000-1

8.4 DIRECTLY ASSIGNING CORRECTOR FACTORS ALONG THE SUPPORTING EDGES

It had been seen that the boundary effects, which can be reflected and revised by the corrector factors, have major influence on the FEA analysis. To further investigate the boundary effects or say to further investigate the physical meaning of corrector factors, in this section, studies are carried out without using the constraint functions. Corrector factors are directly assigned to the area adjacent to the supporting boundaries (see Figure 8.23), in which the panel is divided into 4 zones and accordingly 4 independent corrector factors are assigned. Similar to section 8.2.2, in total 4 kinds of possibly defined boundary conditions are investigated; they are 001-1,110-1,111-1,000-1.
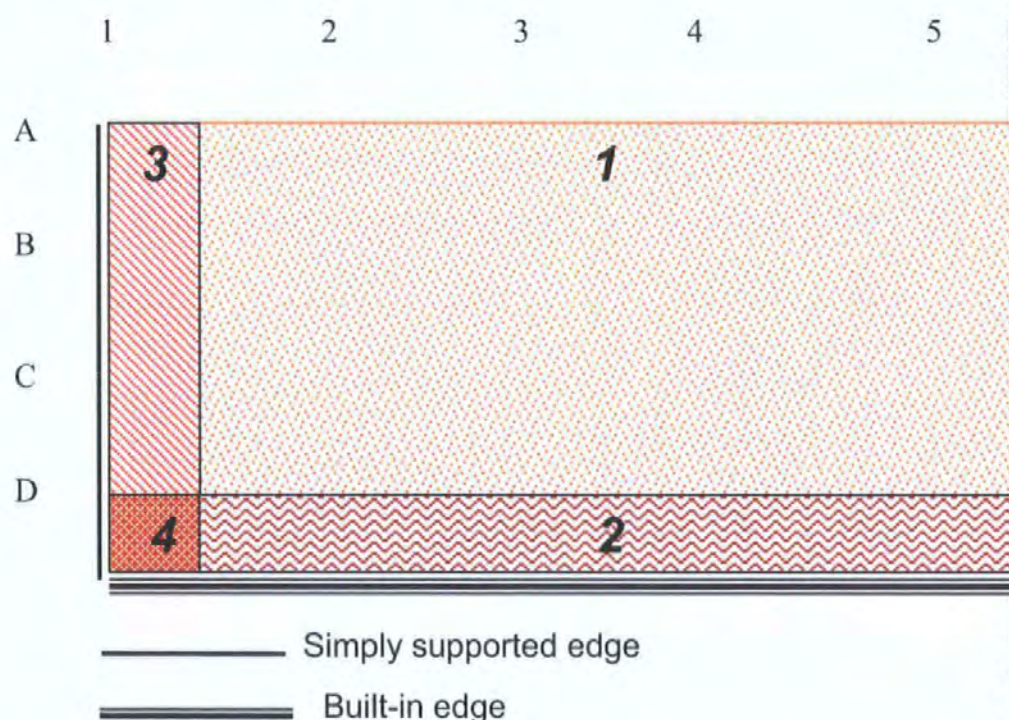
Figure 8.23, Zones for assigning corrector factors adjacent to the supported boundaries

8.4.1 Defining boundary condition as 001-1

Table 8.19 and Figure 8.24 show the obtained corrector factors when defining boundary conditions as 001-1. It can be seen that, the distribution of the corrector factors derived herein are quite similar to 001-1/iiio as shown in Figure 8.5. This means that for SBO1, defining the bottom edge to be built-in over constrain this edge, smaller corrector factors neighbour to this edge revise the boundary effect to match the actual boundary condition. For the two vertical edges, the corrector factors that are adjacent to them are smaller than those in the centre of the panel, but the difference is very small. Examining Figure 8.3, 8.5 and 8.21, it can be concluded that these three figures are almost identical, which indicate that defining the two vertical edges to be simply supported close to their actual boundary condition.

Table 8.19, Corrector factors by directly assignment under 001-1

001-1	1	2	3	4	5
A	1.021	1.112	1.112	1.112	1.112
B	1.021	1.112	1.112	1.112	1.112
C	1.021	1.112	1.112	1.112	1.112
D	0.277	0.212	0.212	0.212	0.212
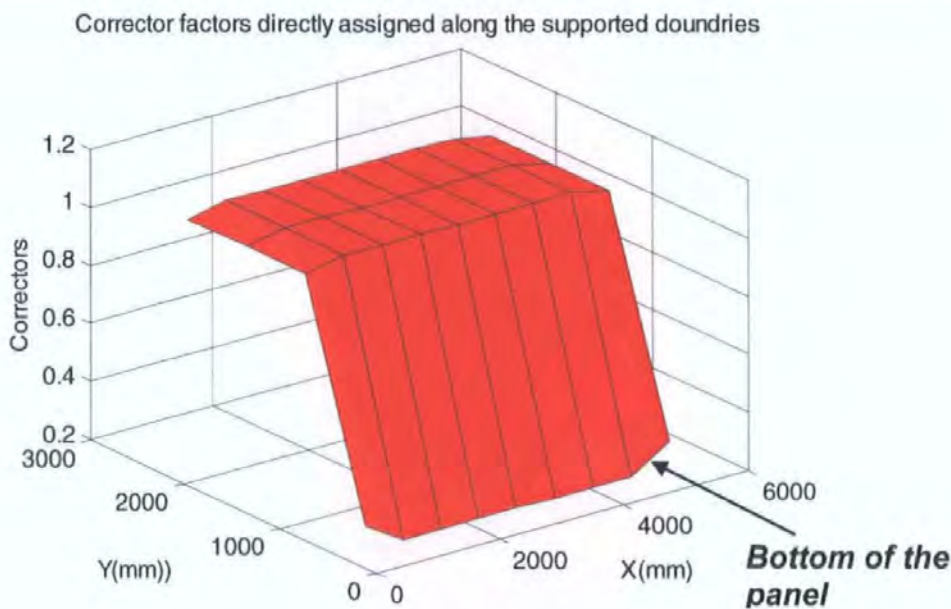
Figure 8.24, 3D-plot of corrector factors by directly assignment (001-1)

8.4.2 Defining boundary condition as 110-1

Table 8.20 and Figure 8.25 show the obtained corrector factors when defining the two vertical edges to be built-in and bottom edge simply supported and top free (110-1). It is seen that corrector factors in the area adjacent to the vertical edges are decreased but those in the area adjacent to the bottom is increased, the defined built-in vertical edges are revised to be less constrained and the defined simply supported edges to be more constrained, which in accordance with the physical meaning of corrector factors confirmed in section 8.3.2.2.

Table 8.20 Corrector factors by directly assignment under 110-1

110-1	1	2	3	4	5
A	0.259	0.763	0.763	0.763	0.763
B	0.259	0.763	0.763	0.763	0.763
C	0.259	0.763	0.763	0.763	0.763
D	0.726	1.213	1.213	1.213	1.213

Corrector factors directly assigned along the supported doundries
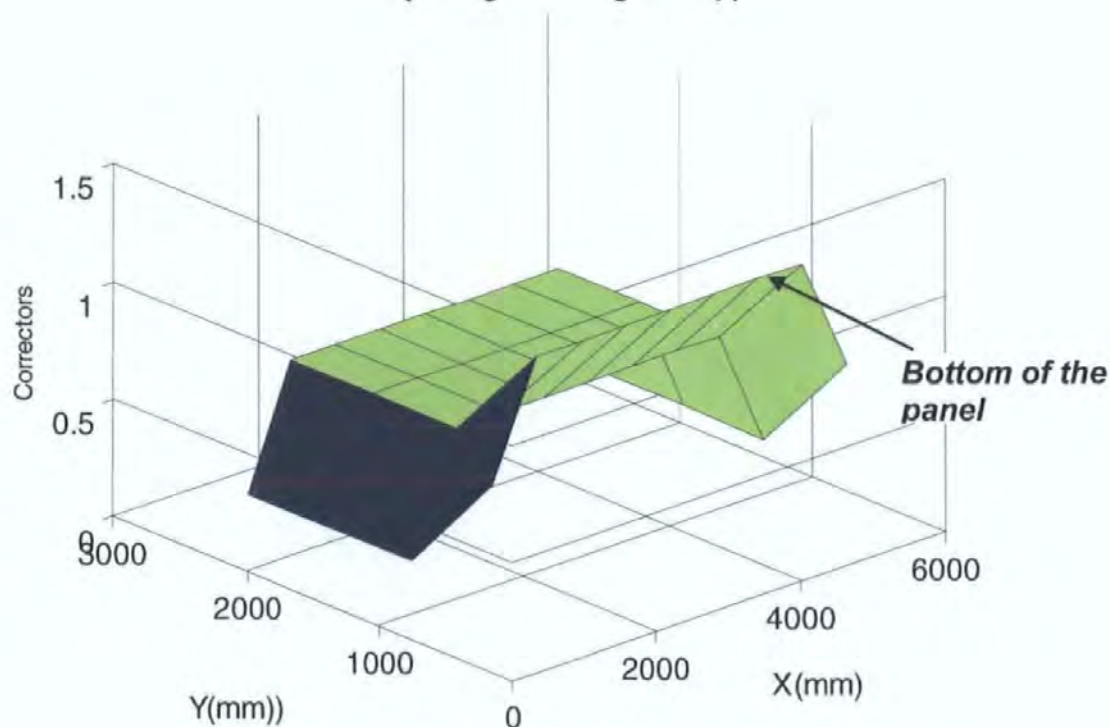
Figure 8.25, 3D-plot of corrector factors by directly assignment (110-1)

8.4.3 Defining boundary condition as111-1

Table 8.21 and Figure 8.26 show the obtained corrector factors when defining all vertical and bottom edges built-in (111-1), it can be seen that all corrector factors along these edges are small than those in the centre of the panel, which mean the corrector factors tend to make the all supported boundaries to be less constrained due to they were defined as fixed. Furthermore, those corrector factors that are adjacent to the bottom edge are slightly larger than those near the vertical edge, which indicates that for the actual boundary conditions, the bottom edge are more constrained than the vertical edges.

Table 8.21 Corrector factors by directly assignment under 111-1

111-1	1	2	3	4	5
A	0.050	1.586	1.586	1.586	1.586
B	0.050	1.586	1.586	1.586	1.586
C	0.050	1.586	1.586	1.586	1.586
D	0.054	0.218	0.218	0.218	0.218

Corrector factors directly assigned along the supported boundries 111-1
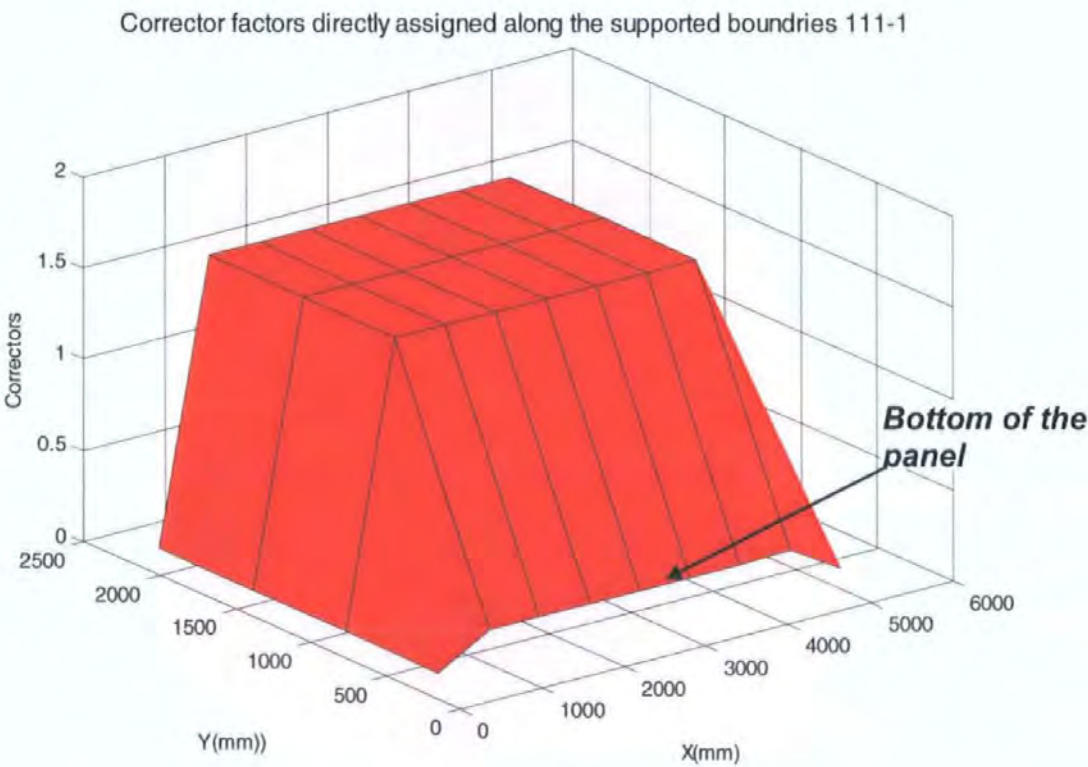
Figure 8.26, 3D-plot of corrector factors by directly assignment (111-1)

8.4.4 Defining boundary condition as 000-1

Table 8.22 and Figure 8.27 show the obtained corrector factors when defining all supported edges in FEA as simply supported. It can be seen that all corrector factors neighbouring the supported edges are increased (except those in the corner of the

panel which is a smaller value). Because the boundary effects are mainly from the boundary itself rather than from the corner, it can still be concluded that the defined simply supported edges are revised to be more fixed.

From the above investigation, it can be concluded that the derived corrector factors in Chapter 7 and their physical meaning are reliable.

Table 8.22 Corrector factors by directly assignment under 000-1

000-1	1	2	3	4	5
A	1.695	1.560	1.560	1.560	1.560
B	1.695	1.560	1.560	1.560	1.560
C	1.695	1.560	1.560	1.560	1.560
D	1.283	1.716	1.716	1.716	1.716

Corrector factors directly assigned along the supported doundries
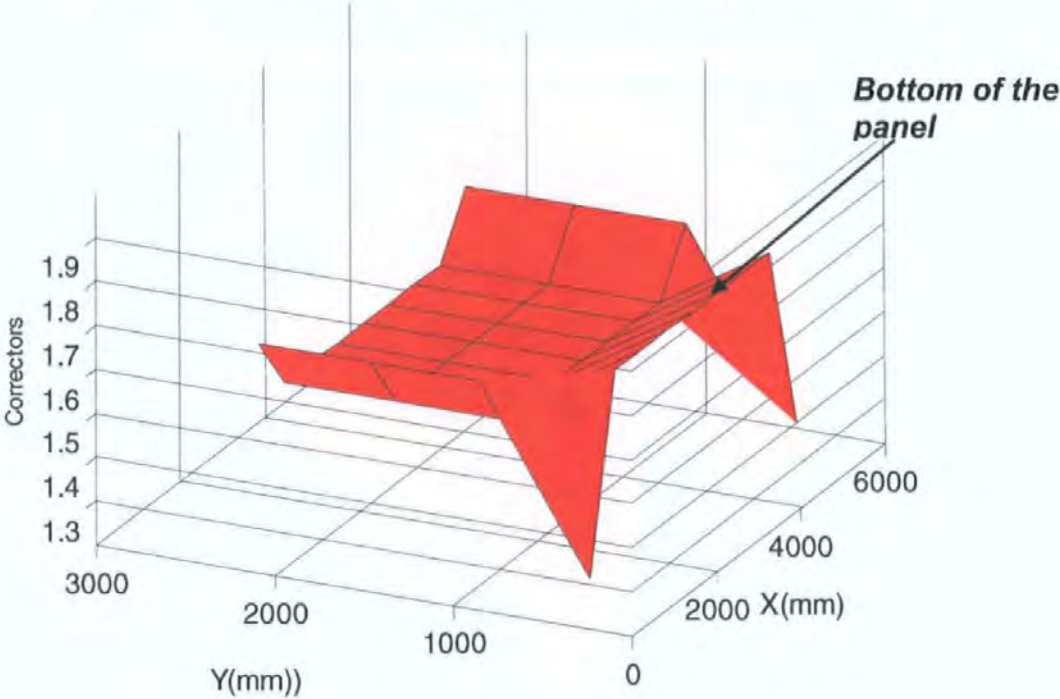
Figure 8.27, 3D-plot of corrector factors by directly assignment (000-1)

8.5 CORRECTOR FACTORS UNDER DIFFERENT MESH SIZES IN FEA

Because FEA results are sometimes affected by the mesh size, it is necessary to investigate the corrector factors by changing the mesh sizes. In previous sections as 8.2, 8.3, 8.4, the panel SBO1 is divided into 18 x 8=144 elements. In this section, the smaller mesh size is produced by increasing the element number to 20x10=200. Corrector factors will be compared between these two divisions.

8.5.1 Corrector factors using constraint-functions with smaller mesh size

Similar to section 7.4.4.2 and section 8.2.2.1, the corrector factors are derived again by defining two vertical edges simply supported and bottom built-in and top free using the constraint function. The corrector factors obtained are shown in Table 8.23 and Figure 8.28.

Compare Figure 8.28 with Figure 8.3, it could be found that the 3D plot of the derived corrector factors under two different mesh sizes are quite similar, which means the mesh size does not affect the distribution tendency of the corrector factors.

Table 8.23, Corrector factors by constraint function under iido with 200 meshes

001-1	1	2	3	4	5
A	1.080	1.013	1.000	0.998	0.997
B	1.072	1.006	0.993	0.991	0.990
C	1.031	0.965	0.952	0.950	0.949
D	0.856	0.790	0.777	0.775	0.774
E	0.231	0.165	0.152	0.149	0.149

Corrector factors of SBO1 using constraint function and 200 meshes
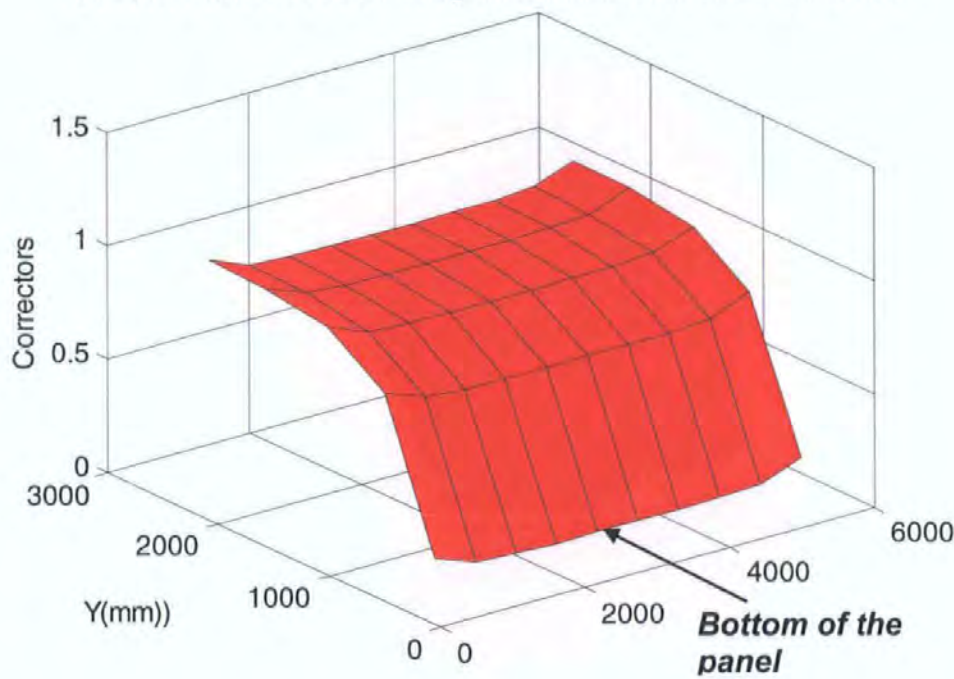
Figure 8.28, 3D plot of corrector factors under 001-1/ddio and by 200 elements

8.5.2 Directly assign corrector factors along the supported boundaries with smaller mesh size

As in Chapter 8.4, corrector factors are directly assigned to zones neighbour to the supported edges. The results are shown in Table 8.24 and Figure 8.29. Compare Table 8.24 with Table 8.19 and Figure 8.29 with Figure 8.24, it can be seen that when using 200 elements, the distribution of the obtained corrector factors are quite similar. They appear smaller values along the bottom edge but appear very limited change along the vertical edges. This result shows that the distribution tendency of corrector factors is not affected by the mesh size in FEA.

Table 8.24, Corrector factors directly assigned of SBO1 with 200 meshes

001-1	1	2	3	4	5
A	1.041	1.006	1.006	1.006	1.006
B	1.041	1.006	1.006	1.006	1.006
C	1.041	1.006	1.006	1.006	1.006
D	1.041	1.006	1.006	1.006	1.006
E	0.396	0.148	0.148	0.148	0.148

Corrector factors directly assigned along
the supported boundries (200 meshes)
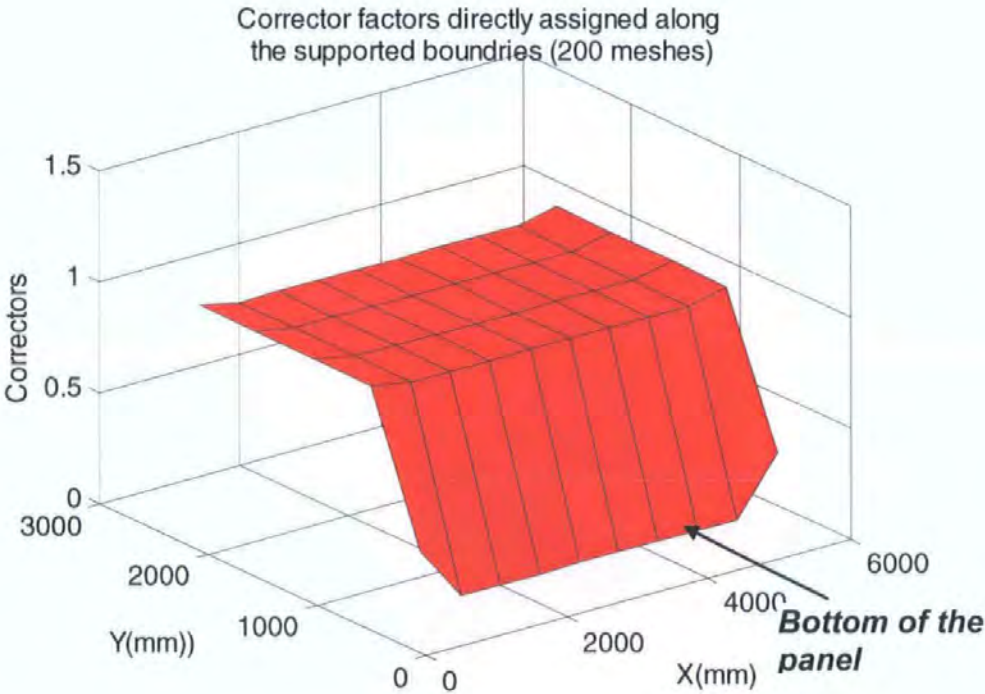
Figure 8.29, 3D plot of corrector factors by directly assignment with 200 meshes (001-1)

8.6. SUMMARY

In this Chapter, the validity of the corrector factors derived in Chapter 7 is studied in the following ways:

1. In consideration of all the possible boundary effect using the permutation of two kinds of constraint functions, the corrector factors are studied. All the derived corrector factors reveal that, to masonry panel SBO1, the bottom edge is not fully fixed but appear to have some degree of flexibility. It is not reasonable to define the bottom edge as fully fixed in the FEA model. However, stiffness of the zones in the area near to the vertical edges which were defined to be simply supported are less changed, which means that defining a vertical edge to be simply supported is acceptable.

2. In the FEA model, altering the definition of the boundary condition of the panel with all possible permutations of the support types, the derived corrector factors again showed that, all the defined built-in edges are always tends to be relaxed by corrector factors. On the other hand, and the defined simply supported edges always tend to be a bit more constrained.

3. Changing the flexural stiffness in the area adjacent to the supporting boundaries show that, the defined fully fixed boundaries in the FEA model always tend to be relaxed by assigning smaller corrector factors to these zones, and the defined simply supported edges tend to be constrained by increasing the corrector factors in these regions.

4. Changing the mesh size has no influence on the distribution of corrector factors, which means the physical meaning of corrector factors is not affected by mesh size.

5. Comparing the error among cases of all the permutations of constraint function under different defined boundary conditions in FEA show that the

corrector factors derived in Table 7.10 in Chapter 7 make a smaller error, which means these corrector factors are reliable.

6. The study in this chapter reveals that, the physical meaning of corrector factors is a revision of the inadequate defined boundary conditions in FEA, to make the defined built-in edge to be less constrained and to make the defined simply supported edges to be slightly more constrained.

Consequently, the obtained corrector factors shown as in Table 7.10 are reliable, for the intended use for more general panels with different boundary conditions, different dimensions and/or with openings. This will be further investigated in Chapter 9.

9. PRACTICAL APPLICATION OF CORRECTOR FACTORS

9.1 INTRODUCTIONS

In Chapter 7, the concept of corrector factors, which was based on numerical model updating methods, was introduced. From the derived corrector factors in Chapter 7, it was seen that boundary effects have a major influence on the response of masonry panels to lateral load. The unique nature of corrector factors was studied in Chapter 8 which led to the understanding of the physical meaning of corrector factors.

In this chapter, the practical application of corrector factors will be demonstrated. A number of cases will be studied and will demonstrate that corrector factors can improve the FEA analyses of laterally loaded masonry panels. The study further demonstrates the general nature of corrector factors and shows the strong effect of boundary conditions on the response of laterally loaded masonry panels. In this chapter, a number of masonry panels tested by different sources which have different dimensions, boundary conditions and panels with or without openings are analysed using corrector factors. Meanwhile, the concept of similar zones is used to generalise the application of corrector factors. The Cellular Automata (CA) model that were developed by Zhou, *et al.*(2003, 2006) will be used to identify similar zones between the base panel and the new panel, by which corrector factors from the base panel are assigned to similar zones on the new panel. A nonlinear FEA program will be used to analyse the response of the new panels subjected to lateral loading within the full linear and nonlinear regions. Results from these case studies show that the improved predictions are obtained by modifying the flexural stiffness and the strength of the panel using corrector factors.

9.2 GENERALIZATION

Generalization is a concept of obtaining corrector factors for any new masonry wall panel to be analysed from similar zones on the base panel (SBO1). These obtained corrector factors are then used to modify the flexural stiffness and strength of the new panel to improve the analysis of any new masonry panels which have different dimensions, boundary conditions and walls panels with or without openings. In this section, the method of generalization will be demonstrated. The generalization directly relates to two issues: (a), corrector factors from the base panel, (b) the criteria of modelling similar zones by CA.

9.2.1 The corrector factors used for generalization

From Chapter 7 & 8, it was found that values in all Table 7.9, 7.10, 8.19, 8.23 are capable of reducing the discrepancy between the FEA and the experimental results, i.e. to improve the analysis of SBO1; therefore, all of them could be regarded as acceptable corrector factors.

In order to select the most suitable corrector factors among these results for practical applications, errors between the experimental and the predicted results were compared and a summary of this study is presented in Table 9.1. It has been found that those values in Table 7.10 lead to the smallest error. Therefore corrector values in Table 7.10 are selected for practical application and they are shown in Table 9.2 here again for convenience.

Table 9.1, Error of using different corrector factors

Table number	Table 7.9	Table 7.10	Table 8.19	Table 8.23
Error (%)	0.3468	0.1366	0.1521	0.2027

SBO1	X1	X2	X3	X4	X5	X6(X4)	X7(X3)	X8(X2)	X9(X1)	height of zones(mm)
Y4	1.283	1.278	1.277	1.277	1.277	1.277	1.277	1.278	1.283	618.75
Y3	1.187	1.181	1.181	1.181	1.181	1.181	1.181	1.181	1.187	618.75
Y2	0.926	0.921	0.92	0.92	0.92	0.92	0.92	0.921	0.926	618.75
Y1	0.223	0.218	0.217	0.217	0.217	0.217	0.217	0.218	0.223	618.75
Length of zones(mm)	622.22	622.22	622.22	622.22	622.22	622.22	622.22	622.22	622.22	

Figure 9.2 The zone divisions and corrector factors of the base panel SBO1

9.2.2 The modification to CA criteria

Zhou, et al.(2003, 2006)　developed the concept of zone similarity to assign the corrector factors from a base panel (SBO1) to other general masonry panel of different dimensions, boundary conditions and panels with or without openings. These corrector factors were used to modify the flexural stiffness and strength of the new panel to improve the predicted response of it. Since manually matching of similar zones for the new panel is not easy as it needs a deeper understanding of the corrector factors and deep domain knowledge, a CA model was proposed by Zhou, et al.(2003, 2006) to match similar zones between the base panel and any new panel. Zone similarity is related to the relative distances of zones from similar boundary types (Zhou 2002) (also see equation (3-4), (3-5), (3-6), (3-7), (3-8) in Chapter 3).

The CA criteria for assigning corrector factors from the base panel to the new panel were summarized as follows (Zhou2002)

1. The division of zones of the new panel:

    a. When the length (or height) of the new panel is larger than the corresponding length (or height) of the base panel, the number of zones along this length (or height) on the new panel is equal to the number of new zones along the corresponding length (or height) on the base panel,

i.e. the zone number is kept unchanged but the zone size are proportionally increased.

b. When the length (or height) of the new panel is smaller than that of the base panel, the number of zones along this length (or height) on the new panel is reduced proportionally, i.e. zone sizes on the new panel are approximately equal to those of the base panel.

2. Any zone on the new panel is matched to a specific zone on the base panel using the concept of similar zones.

3. A similar zone on the new panel has the same corrector factor value as that on the base panel. This means the corrector factor values of any zone of the new panel could be derived directly from the corrector factor value of its similar zone on the base panel.

However, the following two irregularities exist when using the CA criteria:

I. For panels with 4 sides simply supported, corrector factors on the corner of the new panel derived from the base panel do not seem to be logically correct.

II. When the size of the new panel is much smaller than the base panel (although there are seldom such small masonry panels in reality), the CA criteria resembles a smeared material model, i.e. only one zone on the panel.

To demonstrate this, two hypothetical examples are demonstrated below.

Two hypothetical masonry panels with 4 sides simply supported, panel A and panel B, their dimensions are assumed to be 1500 x1000mm and 800 x 800mm respectively. Their corrector factors are derived using the CA criteria developed by Zhou(2002). Figure 9.2 & 9.3 show the zone division and the derived corrector factors of these two

hypothetical masonry panel directly using CA criteria based on corrector factors presented in Figure 9.1.

Panel A	X1	X2	X3
Y2	0.223	1.187	0.223
Y1	0.223	1.187	0.223

Figure 9.2, Zone division and corrector factors of panel A

Panel B	X1
Y1	0.223

Figure 9.3, Zone division and corrector factors of panel B (one zone only)

Examining the zone division and corrector factors in Figure 9.2, it can be seen that the zone number of the hypothetical panel "*A*" is reduced due to its smaller size compared with the base panel SBO1. Also the derived corrector factors adjacent to the vertical simply supported edges of panel "*A*" are reduced which corresponds to the corner on the base panel. This reduction represents a built-in edge of the panel, but all edges of panel *A* have been assumed to be simply supported, obviously, the assigned data is not logically correct.

Examining the zone division and corrector factors in Figure 9.3, it can be seen that, due to the smaller size of panel *B*, only one zone is assigned by the CA criteria. This model has become a smeared model, and its derived corrector factor value reflects the influence from the built-in edge while in reality the panel is simply supported on 4 sides. These two examples demonstrate the existence of irregularities in the CA criteria which needs to be revised.

The irregularities are avoided by modifying the CA criteria in the following ways:

1. To the new panel with two adjacent simply supported edges, corrector factors at the corner of these two simply supported edges are assigned with the mean value of its two neighbouring zones.

2. Make the size of zones adjustable when running the CA model, so as to use smaller zone sides to better describe the boundary effects when analysing the small panels.

These revised CA criteria will be used for the case studies in section 9.3. Corrector factors derived in this way are listed in Appendix 3 which covering the corresponding 29 panel types in BS 5628.

9.2.3 The Code of FEA, CA and the GA

All the analyses using corrector factors are based on the Fortran 77 code FEA software developed by May and Tellett(1986) and late was modification a little bit by Chong (1993) and Zhou (2002), as have been introduced in Chapter 3. The CA code was developed by Zhou (2002). The GA code was developed in this research using Matlab 7.0. All these three modules were combined into the Matlab 7.0 for the practical analysis.

9.3 CASE STUDIES OF LOAD DEFLECTION RELATIONSHIPS

In this section, a number of masonry panels with different boundary conditions, different dimensions and panels with and without openings are analysed to demonstrate the generality of the method proposed in this thesis. The revised CA criteria, introduced in section 9.1, are used for determining the corrector factors for the new panels. In the case studies, the material properties used are from those original sources. Nevertheless, if these properties are not available, the data from tests in the University of Plymouth (Chong 1993) are referred.

9.3.1 The analyses of masonry wall panels tested in University of Plymouth

In this section, 3 full scale single leaf masonry wall panels (SBO2, SBO2, SBO4) tested in the University of Plymouth (Chong 1993) are selected for validation. These panels have the same dimensions and boundary conditions as SBO1, but with openings of different size and position. Figures 9.4, 9.5, 9.6 are the configurations of these panels. For the analyses purpose, the following material properties are used (Chong 1993):

Elastic stiffness E=12 kN/mm^2

Flexural strength perpendicular to the bed joints fx=2.28 N/mm^2.

Flexural strength parallel to the bed joints fx=0.965 N/mm^2.

Poisson's ratio v=0.2.

Using stiffness corrector factors as shown in Table 7.10 and the revised CA model, stiffness correctors for these 3 panels are shown in Figure 9.4, 9.5, 9.6. The strength corrector factors used are those shown in Table 7.11.

Figures 9.10, 9.11, 9.12 show the load deflection relationships at different position on these masonry panels derived by using corrector factors. It can be seen that, for all three panels, a substantial improvement has been achieved, and the load deflection relationships agree well with the experimental results. It is clear that the load deflection relationships are improved at all the 36 measuring points. However, from these figures, it can be seen that, for all the three panels, the predicted failure loads are smaller than those of experimental results. This could have been caused by the strengthening from the wooden frame around the opening area on the masonry walls while testing in the laboratory.

Panel SBO2 with opening
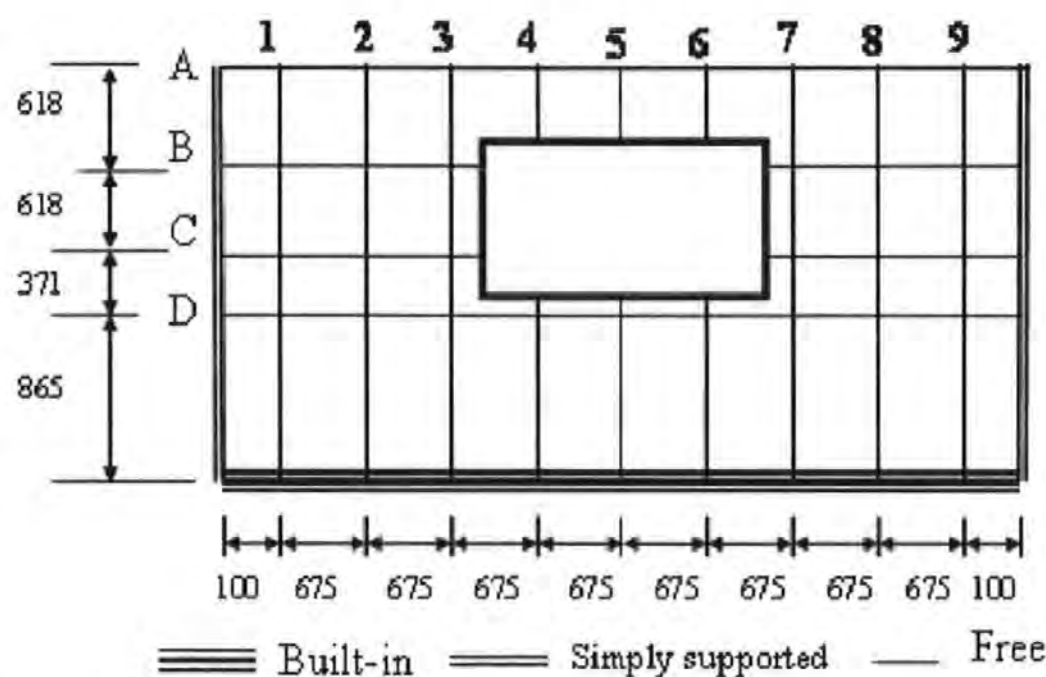
Figure 9.4, Configuration of SBO2 and the measuring points

Panel SBO3 with opening
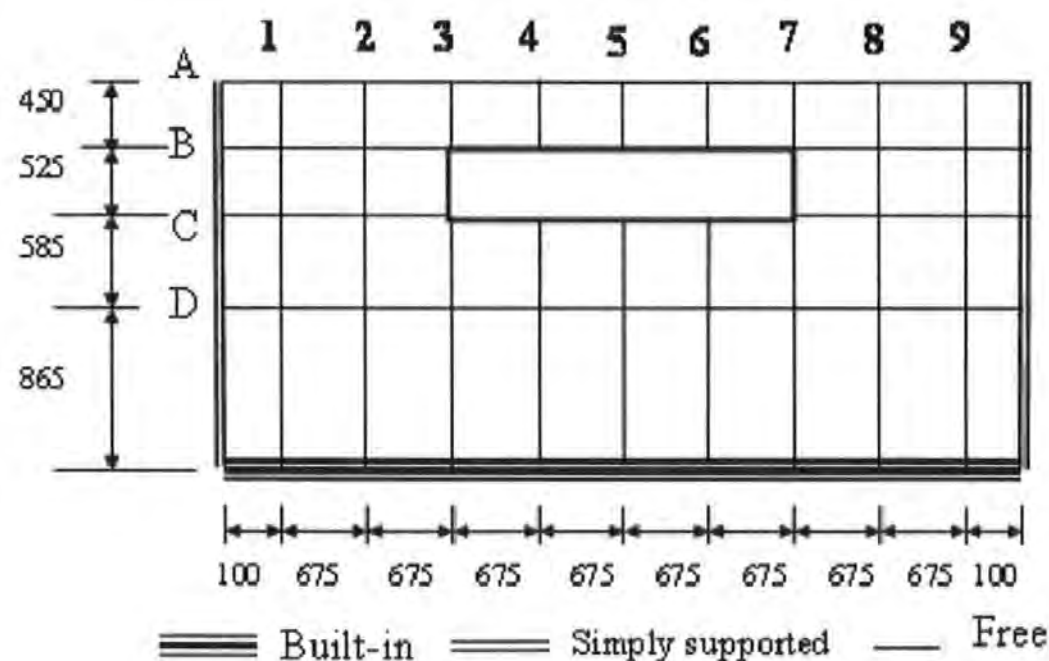
Figure 9.5, Configuration of SBO3 and the measuring points

Panel SBO4 with opening
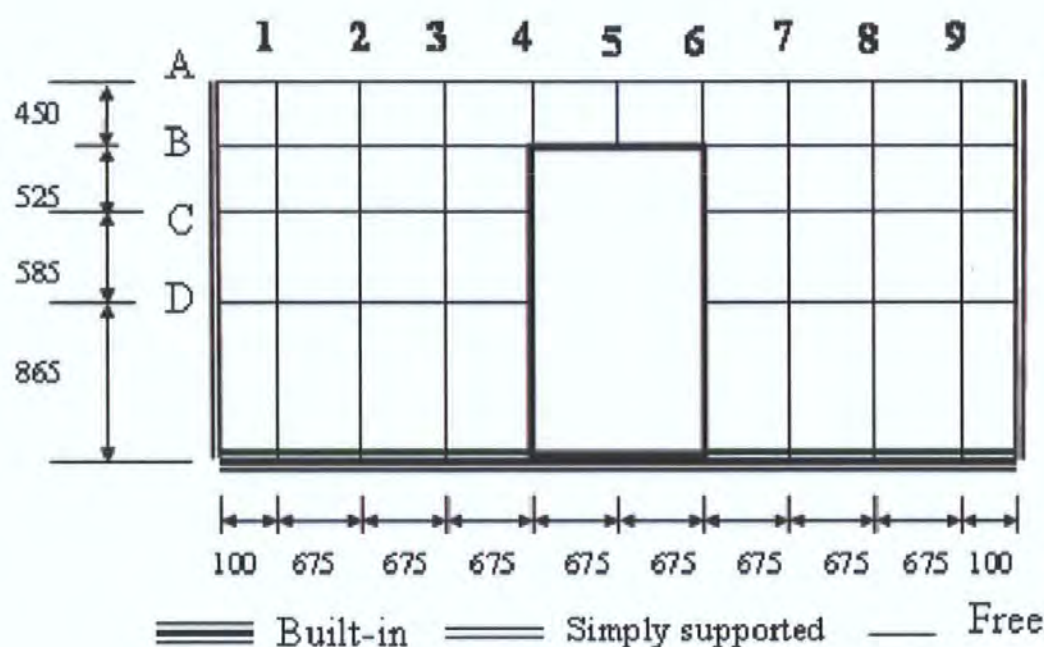
Figure 9.6, Configuration of SBO4 and the measuring points

SBO2	X1	X2	X3	X4	X5	X6	X7	X8	X9	X10	Height of zones(mm)
Y5	1.283	1.278	1.278	1.278	1.278	1.278	1.278	1.278	1.278	1.283	450
Y4	1.187	1.181	1.278	0.001	0.001	0.001	0.001	1.278	1.181	1.187	562.5
Y3	1.187	1.181	1.278	0.001	0.001	0.001	0.001	1.278	1.181	1.187	562.5
Y2	1.187	1.181	1.181	1.277	1.277	1.277	1.277	1.181	1.181	1.187	450
Y1	0.223	0.217	0.217	0.218	0.218	0.218	0.218	0.217	0.217	0.223	450
Length of zones(mm)	556.66	556.66	556.66	565	565	565	565	556.66	556.66	556.66	

Figure 9.7, Zones divisions and corrector factors of SBO2

SBO3	X1	X2	X3	X4	X5	X6	X7	X8	X9	X10	Height of zones(mm)
Y5	1.283	1.278	1.278	1.278	1.278	1.278	1.278	1.278	1.278	1.283	450
Y4	1.187	1.278	1.278	0.001	0.001	0.001	0.001	1.278	1.278	1.187	525
Y3	1.187	1.277	1.277	1.277	1.277	1.277	1.277	1.277	1.277	1.187	500
Y2	0.926	0.921	0.921	0.921	0.921	0.921	0.921	0.921	0.921	0.926	500
Y1	0.223	0.217	0.218	0.218	0.218	0.218	0.218	0.218	0.217	0.223	500
Length of zones(mm)	446.67	446.67	446.67	730	730	730	730	446.67	446.67	446.67	

Figure 9.8, Zones divisions and corrector factors of SBO3

SBO4	X1	X2	X3	X4	X5	X6	X7	X8	X9	X10	Height of zones(mm)
Y5	1.283	1.278	1.278	1.278	1.278	1.278	1.278	1.278	1.278	1.283	450
Y4	1.187	1.181	1.181	1.278	0.001	0.001	1.278	1.181	1.181	1.187	525
Y3	1.187	1.181	1.181	1.278	0.001	0.001	1.278	1.181	1.181	1.187	500
Y2	1.187	1.181	1.181	1.278	0.001	0.001	1.278	1.181	1.181	1.187	500
Y1	0.223	0.218	0.218	1.278	0.001	0.001	1.278	0.218	0.218	0.223	500
Length of zones(mm)	587.5	587.5	587.5	587.5	450	450	587.5	587.5	587.5	587.5	

Figure 9.9, Zones divisions and corrector factors of SBO4
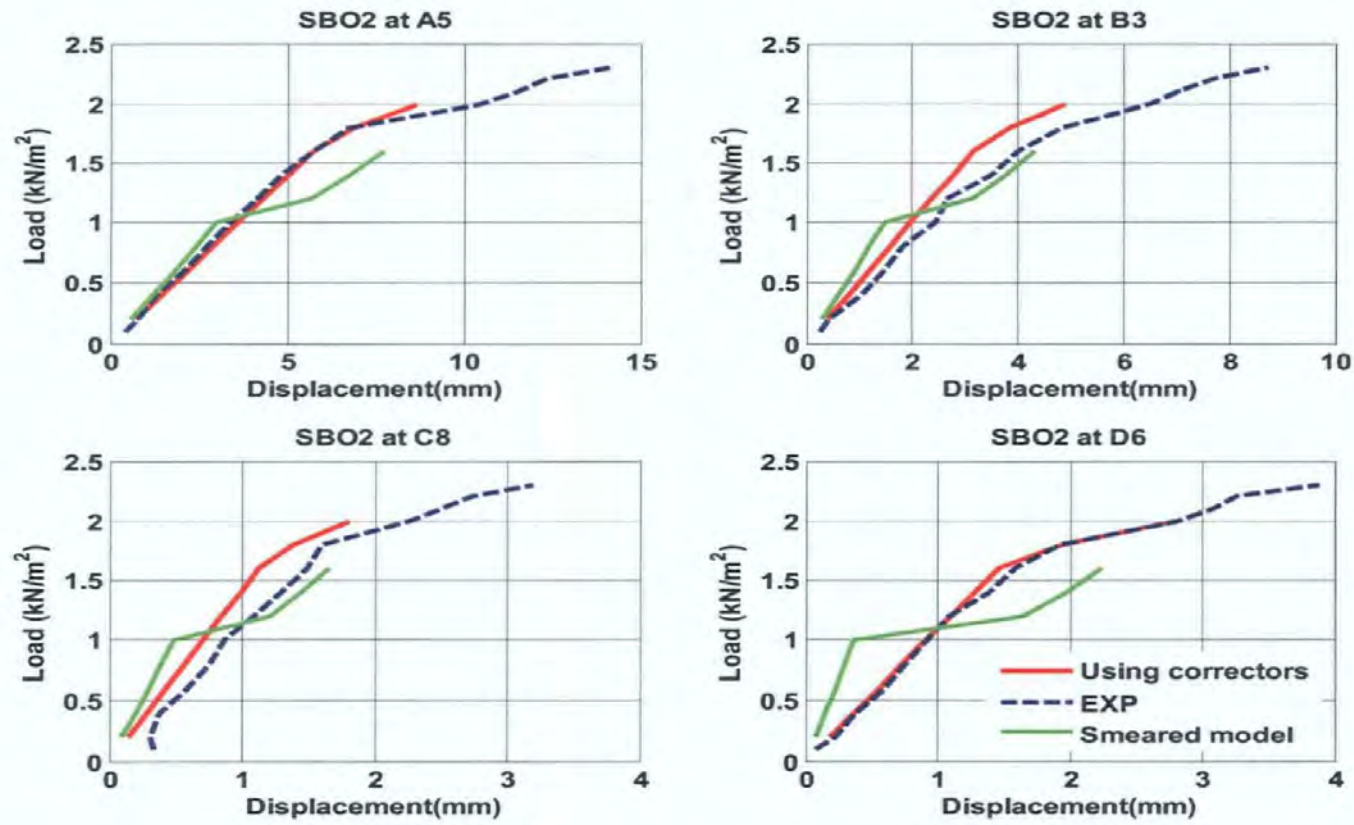
Figure 9.10. The improved load deflection relationships of SBO2
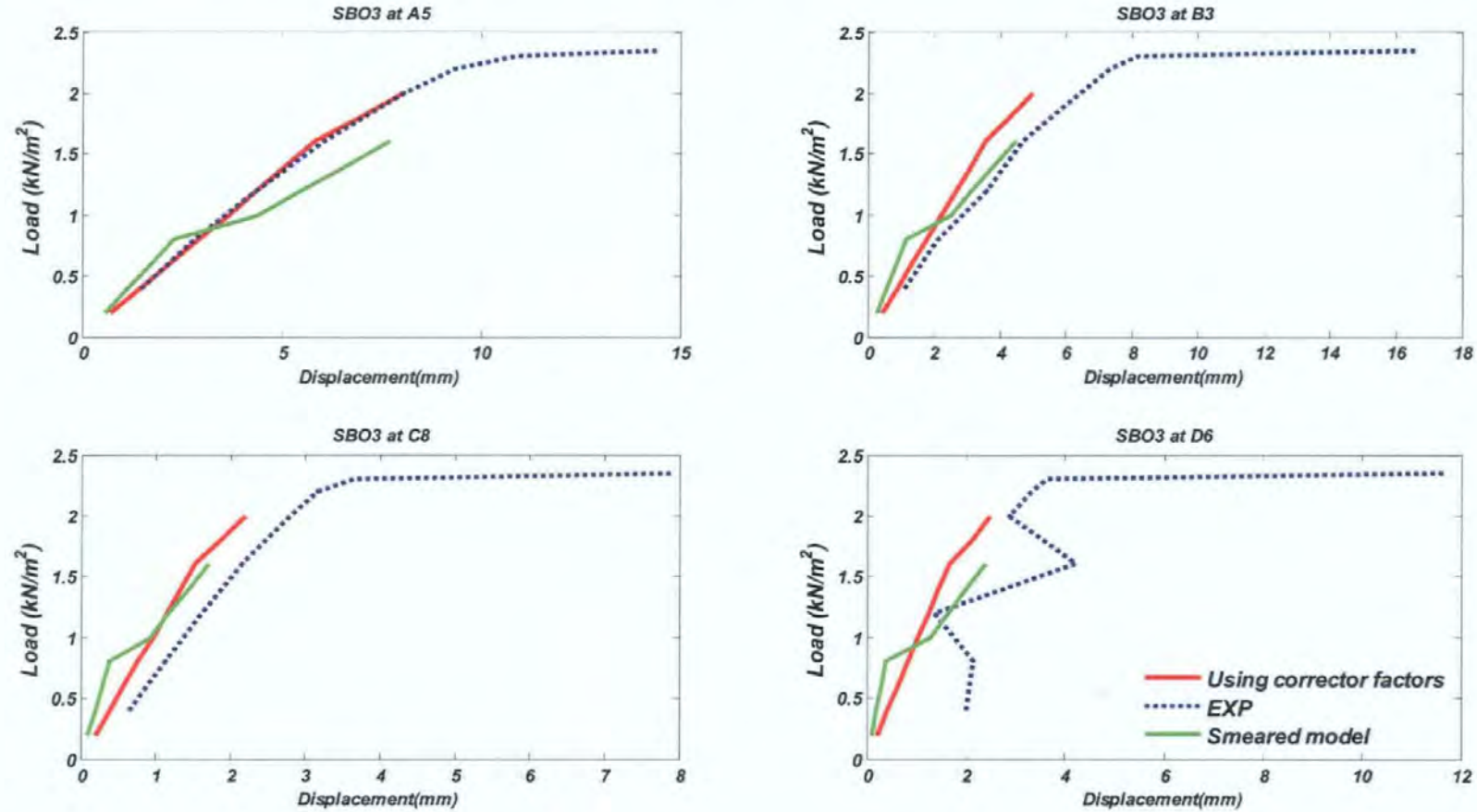
Figure 9.11, The improved load deflection relationships of SBO3
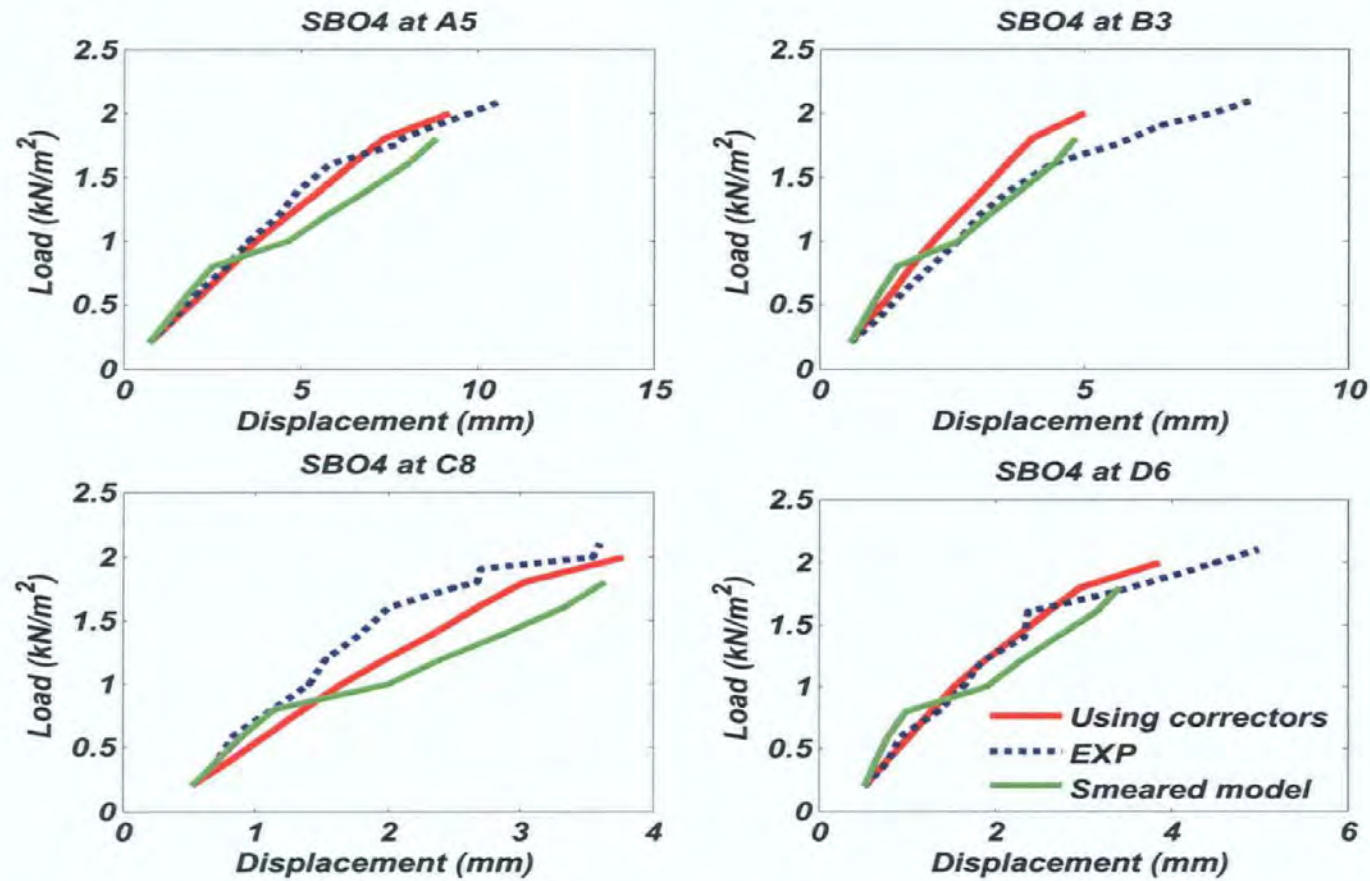
Figure 9.12 The improved load deflection relationships of SBO4

9.3.2 The analyses of masonry wall panels tested in the University of Edinburgh

Liang(1999) in the University of Edinburgh tested 14 masonry panels with different boundary conditions and aspect ratios. Details of these panels are summarised in Table 9.2. These tables are divided into 3 groups:

1) 4 edges simply supported:

   Wall 1, wall 2, wall 3, wall 8, wall 12 wall 14, wall 15

2) 3 edges simply supported and top edge free:

   Wall 4, wall 5, wall 9, wall 13

3) 3 edges simply supported and the right vertical edge free

   Wall 6, wall 7, wall 10, wall11

Table 9.2, Masonry panels tested by Liang(1999)

Support conditions	Wall NO.	Dimension (mm)	Aspect ratio	Flexural strength (N/mm2)		Cracking pressure (KN/m2)	Failure pressure (KN/m2)
		(Length * High)	(Lx/Ly)	fx	fy	EXP	EXP
4 sides simply supported	Wall 1	1140*1140	1	1.79	0.7	6.4	7.46
	Wall 2	1150*1150	1	3	0.75	6.5	12
	Wall 3	1150*1150	1	3.07	0.75	6.8	12.55
	Wall 8	795 *1190	0.67	3	0.9	----	25
	Wall 12	795 * 1190	0.67	3.5	0.98	----	31.8
	Wall 14	1130 * 755	1.5	2.9	0.75	9.9	20.6
	Wall 15	1130 * 755	1.5	2.8	0.74	10.7	18.9
3 sides simply supported and top free	Wall 4	1140*1140	1	2.9	0.75	----	8.54
	Wall 5	1140*1140	1	2.9	0.75	----	8.55
	Wall 9	795*1190	0.67	3.5	0.98	----	23.5
	Wall 13	795*1190	0.67	3.5	1.1	----	27.8
3 sides simply supported and 1 side free	Wall 6	1200*1200	1	3	0.74	2.8	5.2
	Wall 7	1200*1200	1	2.95	0.71	2.2	4.51
	Wall 10	795*1190	0.67	3.65	1.1	7	12.2
	Wall 11	795*1190	0.67	3.5	0.9	6.5	11.9

In this case study, all these panels, except wall 2 which is taken to get the strength corrector factors, are used for the failure load validation. Walls 1, 8, 4, 9, 6, 10 are also used for deflections validation using the corrector factors in Table 7.10. During the validations, the wallette flexural strength perpendicular and parallel to the bed joints shown in Table 9.2 are used. For the elastic modulus, E=12 kN/mm^2 is used as this is the mean value of the elastic modulus E in the two directions (perpendicular and parallel to bed joint) obtained from the test carried out by Liang(1999) in the University of Edinburgh.

The stiffness corrector factors are derived from the base panel SBO1 using the criteria described in section 9.1. These stiffness corrector factors are shown in Table 9.3 to Table 9.9. Meanwhile, the strength corrector factors used here are derived from the laboratory test using wall 2 in Table 9.2 (cfx=1.15, cfy=1.04), which are different from those in Table 7.11. The predicted failure loads of these panels are presented in Table 9.10 and the load deflection relationships of walls 1, 8, 4, 9, 6, 10 are presented as Figure 9.13 to Figure 9.18.

Table 9.3, Corrector factors for wall 1, wall 2, and wall 3

Wall 1 & 2 & 3	1	2	3	4	5
y5	0.926	0.926	0.926	0.926	0.926
y4	0.926	0.921	0.920	0.921	0.926
y3	0.926	0.921	0.920	0.921	0.926
y2	0.926	0.921	0.920	0.921	0.926
y1	0.926	0.926	0.926	0.926	0.926

Table 9.4. Corrector factors for wall 8 and wall 12

Wall 8 & 12	1	2	3
y5	0.926	0.926	0.926
y4	0.926	0.921	0.926
y3	0.926	0.921	0.926
y2	0.926	0.921	0.926
y1	0.926	0.926	0.926

Table 9.5. Corrector factors for wall 14 and wall 15

Wall 15	1	2	3	4	5
y3	0.926	0.926	0.926	0.926	0.926
y2	0.926	0.921	0.920	0.921	0.926
y1	0.926	0.926	0.926	0.926	0.926

Table 9.6. Corrector factors for wall 4 and wall 5

Wall4&5	X1	X2	X3	X4	X5
Y5	1.283	1.278	1.278	1.278	1.283
Y4	1.187	1.181	1.181	1.181	1.187
Y3	1.187	1.181	1.181	1.181	1.187
Y2	1.187	1.181	1.181	1.181	1.187
Y1	1.187	1.187	0.926	1.187	1.187

Table 9.7, Corrector factors for wall 9 and wall 13

Wall 9&13	X1	X2	X3
Y1	1.283	1.278	1.283
Y2	1.187	1.181	1.187
Y3	1.187	1.181	1.187
Y4	1.187	1.181	1.187
Y5	1.187	1.187	1.187

Table 9.8, corrector factors for wall 6 and wall 7

Wall 6, 7	X1	X2	X3	X4	X5
Y5	1.187	1.187	0.926	1.187	1.283
Y4	1.187	1.181	0.921	1.187	1.278
Y3	1.187	1.181	0.921	1.187	1.278
Y2	1.187	1.181	0.921	1.187	1.278
Y1	1.187	1.187	0.926	1.187	1.283

Table 9.9, Corrector factors for wall 10 and wall 11

wall 10 & 11	X1	X2	X3
Y5	1.187	1.082	1.283
Y4	1.187	1.137	1.283
Y3	1.187	1.137	1.283
Y2	1.187	1.137	1.283
Y1	1.187	1.082	1.283

Table 9.10, Analytical failure load using corrector factors

Support conditions	Wall NO.	Cracking pressure (KN/m2)		Failure pressure (KN/m2)	
		EXP	FEA using corrector factors	EXP	FEA using corrector factors
4 sides simply supported	Wall 1	6.4	6.5	7.46	7.5
	Wall 2	6.5	8	12	*
	Wall 3	6.8	8	12.55	12
	Wall 8	----	----	25	27
	Wall 12	----	----	31.8	28
	Wall 14	9.9	----	20.6	16.5
	Wall 15	10.7		18.9	
3 sides simply supported and top free	Wall 4	----	---	8.54	9.5
	Wall 5	----	---	8.55	9.5
	Wall 9	----	---	23.5	22
	Wall 13	----	---	27.8	22
3 sides simply supported and 1 side free	Wall 6	2.8	3	5.2	5
	Wall 7	2.2	2.4	4.51	4.8
	Wall 10	7	4.4	12.2	8.6
	Wall 11	6.5	4.4	11.9	8.6

* Wall 2 was utilized to get strength corrector factors used in this section
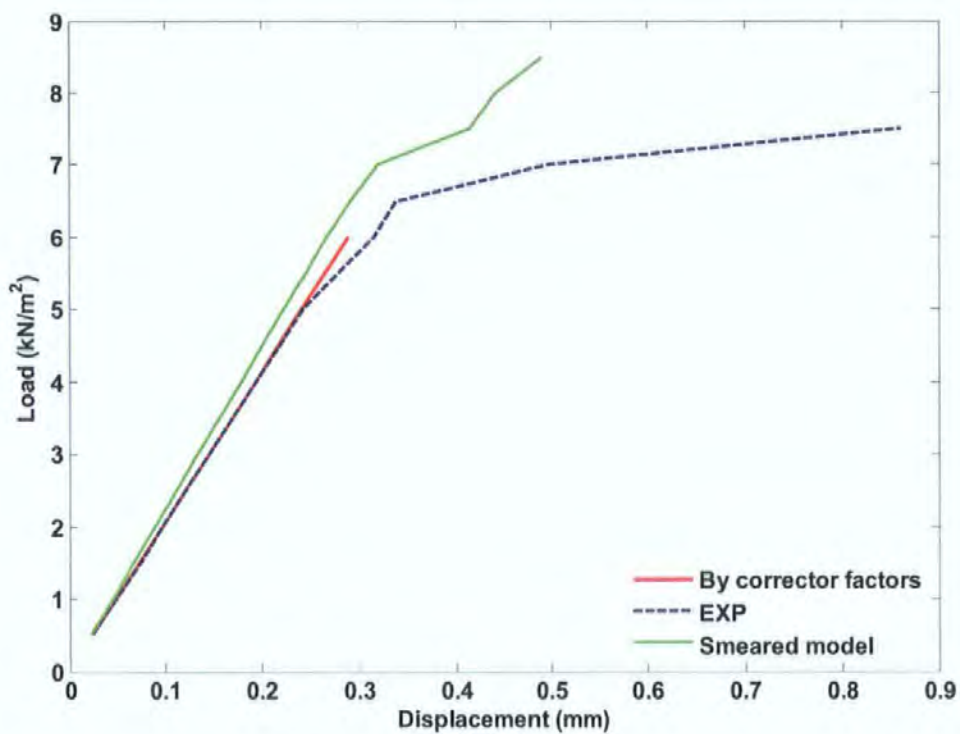
Figure 9.13, The improved load deflection relationships of wall 1
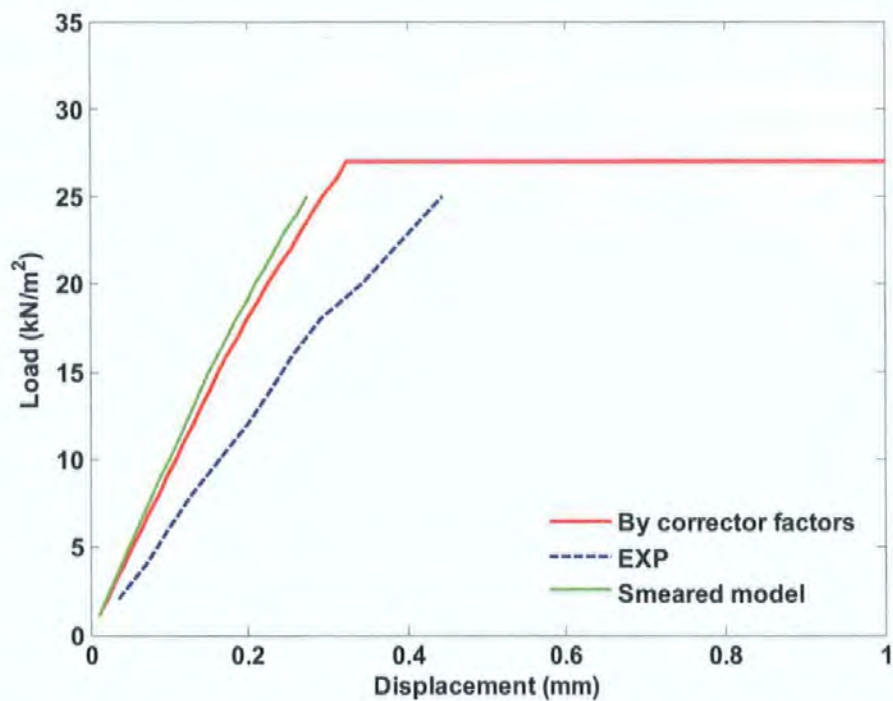
Figure 9.14 The improved load deflection relationships of wall 8
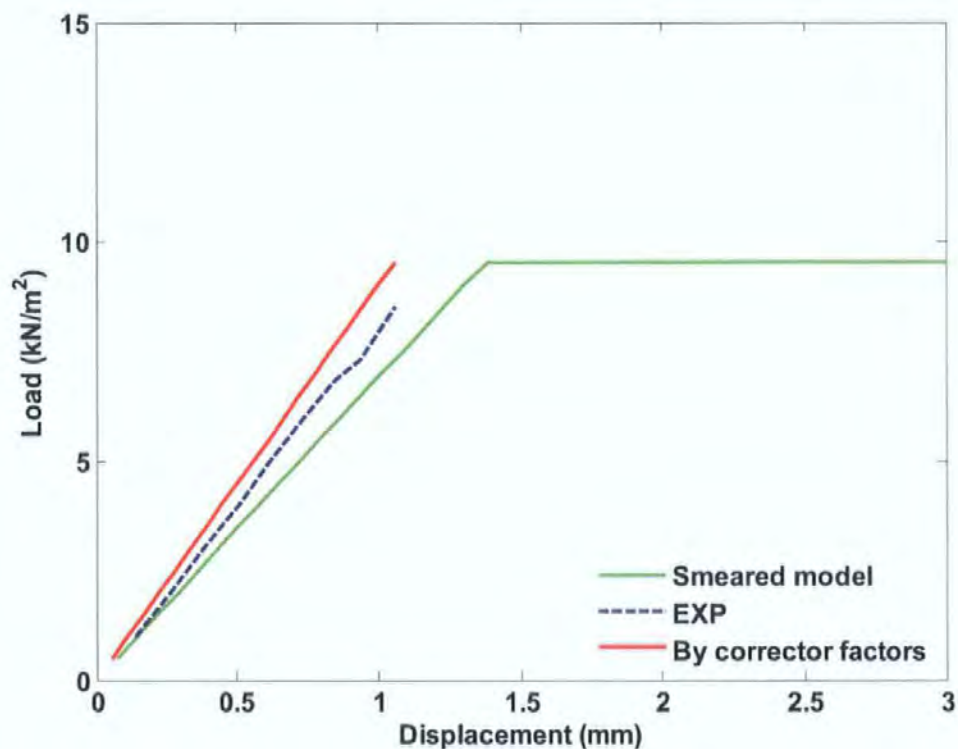
Figure 9.15, The improved load deflection relationships of panel "wall 4"
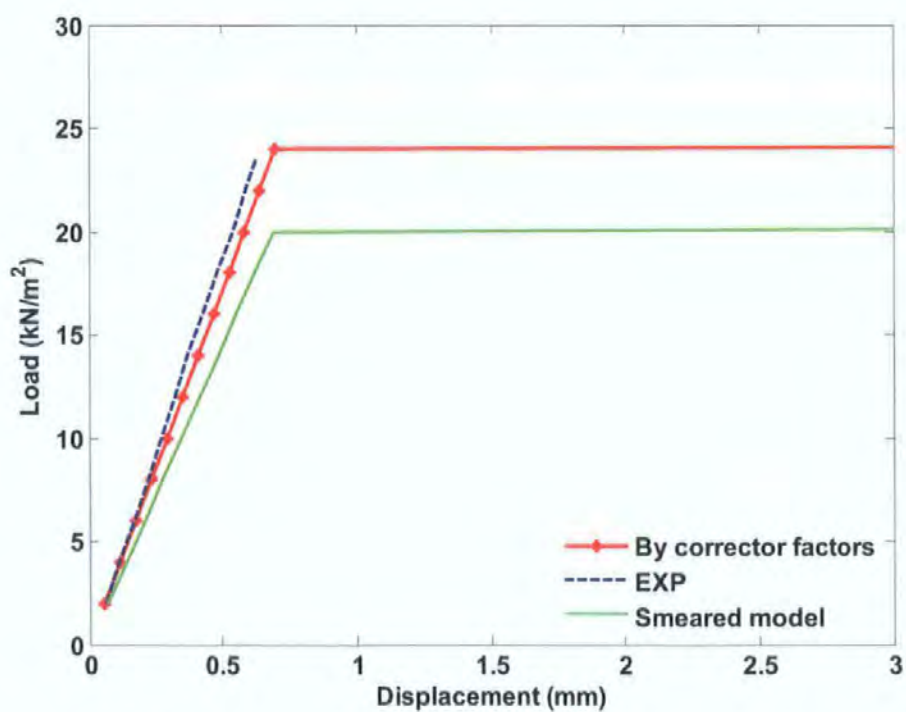
Figure 9.16, The improved load deflection relationships of panel "wall 9"
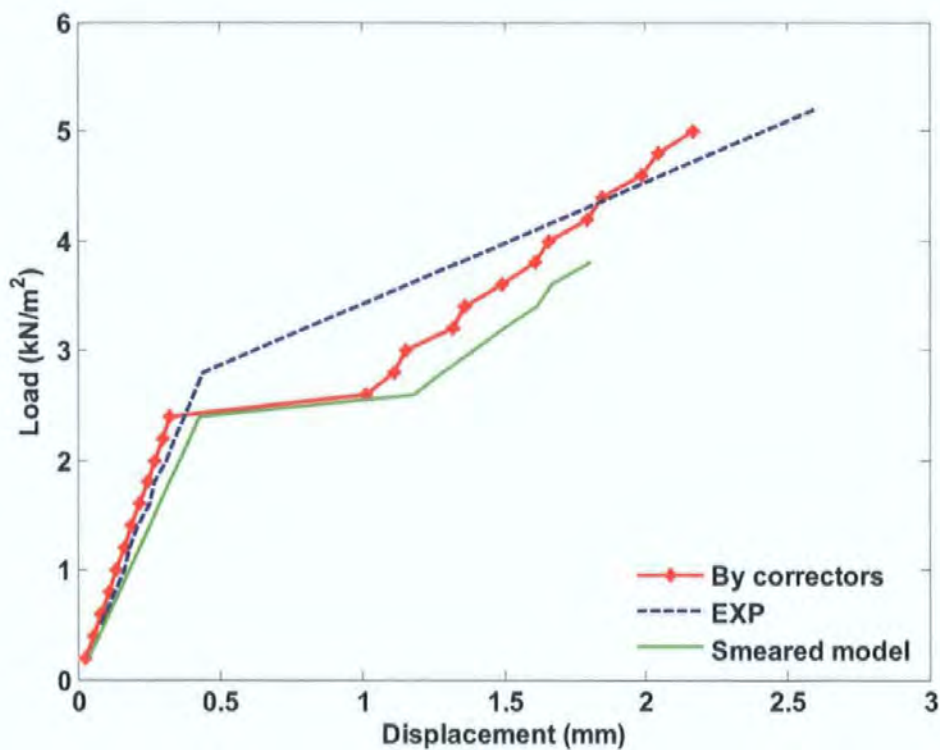
Figure 9.17 the improved load deflection relationships of panel "wall 6"
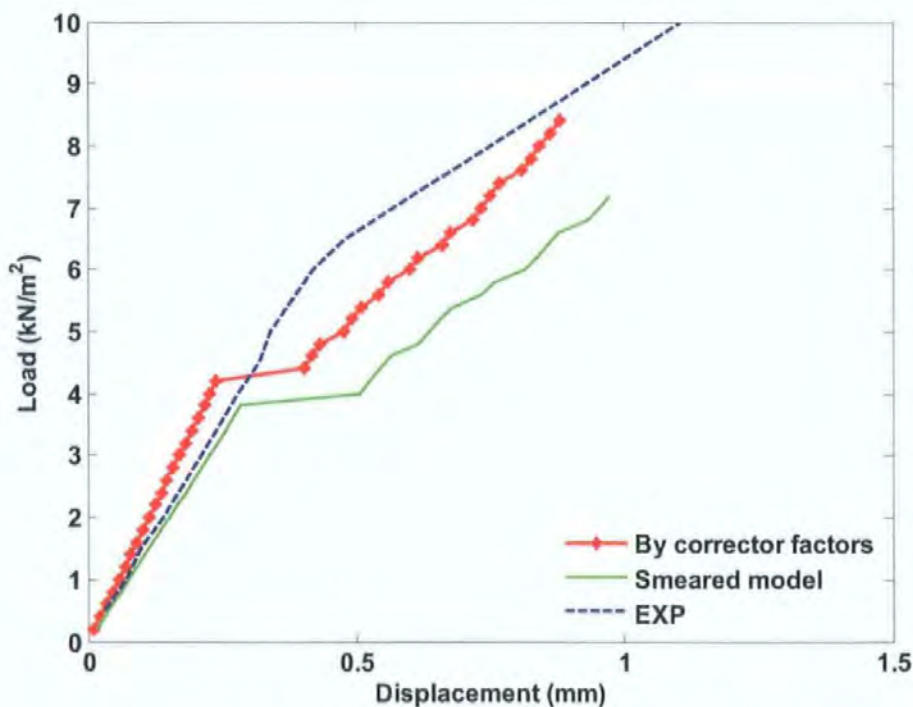
Figure 9.18, The improved load deflection relationships of panel "wall 10"

From the failure loads shown in Table 9.10 and the load deflection curves presented in Figures 9.13 to 9.18, it can be seen that using corrector factors effectively improves the failure load and deflections. For the wall 10 and wall 11, there is slightly larger difference between the experimental and the predicted failure load. This might have been caused by the zone division in the horizontal direction, which could have led to an improper assigning of corrector factors to the column zones of the centre of the panel.

9.3.3 The analyses of masonry wall panels tested in CERAM

A large number of laterally loaded masonry walls panels were tested by CERAM (former British Ceramic Research Association). However, most of the available information from CERAM tested panels is cavity wall panels, which are not covered in this study. Among the available information, 2 single leaf solid brick masonry panels Wall CR 1 and Wall CR 2 are selected for verification, their experimental deflection data are listed in Appendix 3.

9.3.3.1 Wall CR1

Wall CR1a tested by Edgell (1995b) is a single leaf masonry panel constructed with Fletton brick with three sides simply supported and the top edge free. Its dimension is 2.8 x 3.6m. The configuration of wall CR1 is as shown in Figure 9.19 with 11 measuring points at which the load deflection relationships of this wall were measured. The flexural strengths measured from the wallette tests for this panel are given as: fx =1.4N/mm^2, fy=0.40N/mm^2. However, the elastic modulus E and Poisson's ratio are not indicated in the original data. Therefore the elastic modulus E and Poisson's ratio v are assumed to be : E=12kN/mm2, v=0.2 based on the suggestions by Chong (1993). Here again the stiffness corrector factors are derived from the base panel SBO1 using the criteria introduced in section 9.1 and these corrector factors are shown in Figure 9.20.The strength corrector factors used here are the same with those obtained in

Chapter 7 with consideration of the difference between the experimental results and that of Monte Carlo simulations, they are the load deflection curves are shown in Figure 9.21. From Figure 9.21, it can be seen that using corrector factors both the predicted failure load and load deflection relationships are greatly improved.
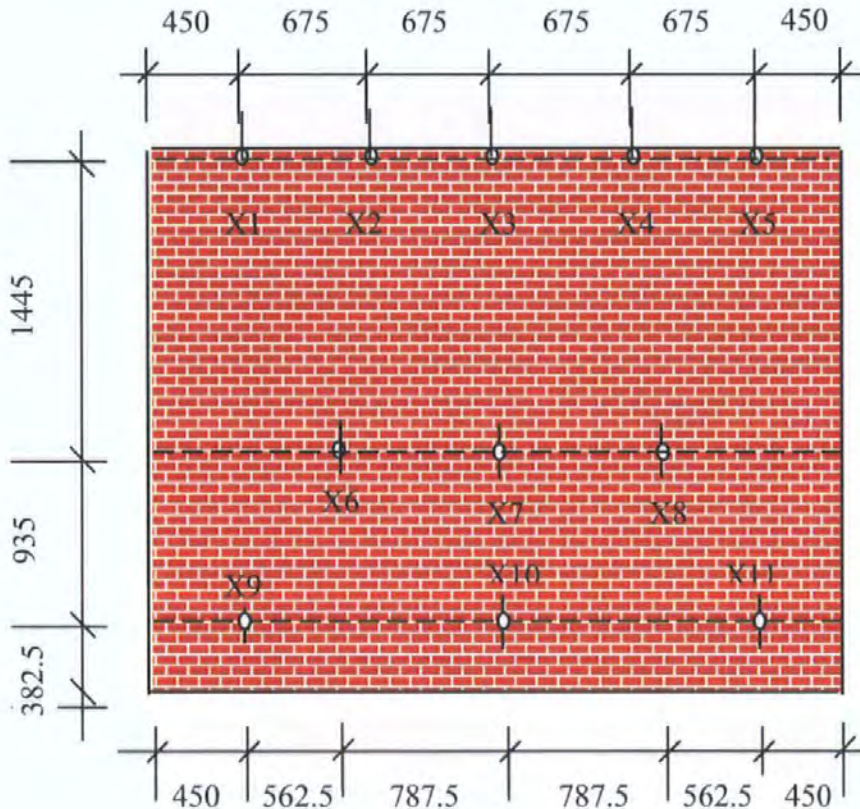
Figure 9.19, Configuration of wall CR 1

Wall CR1	X1	X2	X3	X4	X5	X6
Y5	1.283	1.278	1.278	1.278	1.278	1.283
Y4	1.187	1.181	1.181	1.181	1.181	1.187
Y3	1.187	1.181	1.181	1.181	1.181	1.187
Y2	1.187	1.181	1.181	1.181	1.181	1.187
Y1	1.187	1.187	1.187	1.187	1.187	1.187

Figure 9.20, Corrector Factors of Wall CR1

216
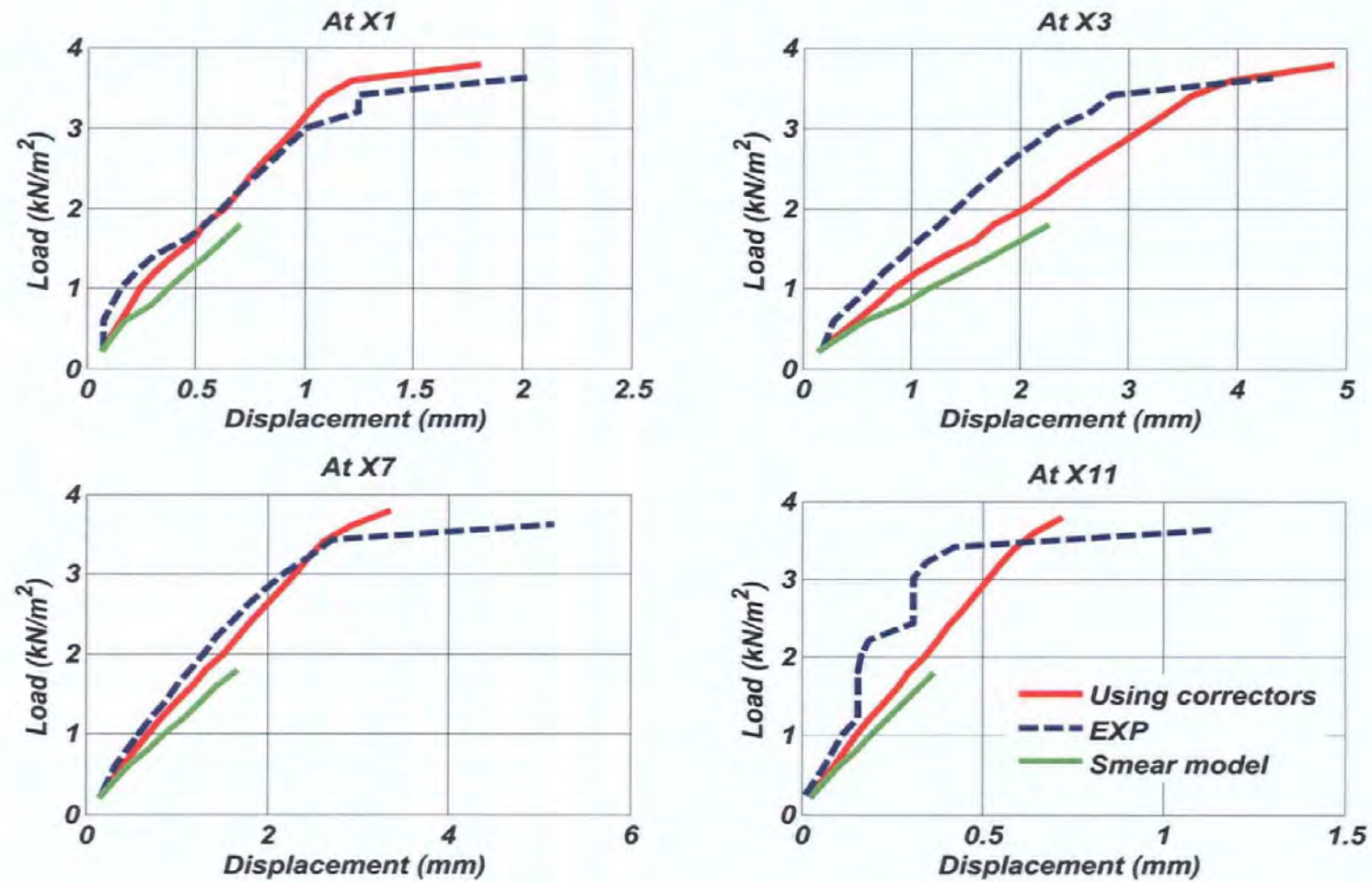
Figure 9.21, The improved load deflection relationships on wall CR1

9.3.3.2 Wall CR2

Wall CR2 tested by Edgell (1995a) is a single leaf masonry panel tested by CERAM with a central opening and constructed with Fletton bricks with three sides constrained and the top edge free. Its dimension is 5.5 x 2.8m with the opening size 2m x 1.2 m. The configuration of wall CR2 is as shown in Figure 9.22; there were 15 measuring points at which the load deflection relationships for this wall were measured.

The mean flexural strengths for this wall measured from the wallette tests are: fx $=1.37N/mm^2$ and fy=0.42 N/mm^2. However, the elastic modulus E and Poisson's ratio are not included in the original data, therefore the elastic modulus E and Poisson's ratio v are assumed to be : $E=12kN/mm^2$, v=0.2 based on the suggestions by Chong (1993).

Since the 3 edges of the wall panel were under restraint and top edge was free during the test, the 3 edges are defined to be simply supported in FEA model, and the corresponding corrector factors and zone divisions are as shown in Figure 9.23. These corrector factors are obtained from the base panel SBO1 using the criteria introduced in section 9.1. The strength corrector factors used here are the same as those obtained in Table 7.11 with considering the ratio between the experimental results and that of Monte Carlo simulations of the base panel SBO1 Chong(1993). The load deflection relationships for this panel are shown in Figure 9.24 using corrector factors.

From Figure 9.24, it is clear that using corrector factors, both the analysis of failure load and deflections are improved. The predicted failure load is smaller than the experimental one which might be caused by the existence of the frame at the top of opening which was not considered during the analysis.
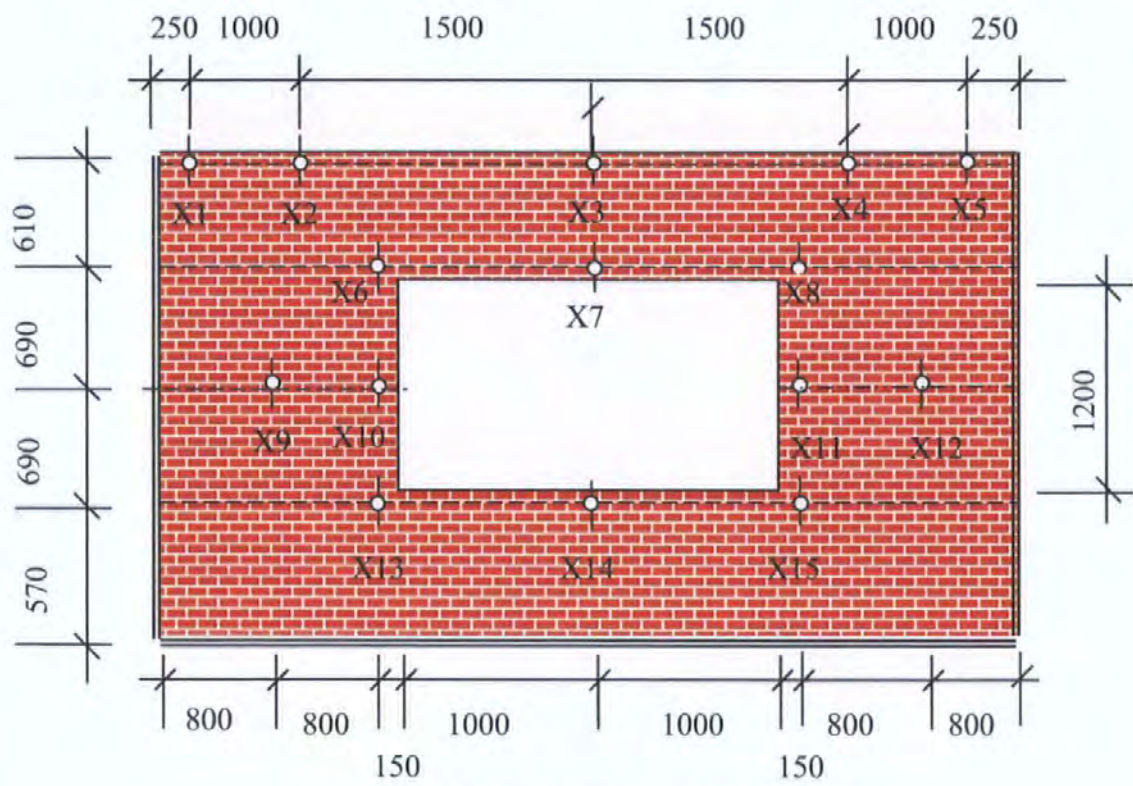
Figure 9.22, Configuration of wall CR 2

Wall CR2	X1	X2	X3	X4	X5	X6 (X5)	X7 (X4)	X8 (X3)	X9 (X2)	X10 (X1)
Y4	1.283	1.278	1.278	1.278	1.278	1.278	1.278	1.278	1.278	1.283
Y3	1.187	1.181	1.278	0.01	0.01	0.01	0.01	1.278	1.181	1.187
Y2	1.187	1.181	1.278	0.01	0.01	0.01	0.01	1.278	1.181	1.187
Y1	1.187	1.187	1.187	1.187	1.187	1.187	1.187	1.187	1.187	1.187

Figure 9.23, Zone divisions and corrector factors for wall CR 2
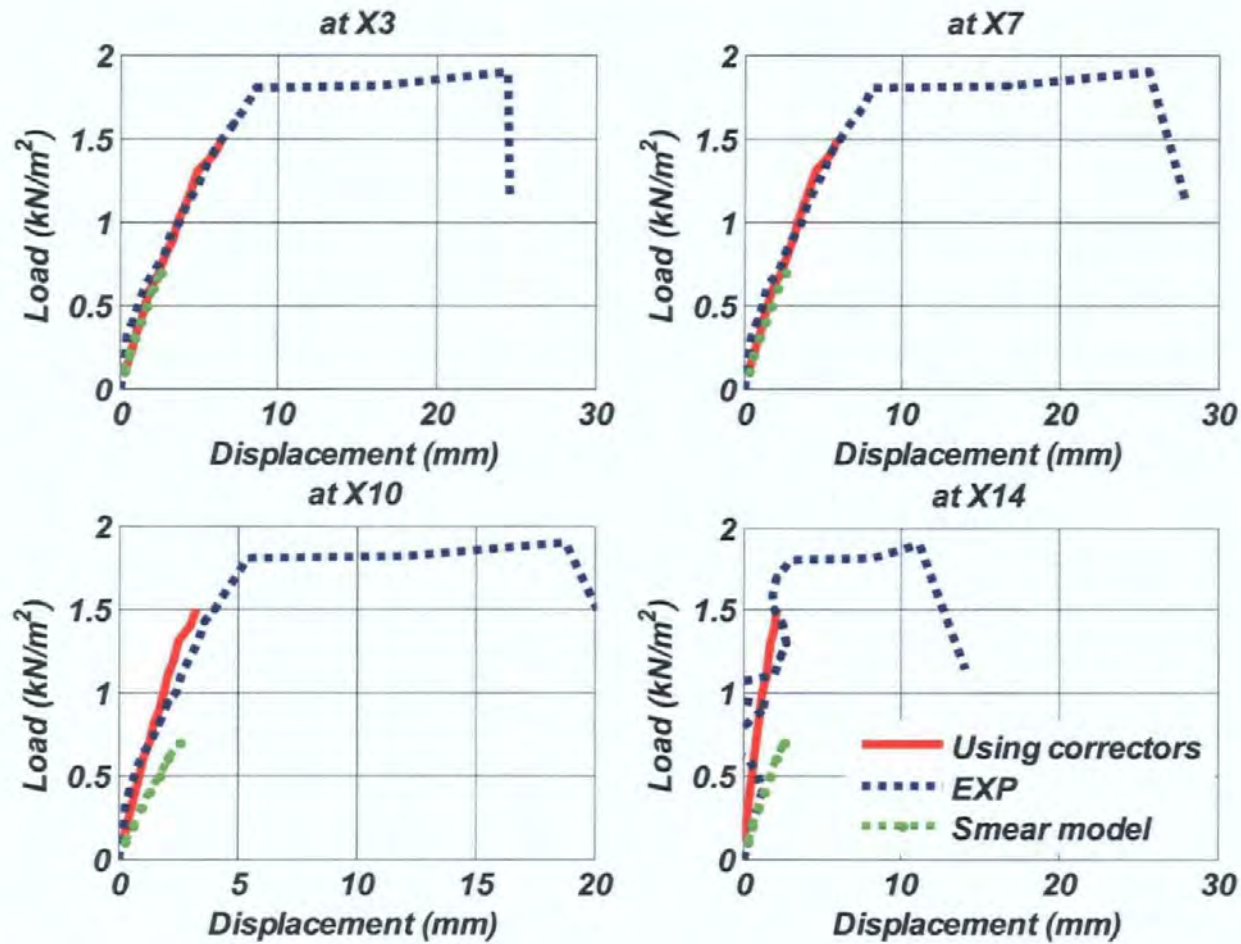
Figure 9.24, The improved load deflection relationships of wall CR 2 using corrector factors

9.4 CASE STUDIES OF FAILURE PATTERN

In section 7.6, it was shown that, to the base panel SBO1, the failure pattern of using

corrector factors is reasonable agree with the experimental one. In this section, the

failure patterns of more general masonry panels using corrector factors are studied.

Masonry panel have been using in this chapter, except those from the University of

Edinburgh, are utilised again, for the study of failure patterns, they are: SBO2, SBO3,

SBO4, CR1, CR2.

Figure 9.25 to Figure 9.34 are the comparison of the experimental failure patterns and

the analytical ones using correctors, the used correctors are those have been used in

section 9.3 in this chapter.

From these Figures, It can be concluded that, using corrector factors can give a better

prediction to failure pattern as well.
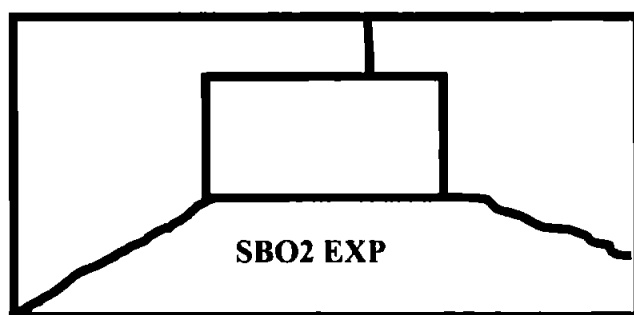
Figure 9.25, the experimental failure pattern of SBO2

Principal stress contour of SBO2 using correctors at 2.0 KN/m²
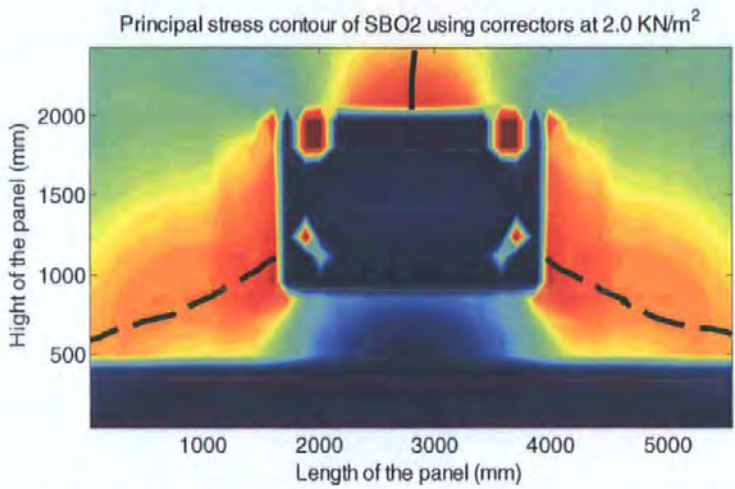
Figure 9.6, the analytical failure pattern of SBO2 using corrector factors

SBO3 EXP
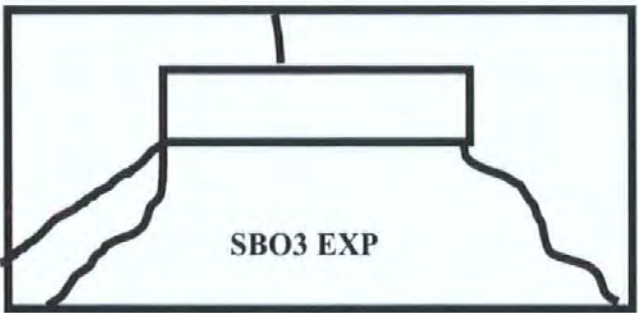
Figure 9.27, the experimental failure pattern of SBO3

Principal stress contour of SBO3 on the outer surface at 2 kN/m²,
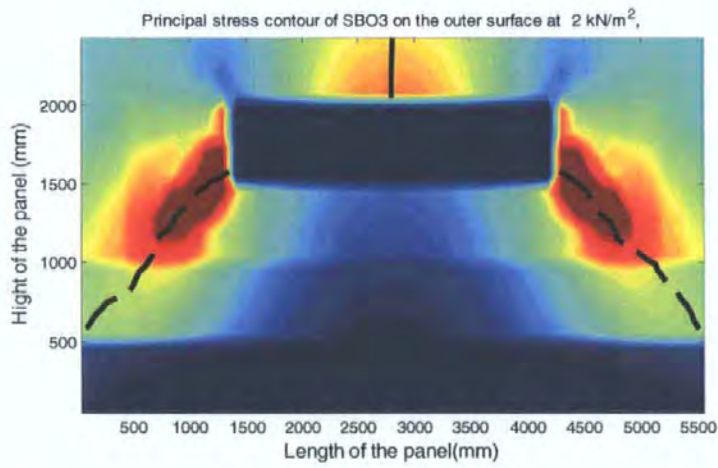
Figure 9.28, the analytical failure pattern of SBO3 using corrector factors
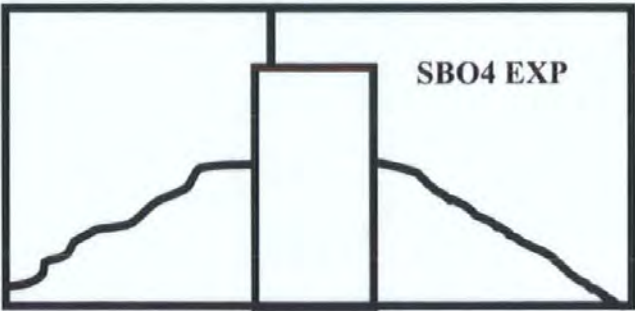
Figure 9.29, the experimental failure pattern of SBO4
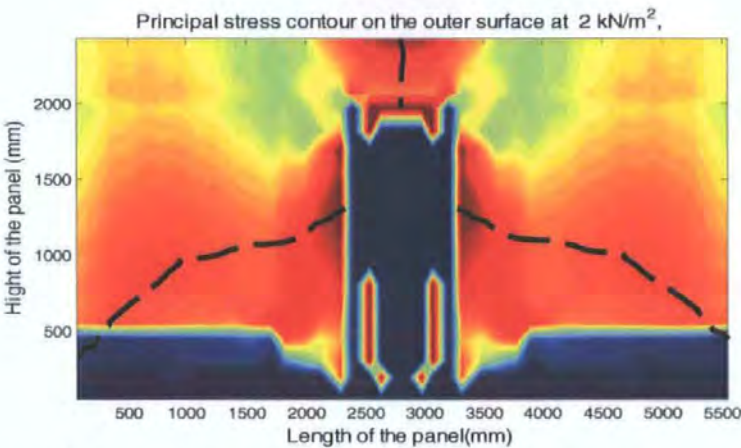
Figure 9.30, the analytical failure pattern of SBO4 using corrector factors
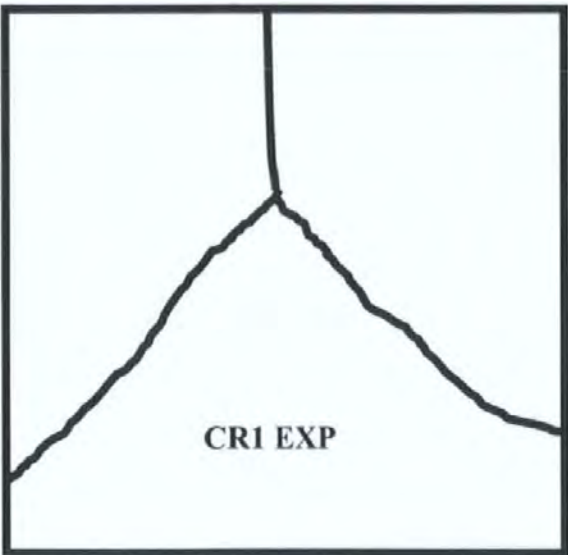
Figure 9.31, the experimental failure pattern of CR1

Principal stress contour of CR1 using correctors on the outer surface at 3.8 kN/m^2,
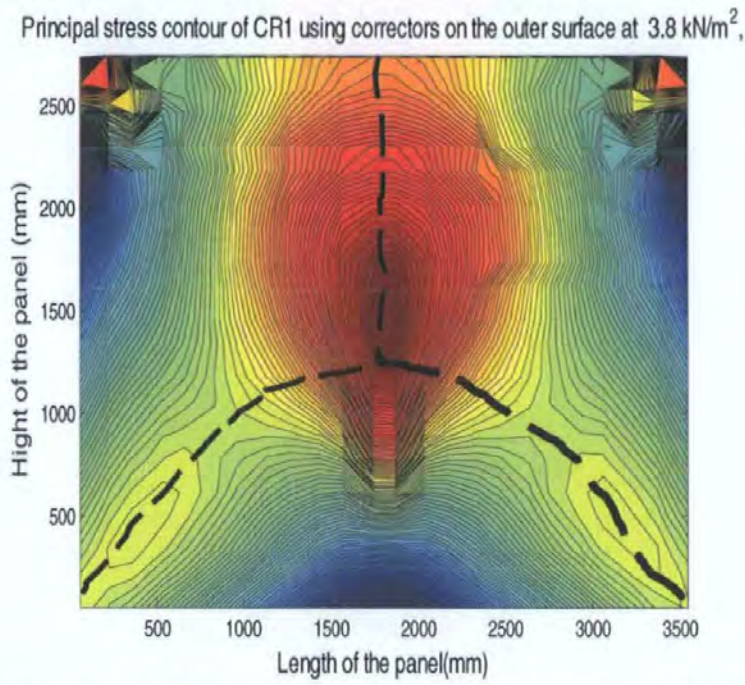
Figure 9.32, the analytical failure pattern of CR1 using corrector factors

CR2 EXP
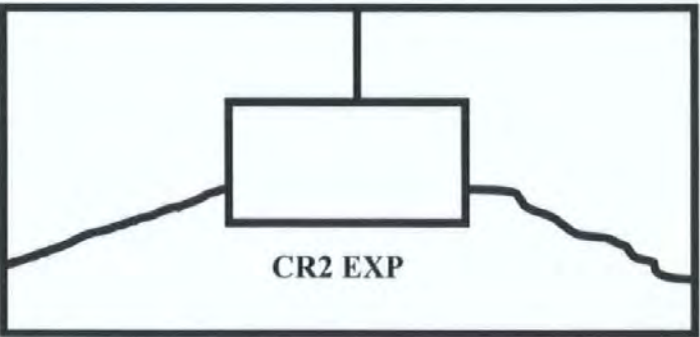
Figure 9.33, the experimental failure pattern of CR2

Principal stress contour of wall CR2 using correctors on the outer surface at 1.4 kN/m^2,
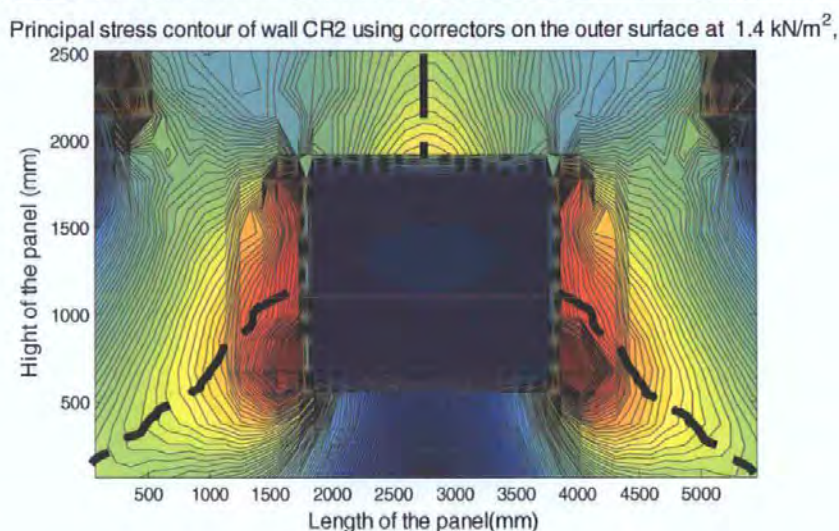
Figure 9.34 the analytical failure pattern of CR2 using corrector factors

9.5 SUMMARY

From the results obtained from these case studies in this chapter, several conclusions can be drawn:

1. Using the stiffness and strength corrector factors derived in Chapter 7, along with using the revised CA criteria, the non-linear FEA analysis using corrector factors gives a very good correlation with the experimental results. The predicted failure loads are improved and the predicted load deflection relationships and failure pattern closely agree with the experimental results.

2. Due to the improved results using corrector factors, it was confirmed that the boundary conditions have a decisive influence on the behaviour of lateral loaded masonry panels. Therefore, the validation of any FEA models for analysing laterally loaded masonry panels without considering the effects of boundary conditions is suspicious. This also means that further experimental studies of the boundary constraints are necessary.

3. The criteria of using cellular automata (CA) to model similar zones, still needs to be further studied to get more accurate analytical results.

4. Most of the predicted failure loads using corrector factors still appear slightly lower than the experimental results, which mean that the physical meaning of the strength corrector factors should be further investigated.

10. CONCLUSIONS AND PERSPECTIVES

10.1 CONCLUSIONS

In this research, the following conclusions have been drawn:

1. This dissertation describes a methodology for the refinement of corrector factors, to improve the prediction of the response of laterally loaded masonry wall panels. Using the refined corrector factors via finite element analysis (FEA), the analysis on both the failure load and the deformations of the entire panels are effectively improved.

2. Because laterally loaded masonry wall panel consists of two kinds of materials and its experimental deflection data are irregular, but macro-modelling regards masonry as one material and the analytical deflections should be regular, in order to compare like with like and make a more accurate numerical analyses, a methodology to refine these irregular data is studied. The methodology expresses the lateral deflections using the continuous formulae and makes the lateral deflections at any position on the panel available, which improves the further numerical analysis. This technique was necessary for use in the GA model to achieve a suitable set of corrector factors for the base panel.

3. A methodology to derive corrector factors using a model updating method and the genetic algorithm (GA) is studied. The objective function and the constraint-function are proposed in this study, which are suitable to derive corrector factors that improve the FEA to match the experimental results well at all load levels on the entire masonry panel. Moreover, compare with the method proposed by the previous researcher, this method can derive corrector factors at any position of

the masonry panel without the limitation of the measuring points, which is ideal for further studying and utilising corrector factors.

4. The genetic algorithm (GA) is shown to be a powerful tool for model updating, particularly when the problem concerns many variables and in a discontinuous solution space like this research.

5. This research directly reveals that boundary effects have a large influence on the behaviour of laterally loaded masonry wall panels. The derived corrector factors and the uniqueness study indicated that the actual boundary conditions of a masonry panel are not fully fixed or purely simply supported. The improper definitions of boundary conditions in a FEA results in the inaccuracy of the FEA.

6. Accurately quantifying and modelling the boundary effects have been difficult both for engineers and researchers, but this problem is sorted out by using corrector factors.

7. Using the modified criteria of matching similar zones, the corrector factors from the base panel are successfully applied to more general masonry wall panels. The verification through 19 masonry panels of different boundary conditions and materials shows that the derived corrector factors can effectively improve the prediction of the behaviour of laterally loaded masonry wall panels. The investigation through 5 masonry panels shows that using corrector factors can predict the failure pattern as well.

10.2 FURTHER RESERRCH

1. So far, the physical meanings of stiffness corrector factors are clear. However, the physical meaning of strength corrector factors is still not identified. It would be a meaningful work to combine the model updating method proposed in this

research with micro-modelling and homogeneous techniques, to identify the physical meaning of strength corrector factors.

2. Strength corrector factors might be due to the variation of the material properties or the physical combination of units and mortar. It is meaningful to do such experiments: using panels of isotropic materials with grooves on its surface to simulate the mortar. The advantage of this method is to minimise the variation of material properties.

3. It is necessary to test masonry panels with recordings of the boundary rotation and movements, to further validate the findings in this research.

4. The criteria of using cellular automata should be further investigated including its transition function and its parameter values.

5. Quantifying the boundary effect directly using boundary parameters should be investigated along with modifying the constitutive relationships using model updating techniques.

6. This research should be extended to other FEA models such as those studied by Lourenco. Moreover, further investigation should be carried out on applying corrector factors to other masonry panels such as block masonry panels and reinforced masonry panel.

7. So far an isotropic model for the masonry matrail has been considered in the FE analysis. It would be better if suitability of an orthotropic model is investigated that may suit better a highly composite material like masonry.

REFERENCES

AHMADIAN, H., (2001), *Boundary Condition Identification by Solving Characteristic Equations*, Journal of Sound and Vibration 247, (5), 75-763

AL-QAISIA, A., CATANIA, G. and MENEGHETTI, U., (2003), *Crack Localization in Non-Rotating Shafts Coupled to Elastic Foundation Using Sensitivity Analysis Techniques* Journal of Quality in Maintenance Engineering, 9, (2), 176-201

ANDERSON, C., (1984), *Transverse Laterally Loaded Tests on Single Leaf and Cavity Walls*, CIB Third International Symposium on Wall Structures. Warsaw,

ANDERSON, C., (1985), *Tests on Walls Subjected to Uniform Lateral Loading and Edge Loading*, Proceedings-7th International Brick Masonry Conference, Melbourne, Australia, Vol.2 February, 1985, 889-900.

ANDERSON, C., (1987), *Lateral Strength from Full-Sized Tests Related to the Flexural Properties of Masonry*, Masonry International, 1, (2), 51-55

ANGELIS, M. D., LUS, H., BETTI, R. and W.LONGMAN, R., (2002), *Extracting Physical Parameters of Mechanical Models from Identified State Space Representations*, Journal of Applied Mechanics, 69, (5), 617-625

ANTHOINE, A., (1997), *Homogenisation of Periodic Masonry: Plane Stress, Generalised Plane Strain or 3d Modelling*, Communication in numerical method in Engineering, 13, 319-326

ARTHOINE, A., (1995), *Derivation of the in-Plane Elastic Characteristic of Masonry through Homogenisation Theory*, International Journal of Solid and Structures, 32, (2), 137-163

ASTEROM, K. J. and EYKHFF, P., (1971), *System Identification-a Survey*, Automatica, 7, 123-126

ATALLA, M. J., (1996), *Model Updating Using Neural Networks*, Virginia Polytechnic Institute and State University, 1-146

BAKER, L. R., (1972), *Brickwork Panels Subject to Face Wind Loads*, M. EngSc Thesis, University of Melbourne,

BAKER, L. R., (1973), *Structural Action of Brickwork Panels Subject to Wind Loads* Journal Australian Ceramic Society, 9, (1), 1-36

BAKER, L. R., (1979), *A Failure Criterion for Brickwork in Bi-Axial Bending* Proceedings of Fifth International Brick Masonry Conference, Washington, D.C., October,

BAKER, L. R., (1980), *Lateral Loading of Masonry Panels*, Structural design of masonry, Cement and Concrete Association of Australia,, Melbourne,

BAKER, L. R., (1982a), *An Elastic Principal Stress Theory for Brickwork Panels in Flexure*, Proceedings of the 6th International Brick Masonry Conference,Rome,1982, 523-537.

BAKER, L. R., (1982b), *A Failure Criterion for Brickwork in Biaxial Bending*, Proceedings of the 5th International Brick Masonry Conference, Washington D.C, BIA,

BAKER, L. R., (1982c), *A Principal Stress Failure Criterion for Brickwork in Bi-Axial Bending*, Proceedings of the 6th International Brick Masonry Conference, Rome, 1982

BAKVALOV, N. and PANASENKO, G., (1989), *Homogenisations: Averaging Processes in Periodic Media* Math. Appl. (Soviet Ser.) 36 Kluwer. Academic Publishers, 1989,

BANAN, M. R., BANAN, M. R. and HJELMSTAD, K. D., (1992), *Parameter Estimation in Complex Linear Structures*, Probabilistic mechanics and structural and geotechnical reliability, Denver, Co, USA 571-574.

BANAN, M. R., BANAN, M. R. and HJELMSTAD, K. D., (1994a), *Parameter Estimation of Structures from Static Response*, II: Numerical simulation studies, Journal of structural engineering, 120, (11), 3259-3283

BANAN, M. R., BANAN, M. R. and HJELMSTAD, K. D., (1994b), *Parameter Estimation of Structures from Static Response, I: Computational Aspects*, Journal of structural engineering, 120, (11), 3243-3258

BANAN, M. R., BANAN, M. R. and HJELMSTAD, K. D., (1999), *Time-Domain Parameter Estimation Algorithm for Structures*, .II: Numerical simulation studies, Journal of Engineering Mechanics, 121, (3), 435-447

BERRET, R. and COGAN, S., (1992), *Updating Finite Element Models Using Static Deformations.*, computers & structures, 45, (4), 649-654

BERTRAND, M., (1989), *an Introduction to the Numerical Analysis of Spectral Methods*, 154 Springer-Verlag New York, Inc. New York, NY, USA ISBN: 0-387-51106-7

BESDO, D., (1985), *Inelastic Behaviour of Plane Frictionless Block System Described as Cosserat Media*, Archives in Mechanics, 37, (6), 603-619

BIGONI, D. and PICCOLROAZ, A., (2004), *Yield Criteria for Quasi-Brittle and Frictional Materials*, International Journal of Solids and Structures 4, 2855-2878

BRADSHAW, R. E. and ENTWISTLE, F. D., (1965), *Wind Forces on Non-Load Bearing Brickwork Panels*, Clay Products Technical Bureau, London, CPTB Technical Notes, Vol. 1, No. 6, May 1965,

BRARUCH, M., (1982), *Optical Correction of Mass and Stiffness Matrices Using Measured Modes*, AIAA Journals, 20, 1623-1626

BRENNER, S. C. and SCOTT, R., (2002), *The Mathematical Theory of Finite Element Methods*, 294 pages Springer Verlag,2nd edition, ISBN:0387954511

BRINKER, R., (1984), *Yield-Line Theory and Materials Properties of Laterally Loaded Masonry Walls*, International Journal of Masonry Construction Masonry, No. 1, April, 1984, 8-17

British Standards Inst 1970, Code of Practice for Structural Use of Masonry, Part 1, CP111; Part 1, London.

BROOKS, J. J. and BABER, B. H. A., (1998), *The Modulus of Elasticity of Masonry*, Masonry International, 12, (2), 58-63

BROWNJOHN, J. M. W., HONG, H. and CHIEN, P. T., (2001), *Assessment of Structural Condition of Bridges by Dynamic Measurements*, Applied Research Project No. RG 5/97, School of Civil and Structural Engineering, Nanyang Technological University, Singapore, 2001,

CAESAR, B., (1987), *Updating System Matrices Using Model Test Data*, Proceedings of 5th international modal analysis conference, London UK, 453-459.

CAJDERT, A., (1980), *Laterally Loaded Masonry Walls,* Division of Concrete Structures. Chalmers University of Technology ISBN 91-7032-016-0

CANDY, C. C. E., (1988), *The Energy Line Method for Masonry Panel under Lateral Loading*, proceedins-8th International Brick/Block Masonry Conference, Vol. 2, September 1988, 1159-1170.

CECCHI, A. and RIZZI, N. L., (2001), *Heterogeneous Elastic Solids: A Mixed Homogenization-Rigidication Technique*, International Journal of Solids and Structures 38, 29-36

CECCHI, A. and SAB, K., (2002a), *A Multi-Parameter Homogenization Study for Modelling Elastic Masonry* European Journal of Mechanics - A / Solids 21, (2), 249-268

CECCHI, A. and SAB, K., (2002b), *Out of Plane Model for Heterogeneous Periodic Materials: The Case of Masonry* European Journal of Mechanics - A / Solids 21, (5), 715-746

CECCHI, A. and SAB, K., (2004), *A Comparison between a 3d Discrete Model and Two Homogenised Plate Models for Periodic Elastic Brickwork*, International Journal of Solids and Structures, 41, 2259-2276

CHAKRABORTY, S. and MUKHOPADHYAY, M., (2000), *Estimation of in-Plane Elastic Parameters and Stiffener Geometry of Stiffened Plates*, Journal of Sound and vibration 23, (1), 99-124

CHAKRABORTY, S., MUKHOPADHYAY, M. and SHA, O. P., (2002), *Determination of Physical Parameters of Stiffened Plates Using Genetic Algorithm*, Journal of computing in civil engineering, 16, (3), 206-221

CHANG, C. C., CHANG, T. Y. P. and XU, Y. G., (2000), *Adaptive Neural Networks for Model Updating for Structures*, Smat Mater Struct, 9, 59-68

CHEN, X., ZHU, H. and CHEN, C., (2005), *Structural Damage Identification Using Test Static Data Based on Grey System Theory*, J Zhejiang Univ SCI, 6A, (8), 790-796

CHONG, V. L., (1993), *The Behaviour of Laterally Loaded Masonry Panels with Openings*, PhD thesis, School of Engineering, University of Plymouth,

CHONG, V. L., MAY, I. M., SOUTHCOMBE, C. and MA, S. Y. A., (1992a), *An Investigation of the Behaviour of Laterally Loaded Masonry Panels Using Non-Linear Finite Element Program*, 3rd Int. masonry conference, London, The British masonry society,

CHONG, V. L., SOUTHCOMBE, C. and MAY, I. M., (1992b), *The Behaviour of Laterally Loaded Masonry Panels with Openings*, 3rd Int. masonry conference, London, the British masonry society,

CHRISTIANSEN, P., (1996), *Theoretical Determination of Flexural Strength of Unreinforced Masonry.*, Masonry international, 9, (3), 84-90

DASCOTTE, E., (1991), *Applications of Finite Element Model Updating Using Experimental Modal Data*, Based on an article published in Sound and Vibration / June 1991. (http://www.femtools.com/download/docs/sv91.pdf),

DAVEY, N. and THOMAS, F. G., (1950), *the Structural Use of Masonry Brickwork*, Proceedings of Institution of Civil Engineers, Structural Building Paper NO.24,

DIANA, T., (2005 published), *Finite Element Analysis (FEA) Software*, http://www.tnodiana.com/index-vervolg.php?scherm=2&pagina_id=18,

DUARTE, R. B., (1993), *a Study of the Lateral Strength of Brickwork Panels with Openings*, PhD Thesis, University of Edinburgh,

DUARTE, R. B., (1998), *the Design of Unreinforced Brickwork Panels with Openings under Lateral Pressure*, Masonry International, 11, (3), 97-101

ECHERT, L. and CAESAR, B., (1991), *Model Updating under Incomplete and Noisy Modal Test Data*, Proceedings of 9th international modal analysis conference, Florence,Italy,15-18,April,

EDGELL, G. J., (1987), *Factors Affecting the Flexural Strength of Brick Masonry*, Masonry International, 1, (1), 16-24

EDGELL, G. J., (1995a), *Additional Work on Wide Cavity Walls*, Masonry research strategy committee additional work on wide cavity walls, Ref: MRSC/5, May 1995, CERAM research report,,

EDGELL, G. J., (1995b), *Dynamic and Static Lateral Loading of Story Height Walls*, Structural masonry strategy committee gust loading of story height walls, Reference: SM / SMSC .D .1, January 1995, CERAM research report,

EDGELL, G. J., (2005), *Masonry*, Structural Engineer, 83, (9), 27-31

EDGELL, G. J. and KJAER, E., (2000), *Lateral Load Behaviour of Walls with Openings*, Conference, Name, Madrid, Spain, 537-544

EDGELL, G. J., N.J.BRIGHT and M.HEALTH, (2002), *Characteristic Compressive Strength of UK Masonry: A Review*, Proceedings of the British Masonry Society, the Society Stoke-on-Trent, 9, 109-120.

EPUREANU, B. I. and YIN, S.-H., (2004), *Identification of Damage in an Aero elastic System Based on Attractor Deformations*, Computers and Structures, 82, 2743–2751

ESSAWY, A. S., DRYSDALE, R. G. and MIRZA, F. A., (1985), *Non-Linear Macroscopic Finite Element Model for Masonry Walls*, Proc. of New Analysis Techniques for Structural Masonry, ASCE Structures Congress'85, Chicago, Illinois, 19-45.

FANG, X., LUO, H. and TANG, J., (2005), *Structural Damage Detection Using Neural Network with Learning Rate Improvement*, Computers and Structures 83 (2005) 2150–2161,

FRIED, A. N., (1989), *Laterally Loaded Masonry Panels - the Significance of Analytical Techniques and Materials Properties*, PhD thesis, South Bank Polytechnic,

FRISWELL, M. I. and MOTTERSHEAD, J. E., (1995), *Finite Element Model Updating in Structural Dynamics,* Kluwer Academic Publishers, ISBN 0792334310

FRISWELL, M. I., PENNY, J. E. T. and GARVEY, S. D., (1998), *A Combined Genetic and Eigensensitivity Algorithm for the Location of Damage in Structures*, Computers and Structures 69   547-556

GAIRNS, D. A., (1983), *Flexural Behaviour of Concrete Block work Panels". Master of Building Science Thesis, University of Melbourne,*

GE, M. and LUI, E. M., (2005), *Structural Damage Identification Using System Dynamic Properties*, Computers and Structures, 83 2185-2196

GEN, M. and CHENG, R., (1997), *Genetic Algorithms and Engineering Design* John Wiley & Sons Inc ISBN: 978-0-471-12741-3

GOLDING, J. M., (1991), *Practical Design of Laterally Loaded Masonry Panels*, construction and building materials, 1, (3), 135-146

HAJELA, P. and SOEIO, F. J., (1989), *Structural Damage Detection Based on Static and Modal Analysis*, AIAA Journal, 28, (6), 1110-1115

HANGANU, A. D., ONATE, E. and BARBAT, A. H., (2002), *A Finite Element Methodology for Local/Global Damage Evaluation in Civil Engineering Structures*, Computers and Structures, 80, 1667–1687

HASELTINE, B. A. and HODGKINSON, H. R., (1973), *Wind Effects on Brick Panel Walls-Design Information"*. Proc. 3rd International Brick Masonry Conference, Essen, Jane 1973, 399-406.

HASELTINE, B. A., HODGKINSON, H. R. and WEBB, W. F., (1973), *Lateral Loading Tests on Walls with Different Boundary Conditions*, Third International Brick Masonry Conference, Essen,

HASELTINE, B. A. and WEST, H. W. H., (1976), *Design of Laterally Loaded Wall Panels: Part 2*, Technical Note, No. 248, The British Ceramic Research Association,

HENDRY, A. W., (1973), *the Lateral Strength of Unreinforced Brickwork*, the Structural Engineer, 51, (2), 43-50. Discussion, Vol.51, (48) August, 1973, 1277-1284

HENDRY, A. W. and KHEIR, A. M. A., (1976), *The Lateral Strength of Certain Brickwork Panels*, Proc. 4th International Brick Masonry Conference, Bruges April, 1976,

HENDRY, E. A. W., (2001), *Masonry Walls: Materials and Construction*, Construction and Building Materials, 15, (8), 323-330

HILLERBORG, A., (1976), *Strip Method of Design* Scholium Intl, ISBN: 0721010121

HJELMSTAD, K. D., BANAN, M. R. and BANAN, M. R., (1999), *Time-Domain Parameter Estimation Algorithm for Structures,I: Computation Aspects*, Journal of Engineering Mechanics, 121, (3), 424-447

HJELMSTAD, K. D. and SHIN, S., (1997), *Damage Detection and Assessment of Structures from Static Response*, Journal of Engineering Mechanics, 123, (6), 568-576

HU, N., (2001), *Damage Assessment of Structures Using Model Test Data.* International Journal of Solids and Structures, 38, 3111-3126

JAISHI, B., (2005), *Finite Element Model Updating of Civil Engineering Structures under Operational Conditions*, College of Civil Engineering and Architecture, Fuzhou University,

JOHANSEN, K. W., (1972), *"Yield Line Formulae for Slabs"*. London, Cement & Concrete Association, London 1972. ISBN:0721008194, OCLC: 533031

KANYETO, O. J., FRIED, A. N., ALI, J. and ROBERTS, J. J., (2006), *Behaviour of Laterally Loaded Concrete Block work Panels Constructed with Thin Layer Mortar,*, 7th International Masonry Conference 30/31 October – 1 November, London,

KELCH, N. W., (1932), *Method Used in Testing Masonry Specimen for Bending, Tension and Shear*, Journal of American Ceramic Society, 14, (2), 125-132

KOH, C. G., CHEN, Y. F. and LIAW, C.-Y., (2003), *A Hybrid Computational Strategy for Identification of Structural Parameters*, Computers and Structures, 81, 107–117

KOŁAKOWSKI, P., MUJICA, L. E. and VEHÍ, J., (2006), *Two Approaches to Structural Damage Identification Model Updating Vs. Soft Computing*, Journal of Intelligent Material Systems and Structures, 17, (1), pp. 63-79

LARBI, J. A., (2004), *Microscopy Applied to the Diagnosis of the Deterioration of Brick Masonry*, Construction and Building Materials 18, 299-307

LAUWAGIE, T., SOL, H. and DASCOTTE, E., (2002), *Damage Identification in Beams Using Inverse Methods*, PROCEEDINGS OF ISMA2002 - VOLUME II, 715-722.

LAWRENCE, S. J., (1983), *Behaviour of Brick Masonry Walls under Lateral Loading.* , PhD thesis, Volumes 1 and 2, University of New South Wales,

LAWRENCE, S. J., (1994), *Out-of-Plane Lateral Load Resistance of Clay Brick Panels* Australia Structural Engineering Conference, Sydney,

LAWRENCE, S. J., (1995), *The Behaviour of Masonry in Horizontal Flexure*, Seventh Canadian Masonry Symposium, Hamilton, Ontario,, McMaster University,

LAWRENCE, S. J. and CAO, H. T., (1988), *Cracking of Non-Load bearing Masonry Walls under Lateral Forces* 8th International Brick/Block Masonry Conference, Dublin,

LAWRENCE, S. J. and LU, J. P., (1991a), *An Elastic Analysis of Laterally Loaded Masonry Walls with Openings*, International Symposium on Computer Methods in Structural Masonry, pp 39-48, Swansea(Wales),

LAWRENCE, S. J. and LU, J. P., (1991b), *An Investigation of Laterally Loaded Masonry Walls with Openings,* Computer method in structural masonry, pp.39-48, Books and Journals International,

LEE, J. S., PANDE, G. N., MIDDLETON, J. and .., K., (1996), *Numerical Modelling of Brick Masonry Panels Subject to Lateral Loadings*, Computer and Structures, Vol. 61, No. 4, pp 735-745,

LEE, U., CHO, K. and SHIN, J., (2003), *Identification of Orthotropic Damages within a Thin Uniform Plate*, International Journal of Solids and Structures, 40, 2195–2213

LI, Y. Y., CHENG, L., YAM, L. H. and WONG, W. O., (2002), *Identification of Damage Locations for Plate-Like Structures Using Damage Sensitive Indices, Strain Modal Approach*, Computers and Structures, 80, 1881-1894

LIANG, J. X., (1991), *A Finite Element Equivalent Material Model for Structural Masonry*, PhD Thesis, University College of Swansea,

LIANG, N. C., (1999), *Experimental and Theoretical Investigation of the Behaviour of Brickwork Cladding Panel Subjected to Lateral Loading*, School of Engineering and Electronics, University of Edinburgh, 246

LINK, M., (1993), *Updating of Analytical Models-Procedure and Experience*, Proceedings of Conference on modern practice in stress and vibration analysis Sheffield,UK, 35-52.

LINK, M., (1999), *Updating of Analytical Models-Review of Numerical Procedures and Application Aspects*, in proceedings of the structural dynamics forum SD 2000, Los Alamos,

LIU, P.-L. and CHIAN, C.-C., (1997), *Parameter Identification of Truss Structures Using Static Strains*, Journal of structural engineering, 123, (7), 927-933

LOSBERG, A. and JOHANSSON, S., (1964), *Sideway Pressure on Masonry Walls of Brickwork*, CIB Symp. On Load bearing Walls, Warsaw,

LOURECO, P. B., (1997), *an Anisotropic Plasticity Model for Quasi-Brittle Composite Shells*, 5th Int. Conf. Comput. Plast, Owen, CIMNE, pp., 1192-1199.

LOURENCO, P. B., (1994), *Analysis of Masonry Structures with Interface Elements.*, Faculty of Civil Engineering, Delft University of Technology,

LOURENCO, P. B., (1996), *A User/Programmer's Guide for the Micro-Modelling of Masonry Structures.*, Department of Civil Engineering, University of Minho,

LOURENCO, P. B., (1997a), *an Anisotropic Macro-Model for Masonry Plates and Shells: Implementation and Validation.*, Faculty of Civil Engineering, Delft University of Technology. The Netherlands,

LOURENCO, P. B., (1997b), *Two Aspects of Masonry Modelling, Size Effect and Parameter Sensitivity.*, University of Minho,

LOURENCO, P. B., (1998), *Experimental and Numerical Issues in the Modelling of the Mechanical Behaviour of Masonry, in Structural Analysis of Historical Constructions*, II,Eds. P. Roca et al., CIMNE, Barcelona, , p. 57-91

LOURENCO, P. B., (2000a), *Anisotropic Softening Model for Masonry Plates and Shells*, J. Struct. Engrg., 126, (9), 1008-1016

LOURENCO, P. B., (2000b), *Anisotropic Softening Model for Masonry Plates and Shells* Journal of Structural Engineering, 126, (9), 1008-1016

LOURENCO, P. B., (2001), *A Review of out-of-Plane Behaviour of Masonry*, Masonry international, 14, (3), 67-73

LOURENCO, P. B., (2004), *Current Experimental and Numerical Issues in Masonry Research*, Universidade do Minho, Guimarães,Portugal,
http://www.civil.uminho.pt/masonry/Publications/Update_Webpage/2004_Lourenco.pdf

LOURENCO, P. B., (1996), *Computational Strategies for Masonry Structures* Delft University of Technology, Países Baixos, 206

LOURENCO, P. B., ALMEIDA, J. C. and BARROS, J. A., (2005), *Experimental Investigation of Bricks under Uniaxial Tensile Testing*, Masonry International, 18, (1), 11-20

LOURENCO, P. B. and ROTS, J. G., (2000), *An Anisotropic Failure Criterion for Masonry Suitable for Numerical Implementation*, TMS Journal, 18, (1), 11-18

LOURENCO, P. B., ROTS, J. G. and PLUIJM, R., (1999), *Understanding the Tensile Behaviour of Masonry under Tension Parallel to the Bed Joints*, Masonry International, 12, (3), 96-103

LUCIANO, R. and SACCO, E., (1997), *Homogenization Technique and Damage Model for Old Masonry Material*, International Journal of Solids and Structures, 34, (24), 3191-3208

LUCIANO, R. and SACCO, E., (1998), *A Damage Model for Masonry Structures*, European Journal of Mechanics - A/Solids, 17, (2), 285-303

MA, S. Y. A. and MAY, I. M., (1984), *Masonry Panels under Lateral Loads.* , Report No. 3, Dept of Engineering, University of Warwick,

MA, S. Y. A. and MAY, I. M., (1986), *A Complete Biaxial Stress Failure Criterion for Brick Masonry*, Proceedings of Masonry Society, 1ST International for Brick Masonry 2, 115-117.

MACKERLE, J., (1998), *Finite Element Methods and Material Processing Technology, an Addendum (1994-1996)* Engineering Computations, 15, (5), 616-690

MACKERLE, J., (2000), *Finite Element Analyses and Simulations in Biomedicine: Bibliography (1985-1999) Engineering Computations*, 17, (7), 813-865

MACKERLE, J., (2000a), *Finite Element Linear and Nonlinear, Static and Dynamic Analysis of Structural Elements - an Addendum - a Bibliography (1996-1999)*, Engineering Computations; , 17, (3), 274-360

MACKERLE, J., (2001), *Error Estimate S and Adaptive Finite Element Method Bibliography (1999-2000)*, Engineering Computations, 18, (5 / 6),

MACKERLE, J., (2002), *Finite Element Analyses of Sandwich Structures: Bibliography (1980-2001) Engineering Computations*, 19, (2), 206-245

MACKERLE, J., (2002b), *Finite Element Linear and Nonlinear, Static and Dynamic Analysis of Structural Elements, an Addendum: Bibliography (1999-2002) Engineering Computations*, 19, (5), 520-594

MACKERLE, J., (2004), *Finite Element Modelling and Simulation of Indentation Testing: A Bibliography (1990-2002)* Engineering Computations, 21, (1), 23-52

MACKERLE, J., (2005), *Finite Element Modelling of Ceramics and Glass, an Addendum - a Bibliography (1998-2004)* Engineering Computations, 22, (3), 297-373

MAHNKEN, R., JOHANSSON, M. and RUNESSON, K., (1998), *Parameter Estimation for a Viscoplastic Damage Model Using a Gradient-Based Optimization Algorithm* Engineering Computations, 15, (7), 925-955

MAIA, N. M. M. and SILVA, J. M. M., (1997), *Theoretical and Experimental Modal Analysis* Research Studies Press Ltd, Hertfordshire, ISBN 0863802087

MASSART, T., PEERLINGS, R., GEERS. M. D. and SGOTTCHEINER, (2005a), *Mesoscopic Modelling of Failure in Brick Masonry Accounting for Three-Dimensional Effects*, Engineering Fracture Mechanics 72, 1238-1253

MASSART, T., PEERLINGS, R., GEERS., M. D. and SGOTTCHEINER, (2005b), *Mesoscopic Modelling of Failure in Brick Masonry Accounting for Three-Dimensional Effects*, Engineering Fracture Mechanics 72, 1238-1253

MASSART, T. J., PEERLINGS, R. and GEERS, M., (2004), *Mesoscopic Modelling of Failure and Damage-Induced Anisotropy in Brick Masonry.*, Eur.J Mech A/Solids 23, (7), 19-35

MASSART., T. J., PEERLINGS, R. and GEERS, M., (2004), *Mesoscopic Modelling of Failure and Damage-Induced Anisotropy in Brick Masonry.*, Eur.J Mech A/Solids 23, (7), 19-35

MATHEW, A., KUMAR, B., SINHA, B. P. and PEDRESCHI, R. F., (1999), *Analysis of Masonry Panel under Biaxial Bending Using ANNs and CBR,* J. Comp. in Civ. Engrg., 13, (3), 170-177

MAY, I. M. and TELLETT, J., (1986), *Non-Linear Finite Element Analysis of Reinforced and Unreinforced Brickwork* Proceeding of the British Masonry Society, ETY,No 1, 96-99.

MINAS, C. and INNMAN, D. J., (1988), *Correcting Finite Element Models with Measured Modal Results Using Eigenstructure Assignment Models*, Proceeding on 6th international model analysis conference,, Orlanto,USA,, 583-587.

MONK, C. B., (1954), *Transverse Strength of Masonry Walls*, ASTM Special Technical Publication NO 166,Symposium on Methods of Testing Building Construction,Chicago,June 1954 21-50.

MONK, C. B. and HALLEN, M., (1967), *Compressive, Transverse and Racking Strength Tests of 4-in Structural Clay Facing Tile Walls*, Structural Clay Products Research Foundation,

MORBIDUCCI, R., (2003), *Nonlinear Parameter Identification of Models for Masonry*, International Journal of Solids and Structures, 40, 4071–4090

MOTTERSHEAD, J. E. and FRISWELL, M. I., (1993), *Model Updating in Structural Dynamics: A Survey.*, Journal of Sound and Vibration, 167, (2), 347-375

MOTTERSHEAD, J. E. and FRISWELL, M. I., (1998), *Introduction to the Model Updating (Editorial)*, Mechanical Systems and Signal Processing 12, (1), 1-6

NICHOLS, J. M. and ABELL, A. B., (2003), *Implementing the Degrading Effective Stiffness of Masonry in a Finite Element Model*, 9th Ninth North American Masonry Conference (9NAMC), Clemson SC, ,

PANDE, G. N., LIANG, J. X. and MIDDLETON, J., (1989), *Equivalent Elastic Moduli for Brick Masonry*, Computer and Geotechnics, 8, 243–265

PAPAZOGLOU, V. J., TSOUVALIS, N. G. and LAZARIDIS, A. G., (1996), *Non-Destructive Evaluation of the Material Properties of a Composite Laminate Plate*, Applied composite materials, 3, 321-334

PLUIJM, R. V. D., (1999), *Out-of-Plane Bending of Masonry Behaviour and Strength* Eindhoven University of technology, Eindhoven,The Netherlands,

POTISIRI, T. and HJELMSTAD, K. D., (2003), *Structural Damage Detection and Assessment from Modal Response*, Journal of engineering mechanics, 129, (2), 135-145

PRELLS, U. and FRISWELL, M. I., (1999), *Application of the Variable Projection Method for Updating Models of Mechanical Systems*, Journal of Sound and Vibration 225, (2), 307-325

RAFIQ, M. Y., ZHOU, G. and EASTERBROOK, D. J., (2003), *Analysis of Brick Wall Panels Subjected to Lateral Loading Using Correctors*, Masonry International, 16, (2), 75-82

RAFIQ, Y., SUI, C., EASTERBROOK, D. and GUIDO BUGMANN, (2006), *Prediction of the Behaviour of Masonry Wall Panels Using Evolutionary Computation and Cellular Automata*, Proc. of the 13th International Workshop of the European Group for Intelligent Computing in Engineering, Monte Verita, Ascona Switzerland, Springer Berlin / Heidelberg, pp. 534-544. 978-3-540-46246-0

RICHART, F. E., MOORMAN, R. P. B. and WOODWARTH, P. M., (1932), *Strength and Stability of Concrete Masonry Walls*, University of Illinois, Engineering Station, Bulletin 251, July.5. 1932, Vol 29, / 89, 38pp.

ROBERT-NICOUD, Y., RAPHAEL, B. and SMITH, I., (2000), *Decision Support through Multiple Models and Probabilistic Search*, Proceedings of Construction Information Technology 2000, Icelandic Building Research Institute, Reykjavik, 765-779.

ROBERT-NICOUD, Y., RAPHAEL, B. and SMITH, I., (2002), *Decision Support for System Identification*, Advances in Intelligent Computing in Engineering, Fortschritt-Berichte, VDI Verlag Düsseldorf, 4, 92-101.

ROBERT-NICOUD, Y., RAPHAEL, B. and SMITH, I. F. C., (2004), *Improving the Reliability of System Identification*, 11th International EG-ICE Workshop, Weimar, Germany, May 31 - June. 1. 2004,

ROBERT-NICOUD, Y., RAPHAEL, B. and SMITH, I. F. C., (2005), *System Identification through Model Composition and Stochastic Search*, ASCE Journal of Computing in Civil Engineering, 19, (3), 239-247

RUBINSTEIN, R. Y., (1981), *Simulation and the Monte-Carlo Method*, John Wiley & Sons, Inc. New York, NY, USA ISBN:0471089176

SANAYEI, M., IMBARO, G. R., MCCLAIN, J. A. S. and BROWN, L. C., (1997), *Structural Model Updating Using Experimental Static Measurements*, JOURNAL of STRUCTURAL ENGINEERS, 123, (6),

SANAYEI, M. and ONIPEDE, O., (1991), *Damage Assessment of Structures Using Static Test Data*, AIAA journals, 30, (9), 2299-2309

SANAYEI, M., ONIPEDE, O. and BABU, S. R., (1992), *Selection of Noisy Measurement Locations for Error Reduction in Static Parameter Identification*, AIAA journals, 30, (9), 2299-2309

SANAYEI, M. and SALENIK, M. J., (1996a), *Parameter Estimation of Structures from Static Strain Measurements, I: Formulation*, Journal of Structural Engineering,ASCE,, 122, (5), 555-562

SANAYEI, M. and SALENIK, M. J., (1996b), *Parameter Estimation of Structures from Static Strain Measurements, I: Error Sensitivity Analysis*, Journal of Structural Engineering, ASCE, 122, (5), 563-572

SANDINK, C. A., MCAULEY, K. B. and MCLELLAN, P. J., (2001), *Selection of Parameters for Updating in on-Line Models*, Industrial and Engineering Chemistry Research, 40, (18), 3936-3950

SANTOS, J. V. A. D., SOARES, C. M. M., SOARES, C. A. M. and PINA, H. L. G., (2000a), *A Damage Identification Numerical Model Based on the Sensitivity of Orthogonality Conditions and Least Squares Techniques*, Computers and Structures 78 283-291

SANTOS, J. V. A. D., SOARES, C. M. M., SOARES, C. A. M. and PINA, H. L. G., (2000b), *Development of a Numerical Model for the Damage Identification on Composite Plate Structures*, Composite Structures, 48, 59-65

SHEENA, Z., UNGER, A. and ZALMANOVICH, A., (1982), *Theoretical Stiffness Matrix Correction by Using Static Test Results*, Israel Journal of Technology, 20, (6), 245-253

SING-SANG, P., TOTOEV, Y. and PAGE, A., (2005), *A Numerical Model for Analysis of Lateral Load Distribution in Load bearing Masonry Construction*, School of Engineering, The University of Newcastle, Australia, Research Report No. 256.10.2005, ISBN No. 1 9207 0163 X

SINHA, B. P., (1978), *A Simplified Ultimate Load Analysis of Laterally Loaded Model Brickwork Panels of Low Tensile Strength*, The Structural Engineer, 56B, (4),

SINHA, B. P., (1980), *An Ultimate Load Analysis of Laterally Loaded Brickwork Panels*, International Journal of Masonry Construction, 1, (2),

SINHA, J. K. and FRISWELL, M. I., (2002), *Model Updating: A Tool for Reliable Modelling, Design Modification and Diagnosis*, The Shock and Vibration Digest /, Vol.34,, (NO.1), 27-35

STANG, A. H., PARSONS, D. E. and FOSTER, H. D., (1925/1926), *Compressive and Transverse Strength of Hollow-Tile Walls*, Technical Paper of the Bureau of Standards 20, 347,1925-1926,

STAREK, L. and INMAN, D. J., (1991), *Solution of the Model Correction Problem Via Inverse Method* Proceedings of 9th international modal analysis conference Florence Italy, April 15th-18th, 352-355.

TASKER, H. E., (1947), *Simulated Wind Pressure Tests*, Technical Study No 13, Common Wealth Experimental Building Station, Sydney,

THOMAS, F. G., (1953), *The Strength of Brick Works*, The structural engineer, 131, (2), 35-46

TIMOSHENKO, S. P., (1981), *Theory of Plates and Shells,* 2nd Edition 2nd Edition, Woinowsky-Krieger.S , McGraw-Hill., ISBN:0-07-085820-9

TITURUS, B., FRISWELL, M. I. and STAREK, L., (2003a), *Damage Detection Using Generic Elements: Part I. Model Updating*, Computers and Structures, 81 2273-2286

TITURUS, B., FRISWELL, M. I. and STAREK, L., (2003b), *Damage Detection Using Generic Elements: Part Ii. Damage Detection*, Computers and Structures 81 2287-2299

TROVALUSCI, P. and MASIANI, R., (2003), *Non-Linear Micropolar and Classical Continua for Anisotropic Discontinuous Materials*, International Journal of Solids and Structures, 40, (5), 1281-1297

TROVALUSCI, P. and MASIANI, R., (2005), *A Multifield Model for Blocky Materials Based on Multiscale Description*, International Journal of Solids and Structures, 42, 5778-5794

VISSER, W. J., (1992), *Updating Structural Dynamics Models Using Frequency Response Data*, PhD Thesis, Imperial College Of Science, Technology and Medicine University of London, 238 pages

WAHAB, M. M. A., (1999), *Parameterization of Damage in Reinforced Concrete Structures Using Model Updating*, Journal of Sound and vibration, 228, (4), 717-730

WANG, J. and CHEN, L., (2005), *Damage Detection of Frames Using the Increment of Lateral Displacement Change*, Journal of Zhejiang University SCIENCE, 6A, (3), 202-212

WATSON, J. O., (2003), *Boundary Elements from 1960 to the Present Day*, Electronic Journal of Boundary Elements, 1, (1), 34-46

WEST, H. W. H., (1976), *The Flexural Strength of Clay Masonry Determined from Wallettes Specimens*, Technical Note, No. 247, The British Ceramic Research Association,

WEST, H. W. H., HODGKINGSON, H. R. and HASEITINE, B. A., (1977), *The Resistance of Brick Work to Lateral Loading, Part 1: Experimental Methods and Results of Tests on Small Specimens and Full Sizes Walls*, The structural engineer, 55, (10), 411

WEST, H. W. H., HODGKINSON, H. R. and B.A, H., (1975), *Design of Lateral Loaded Wall Panels*, Technical Note, No. 242, The British Ceramic Research Association,

WEST, H. W. H., HODGKINSON, H. R. and W.F, W., (1974), *The Resistance of Clay Brick Walls to Lateral Loading, Part 2*, Technical Note, No. 226, The British Ceramic Research Association,

WEST, H. W. H., HODGKINSON, H. R. and WEBB, W. F., (1971), *The Resistance of Clay Brick Walls to Lateral Loading*, Proceedings of the 4th symposium on load bearing brickwork, London, 141-164.

WU, J. R. and LI, Q. S., (2006), *Structural Parameter Identification and Damage Detection for a Steel Structure Using a Two-Stage Finite Element Model Updating Method*, Journal of Constructional Steel Research, 62, (3), 231-239

ZHANG, R. and MAHADEVAN, S., (2000), *Model Uncertainty and Bayesian Updating in Reliability-Based Inspection*, Structural Safety, 22, (2), 145-160

ZHOU, G., (2002), *Application of Stiff/Strength Corrector and Cellular Automata in Predicting Response of Laterally Loaded Masonry Panels*, PhD Thesis, School of Engineering, University of Plymouth,

ZHOU, G., RAFIQ, M. Y., EASTERBROOK, D. J. and BUGMANN, G., (2003), *Application of Cellular Automata in Modelling Laterally Loaded Masonry Panel Boundary Effects*, Masonry International, 16 (3), 104-114

ZHOU, G. C., RAFIQ, M. Y., BUGMANN, G. and EASTERBROOK, D. J., (2006), *Cellular Automata Model for Predicting the Failure Pattern of Laterally Loaded Masonry Wall Panels*, Journal of Computing in Civil Engineering, Volume 20, (6), 375-441

ZUBAYDI, A., HADDARA, M. R. and SWAMIDAS, A. S. J., (2002), *Damage Identification in a Ship's Structure Using Neural Networks*, Ocean Engineering, 29, 1187–1200

ZUCCHINI, A. and LOURENCO, P. B., (2002), *A Micro-Mechanical Model for the Homogenisation of Masonry*, International Journal of Solids and Structures, 39, (12), 3233-3255

APPENDIX 1

EXPERIMENTAL DATA

From the University of Plymouth (Chong 1993) (NaN denoted opening area, or data not recorded)

SBO1 Experimental Deflections (mm)

Position Load(kN/m²)	A1	A2	A3	A4	A5	A6	A7	A8	A9
0.2	-0.04	0.04	0.44	0.46	0.48	0.78	0.67	1.4	0.23
0.4	0.18	0.41	0.94	0.93	1.23	1.39	1	1.75	0.28
0.6	0.39	0.83	1.47	1.58	1.87	1.75	1.51	2.28	0.63
0.8	0.31	0.9	1.74	2.01	2.42	2.16	1.97	2.31	0.64
1	0.28	1.24	2.06	2.56	2.7	2.76	2.34	2.63	0.59
1.2	0.37	1.81	2.61	3.09	3.48	3.48	2.91	3.06	1.05
1.4	0.42	1.65	3.21	3.77	3.89	4.09	3.33	3.34	1.04
1.6	0.64	2	3.6	4.26	4.72	4.64	3.75	3.75	1.08
1.8	0.81	2.41	4.15	5.19	5.42	5.46	4.5	4.33	1.48
2	0.52	2.79	4.73	5.62	6.26	5.9	5	4.45	1.47
2.2	0.73	3.15	5.31	6.44	6.96	6.73	5.55	4.87	1.58
2.4	0.92	3.25	5.94	7.16	7.62	7.4	6.17	5.32	1.54
2.6	0.93	3.93	6.54	7.96	8.63	8.36	6.92	5.68	1.87

Position Load(kN/m²)	B1	B2	B3	B4	B5	B6	B7	B8	B9
0.2	-0.25	-0.02	0.54	0.53	0.28	0.84	0.8	1.15	0.19
0.4	0.18	0.38	1.11	0.99	1.17	1.49	0.97	1.39	0.14
0.6	0.48	0.83	1.69	1.45	1.95	1.77	1.45	0.76	0.66
0.8	0.28	0.78	1.84	1.87	2.26	2.06	1.99	1.86	0.53
1	0.14	1.28	2.04	2.35	2.45	2.67	2.26	1.15	0.31
1.2	0.25	1.96	2.71	2.96	3.37	3.52	2.82	2.62	1.38
1.4	0.24	1.52	3.37	3.74	3.5	4.07	3.24	2.91	0.87
1.6	0.66	1.94	3.69	3.85	4.31	4.61	3.51	3.31	0.85
1.8	0.96	2.45	4.3	5.03	5.15	5.41	4.32	3.95	1.28
2	0.43	2.83	4.93	5.54	6.08	5.72	4.83	3.82	1.15
2.2	0.47	3.21	5.14	6.24	6.62	6.5	5.21	4.2	1.11
2.4	0.8	3.11	5.96	6.85	7.12	7.08	5.76	4.65	0.9
2.6	0.71	3.89	6.48	7.46	8.21	8.04	6.59	4.82	1.18

Position Load(kN/m²)	C1	C2	C3	C4	C5	C6	C7	C8	C9
0.2	-0.37	-0.33	0.43	0.2	0.03	0.55	0.37	0.62	0.06
0.4	0.01	0.03	0.72	0.48	0.6	1	0.36	0.76	0.1
0.6	0.32	0.42	1.13	0.82	1.15	0.99	0.65	1.05	0.23
0.8	0.05	0.07	1.08	0.85	1.2	1.2	1.02	0.99	0.22
1	-0.13	0.56	1.12	1.13	1.31	1.5	1.04	1.18	0.01
1.2	-0.04	1.23	1.67	1.56	1.89	2.13	1.54	1.57	0.77
1.4	-0.02	0.57	2.16	2.2	1.83	2.49	1.8	1.73	0.47
1.6	0.3	0.81	2.18	1.99	2.48	2.7	1.76	2.18	0.42
1.8	0.55	1.18	2.61	2.95	2.85	3.19	2.24	2.45	0.73
2	0.06	1.42	3.08	2.97	3.56	3.34	2.74	2.19	0.68
2.2	0	1.89	3.16	3.82	3.91	3.9	2.99	2.52	0.65
2.4	0.42	1.61	3.81	4.14	4.06	4.21	3.26	2.83	0.45
2.6	0.22	2.24	4.08	4.34	4.86	4.82	3.92	2.82	0.66

Position Load(kN/m²)	D1	D2	D3	D4	D5	D6	D7	D8	D9
0.2	-0.47	-0.55	0.27	0.08	0.29	0.21	0.39	0.11	0.13
0.4	-0.08	-0.2	0.58	0.33	0.43	0.67	0.19	0.15	0.15
0.6	0.24	0.23	0.8	0.27	0.74	0.57	0.25	0.32	0.1
0.8	-0.02	-0.36	0.74	0.31	0.72	0.41	0.79	0.37	0.1
1	-0.32	0.13	0.65	0.43	0.57	0.59	0.57	0.38	0.17
1.2	-0.36	0.68	1.09	0.71	1.06	1.21	1	0.72	0.48
1.4	-0.31	0.08	1.45	1.39	0.75	1.4	1.18	0.82	0.19
1.6	0.09	0.09	1.41	0.89	1.07	1.36	0.85	1.03	0.12
1.8	0.28	0.34	1.62	1.74	1.41	1.62	1.14	1.42	0.48
2	0.36	0.87	2.52	2.4	2.5	2.1	3.82	4.05	0.36
2.2	0.46	1.49	2.17	2.49	2.43	2.58	1.89	1.52	1.83
2.4	0.35	0.6	2.5	2.39	2.61	2.27	4.13	4.28	0.51
2.6	0.03	1.25	2.63	2.24	2.66	2.47	2.42	1.48	0.44

SBO2 Experimental Deflections (mm) from the University of Plymouth (Chong 1993)

Position Load(kN/m²)	A1	A2	A3	A4	A5	A6	A7	A8	A9
0.1	0.16	0.22	0.25	0.3	0.44	0.46	0.38	0.48	0.21
0.2	0.09	0.16	0.44	0.55	0.81	0.72	0.65	0.5	0.33
0.4	0.1	0.58	0.94	1.18	1.28	1.33	1.09	0.68	0.46
0.6	0.15	0.77	1.39	1.8	2.09	1.93	1.54	0.97	0.36
0.8	0.05	0.95	1.79	2.32	2.71	2.49	1.95	1.29	0.53
1	0.15	1.13	2.23	2.87	3.4	3.12	2.37	1.49	0.52
1.2	0.12	1.55	2.81	3.72	4.15	3.78	2.94	1.73	0.53
1.4	0.17	0.73	3.31	4.34	4.81	4.42	3.51	2.1	0.54
1.6	0.2	2.01	3.83	5.16	5.74	5.26	3.98	2.43	0.6
1.8	0.16	2.3	4.37	5.9	6.7	6.03	4.4	2.77	0.72
2	0.24	3.09	5.67	8.16	10.43	9.91	6.58	3.67	0.9
2.1	0.19	3.14	6.02	8.88	11.48	10.79	7.13	3.98	0.76
2.2	0.32	3.37	6.5	9.53	12.33	11.62	7.55	4.16	0.88
2.3	0.13	3.76	7.28	10.83	14.09	13.4	8.75	4.8	0.96

Position Load(kN/m²)	B1	B2	B3	B4	B5	B6	B7	B8	B9
0.1	0.38	0.28	0.26	NaN	NaN	NaN	0.36	0.46	0.11
0.2	0.1	0.32	0.41	NaN	NaN	NaN	0.56	0.44	0.05
0.4	0.15	0.5	1.03	NaN	NaN	NaN	0.94	0.71	0.31
0.6	0.25	0.79	1.43	NaN	NaN	NaN	1.48	1	0.19
0.8	0.18	0.89	1.83	NaN	NaN	NaN	1.85	1.25	0.35
1	0.24	1.89	2.42	NaN	NaN	NaN	2.35	1.57	0.4
1.2	0.16	1.32	2.66	NaN	NaN	NaN	2.82	1.71	0.3
1.4	0.36	1.76	3.47	NaN	NaN	NaN	3.3	2.09	0.34
1.6	0.41	1.99	3.99	NaN	NaN	NaN	3.73	2.49	0.52
1.8	0.44	2.49	4.8	NaN	NaN	NaN	4.33	2.67	0.59
2	0.55	3.44	6.49	NaN	NaN	NaN	6.7	3.93	0.85
2.1	0.74	3.88	7.04	NaN	NaN	NaN	7.34	4.46	1.07
2.2	0.98	4.02	7.71	NaN	NaN	NaN	7.97	4.82	1.23
2.3	0.81	4.67	8.74	NaN	NaN	NaN	9.4	5.57	1.46

Position Load(kN/m²)	C1	C2	C3	C4	C5	C6	C7	C8	C9
0.1	0.21	0.09	0.04	NaN	NaN	NaN	0.21	0.33	0.02
0.2	0.08	0.14	0.19	NaN	NaN	NaN	0.33	0.3	0.04
0.4	0.01	0.33	0.52	NaN	NaN	NaN	0.55	0.38	0.16
0.6	0.14	0.46	0.82	NaN	NaN	NaN	0.9	0.58	0.03
0.8	0.03	0.61	0.95	NaN	NaN	NaN	1.1	0.76	0.01
1	0.13	0.72	1.34	NaN	NaN	NaN	1.34	0.87	0.25
1.2	0.19	1.05	1.69	NaN	NaN	NaN	1.73	1.08	0.12
1.4	0.27	1.19	2.05	NaN	NaN	NaN	2.02	1.28	0.22
1.6	0.36	1.3	2.26	NaN	NaN	NaN	2.3	1.49	0.36
1.8	0.31	1.62	2.73	NaN	NaN	NaN	2.58	1.6	0.33
2	0.39	2.16	3.64	NaN	NaN	NaN	3.87	2.25	0.36
2.1	0.33	2.34	3.96	NaN	NaN	NaN	4.19	2.49	0.36
2.2	0.55	2.57	4.4	NaN	NaN	NaN	4.57	2.73	0.51
2.3	0.48	3.98	5.24	NaN	NaN	NaN	5.5	3.19	0.61

Position Load(kN/m²)	D1	D2	D3	D4	D5	D6	D7	D8	D9
0.1	0.21	0.06	0.03	0.09	0.13	0.07	0.13	0.15	-0.19
0.2	0.09	0.01	0.06	0.19	0.24	0.22	0.2	0.1	-0.24
0.4	0.04	0.14	0.27	0.4	0.42	0.38	0.27	0.19	-0.11
0.6	0.18	0.21	0.43	0.63	0.65	0.59	0.49	0.29	-0.28
0.8	0.08	0.3	0.54	0.75	0.82	0.75	0.6	0.42	-0.15
1	0.17	0.35	0.75	0.95	1.02	0.92	0.73	0.5	-0.06
1.2	0.2	0.56	0.92	1.24	1.26	1.08	0.89	0.58	-0.27
1.4	0.24	0.65	1.13	1.45	1.5	1.38	1.13	0.72	-0.16
1.6	0.32	0.73	1.32	1.74	1.79	1.59	1.28	0.88	0.03
1.8	0.34	0.9	1.59	2.01	2.06	1.92	1.46	0.92	-0.09
2	0.42	1.3	2.22	2.8	2.95	2.81	2.25	1.36	0.06
2.1	0.43	1.42	2.41	3.06	3.23	3.08	2.44	1.51	0.04
2.2	0.66	1.47	2.7	3.26	3.52	3.26	2.64	1.59	0.53
2.3	0.51	1.94	3.42	3.99	4.13	3.89	3.2	1.83	0.1

SBO3 Experimental deflections from The University of Plymouth (mm)(Chong 1993)

Position Load(kN/m²)	A1	A2	A3	A4	A5	A6	A7	A8	A9
0.4	0.07	0.65	0.98	1.26	1.5	1.54	1.28	1.01	0.6
0.8	0.14	1.04	1.62	2.21	2.82	2.33	2.24	1.73	1.05
0.1.2	0.2	1.73	2.93	3.87	4.34	4.06	3.29	2.41	1.13
1.6	0.43	2.44	4.03	5.4	6.05	5.56	4.5	3.08	0.89
2.0	0.43	3.02	5.32	7.07	8.05	7.43	5.85	3.85	1.54
2.2	0.47	3.43	5.99	8.13	9.34	8.62	6.61	4.19	1.6
2.3	0.53	3.91	7.08	10.23	10.9	9.49	7.19	4.55	1.53
2.3	0.54	4.15	7.77	11.38	11.70	10.21	7.63	4.69	1.48
2.35	12.14	14.43	15.2	14.82	14.44	14.62	14.97	14.49	12.21

Position Load(kN/m²)	B1	B2	B3	B4	B5	B6	B7	B8	B9
0.4	0.33	0.95	1.13	1.43	1.73	1.54	1.46	1.11	0.58
0.8	0.58	1.58	2.13	2.7	3.38	2.77	2.62	2.09	1.25
0.1.2	0.87	2.41	3.61	4.52	5.07	4.7	3.82	2.83	1.38
1.6	1.13	3.27	4.71	6.36	7.01	6.31	5.06	3.55	1.07
2.0	1.22	3.98	6.41	8.2	9.36	8.55	6.69	4.52	1.91
2.2	1.52	4.65	7.33	9.62	10.85	9.89	7.63	5	2.09
2.3	1.23	4.89	8.18	11.68	12.6	10.88	8.1	5.14	1.65
2.3	1.52	5.30	9.11	13.00	13.59	11.88	8.77	5.53	1.80
2.35	12.7	17.32	16.66	21.64	23.57	19.02	21.07	17.95	14.66

Position Load(kN/m²)	C1	C2	C3	C4	C5	C6	C7	C8	C9
0.4	0.16	0.47	0.65	0.7	0.9	0.73	0.85	0.64	0.33
0.8	0.31	0.75	1.08	1.22	1.68	1.23	1.51	1.13	0.56
0.1.2	0.38	1.34	2.01	2.47	2.54	2.37	2.27	1.62	0.6
1.6	0.61	1.99	2.94	3.48	3.64	3.34	3.12	2.15	0.58
2.0	0.61	2.39	3.98	4.4	4.8	4.56	4.17	2.79	0.97
2.2	0.74	2.86	4.49	5.24	5.63	5.41	4.84	3.16	1.1
2.3	0.82	3.33	5.17	5.93	6.36	5.97	5.6	3.64	1.1
2.3	0.76	3.35	5.63	6.37	6.61	6.43	6.00	3.75	0.98
2.35	4.82	7.88	10.32	9.42	10.5	11.03	8.74	7.93	4.84

Position Load(kN/m²)	D1	D2	D3	D4	D5	D6	D7	D8	D9
0.4	NaN	1.92	1.59	1.35	1.8	2.01	1.56	0.97	0.23
0.8	NaN	1.98	1.49	0.96	2.34	2.14	2.18	2.02	0.33
0.1.2	NaN	2.36	1.78	1.43	1.5	1.37	1.22	0.96	0.34
1.6	NaN	2.88	3.62	3.42	4.18	4.21	5.96	4.58	0.44
2.0	NaN	3.1	2.4	2.6	2.98	2.86	2.62	1.92	0.66
2.2	NaN	2.34	4.02	4.1	3.47	3.32	2.99	2.15	0.76
2.3	NaN	2.03	3.1	3.61	3.91	3.63	3.4	2.37	0.68
2.3	NaN	2.70	3.87	4.98	4.85	4.98	4.67	3.86	0.75
2.35	NaN	11.41	10.93	12.27	11.61	11.7	9.97	11.33	6.67

SBO4 Experimental data from The University of Plymouth (mm Chong 1993)

Position Load(kN/m²)	A1	A2	A3	A4	A5	A6	A7	A8	A9
0.2	0.34	0.7	0.65	0.66	0.76	0.89	0.64	0.49	0.37
0.4	0.73	0.97	1.2	1.29	1.43	1.49	1	0.83	0.56
0.6	0.72	1.35	1.68	1.92	2.11	2.11	1.65	1.14	0.64
0.8	0.93	1.71	2.23	2.64	2.95	2.86	2.14	1.42	0.78
1	0.73	1.94	2.67	3.37	3.55	3.46	2.66	1.79	0.89
1.2	0.87	2.3	3.08	4.01	4.35	4	3.23	1.93	0.83
1.4	0.86	2.49	3.61	4.73	4.94	4.93	3.72	2.42	1.03
1.6	0.89	2.97	4.39	5.26	5.85	5.34	4.24	2.21	1.17
1.75	1.17	3.53	5.53	7.74	7.74	6.93	4	2.97	1.06
1.8	1.13	3.84	5.71	8.21	7.89	7.13	5.23	3.24	1.17
1.9	1.14	3.48	6.11	8.86	8.85	7.76	5.57	3.44	1.09
2.0	1.08	4.33	6.86	10.01	9.77	8.67	6.14	3.62	1.2
2.1	0.81	4.51	7.61	11.04	10.76	9.45	6.52	4.02	1.31

Position / Load(kN/m²)	B1	B2	B3	B4	B5	B6	B7	B8	B9
0.2	0.38	0.56	0.59	0.63	0.76	0.96	0.66	0.44	0.34
0.4	0.71	0.98	1.14	1.22	1.4	1.53	0.97	0.71	0.39
0.6	0.66	1.36	1.58	1.88	2.11	2.15	1.6	1.02	0.46
0.8	0.88	1.52	2.11	2.65	3.01	2.9	2.11	1.3	0.6
1	0.66	1.93	2.65	3.42	3.64	3.58	2.6	1.61	0.67
1.2	0.87	2.22	3.02	4.08	4.5	4.23	3.24	1.87	0.67
1.4	0.82	2.47	3.58	4.9	5.11	5.13	3.74	2.3	0.84
1.6	0.76	2.73	4.41	5.53	6.11	5.56	4.27	2.21	0.95
1.75	1.05	3.57	5.64	8.2	8.13	7.31	4.26	2.92	0.9
1.8	1.12	3.84	5.91	8.8	8.34	7.58	5.36	3.21	0.98
1.9	1.28	3.68	6.49	9.7	9.5	8.37	5.82	3.5	1.03
2.0	1.19	4.61	7.42	10.96	10.54	9.38	6.46	3.69	1.04
2.1	1	4.84	8.22	12.16	11.66	10.24	6.94	4.13	1.13

Position / Load(kN/m²)	C1	C2	C3	C4	C5	C6	C7	C8	C9
0.2	0.15	0.52	0.36	0.53	NaN	0.67	0.49	0.25	0.2
0.4	0.29	0.72	0.75	0.94	NaN	0.99	0.85	0.48	0.22
0.6	0.23	0.84	1.05	1.28	NaN	1.41	1.15	0.7	0.4
0.8	0.58	1.13	1.48	1.92	NaN	1.92	1.56	0.78	0.4
1	0.27	1.41	1.78	2.37	NaN	2.37	1.93	1.1	0.44
1.2	0.47	1.53	1.96	2.85	NaN	2.84	2.14	1.21	0.43
1.4	0.52	1.79	2.4	3.33	NaN	3.48	2.49	1.5	0.57
1.6	0.27	2	3	3.71	NaN	3.66	0.97	1.48	0.59
1.75	0.78	2.49	3.87	5.61	NaN	5	3.01	1.9	0.55
1.8	0.87	2.67	4.11	6.08	NaN	5.23	3.71	2.15	0.65
1.9	1	2.7	4.7	6.92	NaN	5.81	4.01	2.32	0.64
2.0	1.01	3.55	5.44	7.95	NaN	6.56	4.5	2.56	0.68
2.1	1	3.6	6.07	8.99	NaN	7.22	4.96	2.85	0.77

Position Load(kN/m²)	D1	D2	D3	D4	D5	D6	D7	D8	D9
0.2	0.13	0.30	0.21	0.24	NaN	0.52	0.33	0.14	0.12
0.4	0.34	0.42	0.45	0.52	NaN	0.79	0.44	0.28	0.06
0.6	0.27	0.60	0.59	0.79	NaN	0.93	0.67	0.41	0.18
0.8	0.43	0.64	0.89	1.14	NaN	1.36	0.95	0.43	0.22
1	0.31	0.88	1.02	1.49	NaN	1.65	1.17	0.65	0.26
1.2	0.40	0.96	1.16	1.75	NaN	1.85	1.43	0.78	0.22
1.4	0.38	1.13	1.53	2.15	NaN	2.33	1.60	0.96	0.35
1.6	0.46	1.20	1.92	2.44	NaN	2.38	1.84	1.00	0.37
1.75	0.52	1.67	2.46	3.66	NaN	3.30	1.77	1.21	0.33
1.8	0.61	1.85	2.67	4.03	NaN	3.55	2.50	1.40	0.40
1.9	0.68	1.83	3.04	4.58	NaN	4.07	2.74	1.54	0.42
2.0	0.69	2.42	3.66	5.33	NaN	4.51	3.14	1.77	0.46
2.1	0.65	2.40	4.15	6.04	NaN	4.99	3.43	2.01	0.53

Experimental data from The University of Edinburgh (Liang 1999)

In Liang's thesis, the experimental deflections were presented by the plot of load deflection relationships. The experimental information presented here was obtained based on the manual measurements to those figures and proportional calculations. All of them were the data at the maximum deflection points.

Wall 1

Load (KN/m^2)	1	1.5	2	2.5	3	3.5	4
Deflections(mm)	0.048	0.036	0.097	0.121	0.145	0.17	0.194
Load (KN/m^2)	4.5	5	5.5	6	6.5	7	
Deflections(mm)	0.218	0.242	0.291	0.315	0.339	0.497	

Wall 8

Load (KN/m^2)	2	4	6	8	10	12
Deflections(mm)	0.036	0.071	0.1	0.129	0.164	0.2
Load (KN/m^2)	14	16	18	20	22	
Deflections(mm)	0.229	0.257	0.293	0.343	0.443	

Wall 4

Load (KN/m^2)	0.14	0.26	0.38	0.51	0.62
Deflections(mm)	1	2	3	4	5
Load (KN/m^2)	0.74	0.85	0.94	1.06	
Deflections(mm)	6	6.8	7.3	8	

Wall 9

Load (KN/m^2)	2	4	6	8	10	12
Deflections(mm)	0.057	0.114	0.171	0.217	0.274	0.32
Load (KN/m^2)	14	16	18	20	22	
Deflections(mm)		0.434	0.48	0.537	0.594	

Wall 6

Load (KN/m^2)	0.5	1	1.2	1.4	1.6
Deflections(mm)	0.08	0.16	0.18	0.21	0.25
Load (KN/m^2)	1.8	2	2.2	2.5	
Deflections(mm)	0.27	0.31	0.34	0.39	

Wall 10

Load (KN/m^2)	0.5	1	1.5	2	3	4
Deflections(mm)	0.03	0.07	0.1	0.14	0.21	0.28
Load (KN/m^2)	4.5	5	5.5	6	6.5	
Deflections(mm)	0.32	0.34	0.38	0.42	0.48	

Experimental data from CERAM, Wall CR1

Load (KN/m²)	X1	X2	X3	X4	X5	X6	X7	X8	X9	X10	X11
0.000	0.000	0.000	0.000	0.000	0.000	0.000	0.000	0.000	0.000	0.000	0.000
0.248	0.078	0.231	0.186	0.160	0.169	0.150	0.188	0.200	0.001	0.079	0.011
0.600	0.077	0.361	0.280	0.319	0.172	0.224	0.318	0.297	0.051	0.140	0.065
1.000	0.155	0.622	0.605	0.719	0.380	0.446	0.582	0.537	0.104	0.215	0.113
1.226	0.231	0.785	0.745	0.879	0.495	0.558	0.740	0.641	0.145	0.321	0.154
1.411	0.310	1.007	0.931	1.119	0.648	0.670	0.880	0.786	0.145	0.383	0.154
1.629	0.465	1.202	1.085	1.359	0.762	0.784	1.032	0.937	0.146	0.444	0.155
1.812	0.543	1.410	1.259	1.524	0.870	0.898	1.167	1.097	0.146	0.506	0.155
2.025	0.622	1.597	1.427	1.840	1.023	1.062	1.324	1.223	0.155	0.550	0.163
2.225	0.698	1.758	1.582	2.000	1.079	1.175	1.450	1.346	0.179	0.582	0.187
2.433	0.776	1.958	1.751	2.240	1.191	1.294	1.632	1.507	0.301	0.688	0.308
2.622	0.853	2.172	1.936	2.480	1.344	1.451	1.790	1.661	0.301	0.748	0.308
2.815	0.931	2.374	2.134	2.721	1.451	1.575	1.977	1.819	0.301	0.826	0.308
3.019	1.010	2.589	2.322	3.040	1.559	1.744	2.190	1.988	0.301	0.974	0.308
3.210	1.241	2.937	2.646	3.362	1.780	1.963	2.457	2.220	0.338	0.992	0.345
3.419	1.243	3.159	2.832	3.610	1.888	2.184	2.697	2.425	0.415	1.133	0.421
3.628	2.014	4.740	4.317	5.523	2.799	4.826	5.144	4.575	1.130	2.021	1.129
3.628	2.920	33.109	34.581	37.842	15.543	22.523	22.602	23.638	1.387	2.082	1.383

Experimental data from CERAM, Wall CR 2

Load (KN/m^2)	x1	x2	x3	x4	x5	x6	x7	x8	x9	x10	x11	x12	x13	x14	x15
0	0	0	0	0	0	0	0	0	0	0	0	0	0	0	0
0.25	-0.11	0.28	0.42	0.34	0	0.28	0.37	0.35	0.04	0.27	0.27	0.1	0.15	0.74	0
0.3	-0.14	0.34	0.49	0.38	-0.05	0.28	0.46	0.43	0.04	0.31	0.33	0.1	0.15	0.93	0
0.4	-0.11	0.59	0.79	0.61	-0.05	0.52	0.82	0.59	0.12	0.48	0.47	0.1	0.24	1.22	0.05
0.51	0.01	0.97	1.23	0.94	-0.08	0.84	1.22	0.91	0.23	0.75	0.7	0.24	0.36	0.89	0.19
0.61	0.04	1.27	1.61	1.24	-0.08	1.17	1.51	1.21	0.35	0.99	0.93	0.28	0.49	0.31	0.37
0.71	0.18	1.81	2.19	1.71	-0.05	1.65	2.17	1.67	0.53	1.4	1.34	0.46	0.71	-5.52	0.74
0.81	0.51	2.27	2.8	2.22	0.27	2.05	2.66	2.1	0.7	1.73	1.63	0.63	0.86	0.2	0.85
0.93	0.59	2.65	3.29	2.63	0.27	2.46	3.19	2.48	0.82	2.06	1.98	0.77	1.03	1.58	1.06
1	0.73	3.11	3.78	3.03	0.41	2.83	3.64	2.89	0.97	2.39	2.28	0.92	1.16	-3.46	1.17
1.11	0.84	3.52	4.27	3.4	0.49	3.19	4.04	3.24	1.13	2.69	2.57	1.06	1.31	2.03	1.37
1.21	1.04	3.99	4.86	3.89	0.65	3.59	4.57	3.68	1.28	3.04	2.92	1.22	1.48	2.31	1.54
1.3	1.08	4.3	5.28	4.24	0.73	3.91	5.01	4.03	1.38	3.31	3.21	1.33	1.6	2.69	1.7
1.42	1.23	4.8	5.88	4.76	0.92	4.37	5.56	4.55	1.51	3.64	3.58	1.53	1.77	2.5	1.91
1.5	1.36	5.21	6.47	5.22	0.97	4.8	6.07	4.99	1.69	4.02	3.97	1.69	1.98	1.98	2.12
1.59	1.53	5.6	7.14	5.73	1.08	5.29	6.72	5.5	1.86	4.44	4.39	1.88	2.16	1.84	2.38
1.7	1.72	6.51	7.96	6.4	1.36	5.93	7.52	6.17	2.09	4.95	4.97	2.15	2.44	2.15	2.7
1.8	1.81	6.92	8.52	6.8	1.38	6.39	8.09	6.6	2.25	5.39	5.38	2.33	2.71	2.97	2.96
1.81	2.29	11.73	16.3	11.7	1.94	12.06	16.66	12.41	4.47	12.09	11.75	4.64	6.97	8.19	7.2
1.9	1.57	16.16	24.52	14.83	-1.8	17.42	25.65	17.09	6.44	18.76	17.22	5.53	11.33	11.11	11.69
1.14	-3.82	13.64	24.58	9.82	-11.42	17.17	27.84	15.27	6.28	21.23	17.27	3.63	13.56	14.04	13.15

APPENDIX 2

The Refined Experimental Deflection Data of SBO1 (mm)

Load level (kN/m^2) \ Position	D1	D2	D3	D4	D5
0.2	0.058	0.105	0.147	0.176	0.186
0.4	0.112	0.187	0.254	0.298	0.314
0.6	0.164	0.276	0.374	0.438	0.461
0.8	0.214	0.371	0.506	0.596	0.627
1	0.263	0.472	0.652	0.770	0.812
1.2	0.310	0.580	0.810	0.962	1.015
1.4	0.355	0.694	0.981	1.171	1.238
1.6	0.398	0.814	1.165	1.398	1.479
1.8	0.440	0.940	1.362	1.642	1.740
2	0.480	1.072	1.572	1.903	2.019
2.2	0.518	1.211	1.794	2.181	2.317
2.4	0.554	1.356	2.030	2.477	2.633
2.6	0.588	1.507	2.278	2.790	2.969

Load level (kN/m^2) \ Position	C1	C2	C3	C4	C5
0.2	0.065	0.193	0.300	0.371	0.396
0.4	0.126	0.332	0.504	0.618	0.658
0.6	0.186	0.480	0.726	0.889	0.946
0.8	0.245	0.637	0.965	1.182	1.258
1	0.302	0.802	1.221	1.499	1.596
1.2	0.358	0.977	1.495	1.838	1.958
1.4	0.412	1.160	1.786	2.201	2.346
1.6	0.465	1.352	2.095	2.587	2.759
1.8	0.517	1.553	2.421	2.995	3.197
2	0.567	1.763	2.764	3.427	3.660
2.2	0.616	1.982	3.125	3.882	4.148
2.4	0.663	2.209	3.503	4.361	4.661
2.6	0.709	2.446	3.899	4.862	5.199

Position Load level (kN/m²)	B1	B2	B3	B4	B5
0.2	0.086	0.353	0.576	0.724	0.776
0.4	0.161	0.590	0.948	1.186	1.269
0.6	0.234	0.835	1.338	1.672	1.789
0.8	0.305	1.091	1.747	2.183	2.335
1	0.376	1.355	2.174	2.718	2.908
1.2	0.445	1.629	2.620	3.277	3.507
1.4	0.512	1.913	3.084	3.861	4.133
1.6	0.579	2.206	3.567	4.469	4.785
1.8	0.644	2.509	4.068	5.102	5.464
2	0.708	2.821	4.588	5.760	6.170
2.2	0.770	3.142	5.126	6.442	6.902
2.4	0.831	3.473	5.683	7.148	7.660
2.6	0.891	3.814	6.258	7.879	8.446

Position Load level (kN/m²)	A1	A2	A3	A4	A5
0.2	0.089	0.372	0.610	0.767	0.822
0.4	0.164	0.616	0.993	1.244	1.331
0.6	0.238	0.870	1.398	1.748	1.871
0.8	0.311	1.135	1.824	2.281	2.441
1	0.383	1.412	2.272	2.842	3.041
1.2	0.454	1.699	2.740	3.431	3.672
1.4	0.524	1.997	3.230	4.047	4.333
1.6	0.592	2.307	3.741	4.692	5.025
1.8	0.660	2.628	4.273	5.365	5.746
2	0.726	2.959	4.827	6.065	6.499
2.2	0.791	3.302	5.402	6.794	7.281
2.4	0.856	3.656	5.998	7.551	8.094
2.6	0.919	4.021	6.615	8.335	8.937

APPENDIX 3

Corrector factors suggested under different boundary conditions based on cellular automata

1. 0000

0000	X1	X2	X3	X4	X5	X6(x4)	X7(X3)	X8(x2)	X9(X1)
Y4	0.223	0.926	0.926	0.926	0.926				
Y3	0.926	0.921	1.181	0.920	0.920				
Y2	0.926	0.921	1.181	0.920	0.920				
Y1	0.926	0.926	0.926	0.926	0.926				

2. 1000

	X1	X2	X3	X4	X5	X6	X7	X8	X9
Y4	0.223	0.926	0.926	0.926	0.926	0.926	0.926	0.926	0.926
Y3	0.217	0.92	0.92	0.92	0.92	0.92	0.92	0.921	0.926
Y2	0.217	0.92	0.92	0.92	0.92	0.92	0.92	0.921	0.926
Y1	0.223	0.926	0.926	0.926	0.926	0.926	0.926	0.926	0.926

3. 1100

1100	X1	X2	X3	X4	X5	X6(x4)	X7(X3)	X8(x2)	X9(X1)
Y4	0.223	0.926	0.926	0.926	0.926				
Y3	0.217	0.92	0.92	0.92	0.92				
Y2	0.217	0.92	0.92	0.92	0.92				
Y1	0.223	0.926	0.926	0.926	0.926				

4. 1110

1110	X1	X2	X3	X4	X5	X6(x4)	X7(X3)	X8(x2)	X9(X1)
Y4	0.223	0.926	0.926	0.926	0.926				
Y3	0.217	0.920	0.920	0.920	0.920				
Y2	0.217	0.920	0.920	0.920	0.920				
Y1	0.218	0.217	0.217	0.217	0.217				

5. 1010

1010	X1	X2	X3	X4	X5	X6	X7	X8	X9
Y4	0.223	0.926	0.926	0.926	0.926	0.926	0.926	0.926	0.926
Y3	0.217	0.92	0.92	0.92	0.92	0.92	0.92	0.92	0.926
Y2	0.218	0.217	0.217	0.217	0.217	0.217	0.217	0.217	0.223
Y1	0.217	0.92	0.92	0.92	0.92	0.92	0.92	0.92	0.926

6. 1111

1111	X1	X2	X3	X4	X5	X6(x4)	X7(X3)	X8(x2)	X9(X1)
Y4	0.218	0.217	0.217	0.217	0.217				
Y3	0.217	0.920	0.920	0.920	0.920				
Y2	0.217	0.920	0.920	0.920	0.920				
Y1	0.218	0.217	0.217	0.217	0.217				

7. 0010

0010	X1	X2	X3	X4	X5	X6(x4)	X7(X3)	X8(x2)	X9(X1)
Y4	0.926	0.926	0.926	0.926	0.926				
Y3	0.926	0.920	0.920	0.920	0.920				
Y2	0.926	0.920	0.920	0.920	0.920				
Y1	0.223	0.217	0.217	0.217	0.217				

8. 0011

0011	X1	X2	X3	X4	X5	X6(x4)	X7(X3)	X8(x2)	X9(X1)
Y4	0.223	0.218	0.217	0.217	0.217				
Y3	0.926	0.92	0.92	0.92	0.92				
Y2	0.926	0.92	0.92	0.92	0.92				
Y1	0.223	0.218	0.217	0.217	0.217				

9. 1011

1011	X1	X2	X3	X4	X5	X6	X7	X8	X9
Y4	0.218	0.217	0.217	0.217	0.217	0.217	0.217	0.217	0.223
Y3	0.217	0.920	0.920	0.920	0.920	0.920	0.920	0.920	0.926
Y2	0.217	0.920	0.920	0.920	0.920	0.920	0.920	0.920	0.926
Y1	0.218	0.217	0.217	0.217	0.217	0.217	0.217	0.217	0.223

10. 000-1

000-1	X1	X2	X3	X4	X5	X6(x4)	X7(X3)	X8(x2)	X9(X1)
Y4	1.283	1.278	1.283	1.278	1.278				
Y3	1.187	1.181	1.181	1.181	0.921				
Y2	1.187	1.181	1.181	0.921	0.921				
Y1	1.187	1.187	0.926	0.926	0.926				

11. 001-1

001-1	X1	X2	X3	X4	X5	X6(x4)	X7(X3)	X8(x2)	X9(X1)
Y4	1.283	1.278	1.277	1.277	1.277				
Y3	1.187	1.181	1.181	1.181	1.181				
Y2	0.926	0.921	0.92	0.92	0.92				
Y1	0.223	0.218	0.217	0.217	0.217				

12. 100-1

100-1	X1	X2	X3	X4	X5	X6	X7	X8	X9
Y4	1.278	1.277	1.277	1.277	1.277	1.277	1.278	1.278	1.283
Y3	0.218	1.181	1.181	1.181	1.181	1.181	1.181	1.181	1.187
Y2	0.218	0.921	0.92	0.92	0.92	1.181	0.921	1.181	1.187
Y1	0.223	0.926	0.926	0.926	0.926	0.926	0.926	1.187	1.187

13. 101-1

101-1	X1	X2	X3	X4	X5	X6	X7	X8	X9
Y4	1.278	1.277	1.277	1.277	1.277	1.277	1.277	1.278	1.283
Y3	0.218	0.92	0.92	0.92	0.92	0.92	1.181	1.181	1.187
Y2	0.217	0.92	0.92	0.92	0.92	0.92	0.92	1.181	0.926
Y1	0.218	0.217	0.217	0.217	0.217	0.217	0.217	0.218	0.223

14. 110-1

110-1	X1	X2	X3	X4	X5	X6(x4)	X7(X3)	X8(x2)	X9(X1)
Y4	1.277	1.277	1.277	1.277	1.277				
Y3	0.218	1.181	0.92	0.92	0.92				
Y2	0.218	1.181	0.92	0.92	0.92				
Y1	0.223	0.926	0.926	0.926	0.926				

15. 111-1

111-1	X1	X2	X3	X4	X5	X6(x4)	X7(X3)	X8(x2)	X9(X1)
Y4	1.278	1.277	1.277	1.277	1.277				
Y3	0.217	0.920	0.920	0.920	0.920				
Y2	0.217	0.920	0.920	0.920	0.920				
Y1	0.218	0.217	0.217	0.217	0.217				

16. 0-100

0-100	X1	X2	X3	X4	X5	X6	X7	X8	X9
Y4	1.187	1.187	0.926	0.926	0.926	0.926	1.187	1.187	1.283
Y3	1.187	1.181	0.921	0.921	0.926	0.926	1.187	1.187	1.278
Y2	1.187	1.181	0.921	0.921	0.926	0.926	1.187	1.187	1.278
Y1	1.187	1.187	0.926	0.926	0.926	0.926	1.187	1.187	1.283

17. 1-100

1-100	X1	X2	X3	X4	X5	X6	X7	X8	X9
Y4	0.223	0.926	0.926	0.926	0.926	0.926	0.926	1.187	1.283
Y3	0.218	0.92	0.92	0.92	0.92	1.181	0.921	1.181	1.278
Y2	0.218	0.92	0.92	0.92	0.92	1.181	0.921	1.181	1.278
Y1	0.223	0.926	0.926	0.926	0.926	0.926	0.926	1.187	1.283

18. 0-101

0-101	X1	X2	X3	X4	X5	X6	X7	X8	X9
Y4	0.223	0.217	0.217	0.217	0.217	0.217	0.217	0.218	1.278
Y3	0.926	1.181	0.92	0.92	0.92	0.92	1.181	0.921	1.278
Y2	0.926	1.181	0.92	0.92	0.92	0.92	1.181	1.181	1.278
Y1	0.926	0.926	0.926	0.926	0.926	0.926	0.926	1.187	1.283

19. 1-110

1-110	X1	X2	X3	X4	X5	X6	X7	X8	X9
Y4	0.223	0.926	0.926	0.926	0.926	0.926	0.926	1.187	1.283
Y3	0.926	1.181	0.92	0.92	0.92	0.92	1.181	1.181	1.278
Y2	0.926	1.181	0.92	0.92	0.92	0.92	1.181	0.921	1.278
Y1	0.223	0.217	0.217	0.217	0.217	0.217	0.217	0.218	1.278

20. 0-111

0-111	X1	X2	X3	X4	X5	X6	X7	X8	X9
Y4	0.223	0.217	0.217	0.217	0.217	0.217	0.217	0.218	1.278
Y3	0.926	0.92	0.92	0.92	0.92	0.92	0.92	1.181	1.277
Y2	0.926	0.92	0.92	0.92	0.92	0.92	0.92	1.181	1.277
Y1	0.223	0.217	0.217	0.217	0.217	0.217	0.217	0.218	1.278

21. 1-111

1-111	X1	X2	X3	X4	X5	X6	X7	X8	X9
Y4	0.218	0.217	0.217	0.217	0.926	0.217	0.926	0.217	1.278
Y3	0.217	0.920	0.920	0.920	0.920	0.920	0.920	1.181	1.277
Y2	0.217	0.920	0.920	0.920	0.920	0.920	0.920	1.181	1.277
Y1	0.218	0.217	0.217	0.217	0.217	0.217	0.217	0.217	1.278

22. 0-10-1

0-10-1	X1	X2	X3	X4	X5	X6	X7	X8	X9
Y4	1.283	1.278	1.278	1.278	1.278	1.278	1.278	1.278	1.283
Y3	1.187	1.181	1.181	1.181	1.181	1.181	1.181	1.181	1.278
Y2	1.187	1.181	1.181	1.181	1.181	1.181	1.181	1.181	1.278
Y1	1.187	1.187	1.187	0.926	0.926	1.187	1.187	1.187	1.283

23. 0-11-1

0-11-1	X1	X2	X3	X4	X5	X6	X7	X8	X9
Y4	1.283	1.278	1.278	1.277	1.277	1.278	1.278	1.278	1.283
Y3	1.187	1.181	0.921	0.921	0.921	0.921	1.181	1.181	1.278
Y2	0.926	0.921	1.181	0.92	0.92	1.181	0.92	1.181	1.278
Y1	0.223	0.218	0.218	0.217	0.217	0.218	0.218	0.218	1.278

24. 1-10-1

1-10-1	X1	X2	X3	X4	X5	X6	X7	X8	X9
Y4	1.278	1.278	1.277	1.277	1.277	1.278	1.278	1.278	1.283
Y3	0.218	1.181	0.921	0.921	0.921	1.181	1.181	1.181	1.278
Y2	0.218	0.921	0.921	0.921	0.921	1.181	1.181	1.181	1.278
Y1	0.223	0.926	0.926	0.926	0.926	0.926	1.187	1.187	1.283

25. 1-11-1

1-11-1	X1	X2	X3	X4	X5	X6	X7	X8	X9
Y4	1.278	1.277	1.277	1.277	1.277	1.277	1.277	1.278	1.283
Y3	0.218	1.181	1.181	1.181	1.181	1.181	1.181	1.181	1.278
Y2	0.217	0.92	0.92	0.92	0.92	0.92	0.921	1.181	1.278
Y1	0.218	0.217	0.217	0.217	0.217	0.217	0.218	0.218	1.278

PUBLICATIONS

1. Rafiq M. Y., Sui, C., Easterbrook, D. J. & Bugmann, G. (2007), "Generality of using Correctors to Predict the Behaviour of Masonry Wall Panels", accepted for presentation in 14th Int. EG-ICE Workshop, Maribor, June.

2. Chengfei Sui, M. Y. Rafiq , D. Easterbrook, G. Bugmann, G. Zhou, (2006), "More accurate prediction of the behaviour of masonry panel subjected to lateral loads", Proc. of the 7th Int. Masonry Conference, London, British Masonry Society, Paper 19 (CD-ROM), October, ISSN 0950 9615.

3. Chengfei Sui, M. Y. Rafiq, D. Easterbrook, G. Bugmann, G. Zhou, (2006) "Using Timoshenko Formula to Modify the Experimental Error of Masonry Panels", Proc. of the 7th Int. Masonry Conference, London, British Masonry Society, Paper 47 (CD-ROM), October, ISSN 0950 9615.

4. Chengfei Sui, M. Y. Rafiq , D. Easterbrook, G. Bugmann, G. Zhou, (2006), "An investigation into numerical model updating of masonry panels subjected to lateral load", Proc. of the 7th Int. Masonry Conference, London, British Masonry Society, Paper 33 (CD-ROM), October, ISSN 0950 9615.

5. Chengfei Sui, M. Y. Rafiq, D. Easterbrook, G. Bugmann, G. Zhou, (2006), "Uniqueness study of updating the FEA model of laterally loaded masonry panel by genetic algorithm", Proc. of the 7th Int. Masonry Conference, London, British Masonry Society, Paper 36 (CD-ROM), October, ISSN 0950 9615.

6. Guangchun Zhou, Yaqub M. Rafiq, Chengfei Sui and Lingyan Xie, (2006). "A CA and ANN Technique of Predicting Failure Load and Failure Pattern of Laterally Loaded Masonry Panel", International Conference On Computing And Decision Making In Civil And Building Engineering, Paper IC_96, June 14-16, Montreal, Canada.

   http://216.239.59.104/search?q=cache:py4JNzDvfyYJ:www.icccbexi.ca/html/en/Sessions/S171.ht m+A+CA+AND+ANN+TECHNIQUE+OF+PREDICTING+FAILURE+LOAD+AND+FAILURE +PATTERN+OF+LATERALLY+LOADED+MASONRY+PANEL&hl=en&ct=clnk&cd=1

7. Yaqub Rafiq, Chengfei Sui, Dave Easterbrook and Guido Bugmann, (2006). "Prediction of the behaviour of masonry wall panels using Evolutionary Computation and Cellular Automata", Proc. of the 13th International Workshop of the European Group for Intelligent Computing in Engineering, Monte Verita, Ascona Switzerland, Springer under Intelligent computing in engineering and Architecture "Lecture Notes in Artificial Intelligence 4200", Smith, I. F. C. (Edt), ISBN -10 3-540-46246-5, pp. 534-544.

   http://www.springerlink.com/content/r783151147732rtx

8. Rafiq, M.Y., Sui, C., Zhou, G. C., Easterbrook, D. J. and Bugmann, G., (2005). "Using Artificial Intelligence Techniques to Predict the Behaviour of Masonry Panels", Proceedings of The Eighth International Conference on the Application of Artificial Intelligence to Civil, Structural and Environmental Engineering, 30 August to 2 September, Rome, CD-ROM Paper 21, ISBN 1-905088-04-3

GENERALITY OF USING CORRECTORS TO PREDICT THE BEHAVIOUR OF MASONRY WALL PANELS

Rafiq M. Y., Sui, C., Easterbrook, D. J. & Bugmann, G.

School of Engineering, University Plymouth, UK   mrafiq@plymouth.ac.uk

ABSTRACT

The highly composite and anisotropic nature of masonry, which is a result of the variation in the properties of the masonry constituents, makes it very difficult to find an accurate material model to predict its behaviour satisfactorily. Current research by the authors has focused more closely on the behaviour of laterally loaded masonry panel using model updating techniques supported by artificial intelligence (AI) techniques. They developed the concept of *correct factors* which models the variation in the properties over the surface of the masonry wall panels. This research resulted in methodologies, which enables designers to more confidently predict the behaviour of masonry wall panels subjected to lateral loading. The paper will demonstrate the generality of using these techniques to predict the behaviour of laterally loaded masonry wall panels tested by various sources.

1. INTRODUCTION

Masonry is a highly composite and anisotropic material which is constructed from layers of brick joined by thin layers of cement and sand mortar. Research on masonry panels subjected to lateral loading, started from around 1970 and continues to the present date (West et al 1971, 1975, Baker & Franken 1976, Fried 1989, Lawrence 1991, Chong 1993, among others). These researchers have tried to find acceptable models for predicting the behaviour of laterally loaded masonry walls. To date these attempt have not produced a reliable and accurate technique which can confidently predict both failure load and load deflection relationship for laterally loaded masonry wall panels.

Model updating techniques, which are based on minimising the error between the experimental and analytical results to select a suitable analytical model from among many possible alternatives, have produced good results in structural damage detection. The majority of the research on model updating process involves computing sets of stiffness coefficients that help predict observed vibration modes of structures. The location and extent of damage are inferred through a comparison between the stiffness coefficients of damaged and undamaged structures. A comprehensive literature review of various model updating methods is presented by Robert-Nicoud et al (2005). Friswell & Mottershead (1995) provide a survey of model updating procedures in structural damage detection research, using vibration measurements. Recent papers published in this area include Brownjohn et al (2003), Castello et al (2002), Teughels et al (2002), Modak et al (2002), Hemez & Doebling (2001), Sohn & Law (2001), Hu et al (2001).

The authors have used a numerical model updating technique to investigate the behaviour of masonry wall panels subjected to lateral loads (Rafiq et al 2006).

2. A BRIEF SUMMARY OF THE PROPOSED METHOD

Zhou (2002) and Rafiq et al. (2003) developed a numerical model updating technique that more accurately predicts the failure load and failure pattern of masonry wall

panels subjected to lateral loading. In this research they introduced the concept of *stiffness/strength corrector factors*, which assigns different values of flexural rigidity or tensile strength to various zones within a wall panel. These modified rigidities or tensile strength values were then used in a non-linear finite element analysis (FEA) model to predict the deflection and failure load of the masonry panels subjected to lateral loading.

Corrector factors were defined from the comparison of laboratory measured and finite element analysis(FEA) computed values of displacements over the surface of the panel. In this investigation a number of experimental panels with different configuration, geometric properties, aspect ratios, and panels with and without opening were used, and stiffness corrector factors for these panels were determined. From a comparison of the contour plots of corrector factors on these panels it was discovered that there appeared to be regions, termed '*zones*', with similar patterns of corrector factors, which are closely related to their positions within the panel from similar boundary types. In other words, zones within two panels appear to have almost identical corrector factors if these zones were located the same distance from similar boundary types. This pattern was observed for all panels with different boundary condition and geometrical configurations.

Based on this finding Zhou et al. (2003) developed methodologies to establish zone similarities between various panels. In order to achieve a more reasonable and automatic technique for establishing this zone similarity between a *base panel* and any new panel, a cellular automata (CA) model was developed. This CA model propagates the effect of panel boundaries to zones within the panel. The CA assigns a unique value the so called '*state value*' for each zone within the base panel and an unseen panel, based on their relative locations from various boundary types. The CA then identifies similar zones between two panels by comparing similar state values of zones on two panels. Zones on two panels are considered to be similar if they are surrounded by similar boundary types and have similar distances from similar boundary types.

Further investigation of corrector factors (Rafiq et al 2006), using evolutionary computation and regression analysis techniques, revealed that the pattern of corrector factors that modify flexural rigidities were mainly altered around the panel boundaries with relatively minor changes inside the panel. This was a major finding of this research.

Difficulties in correctly modelling boundary types is a well known problem even for material like steel and concrete with well defined and well controlled joint details between various elements and supporting structures. This issue is more critical for masonry panels as standard boundaries such as fully fixed and simply supported boundary types, used in FEA models, are not realistic for masonry. The results of our research proved that a better prediction of panel response to lateral loading would be possible if the panel boundaries are modelled more accurately.

A closer study of the corrector factors revealed that a reduction in the corrector factor values around the fixed boundaries has a softening effect on the zones adjacent to this boundary type. This is a reality as it is impossible to have a fully fixed boundary for masonry panels as there is always some degree of rotation at these supports. Similarly an increase in corrector factors near the simply supported boundaries signifies a degree of restraint to rotation at these boundaries which is perfectly logical (Rafiq et al 2006).

In order to demonstrate the generality of this concept, a single panel (Panel SBO1 Rafiq et al 2006) tested by Chong (1993) was used as a '*base panel*'.

The corrector factor values for this panel are summarised in Table 1. These corrector factors from the base panel are then used to establish an estimate of the corrector factors for any *unseen panels* for which no laboratory tests are available. A cellular automata model was used to establish zone similarities between any unseen panel and the base panel. Zones on two panels are considered to be similar if they are surrounded by similar boundary types and having similar distances from similar boundary types.

Table 1. Corrector actor values for the base panel SB01

SB01	X1	X2	X3	X4	X5	X6	X7	X8	X9
Y4	1.283	1.278	1.277	1.277	1.277	1.277	1.277	1.278	1.283
Y3	1.187	1.181	1.181	1.181	1.181	1.181	1.181	1.181	1.187
Y2	0.926	0.921	0.92	0.92	0.92	0.92	0.92	0.921	0.926
Y1	0.223	0.218	0.217	0.217	0.217	0.217	0.217	0.218	0.223

As was shown in this study, the major factor that affects the behaviour of a panel was the panel boundary types. The corrector factors not only model this, but also take care of the variation in the material and geometric properties and other unknown effects. One of the objectives of this research was to use these corrector factors to predict the behaviour of unseen panels with and without openings and panels for which the boundary conditions are different from the base panel.

3. GENERALIZATION

By generalization we mean to test the generality of the corrector factors for a number of new panels tested by other sources which may be totally different from the base panel in terms of size, aspect ratio, geometry, material and workmanship.

4. CASE STUDIES

In this section, a number of masonry wall panels with different boundary conditions, different dimensions and panels with and without openings obtained from various sources are analysed to demonstrate the generality of the proposed method. The corrector factors for any new masonry wall panel are derived from those of the base panel shown in Table 1. A cellular automata model is used to establish zone similarity between the base panel and the new panel. The results of this study are summarised in the following section. For all examples used in these case studies, the material properties used are from the original sources. However, if these properties are not available, the data from tests carried out in the University of Plymouth Chong(1993) are used.

4.1 ANALYSES OF PANELS TESTED IN UNIVERSITY OF PLYMOUTH

In this section, two full scale single leaf masonry wall panels (SB02 & SB04), tested in the University of Plymouth (Chong 1993), are selected for validation purposes. These panels have the same dimensions and boundary conditions as SB01, but panel SB02 has a single opening at its centre to simulate the existence of a window and panel SB04 has an opening to simulate the existence of a door. Details of the configurations of these panels are shown in Figs 1 & 2 respectively.

It should be noted that these panels were tested by Chong (1993) at the University of Plymouth. The reason for selecting these panels is that it is easy to compare the predicted and experimental result to check the validity of the proposed methods.

Corrector factor values for all panels used in the case studies are derived for the base panel using CA to establish zone similarities between new panels and the base panel.

Corrector factor values for panel SB02 and SB04, derived from the base panel (Table 1), are shown in Tables 2 and 3 respectively. These corrector factors are used to modify the flexural rigidity of each zone in the panel. In this study, for ease of use in the FEA models, only the modulus of elasticity of each zone is multiplied by the corrector factor value of each zone. These corrected values of modulus of elasticity are then used in a non-linear finite element analysis model to evaluate the predicted deflection at the corners of each zone and the failure load for the panel. The corrector factors not only model the boundary effects, but also model variation in the material and geometric properties and other unknown effects.
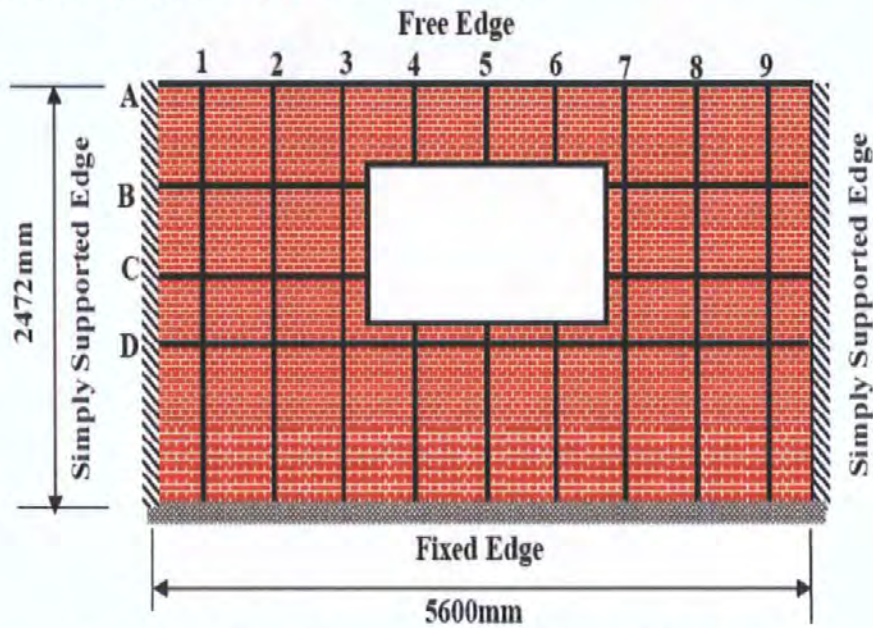
Figure. 1. Panel SB02, measurement points at grid intersections

Table 2. Panel SB02 zone divisions and corrector factors

SBO2	X1	X2	X3	X4	X5	X6	X7	X8	X9	X10
Y5	1.283	1.278	1.278	1.278	1.278	1.278	1.278	1.278	1.278	1.283
Y4	1.187	1.181	1.278					1.278	1.181	1.187
Y3	1.187	1.181	1.278					1.278	1.181	1.187
Y2	1.187	1.181	1.181	1.277	1.277	1.277	1.277	1.181	1.181	1.187
Y1	0.223	0.217	0.217	0.218	0.218	0.218	0.218	0.217	0.217	0.223
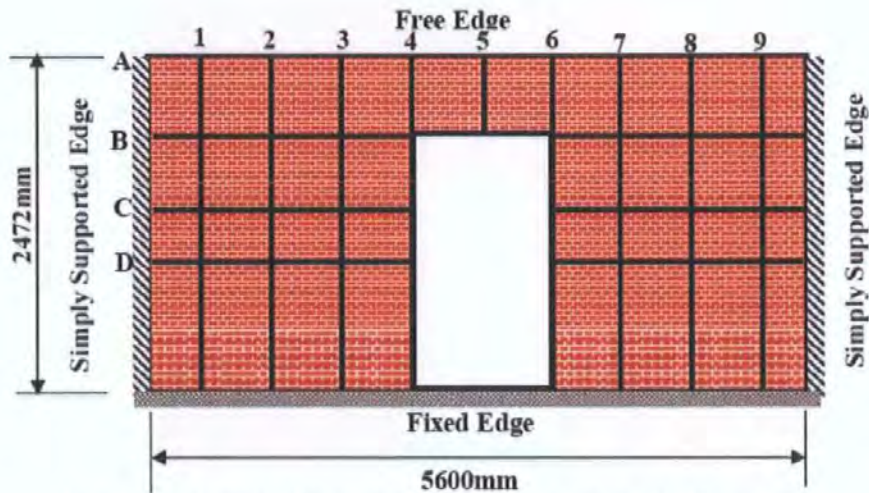
Figure. 2. Panel SB04, measurement points at grid intersections

Table 3. Panel SB04 zone divisions and corrector factors

SBO4	X1	X2	X3	X4	X5	X6	X7	X8	X9	X10
Y5	1.283	1.278	1.278	1.278	1.278	1.278	1.278	1.278	1.278	1.283
Y4	1.187	1.181	1.181	1.278			1.278	1.181	1.181	1.187
Y3	1.187	1.181	1.181	1.278			1.278	1.181	1.181	1.187
Y2	1.187	1.181	1.181	1.278			1.278	1.181	1.181	1.187
Y1	0.223	0.218	0.218	1.278			1.278	0.218	0.218	0.223

Fig. 3 shows a 3D deformed panel shape, comparing the experimental and FEA predicted displacements at various locations on the panel SB02. Apart from minor discrepancies in locations near the boundaries of the opening, FEA results give a good prediction of the displacement over the entire surface of the panel.
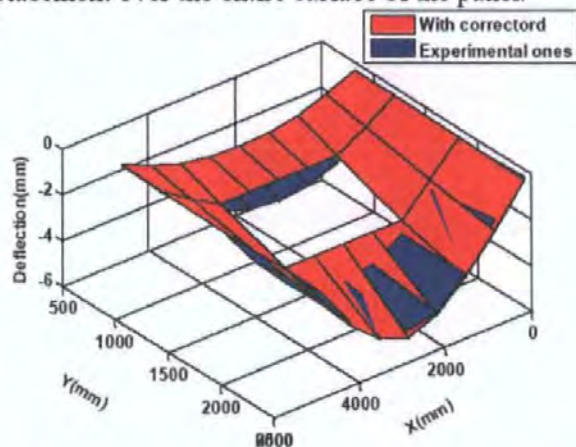
Figure. 3. Panel SB02, comparison of 3D deformed shape showing experimental and the FEA results at 1.4kN/m^2

Figure 4 shows similar information for panel SB04. Once again there is a very good match between experimental and FEA predicted deformed shapes.
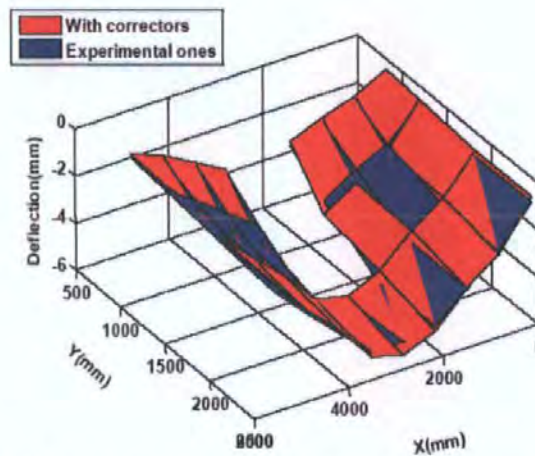
Figure. 4. Panel SB04, comparison of 3D deformed shape showing experimental and the FEA results at $1.4kN/m^2$
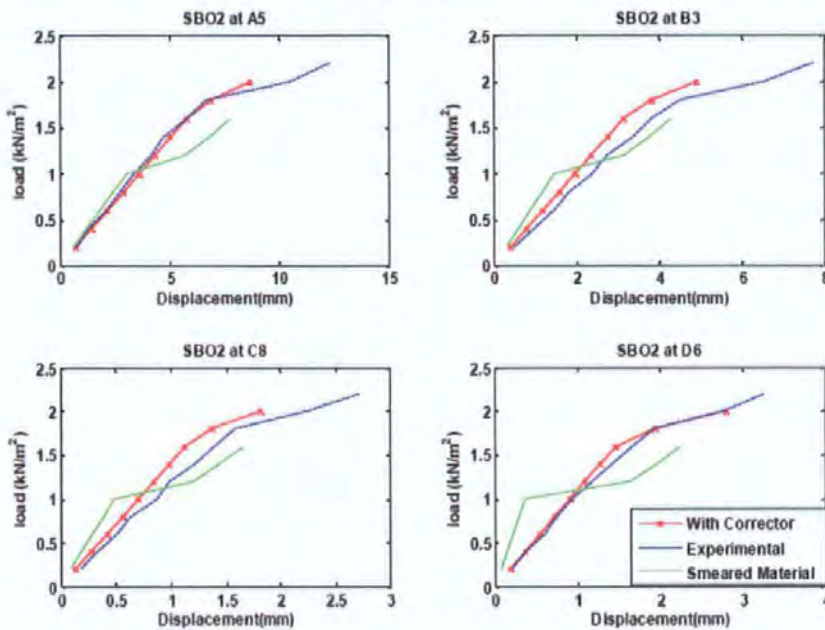
Figure.5. Panel SB02, Comparison of the load deflection relationship showing experimental and the FEA results

To demonstrate the generality of the proposed method, 2D load displacement plots at various locations on the panels SB02 and SB04 are presented in Figs 5 and 6. The reason for selecting these plots is to investigate if there is a consistent correlation between experimental and the FEA predicted deflection at various load levels and at various locations on the panel. The points were selected to be representative of the entire surface. In these Figs. three different curves are plotted (1) the experimental load deflection curve; (2) the predicted load deflection curves using corrector factor values derived from a single base panel (SB01) and the standard smeared material model normally used in FEA analysis. A very good correlation is observed between the experimental and analytical results using the corrector factors. The result from the predicted load deflection using corrector factors is much closer to the experimental results than that of the smeared material model. Moreover, the predicted failure loads

for both panels, using corrector factors, are much better than those of the smeared model.

From this investigation it can be concluded that the proposed method results in an improved prediction of both failure load and load displacement of a panel even if the geometries of the new panels are different from the base panel.

To further examine the generality of the proposed method presented in this paper, a number of panels tested by other sources, for which little or no information on material properties and testing methods are available, are selected. Corrector factors for all these panels were derived from a single base panel (SB01), as has been introduced in this paper. It should be noted that these panels have different dimensions, configuration and boundary conditions than the base panel (SB01).
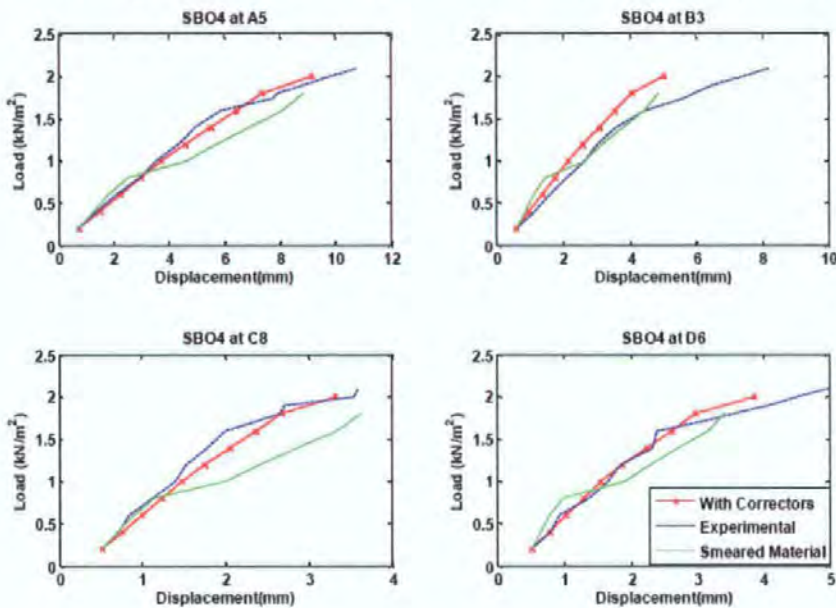
Figure. 6. Panel SB04, Comparison of the load deflection relationship showing experimental and the FEA results

It is also worthwhile mentioning that load deflection data for the panels presented in section 4 and 5 were limited to a few points over the surface of the panel, which was not enough to generate an acceptable 3D load deflection surface plot, therefore, the comparisons were restricted to 2D load deflection plots only.

4.2 ANALYSES OF PANELS TESTED BY (CERAM)

In the UK, CERAM is a reliable source of information on various aspects of masonry. CERAM has been involved in testing of full scale masonry panels investigating various material types, boundary conditions, aspect ratios etc. for over 25 years. In this paper the authors have selected two panels, one solid panel (CR1) and one panel with a single opening central opening (CR2), to investigate the generality of the proposed method. The results of the investigation on both panels are presented in sections 4.2.1 and 4.2.2 respectively.

4.2.1 PANEL CR1

Wall CR1 (Edgell 1995b) is a single leaf masonry panel constructed with Fletton brick with three sides simply supported and the top edge free. This panel has a

dimension of 2.8m x 3.6m. The configuration of wall CR1 is as shown in Fig 7. Measurements of load deflection were recorded at 11 locations on this panel.

The flexural strengths measured from the wallet tests for this panel are given as: $1.40 N/mm^2$ perpendicular to the bed-joints and $0.40 N/mm^2$ parallel to the bed-joints. No information was available for the elastic modulus and Poisson's ratio. Therefore, the elastic modulus E and Poisson's ratio v are assumed to be the same as the base panel SB01. Corrector factors, derived from panel SB01, are shown in Table 4. From Figure 8, it can be concluded that:

- The smeared material model gives a poor correlation with the experimental results.

- The corrector factors improve both load deflection and failure load results which are close to the experimental results at a number of locations.

- The correlation between load deflection at the location of maximum deflection is much better than other locations. This is a good measure of comparison as in practice maximum deflection and stresses are critical design requirements.
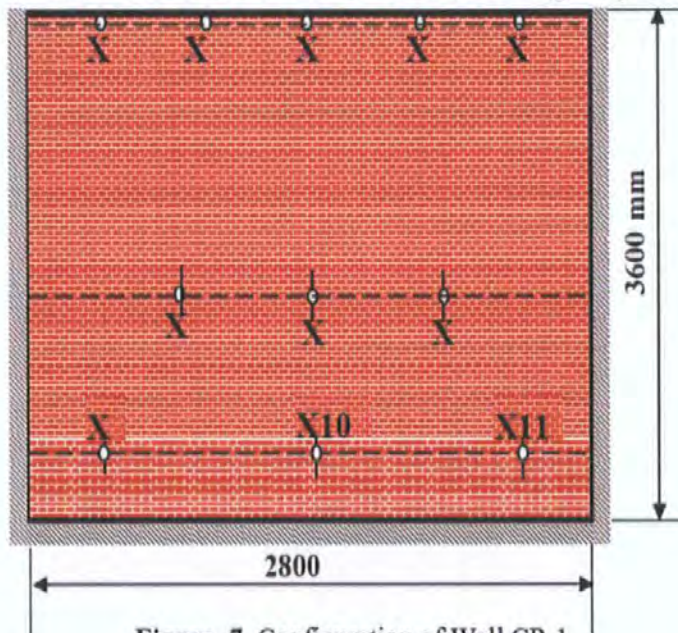
Figure. 7. Configuration of Wall CR 1

Table 4. Corrector Factors of Wall CR1

Wall CR1	X1	X2	X3	X4	X5	X6
Y5	1.283	1.278	1.278	1.278	1.278	1.283
Y4	1.187	1.181	1.181	1.181	1.181	1.187
Y3	1.187	1.181	1.181	1.181	1.181	1.187
Y2	1.187	1.181	1.181	1.181	1.181	1.187
Y1	1.187	1.187	1.187	1.187	1.187	1.187
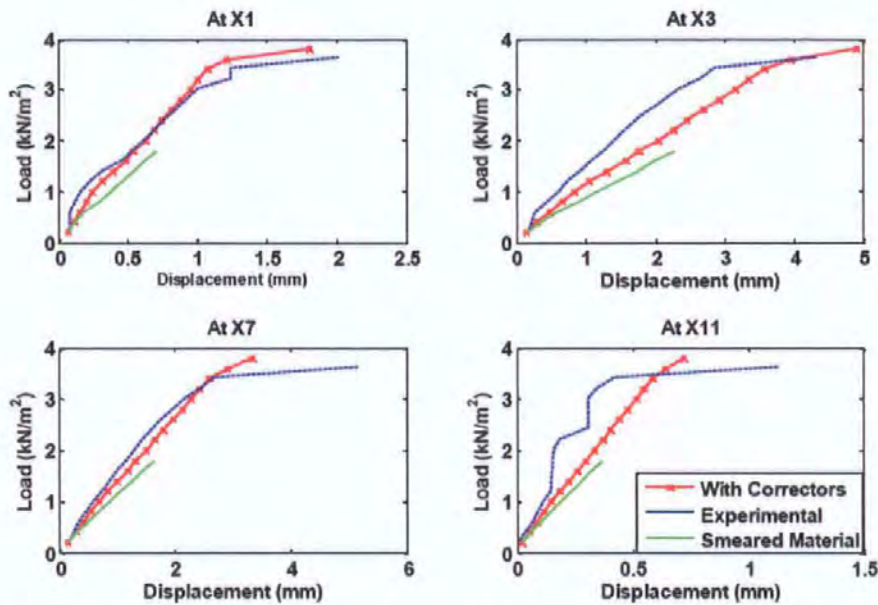
Figure. 8. Panel CR1 Comparison of the load deflection relationship showing experimental and the FEA results

4.2.2 PANEL CR2

Wall CR2 (Edgell 1995a) is a single leaf masonry panel with a single central opening. This panel was also tested by CERAM. The panel was constructed with Fletton brick with three sides simply supported and the top edge is free. The panel dimensions are 5.5m x 2.8m with the opening size 2m x 1.2m. Details of the wall and location of measurement points are shown in Fig 9.
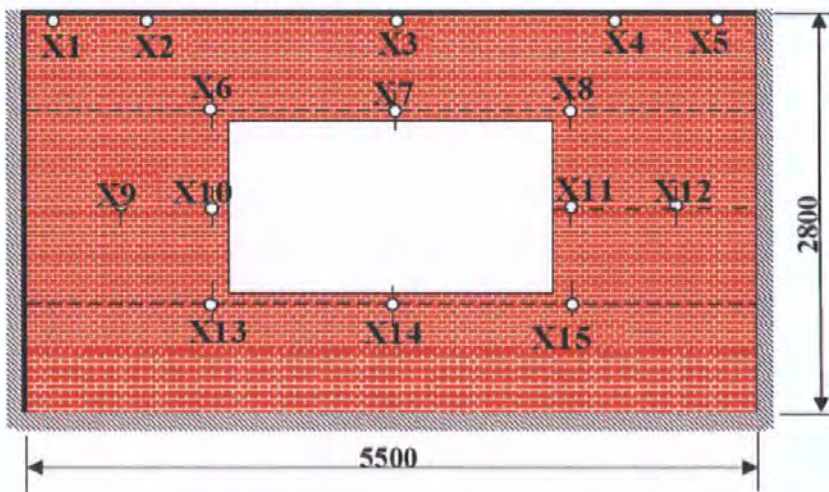
Figure. 9. Configuration of Wall CR 2

The mean flexural strengths for this wall measured from the wallette tests are: $f_x = 1.37 N/mm^2$ and $f_y = 0.42 N/mm^2$. However, the elastic modulus E and Poisson's ratio are not included in the original data, therefore the elastic modulus E and Poisson's ratio v are assumed to be : $E = 12 kN/mm^2$, $v = 0.2$, same as the base panel.

The corresponding corrector factors for zones, derived from panel SB01, are as shown in Table 5. Fig. 10 shows load deflection plots at 4 selected locations on the

panel. From Fig 10, it is clear that using corrector factors, both the failure load and load deflection curves are much closer to the experimental results.

Table 5. Zone Division and Correctors for Wall CR 2

Wall CR2	X1	X2	X3	X4	X5	X6	X7	X8	X9	X10
Y4	1.283	1.278	1.278	1.278	1.278	1.278	1.278	1.278	1.278	1.283
Y3	1.187	1.181	1.278					1.278	1.181	1.187
Y2	1.187	1.181	1.278					1.278	1.181	1.187
Y1	1.187	1.187	1.187	1.187	1.187	1.187	1.187	1.187	1.187	1.187
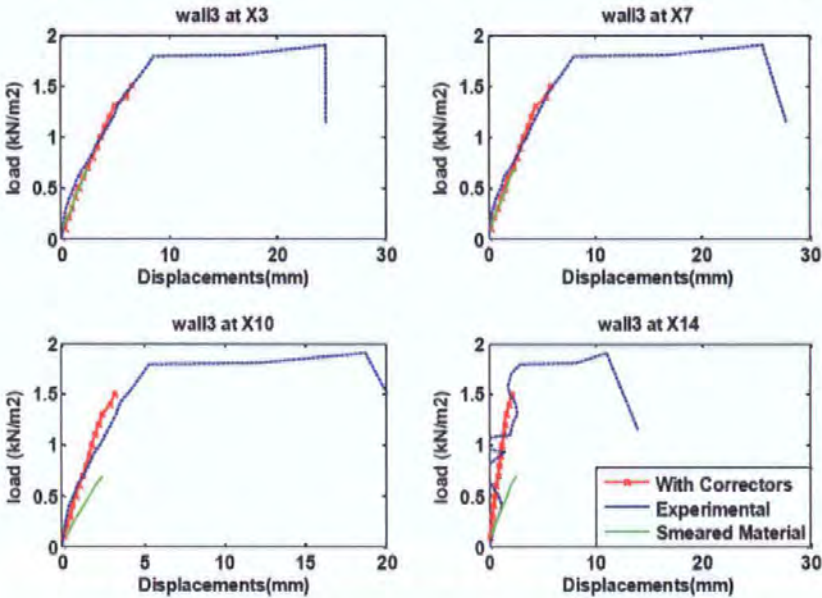
Figure. 10. Load deflection relationships of Wall CR 2 using correctors

4.3 ANALYSES OF PANELS TESTED BY UNIVERSITY OF EDINBURGH

It is worth mentioning again that like the majority of the masonry panels tested around the world the information obtained from panels tested in the University of Edinburgh measures only deflection at a single critical location in the panel. Therefore for panels presented in this section, only 2D plots of load deflection at the location of maximum displacement are presented.

4.3.1 PANEL WALL 9

Wall 9 is a single leaf masonry wall panel, tested in the University of Edinburgh (LIANG 1999). This panel is simply supported on its 3 edges and the top edge is free. The Pane dimension is 795 x 1190 mm. The reason for selecting this panel for investigation is that this is a much smaller panel than the base panel SB01 and its aspect ratio is also different. If the corrector factors from the base panel SB01 are suitable for predicting the failure load and load deflection for this panel then this would give us more confidence on the validity of the proposed method.

Table 6. Correctors of Wall 9

Wall 9&13	X1	X2	X3
Y1	1.283	1.278	1.283
Y2	1.187	1.181	1.187
Y3	1.187	1.181	1.187
Y4	1.187	1.181	1.187
Y5	1.187	1.187	1.187

The flexural strength parallel and perpendicular to the bed joints were obtained from the wallette test, which are respectively 3.5N/mm^2 and 0.98 N/mm^2. The values of corrector factors, derived from the base panel are summarised in Table 6. Fig 11 shows a comparison of experimental and predicted load deflection curves at the location of maximum deflection. From Fig. 11 it is clear that there is a good agreement between experimental and predicted results, which demonstrates the generality of the proposed method.
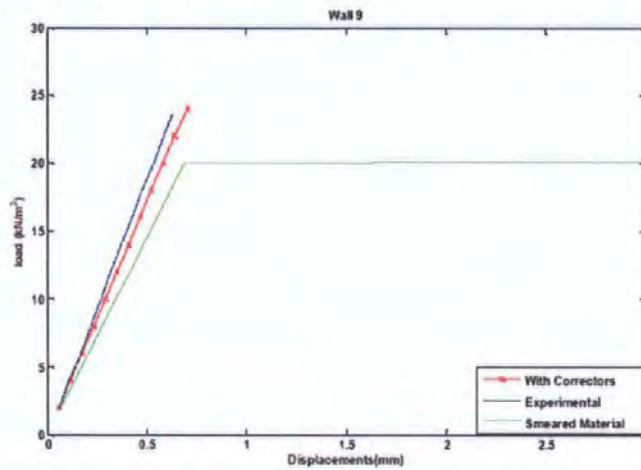
Figure. 11. Load deflection relationships of Wall 9 using correctors

5. CONCLUSION

The research presented in this paper introduces a novel approach using a numerical model updating technique supported by AI for predicting the behaviour of masonry wall panels much better than any other analytical model used so far. This method has the potential to be extended beyond masonry brick walls and could also be used with other materials to reduce the degree of uncertainty in analytical models and analytical results. The simplicity of the model is that once corrector factors for a representative base panel are determined it would be easy to use these factors for any panels using zone similarity techniques.

In this research, corrector factors from a single panel tested in the laboratory were used for a number of unseen panels with different boundary types, size and configurations. The results produced a more accurate prediction of the behaviour of the laterally loaded masonry wall panels.

Modelling boundary types wrongly results in incorrect analytical results. Using corrector factors minimised this error and corrected the error in modelling to a great extent.

REFERENCE

Baker, L. R. and Franken, G. L., (1976). "Variability Aspects of the Flexural Strength of Brick Work", Proc. 4th IBMAC, Brugge.

Brownjohn, J. M. W., Moyo, P., Omenzetter, P., and Lu, Y. (2003). "Assessment of highway bridge upgrading by testing and finite-element model updating." *J. Bridge Eng.* 8 (3), 162–172.

Castello, D. A., Stutz, L. T., and Rochinha, F. A., (2002). "A structural defect identification approach based on a continuum damage model." *Comput. Struct.* 80, 417–436.

Chong, V. L. (1993). *The Behaviour of Laterally Loaded Masonry Panels with Openings.* Thesis (Ph.D). University of Plymouth, UK.

EDGELL, G. J., (1995a), "Additional work on wide cavity walls", CERAM research report, Masonry Research Masonry Strategy Committee additional work on wide cavity walls, MRSC/5.

EDGELL, G. J., (1995b), Dynamic and static lateral loading of story height walls, CERAM research report, Structural Masonry Strategy Committee gust loading of story high walls, SM / SMSC .D .1, January.

Fried, A.N., (1989). Laterally Loaded Masonry Panels-The Significance of Analytical Methods and Material Properties. PhD Thesis, South Bank Polytechnic, London.

Friswell, M. I., and Mottershead, J. E. (1995). *Finite element model updating in structural dynamics.* Kluwer, New York.

Hemez, F. M., and Doebling, S. W. (2001). "Review and assessment of model updating for non-linear, transient dynamics." *Mech. Syst. Signal Process.* 15 (1), 45–74.

Hu, N., Wang, X., Fukunaga, H., Yao, Z. H., Zhang, H. X., and Wu, Z. S. (2001). "Damage assessment of structures using modal test data." *Int. J. Solids Struct.*, 38, 3111–3126.

Lawrence, S.J. and Lu, J.P., (1991). "An Elastic Analysis of Laterally Loaded Masonry Walls with Openings" International Symposium on Computer Methods in Structural Masonry, Swansea (Wales).

LIANG, N. C., (1999), "Experimental and theoretical investigation of the behaviour of brickwork cladding panel subjected to lateral loading", School of Engineering and Electronics, University of Edinburgh.

Modak, S. V., Kundra, T. K., and Nakra, B. C. (2002). "Comparative study of model updating studies using simulated experimental data.", *Comput. Struct.* 80, 437–447.

Rafiq, M. Y.. G. C. Zhou, et al. (2003). "Analysis of brick wall panels subjected to lateral loading using correctors." *Masonry International* 16(2): 75-82.

Robert-Nicoud, Y., Raphael, B., and smith I. F. C. (2005). " System Identification through Model Composition and Stochastic Search", ASCE Journal of Computing in Civil Engineering. Vol. 19. No. 3, pp 239-247.

Sohn H., and Law K.H. (2001), "Damage Diagnosis using Experimental Ritz Vectors." Journal of Engineering Mechanics, ASCE, Vol. 127, No. 11, pp. 1184-1193.

Teughels, A., Maeck, J., and Roeck, G. (2002). "Damage assessment by FE model updating using damage functions." *Comput. Struct.* 80, 1869–1879.

West, H.W.H., Hodgkinson, H.R. and Webb, W.F., 1971. *The Resistance of Clay Brick Walls to Lateral Loading.* Technical Note, No. 176, The British Ceramic Research Association.

West, H.W.H., Hodgkinson, H.R. and Haseltine. B.A., (1975). *Design of lateral Loaded Wall Panels.* Technical Note, No. 242, The British Ceramic Research Association.

Yaqub Rafiq, Y., Sui, C., Easterbrook, D, and Bugmann, G., (2006). "Prediction of the behaviour of masonry wall panels using Evolutionary Computation and Cellular Automata", Proc. of the 13th International Workshop of the European Group for Intelligent Computing in Engineering, Monte Verita, Ascona Switzerland, Springer under Intelligent computing in engineering and Architecture "Lecture Notes in Artificial Intelligence 4200", Smith, I. F. C. (Edt), ISBN -10 3-540-46246-5, pp. 534-544.

Zhou, G. C. (2002). Application of Stiffness/Strength Corrector and Cellular Automata in Predicting Response of Laterally Loaded Masonry Panels. School of Civil and Structural Engineering. Plymouth, University of Plymouth. PhD Thesis.

Zhou, G. C., Rafiq M. Y. Easterbrook, D. J., and Bugmann, G. (2003). "Application of cellular automata in modelling laterally loaded masonry panel boundary effects". *Masonry International*. Vol 16 No 3, pp 104 -114.

More Accurate Predictions of the Behaviour of Masonry Panels Subjected To Lateral Loads

by

C SUI[1], M Y RAFIQ[1], D EASTERBROOK[1], G BUGMANN[1] and G ZHOU[2]

[1] University of Plymouth, UK

[2] Harbin University of Technology (HIT), China

ABSTRACT

Due to the highly anisotropic properties of masonry panels, it is very difficult to predict accurately their behaviour. In the past finite element analysis (FEA) micro and macro models have been used to improve the quality of the FEA to be closer to their experimental results, but still there is no established method(s) that suitably address this problem. Research in the University of Plymouth (UoP) introduced a methodology of model updating that uses the concept of Correctors and Cellular Automata combined with a non-linear FEA, which more accurately predict the behaviour of masonry panels. This paper presents further refinements to the findings of the previous research by the team at UoP and uses evolutionary computation and regression analysis methods. New corrector values obtained by this method further improve the results of the non-linear FEA, which shows better agreement with the experimental results. In this study failure load and the load deflection relationships are studied for comparison.

KEYWORDS

Prediction, masonry panel, behaviour, lateral load, model updating

NOTATION

A, B, C: Constants of constraint function which are used as the GA Variables

CR: corrector factors

X: the distance from the centre of zone to panel boundaries.

1. INTRODUCTION

In spite of over 30 years of research on masonry panels it has been difficult to accurately predict the true behaviour of laterally loaded masonry panels. Since the late 1980s, finite element analysis (FEA) has been used to model the failure characteristics of masonry panels [1-2]. Using FEA of micro-modelling and macro-modelling [3-6], some improvement has been achieved in predicting its failure load but these improvements are still limited. So far most research in this area is still focusing on obtaining more accurate parameter values for material properties, or focusing on constitutive law and failure criteria. Still it has been difficult to find a suitable material model to be used in the FEA to give an accurate prediction of the masonry panel behaviour.

The Conceptual Modelling Research group in the University of Plymouth (UoP) has introduced a novel method of numerical model updating that use corrector factors [7], ZHOU [8-9] introduced the concept of corrector factors and zone similarity using the cellular automata (CA). Zhou improved the prediction of the failure load and failure pattern of masonry wall panels, but his improvements was limited in predicting the load deflection characteristics more accurately.

An improved model updating technique is proposed in this research based on the previous work in the UoP, which refine the corrector values using evolutionary computing (EC) techniques. In this paper, the refined correctors are used to improve the prediction of the behaviour of laterally loaded masonry panels and the method is verified by other cases; one of the main findings in this research is that the panel boundary conditions have a strong influence on the response of the laterally loaded masonry panel. Another innovative finding in the present research is that, because of the sudden decrease of analytical load-displacement relationships after a specific point (see Figure 2), the biaxial failure criteria were regarded as not suitable for masonry by previous researcher [10-11]. But this paper reveal that, the sudden decrease is caused by improper FEA boundary conditions defined, but is not because of the biaxial failure criteria itself.

2. THE CONCEPT OF CORRECTORS AND SIMILAR ZONE

To analyse masonry panels using FEA modelling, the panel is normally divided into elements far larger than brick units and a smeared material model is used. To improve the FEA analysis, research in the UoP introduced corrector factors that modify flexural stiffness values at various locations (zones) over the panel [7,9]; A single panel SBO1 [12] was used as a base panel to obtain the corrector factors, the corrector factors at various zones on this panel were derived directly by compares the experimental deflection with that of FEA at the centre of each zone. As there were 36 reading points on the base panel SBO1(See Figure 1) [12], this panel was divided into 36 zones accordingly and 36 corrector factors were obtained thereby as shown in Table 1 [8], because of the symmetry of the panel, only 20 values are presented in the table.

To apply the correctors obtained to more general panels, the concept of zone similarity was introduced [9]. Zone similarity was based on the position of the zones adjacent to similar boundary types, i.e. zones adjacent to similar boundary types tend to have the same corrector values. Once the corrector factors for an unseen panel were obtained, they were used by FEA to determine failure load and failure pattern of the unseen panels. Cellular Automata (CA) was used to match the similar zones between two panels [9].
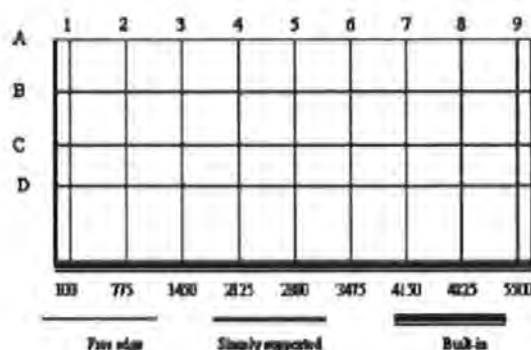
Figure 1   The configuration of SBO1

Table 1
Correctors of Zhou (left half)

	1	2	3	4	5
A	0.637	0.819	1.198	1.262	1.313
B	0.553	0.706	0.935	1.027	1.059
C	0.689	0.759	0.957	1.114	1.218
D	0.53	0.54	0.916	1.268	1.247

3. REFINING CORRECTOR VALUES

In this research the concept of corrector was further investigated to refine the corrector factors. Panel SBO1 shown as Figure 1 was once again used as the base panel as it consists of various boundary types (free at the top, built-in at the bottom and simply supported at the vertical sides).In the present study, more emphasis was placed on the load-deflection relationships on the entire panel rather than failure load only.

Model updating techniques [13] is an effective way to update an existing FEA model. By fitting the experimental results, the values of parameters of the FEA model were adjusted using evolutionary computation techniques. In theory, any optimisation method would be suitable for model updating process, but in this research, the genetic algorithm (GA) was utilised.

3.1 Derive corrector factors by GA and regression

To obtain the suitable corrector factors, at first the GA was used to directly derive the corrector factors at various locations on the panel. Corrector factors at each location were assigned to a GA variable (20 different variables for the symmetrical half model). Corrector factors, identified by the GA, were used to modify the flexural rigidity at each location on the panel. The objective function of the GA was designed as below:

- Deflection error: minimise deviation of the FEA deflection values from the target values over the entire surface of the panel.
- Load error: minimise deviation of the FEA failure load from the target failure load.

At this stage a regression analysis was used to refine corrector factors which were derived by a number of the GA

runs, to obtain a set of corrector factors that represent a best fit for the experimental deflected shape of the panel. The results of this analysis are presented in Table 3.

3.2 Derive corrector factors by GA and constraint function

A careful study of the corrector factors in Table 2 revealed that the flexural rigidities were mainly modified around the panel boundaries with relatively small changes inside the panel. It was therefore necessary to investigate the effect that boundary types may have on the behaviour of the panels. The corrector factors were related directly to the location of zones from different boundaries and the following constraint function was used to define correctors:

$$CR=A\,(1\pm B\,C^{\,x}) \tag{1}$$

Furthermore, gradient error was also added to the objective function above to get results of further smaller error

- Gradient error: minimise deviation of the gradients of the FEA load deflection curve between two adjacent load levels.

Results of this analysis are presented in Table 3 and the corresponding load-deflection relationship is shown in Figure 2.

3.3 Updating the tensile strength of the masonry panel

Using corrector factors presented in Table 3, the load deflection relationship has been improved to be closer to the modified load deflection plots (Figure 2). The load deflection plots demonstrate that the panel failure load was smaller than the experimental failure load. A further study proved that by increasing the tensile strength parallel to the bed joints by about 50%, it would be possible to obtain failure loads closed to the experimental one(see Figure 3).

5. GENERALISATION

In this investigation it is important to test the generality of the concepts presented in this paper. To validate the generality of this finding, corrector values for the base panel (SBO1) summarised in Table 3, are used to derive corrector values for any unseen panels. The cellular automata 'zone similarity' technique is used to estimate corrector values for unseen panels. These corrector factors, plus the tensile strength coefficient obtained in section 3.3, are then used in a non-linear FEA to predict the load deflection, failure load for the unseen panel. The results of this investigation are shown in the case studies below.

5.1 Case study 1

Two masonry panels SBO2 and SBO4 tested also by CHONG [12] are used for validation purposes. These panels had the same dimension and boundary condition as SBO1 has, the only difference is that they have openings with different dimensions and positions on the panel. Their configurations are shown in Figures 4 and 5.

The result of the FEA using corrector derived from Table 3 by CA is shown in Figures 6 and 7. From these figures, it is clear that by using correctors, the failure load and load-deflection relationships are much closer to their experimental results.

5.2 Case study 2

Wall 1 was tested by British Ceramic Research Association in 1995 [16]; it was a single leaf panel 3600 x 2800mm with the top free and the other sides simply supported (see Figure 8). The panel was meshed (12 x 10) elements in the FEA analysis; the corrector factors for this panel were also derived from Table 3 by CA. Figure 5 presents the results of this investigation. From Figure 9 it is clear that the proposed method reasonably predicted the failure load and load deflection relationships. The deviation from the experimental results could be due to the scaling effects which needs further investigation.
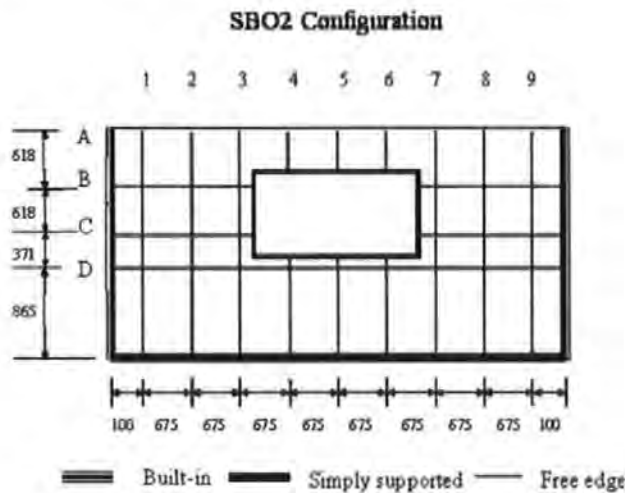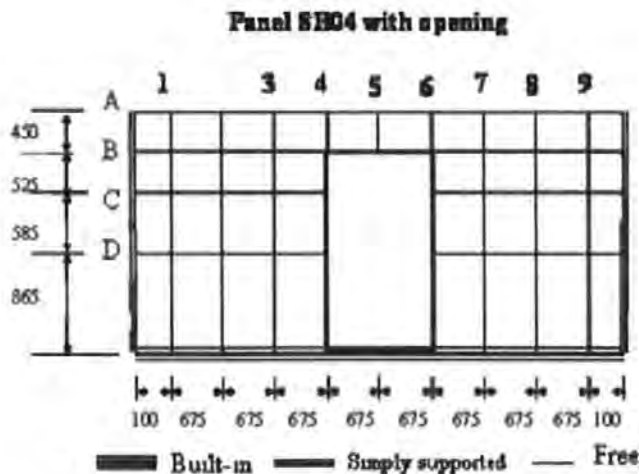
SBO2 Configuration

Figure 4   SBO2 configuration

Panel SBO4 with opening

Figure 5   SBO4 configuration

Table 2
Corrector factors derived by the GA and refined by regression

	1	2	3	4	5
A	0.697	0.981	1.125	1.152	1.153
B	0.704	1.016	1.174	1.204	1.205
C	0.716	1.076	1.258	1.292	1.294
D	0.749	1.237	1.484	1.531	1.533

Table 3
Corrector factors derived by the GA with adding gradient objective function

	1	2	3	4	5
A	1.283	1.278	1.277	1.277	1.277
B	1.187	1.181	1.181	1.181	1.181
C	0.926	0.921	0.920	0.920	0.920
D	0.223	0.218	0.217	0.217	0.217
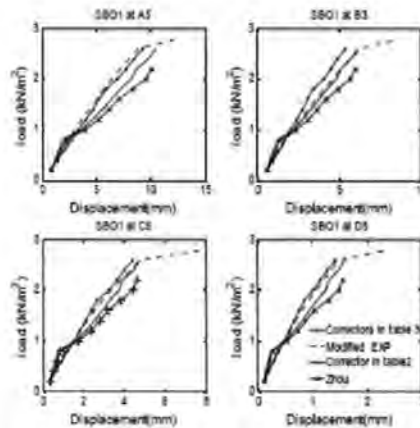
Figure 2 Updating results by correctors
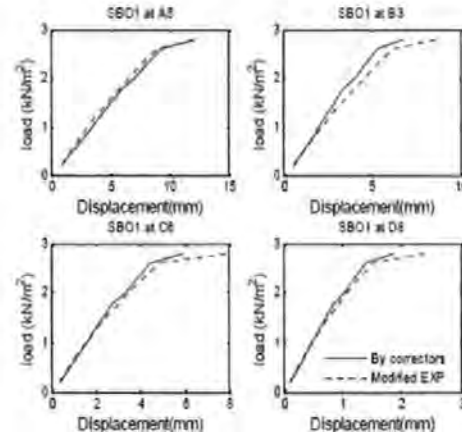
Figure 3 Updating results by correctors and strength coefficients

4. ANALYSES TO THE CORRECTOR FACTORS

Compare Tables 1, 2 and 3, It could be found that, values in Table 1, 2 appear the same pattern, i.e. all values adjacent to the supported edges are smaller than those in the central parts of the panel. But values in Table 3 appear different pattern; compare with the central parts of the panel, values adjacent to the built-in edge are smaller buy those neighbour to the simply supported edges are bigger. In Figure 2, it could be found that, the load deflection curves of using corrector factors as shown in Table 1, 2 have the kinks around $0.8kN/m^2$, whereas that of using Table 3 hasn't the apparent kink (see Figure 2).

In this study, corrector factors are used to modify the flexural stiffness of the FEA, smaller corrector factor (<1) means to decrease the stiffness but bigger corrector factor (>1) means to increase the stiffness. Therefore, from Table 3 it could be deduced that in the real experiments, the built-in bottom edge of the panel was not totally fixed, but appear some rotation or movement; whereas in the simply supported vertical edges the panel appeared to be

constraint to some extent. This means that assuming the bottom edge to be totally fixed and vertical edges ideally simply supported in FEA model do not represent the real boundary conditions. More comprehensive studies of the effects of different boundary types can be found elsewhere [14].

Because of the big difference between the analytical and experimental load deflection relationships after the cracking of the masonry panel (kink in Figure 2), previous researcher questioned the validity of using biaxial failure model to analyse masonry panels [15], but Table 3 indicated that the difference was caused by improper modelling of boundary conditions in the FEA.

Table 3 also indicated that, some models proposed recently, although their analytical load deflection relationship match the experimental one well (no kink), might need some further investigation if the boundary condition effect was not considered, because boundary conditions might have a strong influence to the analysis; and to the common sense, it is impossible that the boundary conditions appear absolutely fixed or free of rotation in the real experiments.
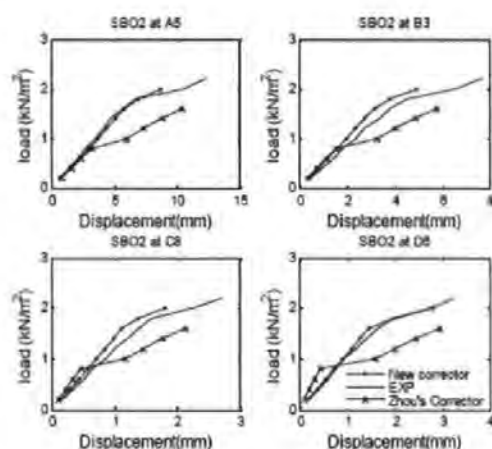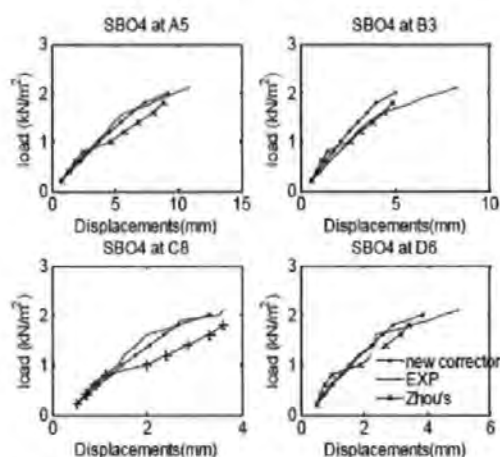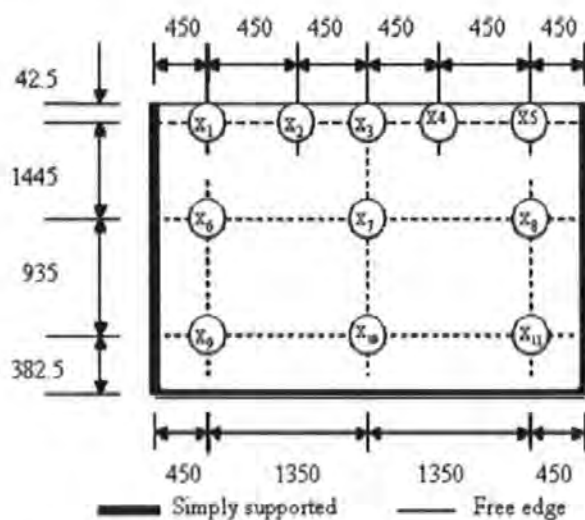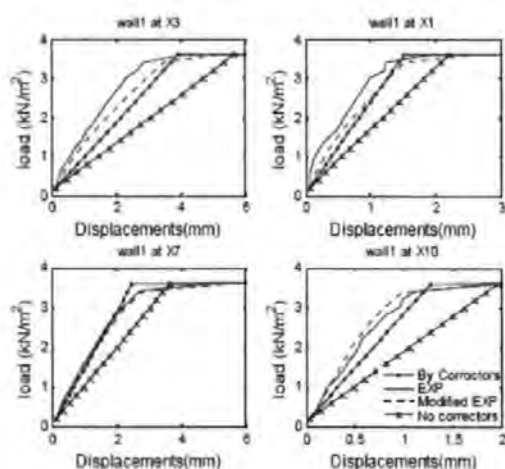
Figure 6   SBO2 validation

Figure 7   SBO4 validation

Figure 8   Wall 1 configuration

Figure 9   Wall 1 validation

6. CONCLUSION

- Corrector factors derived from model updating methods revealed that, the improper modelling of boundary conditions was one of the main causes leading to the inaccuracy of FEA analysis.
- By using corrector values, the prediction of both failure load and load deflection relationships across the entire surface of the masonry panel were improved. This meant that, it is possible to predict the load-deflection behaviour of masonry panels using correctors.
- This paper also shows that the model updating method is an effective way to update the FEA model.

ACKNOWLEDGEMENTS

REFERENCES

1. ESSAWY, A S, DRYSTALE, R G and MIRZA, F A. "Non-linear macroscopic finite element model for masonry walls". Proc. of New Analysis Techniques for Structural Masonry, ASCE Structural Conference 1985, Chicago, Illinois, September 1985.
2. MA, S Y A and MAY, I M. "A complete biaxial stress failure criterion for brick masonry". Proceedings of Masonry Society, 1st International for Brick Masonry 2), pp. 115-117, 1986.
3. LOURENÇO, P B. "An anisotropic macro-model for masonry plates and shells: Implementation and validation", TUD-03-21-22-0-01, TNO-94-NM-R0762, Faculty of Civil Engineering, Delft University of Technology, pp 34 (1997).
4. LOURENCO, P B. "Anisotropic softening model for masonry plates and shells". Journal of Structural Engineering, vol. 126, (9), pp. 1008-1016 September 2000.
5. MASSART, T J, PEERLINGS, R H J and GEERS, M G D. "Mesoscopic modeling of failure and damage-induced anisotropy in brick masonry". European Journal of Mechanics - A/Solids, vol. 23, (5), pp. 719-735 September-October, 2004.
6. ZUCCHINI, A and LOURENÇO, P B. "A micromechanical model for the homogenisation of masonry". Int. J. Solids and Structures, vol. 39, (12), pp. 3233-3255, 2002.
7. RAFIQ, M Y, ZHOU, G and EASTERBROOK, D J. "Analysis of brick wall panels subjected to lateral loading using correctors". Masonry International, vol. 16, (2), pp. 75-82, 2003.
8. ZHOU, G. "Application of stiff/strength corrector and cellular automata in predicting response of laterally loaded masonry panels". PhD Thesis, School of Engineering, University of Plymouth, 2003.
9. ZHOU, G, RAFIQ, M Y, EASTERBROOK, D J and BUGMANN, G. "Application of cellular automata in modelling laterally loaded masonry panel boundary effects," Masonry International, vol. 16 (3), pp. 104-114, 2003.
10. CHONG, V L, SOUTHCOMBE, C and MAY, I M. "The behaviour of laterally loaded masonry panels with openings". The British Masonry Society, 3rd Int. masonry conference, London, October 1992.
11. LAWRENCE, S J and LU, J P. "An investigation of laterally loaded masonry walls with openings". Computer method in structrural masonry. Eds. J Middleton and G N Pande. Books and Journals Int. pp.39-48, 1991.
12. CHONG, V L. "The behaviour of laterally loaded masonry panels with openings". PhD thesis, School of Engineering, University of Plymouth, 1993.
13. FRISWELL, M I and MOTTERSHEAD, J E. "Finite element model updating in structural dynamics". Kluwer Academic Publishers, New York, ISBN 0-7923-3431-0, pp. 286, 1995.
14. SUI, C, RAFIQ, M Y, EASTERBROOK, D, BUGMANN, G and ZHOU, G. "Uniqueness study of updating the fea model of laterally loaded masonry panel by genetic algorithm". 7th International Masonry Conference, London, 30/31 October - 1 November, 2006.
15. CHONG, V L, MAY, I M, SOUTHCOMBE, C and MA, S Y A. "An investigation of the behaviour of laterally loaded masonry panels using non-linear finite element program". The British Masonry Society, 3rd Int. Masonry Conference, London, October 1992.
16. BRITISH CERAMIC RESEARCH ASSOCIATION. "Dynamic and static lateral loading of storey height walls". Structural Masonry Strategy Committee Gust loading of Storey Height Walls, Reference: SM / SMSC.D.1, January, 1995.

Using Timoshenko-Like Formula to Reduce the Experimental Error of Laterally Loaded Masonry Panels

by

C SUI [1], M Y RAFIQ [1], D EASTERBROOK [1], G BUGMANN [1] and G ZHOU [2]
[1] University of Plymouth, UK
[2] Harbin University of Technology (HIT), China

ABSTRACT
Naturally there are errors in laboratory experimental data. These errors are more apparent in data obtained from testing of anisotropic composite materials such as masonry. In this paper a methodology for minimising errors in experimental data is proposed and two types of modifications are used (i) 3D-surface fitting of the experimental data to smoothen irregularities in overall deformed shape of the laterally loaded masonry panel, (ii) load deflection curve fitting to further smoothen irregularities in load deflection curves that are not sufficiently modified by the surface fitting process, which is mainly effective near the panel boundaries. The investigation proved that a Timoshenko-like formula is a better fit for the experimental data.

KEYWORDS: masonry, experimental error, modified deflection, surface fitting.

NOTATION

a : the length of the plate
Ai, Bi, C, Am, Bm, Cm, Dm, A0, A1, A7: the constants.
i : term's number
Lx, Ly: panel's length and height respectively.
M: odd numbers of 1 3 5... in Timoshenko's formula
n: total numbers of terms in the series.
Q: the load level. .
W: the deflection of the panel
X ,Y : co-ordinates of point i.

1. INTRODUCTION

Deflections are very important criteria when evaluating the behaviour of structures. Experimental load deflection relationships have been widely used to verify the validity of FEA models in structural analysis. However, for out-of-plane laterally loaded masonry panels, such as those tested by CHONG [1] in the University of Plymouth (UoP), the deflections appear more irregular over the surface of the panel with substantial error near the panel boundaries. These irregular deflections are unavoidable even under strict laboratory conditions, because it is very hard to provide a perfect support for the masonry panels which have irregular surfaces, even with very careful workmanship; furthermore, masonry is a highly composite material, consisting of two different types of materials (brick

and mortar), that might cause an uneven strain within the panel that results in irregular deflection.

This paper proposes a novel method of reducing the deflection error using mathematical regression techniques, to fit the experimental deflection data by suitable mathematical formulae. In this process, values of some of the parameters in these formulae are determined by regressions to minimise the error between the experimentally recoded data and those resulting from mathematical formulae. One of the formulae used is a TIMOSHENKO [2] like formula, which is derived from solving differential equations that are suitable for deflection of isotropic plates and shells. Although Timoshenko formulae are mainly for isotropic materials such as steel and reinforced concrete, they could be used to approximate the deflected shape of the masonry panels with reasonable accuracy.

2. REASONS FOR FITTING EXPERIMENTAL DATA

CHONG [1] tested 18 full scale laterally loaded masonry wall panels. In this research, one of the tested panels SBO1 is selected as the example, to demonstrate the process of reducing experimental error.

Panel SBO1 is a solid single leaf brick panel, constructed from perforated class B facing clay bricks. This panel is 5600mm long, 2472mm high and 102.5mm thick with the two vertical edges simply supported, the bottom edge built-in and the top edge free. Its configuration is shown in Figure 1. For this panel the experimental deflections are recorded at the intersections of gridline A~D and 1~9. Figures 2 and 3 respectively shows the experimental deflections and the load-deflection curve along gridline C; it is clear that the deflections are irregular over the entire surface particularly near the supported boundaries.

Obviously it is very necessary and meaningful to reduce the error of experimental deflections. Firstly, it is nearly impossible to utilise these irregular experimental data for further analysis, which means some of the nature of the structure could not be revealed. Secondly, evaluating deflection of the panel using numerical modelling techniques, such as finite element analysis (FEA), results in a regular surface. To compare like with like, the experimental results should also be as regular as possible especially for a symmetrical wall panel [3]. This requires assessing the experimental data and reducing these irregularities.
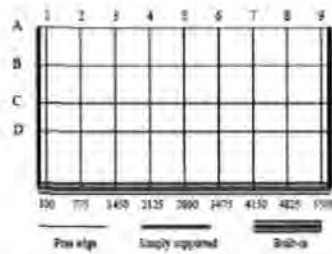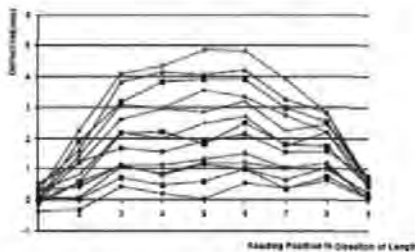
Figure 1 The configuration of SBO1

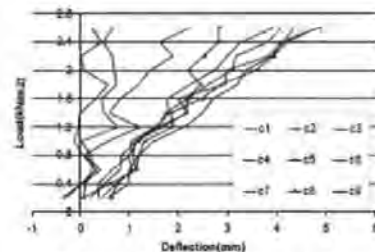**Figure 2 Experimental deflections at different load levels along grid C of SBO1**

Figure 3 Experimental load-deflection curves on grid C of SBO1

3. PROCESS OF REDUCING ERROR IN EXPERIMENTAL DATA

It is reasonable to assume that when the panels are loaded laterally their deflection follows some logical rules of regularity, such as the deflections should be symmetric for the symmetric boundary conditions and steadily increase from the supported boundary to the centre of the panel. Also, the load-deflection curves should increase continuously as the load increases.

To reduce the experimental error for the panel SBO1, with three sides supported and the fourth side free, the following rules should be observed:
1. The experimental deflections should be symmetrical about the central grid line (X = 2800).
2. Deflections should increase from the bottom to the top and from two vertical edges to the centre of the panel.
3. Deflections should increase as the load is increased.

The above rules could be divided into two categories: the rule of deflection surfaces and the rule of load-deflection curves. Accordingly, some mathematical formulae which represent these rules could be used for fitting the deflected surface using regression and two kinds of data fitting may be necessary:
i. Deflection surface-fitting: using regression with various rules to fit the experimental data to a smooth surface.
ii. Load-deflection curve modification: to make sure that load deflection curves at each recording location closely follow the above rules.

It is suggested to always undertake surface fitting first; only when the load-deflection relationships from surface fitting are still disobey the rule 3 above, the load-deflection fitting would be implemented because load-deflection curve fitting could impose a higher risk of changing the characteristics of the panel.

3.1 Applying weights to various recording points

After carefully examine the experimental deflection plots (Figures 2 and 3), it is found that:
1. At lower load levels (below 1.6kN/m2), the deflections appear more irregular than those above (1.8kN/m2 - 2.6kN/m2). The reason for this might be that at the lower load levels, the panel sides are not fully touching the surrounding supports completely. As the load increases the panel moves towards the supports and the full length of the panel edges touch the surrounding supports.
2. At recording points C3-C7, the deflection increases as the load increase, as expected; whereas recording points near the supports such as C1-C2 and C8-C9, sometimes the deflections decrease when load increases. This is not expected.

Therefore, it is justifiable to apply different weightings when performing regression analysis to minimise the error at various recording points and load levels when fitting experimental data to mathematical curves. Figure 4 shows a flowchart of the above process.

Weight values are determined based on deflection surface and load-deflection curves at recorded locations. Part of the surface and load deflection curve which are smoother are considered to be more reliable and higher weight values are assigned to them accordingly. Referring to Figures 2 and 3 it can be seen that the load-deflection curves at locations adjacent to the panel boundaries (e.g. C1-C2 & C8-C9) appear more irregular, this means that the corresponding recording values contain larger errors. Therefore, lower weights are assigned to these points. On the other hand load-deflection curves at points further away from the panel boundaries (e.g. C3-C7) are more regular, higher weights are assigned to these points. Weight values for all location on the panel are shown as in Table 1.

Figure 4 Flow chart of modifying the deflections of the masonry panel

Table 1
Weights dissemination in the panel

Position	1	2	3	4	5	6	7	8	9
A	0.5	1	1	1	1	1	1	1	0.5
B	0.5	0.5	1	1	1	1	1	0.5	0.5
C	0.5	0.5	1	1	1	1	1	0.5	0.5
D	0.5	0.5	0.5	0.5	0.5	0.5	0.5	0.5	0.5

4. REGRESSION FORMULAE FOR SURFACE FITTING

4.1 Formulae for surface fitting

We know that any formula could be expressed by a polynomial or trigonometric series, and Timoshenko's formula is the most typical one to describe the deflections of the panel. After a number of initial trial investigations it is found that these three formulae are appropriate for the detailed investigation. Therefore, based on the rules specified above, three candidate formulae are investigated for 3D deflected surface fitting; they are polynomial, trigonometric and Timoshenko-like formulae and are used as below.

4.1.1 Polynomial formula

$$Let\ F_1 = \sum_{i=1}^{n} AI * (ABS (X / L_x))^i \quad and \quad F_2 = \sum_{i=1}^{n} BI * (Y / L_y)^i$$

Then
$$W = A_0 * F_1 * F_2 + C \tag{1}$$

4.1.2 Trigonometric formula

The following trigonometric formula proved to be a good fit for the data

When
$$F_1 = COS^2 (ABS (\pi / 2 * (X / (0.5 * L_x) * A_1))^{A_2})$$
and
$$F_2 = \sum_{i=1}^{n} BI * (Y / L_y)^i$$
Then
$$W = A0 * F_1 * F_2 + C \tag{2}$$

4.1.3 Timoshenko-like formula

Timoshenko-like formula [2], which is derived from solving differential equations that are suitable for deflection of isotropic plates and shells with various kinds of boundary types. These formulae consist of trigonometric and hyperbolic terms with constants which are directly related to the material properties of the plate, such as modulus E and Poisson ratio. An advantage of a Timoshenko-like formula is that it can satisfy the boundary conditions better than other types of formula. Boundary conditions can be applied as:

$$\frac{\partial^2 w}{\partial x^2}\bigg|_{(y=0,\ L_x)} = 0,\ \frac{\partial w}{\partial y}\bigg|_{y=0} = 0,\ \frac{\partial w}{\partial x}\bigg|_{(x=L_x/2)} = 0.$$

During the fitting process, the original Timoshenko constants in each term are replaced by the new coefficients values of which are determined by regression analysis.

For the panel SBO1, with two vertical edges simply supported the bottom edge built-in and the top edge free and for a uniformly distributed load the following expression is given by Timoshenko:

$$W = (\frac{4qa^4}{\pi^5 D} \sum_{m=1,3,5}^{\infty} m^{-5} sin\frac{m\pi x}{a}) + (\sum_{m=1,3,5}^{\infty} Y_m sin\frac{m\pi x}{a})$$

$$Y_m = \frac{qa^4}{D}(A_m\ cosh\frac{m\pi y}{a} + B_m\frac{m\pi y}{a}sinh\frac{m\pi y}{a} + C_m\ cosh\frac{m\pi y}{a} + D_m\frac{m\pi y}{a}cosh\frac{m\pi y}{a})$$

Our intensive investigation showed that the higher order of m (above 5) lead to over-fitting, which means the formula tries to fit irregular data points too closely, the surface would undulate but does not agree with the rules above. In this investigation It is decided to use m = 1, 3, 5, they resulted in a reasonable fitting of the surface and their results are very similar. When m = 5, the formula then becomes the style below.

$$W = A_9 [sin (\pi x/a) + sin (3\pi x/a)/243 + sin (5\pi x)/3125]$$
$$+ F_1 sin (\pi x/a) + F_2 sin (3\pi x/a) + F_3 sin (5\pi x/a) + A10 \tag{3}$$

Where:
F1= A_0cosh ($\pi y/a$) +A_1 ($\pi y/a$) sinh ($\pi y/a$) +A_2sinh ($\pi y/a$)-A_2 ($\pi y/a$) cosh ($\pi y/a$)
F2= A_3cosh ($3\pi y/a$) +A_4 ($3\pi y/a$) sinh ($3\pi y/a$) +A_5sinh ($3\pi y/a$)-A_5 ($3\pi y/a$) cosh ($3\pi y/a$)
F3= A_6cosh ($5\pi y/a$) +A_7($5\pi y/a$) sinh ($5\pi y/a$) +A_8sinh ($5\pi y/a$)-A_8 ($5y\pi/a$) cosh ($5\pi y/a$)

4.2 Surface fitting by the candidate formulae

The comparisons of the results by surface fitting using the three candidate formulae are shown in Figures 5 and 6. From the comparison of results the following conclusions can be drawn:

1. At the lower load level, the polynomial and trigonometric formulas give a flat curve at the central part of the panel (refer to Figure 5).
2. At the higher load level all three formulae give similar results (refer to Figure 6).

Consequently, the Timoshenko formula is regarded to be a better representation of the experimental results and this formula is selected for further investigation.
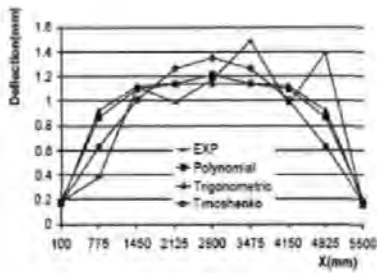
Figure 5   The modified deflections at 0.4kN/m^2 on grid C
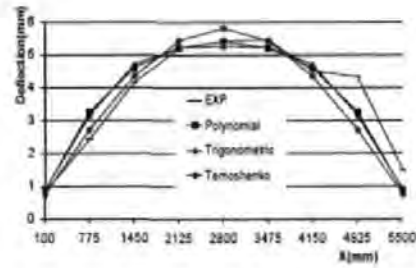
Figure 6   The modified deflection at 1.8kN/m^2 on grid C
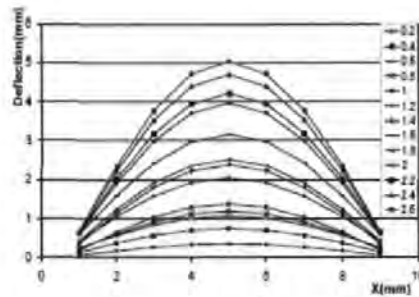
Figure 7   The modified deflections in grid C
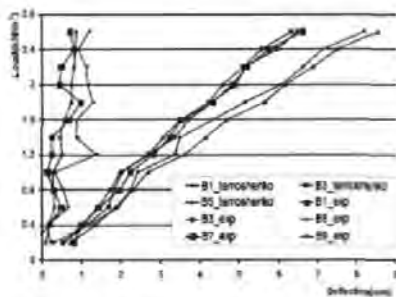
Figure 8   The load-deflection curve after surface modification at B1 B3 B5
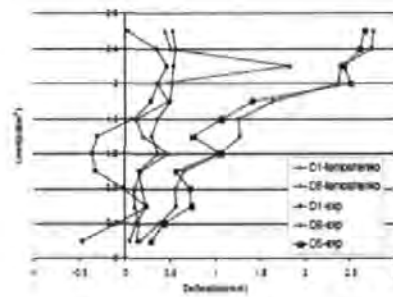
Figure 9   The load-deflection curve after surface modification at D1, D5

4.3 Analysis to the surface fitting modification

Results of the modified deflection curves, using Timoshenko-like formula of Equation (3), are presented in Figure 7, and associated load-deflection curves are presented in Figures 8 and 9. It is clear that all curves are more regular compared with the experimental one as shown in Figure 2, the load-deflections curves are also more regular compared with the experimental one as shown in Figure 3.

However, some of the load-deflection curves, such as those close to the boundaries (e.g. B1 in Figure 8 and D1 in Figure 9) are still not regular. This means that although the Timoshenko-like formula is a good fit for the experimental data, further modification is still necessary.

5. LOAD DEFLECTION MODIFICATION

The need for adjusting load deflection curves to further smoothen the deformed shape is discussed in section 3.

The following section briefly discusses the implementation process.

5.1 Adjusting the weight values at load levels

From Figures 8 and 9 it is clear that surface fitting could not fully eliminate the irregularities, particularly at lower load levels. Moreover, it is clear that load-deflection curves at the lower load levels are more irregular than those at higher load level. When the load levels exceed 1.6kN/m^2, the curves become more regular. Our investigations showed that if a smaller weighting of 0.5 is applied at lower load levels (below 1.6kN/m2) and a larger weighting of 1.0 at load levels above 1.6kN/m^2 it would result in a much smoother deformed shape.

5.2 Select formula for load deflection curves

The rules specified in section 3 are still valid for selecting formula for load-deflection curves. We tried various types of formulae (logarithmic, exponential and polynomial). It is

found that the polynomial formulae give a best fit to the data (see Figure 10). Consequently, a polynomial line expressed in Equation (4) is selected for the load-deflection line modification.

$$W = \sum_{i=0}^{n} Ai * (Qi)^i \qquad (4)$$

Once again our investigation showed that $n > 4$ will lead to over fitting and hence in this investigation $n = 3$ is selected. Figure 11 demonstrates the result of this investigation.

5.3 Determine the number of lines used for load deflection modification

This investigation studies the behaviour of masonry panels subjected to lateral loading within the full linear and non-linear ranges. Therefore, the full load deflection normally consists of two or more lines. Results of this investigation showed that due to the brittle nature of the masonry material a single line would be sufficient to model the load deflection curve.

6. VERIFICATION OF THE MODIFIED DEFORMED SHAPE

In order to check the generality of the proposed method it is necessary to test this on a number of panels for which

laboratory data is available. In this paper the results of two panels (SBO5 and SBO2) are presented.

6.1 Example 1 Panel Sbo5
SBO5 is a panel tested by CHONG [1] with a bituminous dpc built into the first bed joint. This panel has the same configuration and dimension as SBO1 as shown in Figure 1 and both panels have the same loading condition.

Figure 12 is the comparisons between the modified deflections of SBO5 and SBO1. From this Figure it is clear that, although there are very large differences between experimental data of SBO1 and SBO5, their modified load deflection curves amazingly match each other very well. This fact proves that the method proposed in this paper is effective and reliable.

6.2 Example 1 Panel Sbo2
SBO2 is another panel tested by CHONG [1]. This panel is similar to SBO1 but with central opening, its details are shown in Figure 13. As the experimental data have errors a 3D surface fitting, similar to SBO1 is carried out. This modification is presented in Figure 14. Once again Figure 14 demonstrates that little modification is needed for points at the centre of the panel (A5 and D5) while there are a rather large error in experimental data at locations adjacent to panel boundaries (D1 and A2).
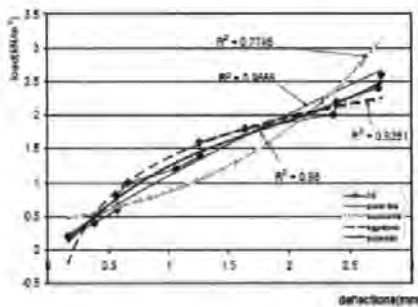
Figure 10   Modification by different kinds of lines formula
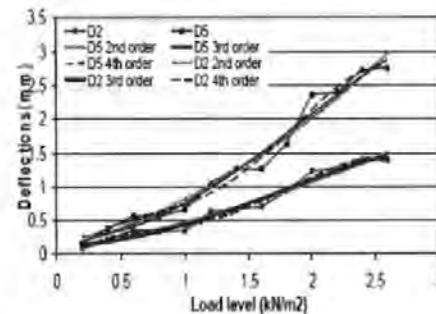
Figure 11   Modification by lines of different order
Notes: (1) the vertical coordinate is deflection;
(2) Lines D2, D5 are deflections by surface modification
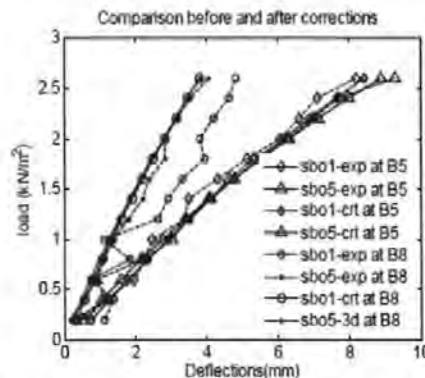
Figure 12   The modified deflections of SBO1 and SBO5 at B8 & B5
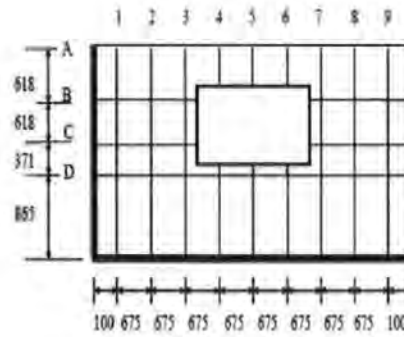
Figure 13   The configuration of SBO2
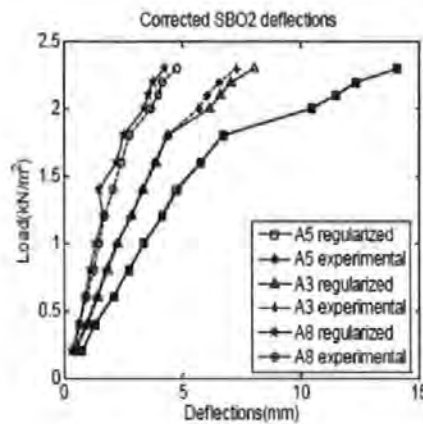
Figure 14   SBO2 modified deflections at A3, A5, and A8

7. CONCLUSION

It is demonstrated that there are unavoidable errors in experimental data. In this paper suitable methodologies are proposed to minimise errors in experimental data. Modifications consist of two elements: (i) 3D-surface fitting and (ii) load deflection curve fitting. 3D-surface modifications play a main role and give a larger contribution to the total modification compared with the load-deflection modification. The load-deflection modification is more effective where near the supported boundaries but makes little change to the regular data far from the supports. The modified deflections can replace the original experimental data for validation of the FEA results. However, because the proposed methodology had only been checked by several masonry panels, it is suggested that further check is given before being widely used.

REFERENCES
1. CHONG, V L. "The behaviour of laterally loaded masonry panels with openings," PhD thesis, *School of Engineering*, University of Plymouth, 1993.
2. TIMOSHENKO. S P. "Theory of plates and shells, "Woinowsky-Krieger.S, McGraw-Hill 1981, ISBN 0-07-085820-9.
3. SUI, C. "Improving predictions of the behaviour of laterally loaded masonry panels using analytical and AI techniques," M. Phil Transfer report, University of Plymouth, 2005.

An Investigation into Numerical Model Updating of Masonry Panels Subjected to Lateral Load

by

C SUI [1], M Y RAFIQ [1], D EASTERBROOK [1], G BUGMANN [1] and G ZHOU [2]
[1] University of Plymouth, UK
[2] Harbin University of Technology (HIT), China

ABSTRACT

The nature of model updating procedure is, in general, a reverse problem solving process. Due to the complexity of the structure and the number of variables involved, a number of models would exist that partially satisfy necessary requirements. Investigation into model updating process shows that due to compensatory effects of large number of variable involved, values of variables obtained during model updating process are different or even sometimes some of the variable values appear to be illogical. It is crucial to identify those variable values that not only improve the prediction of the model, but also do not violate basic established rules. In this paper, an extensive parametric study has been conducted in which an evolutionary computation (EC) technique is used to explore a population of feasible models for masonry wall subjected to lateral load. A non-linear finite elements analysis (FEA) program is called by the objective function of the EC to calculate failure load and load deflection values at various critical locations over the surface of the panel. These values are then compared with the experimental results and the error between the two values are minimised. Domain knowledge is used to select those models with parameter values that do not violate established design rules. The final parameter values are then used to predict failure load, failure pattern and load deflection values of any unseen panel with or without openings.

KEYWORDS

Uniqueness, model updating, optimisation, masonry panel, lateral load.

NOTATION

As, Bs, Cs, Ds, Es	GA variables for the contributions to corrector factors from simply supported edge
Ab, Bb, Cb, Db, Eb	GA variables for the contributions to corrector factors from built-in edge
A_i, B_i, C_i	GA variables for the increasing tendency formula
Ad,Bd,Cd	GA variables for decreasing tendency formula
C_{fx}, C_{fy}	Corrector factors of tensile strength in direction perpendicular and parallel to bad joints
CR	Corrector factors
CRl ,CRr,CRb	the contribution to the corrector factors from left, right and bottom edges of the panel
CRi,CRd	Corrector factors of using decreasing and increasing tendency constraint function
F,D,G	Load, deflection and gradient respectively
Df,De	the deflections of FEA and experiment respectively
E	stiffness matrix of the masonry panel
EXP	Experimental results

Fx.fy	tensile strength of masonry panel at direction perpendicular and parallel to bed joints
Ff,Fe	FEA and experimental loads respectively
j	load level
k	position measurement points on the panel
Wl,Wd,Wg	weights of failure load deformations and gradient respectively
Xs,Xb	distance from centre of the element to the corresponding panel edges of simply supported and built-in
V	Poisson ratio of the masonry panel
δ	objective function which express the discrepancy between analytical and experimental results
δl,δd,δg	discrepancy of the failure load, deformation and the discrepancy respectively

1. INTRODUCTION

In order to predict more accurately the behaviour of masonry panels subjected to lateral load, considerable research has been carried out. In recent years, finite element analysis (FEA) using macro-modelling and micro-modelling plus more advanced model have been studied by many researchers [1-5]. Unfortunately the results obtained from this method do not accurately predict the deformation over the surface of the panel. Conceptual Modelling Research group in the University of Plymouth has introduced a novel method of numerical model updating techniques that use corrector factors [6-7] to modify flexural stiffness to improve the FEA results. The refined corrector factors, derived by model updating techniques have given very good agreements both for failure load and deformation on the entire panel [8].

Model updating techniques introduced in 1990s [9-10] have been widely used for model calibration, parameterization and damage detection and diagnosis. It has become an effective way to analyse and revise the error of the model [11], model updating process aims to minimise the discrepancy between experiment and FEA by changing the values of model parameters, this procedure is normally completed through optimisation. Although most cases of model updating have been applied to vibration frequencies in dynamic test, there are cases of using static deflections [12-15]. This paper presents the example of updating the FEA model using the method for static deflections of laterally loaded masonry panel.

When carrying out a FEA analysis, it is important to consider three kinds of modelling errors [9]: (a) model parameter errors, which would typically include the application of improper boundary conditions and inaccurate assumptions used in order to simplify the model; (b) Model order errors, which arise in the discretization of complex system and can result in a model of insufficient order;

(c) Model structural errors are liable when there is an uncertainty concerning the governing equations – such error might occur typically in the modelling of neurophysiologic process and strongly non-linear behaviour in certain engineering systems. What concerned in this paper is dealing with model parameter errors.

Model updating process is not just an optimisation problem, it required a understand of the exiting model so as to choose proper parameters for updating and to minimise the underlying modelling errors [16]. Once the model is fully understood, it is time for formulating the objective function that aims to minimise the errors between the experimental and the analytical results. This process requires a large amount of trial and exploration.

This paper presents details of the numerical updating of a FEA model of a laterally loaded masonry panel, which includes model analysis, parameter selection, determining the objective function and the updating strategy. Model updating process is generally performed by traditional optimisation method. In this paper an evolutionary computation (EC) method such as the genetic algorithm (GA) is used to minimise modelling errors.

2. MODEL UPDATING STRATERGIES

2.1 Model analysis

The FEA program used in this study was initially created and later modified by MAY and CHONG [17-18]. In this model, masonry was regarded as an isotropic material with different strengths in two directions parallel and perpendicular to the bed joints, but other material properties are kept the same in both directions. In this program, masonry is modelled as tri-linear and as an elastic-plastic material in compression and as a uniaxial material in tension. Linear-elastic-brittle behaviour was assumed for the bending parallel and perpendicular to the bed joints. Biaxial failure criteria to describe the failure and the stress state of the masonry are divided into three kinds in four quadrants: tension-tension, tension-compression (compression-tension) and compression-compression quadrants. Also masonry failure is assumed of two kinds: crushing by compression when the stress reaches its ultimate capacity; or by cracking when the tensile strength reaches the limit of tensile strength. After crushing occurs, the stress of masonry is completely lost. The crack direction is assumed to be normal to the direction

of principal stress; and after cracking occurs; masonry loses its strength normal to the crack direction but still resists stress in the crack direction. Furthermore, a four-nod flat shell element was adopted and 2 x 2 point Gauss-quadrature iteration scheme was employed and a constant stiffness matrix was used during the incremental approach.

It should be mentioned that, in recent years, the assumption of a sudden drop to zero stress level upon violation of the tensile or compressive strength is considered to be unreasonable by some researchers [19-20], so a softening stress-strain relationship is used instead of the assumption in this model; but anyway, the model updating process based on the existing model was still meaningful as the updating procedure would be quite similar.

2.1.1 Analysis to the existing model

The objective of model analysis is to clarify how each parameter affects the analysed results and to find appropriate parameters for updating. Only those parameters which strongly affect the analytical results are selected.

In this study parameters related to the masonry material properties are investigated such as modulus E, Strength fx and fy, Poisson's ratio v. Figures 1 to 4 are load-deflection plots achieved by changing these parameters. Figure 1 shows that the modulus E has a stronger influence on deflections but little influence on the failure load. Figure 2 shows that the tensile strength perpendicular to bed joints fx could dramatically affect the failure load but the shapes of the load deflection relationships are not affected. Nevertheless, Figure 3 shows that the tensile strength parallel to the bed joints fy mainly affects the shape of the load deflection curve, the higher the value of fy is the longer the linear stage (from beginning to kink position) would be, but this has a very small effect on the failure load. Figure 4 shows the influence of the Poisson's ratio v and it is clear that only a small influence to both failure load and deformations is visible.

Consequently, modulus E and tensile strengths fx and fy are selected for the model updating process. As the modulus E mainly affects deflections and tensile strengths fx and fy affect the panel failure load, modulus E is modified at each zone within the panel using corrector factors. This modification is intended to model the combined effects of variations in material and geometric properties and the effects from panel boundary types.
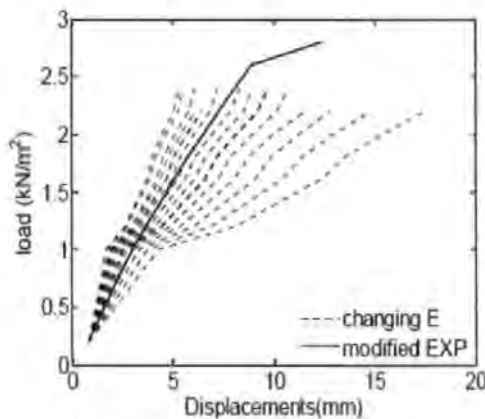

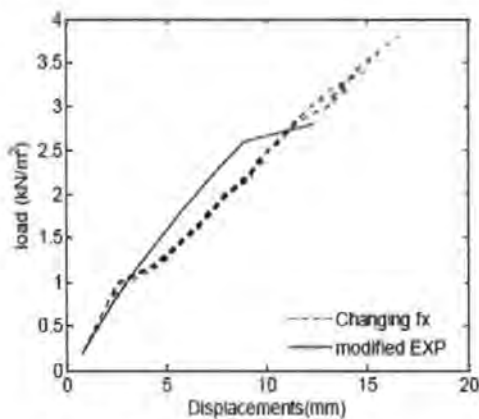**Figure 1   Deflections are decreased by increasing E**

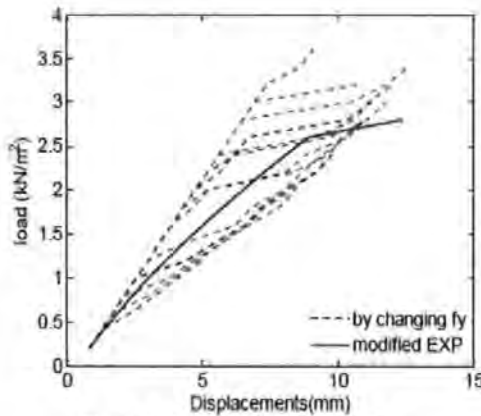**Figure 2   Failure load is increased by increasing fx**

Figure 3   Load level of first crack
is increased by increasing fy
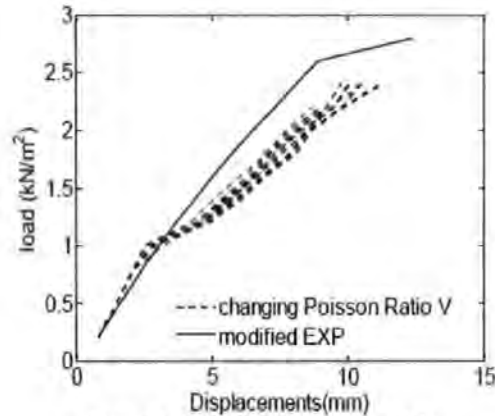
Figure 4   Load-deflection relationships
by changing Poisson ratio V

2.2 Target information

To compare the FEA results with the experimental ones (load deflection and failure load), the results from the base panel (SBO1) is used as the target for comparison purposes. Panel SBO1 was a solid single leaf masonry panel which was tested by CHONG [21]. This panel was constructed using perforated class B facing bricks with dimensions of 5600mm long, 2472mm high and 102.5mm thick. The panel boundary conditions were such that two vertical edges were simply supported, the bottom edge was built-in and the top edge was free. The deflection readings were obtained at 36 locations on the panel. These deflection readings and failure load were used for updating the FEA model.

Because most experimental readings appeared irregular, it is not feasible to directly use these readings. Therefore, some rectification has been carried out by a computational regression method using Timoshenko's formula. More details of the modification can be found elsewhere [22]. Another benefit of this modification is that the formula results in a continuous deformation surface for every load level; this means deflections of the whole panel are available beside the 36 measuring points. This is more convenient for further computational purposes.

2.3 Updating tools

In this study the genetic algorithm (GA) optimisation technique is used to minimise the errors between the experimental and analytical results. The practical obstacle in this study is that there are 20 GA variables which due to the compensatory effects it is difficult to find a unique solution for practical purpose. The genetic algorithm (GA) is an evolutionary optimisation approach, it is more appropriate for solving multi-dimensional problems with non-linear complex models where the global optimum is difficult to locate. Therefore, GA is selected in this study, parameters for GA search is shown as Table 1.

2.3.1 Objective function

The objective function is used to express the error between the analytical and experimental results. Normally, when analysing masonry panels, better agreement is sought for the prediction of: (a) failure load; (b) deformation; (c) failure pattern. As it is hard to express the failure pattern by a function, only failure load and deflections are considered. The error is defined as:

1. Deflection error: deviation of the FEA deflection values from the target values over the entire surface of the panel.
2. Load error: deviation of the FEA failure load from the target failure load.

The objective functions can be expressed as:

$$\delta d = (\frac{1}{m} * \frac{1}{n}(\sum_{k}^{m}\sum_{j=1}^{n}(\frac{Dfj-Dej}{Dej})^2)_k)^{0.5} \qquad (1)$$

$$\delta l = abs(\frac{Ff-Fe}{Fe}) \qquad (2)$$

$$\delta = wl * \delta l + wd * \delta d \qquad (3)$$

It is found that, using Equation (3) as the objective function, the GA becomes stuck to local optima. To obtain the global optimised solution, gradient error, which is defined as the deviation of the gradients of the load deflection curve between two adjacent load levels shown as Equation (4) and (5), is added to the objective function and the objective function becomes as shown in Equation (6)

$$G_i = \frac{F_{i+1} - F_i}{D_{i+1} - D_i} \qquad (4)$$

$$\delta g = (\frac{1}{m} * \frac{1}{n-1}(\sum_{k}^{m}\sum_{j=1}^{n-1}(\frac{Gfj-Gej}{Gej})^2)_k)^{0.5} \qquad (5)$$

$$\delta = wl * \delta l + wd * \delta d + wg * \delta g \qquad (6)$$

In this research, wl = 0.5, wd = 0.2, wg = 0.3 are proved to be adequate.

Table 1
Parameters definition for genetic algorithm search

Parameters kinds	Population (Npop)	Probability of crossover(Pc)	Probability of mutation(Pm)	Number of generations(Ngen)
Range	20-200	0.25-1.0	0.001-0.75	10-3000
Mostly used	80-200	0.5-0.8	0.01-0.03	50-300
This research	200	0.65	0.01	100

Table 2
The updated corrector values for smeared global properties (left half panel)

	1	2	3	4	5
A	0.5	0.5	0.5	0.5	0.5
B	0.5	0.5	0.5	0.5	0.5
C	0.5	0.5	0.5	0.5	0.5
D	0.5	0.5	0.5	0.6	0.5
Cfx=0.554 Cfy=2.943 error=15.73%					

Table 3
Corrector factors derived by the GA (left half panel)

	1	2	3	4	5
A	1.607	1.106	1.132	1.138	1.140
B	1.587	1.086	1.112	1.118	1.119
C	1.526	1.025	1.051	1.057	1.059
D	0.717	0.216	0.242	0.248	0.250
Cfx=1.473 Cfy=1.040 error=0.1543%					

3. UPDATING PROCESS

In the updating process the objective function, discussed in section 2.3.1 is used for all cases and the following design parameters are considered:
- Corrector factors: These take account of variation in flexural stiffness in elements of FEA and also effect of panel boundary types.
- Tensile strength values both parallel and perpendicular to bed joints

3.1 Smeared properties – constant corrector factors
In this case, all elements are assigned with the same values of material properties and tensile strengths. In this case there are only 3 independent parameters, used in the optimisation process. Table 2 and Figure 5 show the updated results. Although they show a good correlation with the experimental results, the updated values of tensile strength parallel to bed joints fy is larger than fx, which obviously not acceptable. From these results it can be concluded that use of smeared properties cannot result in a suitable model.

3.2 Updating corrector factors at each element
3.2.1 Corrector factors as the GA variables
At this stage corrector factors at each element are used as the GA variables (a total 20 GA independent variables for the symmetrical half panel). Tensile strength values parallel and perpendicular to the bed joints are also used as the GA variables.

In this process, although the GA is able to find models that improved the predicted deflected shape of the panel, due to the compensatory effects of many variables it is difficult to identify a suitable model. At this stage a regression analysis is used to refine corrector factors, selected from a number of the GA runs, to obtain a set of corrector factors that represent a best fit for the experimental deflected shape of the panel.

3.2.2 Corrector factors with constraint function
Our investigation of the sensitivity analysis showed that the panel boundary types have a strong influence in the response of the panel to lateral loading. The study also showed that the stiffness of elements adjacent to panel boundaries either increases (simply supported boundary as there is some degree of restrain in the rotation at the panel vertical sides) or decrease (for the built-in support as there is some degree of rotation at the base of the panel). This has been reflected in values of the corrector factors (see Figure 6 for details). The equations defining the corrector factors are given below:

For simply supported edges:
$$CR_s = A_s*\exp(B_s/X_s) + C_s*\exp(D_s/X_s) + E_s \qquad (7)$$

For built-in edge:
$$CR_b = A_b*\exp(B_b/X_b) + C_b*\exp(D_b/X_b) + E_b \qquad (8)$$

As there are two simply supported boundary types, one at each vertical edge of the panel and one built-in boundary at the panel base, the combined effect of these is summed in Equation (9):
$$CR = (CR_s + CR_s + CR_b)/3 \qquad (9)$$
In this representation, there are 10 independent GA variables and the corrector factors obtained are summarised in Table 3.
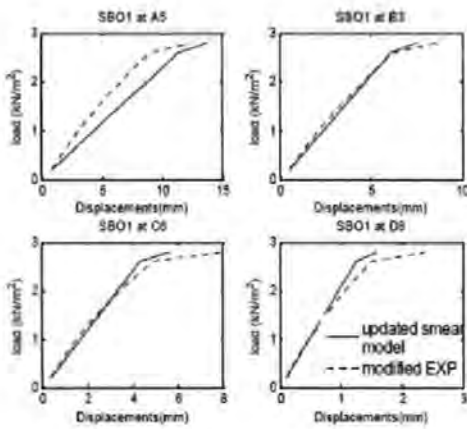
Figure 5 Load-deflection relationships by updating material properties with same value
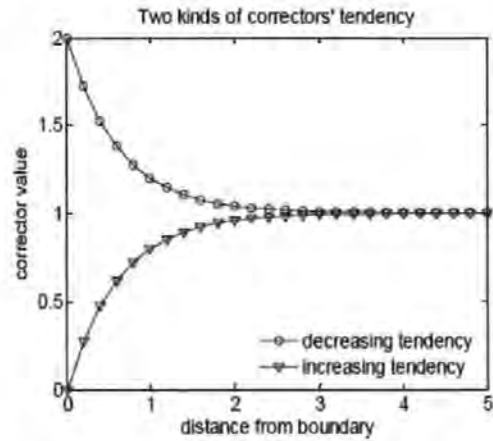
Figure 6 Two kinds of constraint function of expressing boundary effects (or corrector factors)
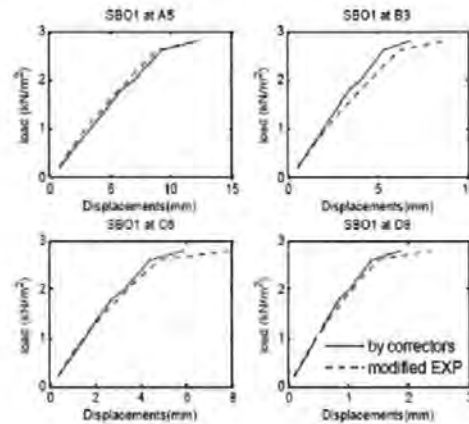
Figure 7 Load-deflection relationships by updating material properties with different values

Table 4
Corrector factors derived by the GA with adding gradient objective function

	1	2	3	4	5
A	1.283	1.278	1.277	1.277	1.277
B	1.187	1.181	1.181	1.181	1.181
C	0.926	0.921	0.920	0.920	0.920
D	0.223	0.218	0.217	0.217	0.217
Cfx=1.473 Cfy=1.040 error=0.1141%					

From Table 3, it can be seen that from row D to row A in each column, corrector factors are increasing but they are decreasing from the vertical supports towards the centre of the panel (from column 1 to 5). Further investigation showed that if Equations (7) and (8) are replaced by Equations (10) and (11) more consistent results are obtained.

$$CR_i = A_i(1 + B_i C_i^{x_i}) \quad (10)$$
$$CR_d = A_d(1 - B_d C_d^{x_d}); \quad (11)$$

In the formulae, When A>0, B>0, 0<C<1, then CR_i represent decreasing tendency and CR_d represent increasing tendency. The updated results by using Equations (10) and (11) are shown in Figure 7 and Table 4.

4. CONCLUSION

Details of an innovative numerical model updating process are introduced in this paper. In this research evolutionary computation techniques are successfully applied to derive corrector factors for use in an FEA model for updating laterally loaded masonry wall panels. These corrector factors modelled the collective effects of variation in material and geometric properties and also the effect of the panel boundary types on the response of masonry wall panels subjected to lateral loading. To cover the whole linear and non-linear range for loading, it is necessary to minimise the error between the gradient of the predicted (FEA) and the target (Experimental) load deflection curves at various load levels. This considerably improved the convergence toward the experimental results.

REFERENCES

1. LOURENCO, P B, BORST, R D and ROTS, J G. "A plane stress softening plasticity model for orthotropic materials," International Journal for Numerical Methods In Engineering, vol. 40, pp. 4033-4057, 1997.
2. MASSART, T J, PEERLINGS, R H J, GEERS, M G D and GOTTCHEINER, S. "Mesoscopic modeling of failure in brick masonry accounting for three-dimensional effects". Engineering Fracture Mechanics, vol. 72 (2005), pp. 1238-1253, 2005.
3. LOURENÇO, P B and ROTS, J G. "Multisurface interface model for analysis of masonry structures". J. Engrg. Mech., vol. 23, (7), pp. 660-668, July 1997.
4. SALERNO, G, BILOTTA, A and PORCO, F. "A finite element with micro-scale effects for the linear analysis of masonry brickwork". Computer Methods in Applied Mechanics and Engineering vol. 190, (34), pp. 4365-4378, 25, May 2001.
5. LEE, J S, PANDE, G N, MIDDLETON, J and KRAU, B. "Numerical modelling of brick masonry panels subject to lateral loadings". Caqwrers & Slrwhwes, vol. Vol. 61, (No. 4), pp. 735-74.5, 1996.
6. RAFIQ, M Y, ZHOU, G and EASTERBROOK, D J. "Analysis of brick wall panels subjected to lateral loading using correctors". Masonry International, vol. 16, (2), pp. 75-82, 2003.
7. ZHOU, G, RAFIQ, M Y, EASTERBROOK, D J and BUGMANN, G. "Application of cellular automata in modelling laterally loaded masonry panel boundary effects". Masonry International, vol. 16 (3), pp. 104-114, 2003.
8. SUI, C, RAFIQ, M Y, EASTERBROOK, D, BUGMANN, G and ZHOU, G. "An investigation into more accurate prediction of the behaviour of masonry panel subjected to lateral loads". 7th International Masonry Conference 30/31 October – 1 November London, 2006.
9. FRISWELL, M I and MOTTERSHEAD, J E. "Finite element model updating in structural dynamics". Kluwer Academic Publishers, New York, ISBN 0-7923-3431-0, pp. 286, 1995.
10. DASCOTTE, E. "Applications of finite element model updating using experimental modal data". Based on an article published in Sound and Vibration / June 1991, 1991.
11. ATALLA, M J. "Model updating using neural networks". PhD Thesis, Virginia Polytechnic Institute and State University pp. 1-146, 1996.
12. SANAYEI, M, IMBARO, G R, MCCLAIN, J A S and BROWN, L C. "Structural model updating using experimental static measurements". Journal of Structural Engineering, vol. 123, (6), pp. 792-798, June 1997.
13. HJELMSTAD, K D and SHIN, S. "Damage detection and assessment of structures from static response". Journal of Engineering Mechanics, vol. 123, (6), pp. 568-576, June 1997.
14. WANG, J and CHEN, L. "Damage detection of frames using the increment of lateral displacement change". Journal of Zhejiang University Science, vol. 6A, (3), pp. 202-212, 2005.
15. SANAYEI, M and ONIPEDE, O. "Damage assessment of structure using static test data". Journal of American Institute of Aeronautics and Astronautics vol. 29, (1174-1179), 1991.
16. JYOTI, K and SINHA, M I F. "Model updating: A tool for reliable modelling, design modification and diagnosis". The Shock and Vibration Digest /, vol. Vol.34, (No.1), pp. 27-35, 2002.
17. MA, S Y A and MAY, I M. "A complete biaxial stress failure criterion for brick masonry". Proceedings of Masonry Sciciety, 1ST International for Brick Masonry 2), pp. 115-117, 1986.
18. CHONG, V L, MAY, I M, SOUTHCOMBE, C and MA, S Y A. "An investigation of the behaviour of laterally loaded masonry panels using non-linear finite element program". The British masonry society, 3rd Int. masonry conference, London, October 1992.
19. LOURENÇO, P B. "An anisotropic macro-model for masonry plates and shells: Implementation and validation". Relatório n° 03.21.1.3.07, Universidade Técnica de Delft, Delft, Países Baixos e Universidade do Minho, Guimarães, 70 pp, 1997.
20. LOURENCO, P B. "Anisotropic softening model for masonry plates and shells". Journal of Structural Engineering, vol. 126, (9), pp. 1008-1016, September 2000.
21. CHONG, V L. "The behaviour of laterally loaded masonry panels with openings". PhD thesis, School of Engineering, University of Plymouth, 1993.
22. SUI, C, RAFIQ, M Y, EASTERBROOK, D, BUGMANN, G and ZHOU, G. "Using timoshenko formula to modify the experimental error of masonry panels". 7th International Masonry Conference, London, 30/31 October - 1 November 2006.

Uniqueness Study to Update FEA Models of Laterally Loaded Masonry Panels by Genetic Algorithm

by

C SUI [1], M Y RAFIQ [1], D EASTERBROOK [1], G BUGMANN [1] and G ZHOU [2]

[1] *University of Plymouth, UK*
[2] *Harbin University of Technology (HIT), China*

ABSTRACT

It is not easy to construct an accurate FEA model for laterally loaded masonry panels. Model updating has been an effective way to improve an existing FEA model, however, model updating is a reverse problem solving process, which means there maybe many solution, some solutions are the local optima which mislead the model to be a wrong physical meaning, or lost the physical meaning. Therefore, the uniqueness study to the solutions is very necessary. In this paper, the uniqueness of the solution of updating a FEA model of laterally loaded masonry panel by genetic algorithm (GA) was studied, so as to clarify whether the obtained solutions reflect the real condition of the structure and could be used to make effective revision to the model. The study is carried out in the following ways: Firstly, compare solutions under all possible permutations of assumed boundary conditions in which the permutation of two kinds of constraint function was used. Secondly, compare solutions under all possible permutations of assumed boundary conditions in which the stiffness close to the supported boundaries are changed. Thirdly, compare the solutions under the condition of changing the mesh sizes. It has been found that the solutions indicate the same physical meaning and reveal the same problem of the existing FEA model; they also make similar revision to the model although their values were different. Consequently, solutions could be regarded as unique and the model updating results by the proposed model updating methodology is credible for improving the existing FEA model.

KEYWORDS

Uniqueness, Model updating, optimisation, masonry panel, FEA, genetic algorithm.

NOTATION

A, B, C   GA variables, as the constants of the constraint formulae
CR   Corrector factors
X   distance from the zone centre to the corresponding edge

1. INTRODUCTION

A FEA model of laterally loaded masonry panel has been successfully updated [1-2] using the experimental results for a solid masonry panel, SBO1, which consists of two vertical edges simply supported and the bottom edge built-in and the top edge free. The flexural stiffness of elements of the FEA mesh was revised by multiplying the corrector factors, as introduced by ZHOU [3]. These corrector factors shown as Table 1 were derived using model updating process with the genetic algorithm (GA). Values in Table 1 indicate that, in a FEA model of SBO1, assuming the bottom edge to be totally fixed and the vertical edges simply supported do not represent the real boundary conditions. In the experiment

the built-in bottom edge of the panel was not totally fixed, but some rotation or movement is expected, whereas the rotation in the simply supported vertical edges appeared to be constrained to some extent.

It is very difficult to find an analytical model which produces results that perfectly match the real behaviour. This situation is worse with masonry due to the highly composite nature of the material constituents of masonry. Model updating techniques are an effective way to verify the suitability of the analytical models. Model updating is a reverse problem solving process, which naturally results in a cluster of good solutions. Sometimes model updating may result in a model that can reasonably simulate the experimental results, but values of some of the parameters may be such that their physical meaning could be lost [4-5]. This paper reports the results of a comprehensive uniqueness study that the proposed methodology can find a practically acceptable solution that closely models the true behaviour of the masonry panels.

Specifically, uniqueness of model updating process can be investigated by the following methods [5-6]: using different numbers of updating parameters; adding some noise to the target information; additional constraint to the parameters to be updated; study the updating results of using different mesh size; directly updating the physical parameters used in the definition of the FEA model.

In this research, the uniqueness study was conducted as follows: (a) investigate the results from different GA runs with different starting points; (b) investigate the effect of all possible boundary conditions; (c) investigate the effect of different FEA mesh sizes; (d) compare the results of using different formulae to derive corrector factors. The main objective of this study was to capture a practically acceptable model that simulates experimental results closely and ensures the values of the parameters are within the acceptable range.

2. DIFFERENT GA RUNS WITH DIFFERENT STARTING POINTS

Due to the interaction and compensatory effects of many variables, it would be difficult to find a unique solution using stochastic search techniques such as the GA.

Many GA process have demonstrated that, by introducing three kinds of discrepancy to the objective function [2], it is possible to capture a cluster of good solutions that improved the quality of the predicted behaviour of the masonry panels. Although the error of each implementation was not exactly the same, they were quite similar. In this process the set of corrector factors derived in each solution appeared to have a similar pattern (refer to Tables 1 and 2 for details). From this study it can be concluded that the set of correctors, captured by the GA (Table 1) are practically acceptable and give a close match with the experimental results, both in load deflection and failure load predictions.

NOTE: In all tables in this paper, Row D (or E) was the zones close to bottom edge, column 1 was zones close to the left edge and column 5 was the middle. Because of symmetry, only the left half of the panel is presented.

Table 1
Corrector factors with bottom edge built-in and vertical edge simply supported [2]

Error = 0.008	1	2	3	4	5
A	1.283	1.278	1.277	1.277	1.277
B	1.187	1.181	1.181	1.181	1.181
C	0.926	0.921	0.920	0.920	0.920
D	0.223	0.218	0.217	0.217	0.217

Table 2
Another corrector factors with bottom edge built-in and vertical edge
simply supported with different GA implementation

Error = 0.102	1	2	3	4	5
A	1.274	1.248	1.247	1.247	1.247
B	1.268	1.242	1.241	1.241	1.241
C	1.196	1.170	1.168	1.168	1.168
D	0.265	0.239	0.238	0.238	0.238

Simply supported edge

Built-in edge
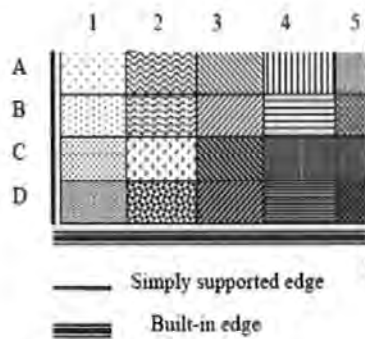
Figure 1 Different corrector factors were assigned to the all zones of the panel

3. INVESTIGATE THE EFFECT OF BOUNDARY CONDITIONS

In this investigation a comprehensive parametric study was conducted in which different combinations of boundary types for both the vertical edges and the base edge of the panel were tried.

3.1 Corrector factors modified at all elements
The model updating results, i.e. corrector factors, as shown in Table 1 were obtained in this way: because in the FEA model, the two vertical sides of the panel were assumed to be simply supported and the base of the panel was assumed to be built-in (the top edge was free). Then two different constraint formulae, one with increasing tendency (to model the degree of rotation at the built-in edge) and another with the decreasing tendency (to model the degree or restraint to rotation in a simply supported edge), were introduced (see Figure 1, Equations (1) and (2) respectively).

$$Cr = A - B \cdot C^z \qquad (1)$$

$$Cr = A + B \cdot C^z \qquad (2)$$

Using Equations (1) and (2), a set of corrector factors, shown in Table 1 was captured which given the smallest error.

The results in Table 1 show that the base of the panel is not fully built-in and there is some degree of rotation at this supporting edge. This has been reflected by the softening of the stiffness of zones adjacent to the built-in support (in this case the base of the panel) which contain 4 elements. Similarly corrector values in Table 1 also show that at simply supported edges there was some degree of restraint to rotation. This was reflected by hardening of the stiffness of elements adjacent to simply supported edges.

To further verify these conclusions, an investigation was conducted to study the effect of changes in boundary types on the response of the panel to lateral loading. In this study the following combinations of boundary types were studied:
1. Left and right edges simply supported with the bottom edge built-in and the top edge free (001-1)
2. Left and right edges built-in with the bottom edge simply supported and the top edge free (110-1)

3. Left and right edges with the bottom edge built-in and the top edge free (111-1)
4. Left and right edges with the bottom edge simply supported and the top edge free (000-1).

Note that the top edge was considered to be free for all cases. It was assumed that the two vertical edges have the same boundary conditions. In the above definitions simply supported, built-in and free edges were expressed as 0 and 1 and -1 respectively as in the brackets.

In order to investigate all possible tendencies of the corrector factors beside defined in Table 1, the following combinations of the Equations (1) and (2) were considered:

1. Left and right edges decreasing tendency but bottom edge increasing tendency (ddi)
2. Left and right edges increasing tendency but bottom edge decreasing tendency (iid)
3. All bottom, left and right edges increasing tendency (iii)
4. All bottom, left and right edges decreasing tendency (ddd)

The increasing and decreasing tendencies above were denoted by i and d respectively as in the brackets.

Consequently there were in total 16 possible cases from all boundary types for updating the FEA model. The corresponding errors between the experimental results and the predicted response using non-linear FEA model for all 16 cases are summarised in Table 3. The model updating details are addressed elsewhere [2].

From the results in Table 3 it can be concluded that the error values along the diagonal of the matrix (Table 3) corresponding to 001-1/ddi, 110-1/iid, 000-1/ddd, and 111-1/iii have the smallest error in each kind of boundary condition. The corresponding updated results for these cases are presented in Tables 1, 4, 5 and 6 respectively. From the four tables it can be seen that the stiffness values for elements adjacent to a built-in boundary are always decreasing and those near the simply supported edges are increasing. This means that all boundaries are neither fully fixed nor totally free of rotation.

Table 3
Discrepancies with different definitions of the boundary
conditions and using different formula combinations

Defined boundary conditions / Constraint functions	ddi	iid	iii	ddd
001-1	0.135	0.217	0.136	0.281
110-1	0.255	0.135	0.148	0.250
111-1	0.221	0.193	0.176	0.261
000-1	0.225	0.223	0.199	0.180

Note: defined boundary conditions, the 4 digits from the left represent
left, right, bottom and top sides respectively, 0 means simply supported,
1 means built-in and -1 means free, then 001-1 means left and right sides simply supported,
bottom built-in and top free. i represent increasing tendency and
d represent decreasing tendency of the constraint function

Table 4
Corrector factors of SBO1 with vertical sides built-in
and bottom edge simply supported (110-1/iid)

Error = 0.135	1	2	3	4	5
A	0.063	0.973	1.480	1.735	1.812
B	0.100	1.010	1.517	1.772	1.849
C	0.179	1.088	1.595	1.850	1.927
D	0.345	1.255	1.762	2.017	2.094

Table 5
Corrector factors of SBO1 with three sides built-in (111-1/iii)

Error = 0.176	1	2	3	4	5
A	0.245	0.431	0.559	0.634	0.659
B	0.243	0.429	0.557	0.632	0.657
C	0.225	0.411	0.538	0.613	0.638
D	0.065	0.251	0.379	0.454	0.479

Table 6
Corrector factors of SBO1 with vertical sides simply
supported and bottom built-in (000-1/ddd)

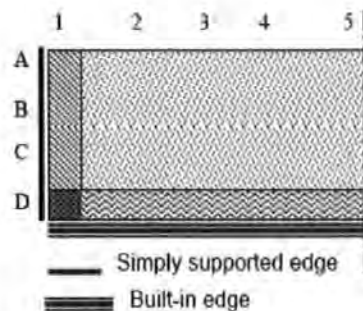| Error = 0.180	1	2	3	4	5
A	1.49	1.483	1.48	1.479	1.479
B	1.495	1.488	1.484	1.483	1.483
C	1.499	1.492	1.489	1.488	1.488
D	1.504	1.497	1.494	1.493	1.493

Figure 2 Different corrector factors were assigned to the zones adjacent to the supported edges

Furthermore, a close examination of Tables 5 and 6 show that, when both the vertical and bottom edges are built-in, the stiffness for elements close to the vertical sides would appear to be much smaller than those close to the bottom edge. On the other hand, when defining all these boundaries as simply supported, the stiffness of elements adjacent to the bottom edge appears to be much larger than those adjacent to the vertical sides, which means the bottom edge tends to be constraint more than the vertical edges.

From the above observations it can be concluded that, when the two vertical sides are defined as simply supported and the base edge is defined as built-in, corrector factors in Table 1 indicated the real problem of the existing FEA model and made proper revision to the FEA model.

3.2 Changing the stiffness only at the supported boundaries

From the investigation in section 3.1, it is also evident that, corrector factors are approximately the same except those adjacent to the supported edges which appear much difference. Therefore it is reasonable to investigate how the corrector factors would be changed if the panel is divided in to 4 zones, and only 4 different corrector factors are used as shown in Figure 2.

In this investigation, all 4 kinds of defined boundary conditions as in section 3.1 were used. The results of this investigation are summarised in Tables 7, 8, 9 and 10. A glance in these tables shows that corrector factors have a similar pattern as those of Tables 1, 4, 5 and 6 respectively described in section 3.1. Compare with the middle part of the panel, corrector factors along the defined built-in boundaries are much smaller but those along the defined simply supported edges are much bigger. Hence the same conclusions on the effects of panel boundaries can be drawn.

4. CHANGING THE MESH SIZE

The above investigation were based on an 18 x 8 grid = 144 FEA mesh size, to correspond to the number of experimental recorded points. To check the updated results, another FEA model using a 20 x 10 grid = 200 mesh was tested. For simplicity only the boundary conditions corresponding to Table 1 and Table 7 was investigated. Corrector factors resulting from this investigation are shown in Tables 11 and 12.

From Table 11 and 12 it can be seen that the corrector factors have the same feature as those in Table 1 and 7 respectively, which means that Table 1 does indicate the practical boundary effects.

Table 7
Corrector factors achieved by only changing values adjacent to
the boundaries (vertical sides simply supported and bottom built-in)

001-1	1	2	3	4	5
A	1.021	1.112	1.112	1.112	1.112
B	1.021	1.112	1.112	1.112	1.112
C	1.021	1.112	1.112	1.112	1.112
D	0.277	0.212	0.212	0.212	0.212

Table 8
Corrector factors achieved by only changing values adjacent to
the boundaries (vertical sides built-in and bottom simply supported)

110-1	1	2	3	4	5
A	0.259	0.763	0.763	0.763	0.763
B	0.259	0.763	0.763	0.763	0.763
C	0.259	0.763	0.763	0.763	0.763
D	0.726	1.213	1.213	1.213	1.213

Table 9
Corrector factors by only changing values adjacent to
the boundaries (with all vertical sides and bottom built-in)

111-1	1	2	3	4	5
A	0.050	1.586	1.586	1.586	1.586
B	0.050	1.586	1.586	1.586	1.586
C	0.050	1.586	1.586	1.586	1.586
D	0.054	0.218	0.218	0.218	0.218

Table 10
Corrector factors by only changing values adjacent to
the boundaries (all vertical sides and bottom simply supported)

000-1	1	2	3	4	5
A	1.695	1.560	1.560	1.560	1.560
B	1.695	1.560	1.560	1.560	1.560
C	1.695	1.560	1.560	1.560	1.560
D	1.283	1.716	1.716	1.716	1.716

Table 11
Corrector factors with 200 elements using constraint function
(bottom edge built-in and vertical edge simply supported)

001-1	1	2	3	4	5
A	1.080	1.013	1.000	0.998	0.997
B	1.072	1.006	0.993	0.991	0.990
C	1.031	0.965	0.952	0.950	0.949
D	0.856	0.790	0.777	0.775	0.774
E	0.231	0.165	0.152	0.149	0.149

Table 12
Changing corrector factors only adjacent to the boundaries
(vertical sides simply supported and bottom built-in with 200 elements)

001-1	1	2	3	4	5
A	1.041	1.006	1.006	1.006	1.006
B	1.041	1.006	1.006	1.006	1.006
C	1.041	1.006	1.006	1.006	1.006
D	1.041	1.006	1.006	1.006	1.006
E	0.396	0.148	0.148	0.148	0.148

5. CONCLUSIONS

As a result of this investigation the following conclusions can be drawn:
- Panel boundary types have a major influence on the corrector values;
- Assumed built-in and simply supported boundary types can not fully define the boundary types in real panels;
- Corrector factors can collectively model the variation in material and geometric properties and also the effects of panel boundaries;
- Larger corrector factor values occur near simply supported edges and smaller values near built-in edges and do not mean that these locations are physically more stiff or less stiff, they rather reflect that the panel boundaries are not defined properly and this adjustment compensates for this modelling error;
- It is also demonstrated that using evolutionary computation techniques, such as genetic algorithms, it is possible to capture a response of the panels that is closely related to the experimental result.

ACKNOWLEDGEMENTS

REFERENCES
1. SUI, C, RAFIQ, M Y, EASTERBROOK, D, BUGMANN, G and ZHOU, G. "An investigation into more accurate prediction of the behaviour of masonry panel subjected to lateral loads". 7th International Masonry Conference, London, 30/31 October – 1 November, 2006.
2. SUI, C, RAFIQ, M Y, EASTERBROOK, D, BUGMANN, G and ZHOU, G. "An investigation into numerical model updating of masonry panels subjected to lateral load". 7th International Masonry Conference, London, 30/31 October - 1 November, 2006.
3. ZHOU, G. "Application of stiff/strength corrector and cellular automata in predicting response of laterally loaded masonry panels". PhD Thesis, *School of Engineering*, University of Plymouth, 2003.
4. JANTER, T and SAS, P. "Uniqueness aspects of model-updating procedures". AIAA IJOURNAL, Vol.28, (3), 1990.
5. DUNN, S A. "Technique for unique optimization of dynamic finite element models". Journal of Aircraft, Vol.36, (6), pp. 919-925, November-December 1999.
6. VISSER, W J. "Updating structural dynamics models using frequency response data". PhD Thesis, Imperial College Of Science, Technology and Medicine University of London, pp. 238, September 1992.

A CA AND ANN TECHNIQUE OF PREDICTING FAILURE LOAD AND FAILURE PATTERN OF LATERALLY LOADED MASONRY PANEL

Guangchun Zhou[1], Yaqub M. Rafiq[2], Chengfei Sui[3] and Lingyan Xie[4]

Abstract

In spite of more than 30 years of research, it is difficult to reliably predict the behaviour of masonry panel subjected to lateral loading. This paper indroduces an innovative technique, which combines the cellular automata (CA) and artificial neural networks (ANN) to predict both failure loads and failure patterns of laterally loaded masonry panels without using conventional techniques.

This paper proposes a new concept, called *generalized panel*, which can project various failure patterns of panels into one panel. In other words, these numerical patterns of the panels are mapped on a generalized panel that symbolizes the failure patterns for the panels having different shapes, sizes and boundary conditions. The data are then transferred as the input for the proposed ANN model. The output from the ANN model is the failure load values of the panels. Finally, the ANN model relates the failure load with the corresponding failure pattern of a panel, and subsequently predicts the failure load of the panel.

KEY WORDS

failure load, failure pattern, artificial neural networks, cellular automata, *generalized panel*, *zone similarity*.

Introduction

In the past numerical analytical tools have been widely used to predict the failure load and the corresponding failure pattern of a panel. The accuracy of numerical analytical models mostly depends on modeling the constitutive relationship for material more accurately. One of the most difficult research subjects is to model the constitutive relationship of masonry and the behaviour of laterally loaded masonry wall panels. This is because masonry is a highly anisotropic composite material.

Researchers have proposed three typical analytical methods. Baker (1982) and Chong (1993) statistically established the smeared material properties for brickwork by testing a

---

[1] Professor. School of Civil Engineering, Harbin Institute of Technology. 202 Haihe Street, Harbin, 150090, China. E-mail: gzhou@hit.edu.cn

[2] Dr. School of Engineering, University of Plymouth. Drake Circus, Plymouth, PL4 8AA, England. E-mail: mrafiq@plymouth.ac.uk

[3] PhD student. School of Engineering, University of Plymouth. Drake Circus, Plymouth, PL4 8AA, England. E-mail: chengfei.sui@plymouth.ac.uk

[4] MSc student. School of Civil Engineering, Harbin Institute of Technology. 202 Haihe Street, Harbin, 150090, China. E-mail: skylar-001@163.com

number of wallets, and applied the cracking criteria related to flexural tensile stress in their finite element analysis (FEA) of laterally loaded masonry panels. Lee et al. (1996) introduced a two-stage of homogenization technique to investigate the elastic-brittle behaviour of masonry panels subjected to lateral loading; one stage for the orthotropic material; and the other for smeared cracking of the material. Lourenco (1997, 2000) proposed an anisotropic softening model so that a process was made for predicting the response of masonry panels subjected to out-of-plane loading. The above three models do not involve modelling variation of masonry properties in local regions within the panel, which considerably affects the accuracy of the existing analytical techniques.

However, the existing analytical techniques on masonry structures, such as the FEA methods based on the above constitutive models, have shown that no mater how accurate the constitutive modes for masonry properties are, they can not predict the failure load and failure pattern of the masonry structure accurately as long as they use global material properties for the whole structure. Lawrence (1991) indicated that "the greatest difficulty with analyzing walls under lateral loading is coping with the high degree of random variation present in masonry materials. ... It is essential to account for this inherent random variation in any theoretical analysis." In other words, it is impossible to make an accurate prediction if the variation of masonry properties in the local working environment of a masonry structure is not included in the analytical techniques. Therefore, some researchers sought the analytical techniques which can quantify the variation of masonry properties at locations within the masonry structure and used the intelligent techniques, such as neural networks and cellular automata, to deal with predicting the response of masonry panels under lateral loading.

Lawrence (Lawrence and Lu 1991) introduced random noise to tensile strengths at various locations on the panel in order to improve the accuracy of the FEA of masonry panels, but in some cases this approach leads to less accurate prediction of cracking load. Mathew et al. (1999) introduced a hybrid system which combines both case-based reasoning and the artificial neural networks (ANN) based analysis to predict the failure load of masonry wall panels under lateral loading. But for some particular sets of parameters involving in structural configurations, boundary conditions and material properties, the trained ANN can not distinguish their differences well and results in that some predicted failure loads have the same value.

Zhou et al (Zhou, 2002; Rafiq et al, 2003) reported that the panel response to lateral loading is influenced by the variation in masonry properties and most importantly by the boundary. They introduced a new concept "the concept of stiffness/strength corrector" to quantify the variation in masonry properties and the effect of panel boundaries. Then they introduced the concept of zone similarity is basically based on the assumption that the corrector values are governed by the relative distances of a zone from similar boundary types. Based on this concept of zone similarity, a technique using Cellular Automata (CA) was developed to establish corrector values for any unseen panels. Rafiq et al (2006) has extended and refined the concept of stiffness/strength corrector to obtain a close match between load-deflection and failure behavior of various panels. Results from a non-linear FEA demonstrated that using corrector values can greatly improve the prediction of both failure load and failure pattern of the panel.

Page 524

Zhou and Rafiq et al (2006) further found that the CA model and corresponding criteria for matching zone similarity can be directly used to predict the failure pattern of unseen panels based on the failure pattern of the base panel.

This paper relates the predicted failure pattern of the corresponding failure load of the panel using a new concept of *generalized panel*. In this approach, the ANN model of the panel is used to predict the failure load of the panel based on the predicted failure pattern, obtained by the above CA model. Thus an artificial intelligent technique (AIT) is implemented to directly predict both the failure load and failure pattern of the panel subject to lateral loading without using any conventional methods such as the FEA.

The CA modelling of boundary effect on zones within a pnel

The CA model properties

Edward (1989) describes CA as discrete space-time models consisting of cells in a lattice network. The "neighborhood" consists of adjacent cells which will influence the behaviour of a particular cell state (Soschinske 1997). Fig. 1 shows a typical 2-D neighborhood cell model developed by von Neumann (Soschinske 1997) and utilised in this paper.
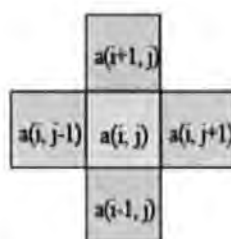
FIG. 2. Cellular Automata Neighbourhoods of von Neumann (1997)

Halpern et al. (1989) formalised the CA transition model in the case of the von Neumann neighbourhood as:

$$a_{i,j}^{(t+1)} = f(a_{i,j}^{(t)}, a_{i,j+1}^{(t)}, a_{i+1,j}^{(t)}, a_{i,j-1}^{(t)}, a_{i-1,j}^{(t)}) \tag{1}$$

where a = cell state value at a given time interval t, i, j = x, y cell coordinates, t = time interval, and f = transition function describing iteration rule.

Rucker and Rudy (1989) summarised the properties of the CA as follows:

Parallel: each cell is updated independent of other cells;

Locality: the state value of a new cell depends on its old cell state value, and the values of its neighbourhood cells at a given time t;

Homogeneity: the same rules are applied to all cells.

Page 525

The CA modelling of boundary effect on zones within a panel

Boundary effect on zones (Zhou and Rafiq et al, 2002, 2003) within panels with similar properties can be suitably described by the CA space properties, parallel, locality and homogeneity. Fig. 3 shows how the boundary effect is modelled using CA:
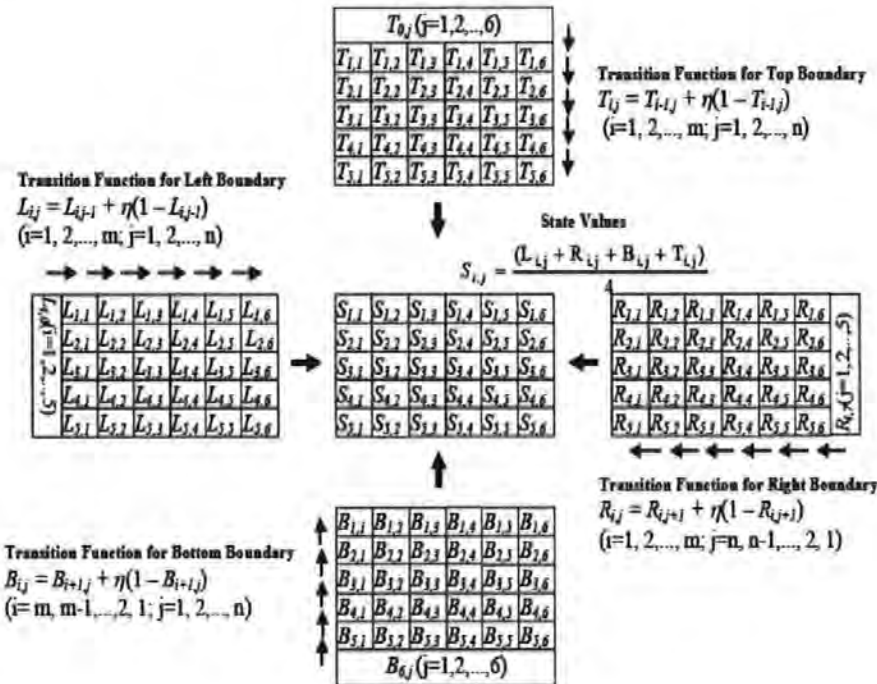
FIG. 3. The CA Model of Boundary Effect on Zones within a Panel

- The panel is divided into a number of zones (cells in a CA model). Boundaries of the panel are described as the specified input initial values of the transition functions which are defined in Eqn (2) below. The position of each cell in the CA model corresponds to the position of a zone within the panel.

- Each cell (zone) receives the boundary effect from its neighborhood cells and in turn propagates the boundary effect to their neighborhood cells. For a two-dimensional panel, the von Neumann model was found to be sufficient for describing the effect of different boundaries from four supports at edges of the panel. Therefore, the CA transition functions, which are defined in Eqn. (2), fully propagate the effect of panel boundaries to individual zones within the panel.

Page 526

$$L_{ij} = L_{ij-1} + \eta(1 - L_{ij-1}) \quad (i = 1, 2,..., M; j = 1, 2,..., N)$$

$$R_{ij} = R_{ij+1} + \eta(1 - R_{ij+1}) \quad (i = 1, 2,..., M; j = N, N-1,..., 2, 1)$$

$$B_{ij} = B_{i+1,j} + \eta(1 - B_{i+1,j}) \quad (i = M, M-1,...,2, 1; j = 1, 2,..., N)$$

$$T_{ij} = T_{i-1,j} + \eta(1 - T_{i-1,j}) \quad (i = 1, 2,..., M; j = 1, 2,..., M)$$

(2)

where M and N are the numbers of columns and rows of divided zones, η is the coefficient of transition, and L, R, B and T are the state values of zones (cells) which are obtained from the propagation of the collective effect from the left, right, bottom and top boundaries respectively.

$L_{i,0}$, $R_{i,N+1}$, $B_{M+1,j}$ and $T_{0,j}$ are the input initial values for the transition functions L_{ij}, R_{ij}, B_{ij} and T_{ij}. These initial values describe different boundary types identified by specific values, for instance, 0.0 defines a free support, 0.2 defines a simple support and 0.4 defines a built-in support. For more details of selecting initial values, refer to Zhou (2002) and Rafiq et al. (2003).

The state value $S_{i,j}$ of every zone within the panel is calculated as the average effect from its four adjacent cells, see Eqn (3), which shows that the state value for each cell is closely related to its four neighbourhoods.

$$S_{i,j} = \frac{(L_{i,j} + R_{i,j} + B_{i,j} + T_{i,j})}{4} \quad (i = 1, 2, ..., M, j = 1, 2, ..., N)$$

(3)

The above proposed CA modelling of boundary effects on zones within the panel reflects the CA properties of parallel, locality and homogeneity. For the property of parallel: the state values of individual cells can be updated independent of other cells/zones to assign unique values to each zone using Eqns (2) and (3). For the property of locality: the new cell/zone state value depends on state values of its neighbouring cells/zones (Eqn 3). For the property of homogeneity: the same rules, Eqns (2) and (3), are applied to all cells/zones within the panel.

criteria for matching zone similarity

The concept of zone similarity (Zhou and Rafiq et al, 2002, 2003) identifies zones within two panels, which are governed by similar boundary types. For this purpose, a criterion needs to be established to match similar zones between a new panel (unseen panel) and a base panel (panel for which the correctors are known) based on the concept of zone similarity. The general criterion for matching zone similarity in the above CA model can be defined as:

Firstly, using the Eqns (4) and (5), calculate state values for all zones within the base panel and the new panel:

$$\left\{S_i^{new}\right\} = \left\{f(B_l, B_r, B_b, B_t; d_{li}, d_{ri}, d_{bi}, d_{ti})\right\}$$

(4)

$$\left\{S_k^{base}\right\} = \left\{f(B_l', B_r', B_b', B_t'; d_{lk}', d_{rk}', d_{bk}', d_{tk}')\right\}$$

(5)

Page 527

where

f is the function relationship.

$\{S_i^{new}\}$ is the state vector related to the zone i on the new panel, which includes the state values of this zone itself and its four neighbourhoods.

$\{S_k^{base}\}$ is the state vector related to the zone k on the base panel, which includes the state values of this zone itself and its four neighbourhoods.

B_l, B_r, B_b, B_t are the boundary type parameters at the left, right, bottom and top edge of the new panel respectively.

B_l', B_r', B_b', B_t' are the boundary type parameters at the left, right, bottom and top edge of the base panel separately.

$d_{li}, d_{ri}, d_{bi}, d_{ti}$ are the distances from the centre of the zone i to the left, right, bottom and top edges of the new panel respectively.

$d_{lk}', d_{rk}', d_{bk}', d_{tk}'$ are the distances from the centre of the zone k to the left, right, bottom and top edges of the base panel respectively.

The equation (6) is used to establish zone similarity between panels

$$S\_Z_j = \overset{MN}{\underset{k=1}{COMPARISON}}\left(\{S_i^{new}\}, \{S_k^{base}\}\right) \tag{6}$$

where S_Z_j is the zone j on the base panel, which is similar to a zone i on a new panel, $MN = M{\times}N$ is the total number of zones on the base panel, M and N represent the numbers of zones in row and column within the base panel, and $COMPARISON$ is the criterion for matching similar zones between a base panel and a new panel.

For laterally loaded masonry wall panels, the Eqns (2) and (3) are proposed as the specific expression of the general Eqns (4) and (5), and the Eqn (7), shown below, is proposed as the specific expression of the general Eqn (6)

$$E_{i,j \to new}^{k,j \to base} = \overset{M,N}{\underset{m=1,n=1}{MIN}}\left(\left|S_{i,j}^{new} - S_{m,n}^{base}\right| + \left|S_{i,j-1}^{new} - S_{m,n-1}^{base}\right| + \left|S_{i,j+1}^{new} - S_{m,n+1}^{base}\right| + \left|S_{i-1,j}^{new} - S_{m-1,n}^{base}\right| + \left|S_{i+1,j}^{new} - S_{m+1,n}^{base}\right|\right)$$

(7)

where $E_{i,j \to new}^{k,j \to base}$ is the minimum error of $M{\times}N$ errors in Eqn. (7), m and n represent the position of a zone on the base panel, i and j represent the position of a zone on the new panel.

Eqn (7) is used to compare the state values of a zone itself and its four neighbourhoods in the new panel with every zone and its four neighbourhood zones on the base panel. An

Page 528

error value is calculated for each zone by Eqn (7). The zone with the minimum error value on the base panel is defined as the sole similar zone to the zone on the new panel.

Predicting failure pattern of panel using the above concept and criteria

The CA model of the panel, which is described by the Eqns. (2) and (3), and the criteria for matching zone similarity has been used to directly (without using FEA) match the failure pattern of the base panel to a new panel using Eqn (7). This technique includes three steps:

The first step: Establish the CA models of the base panel and the new panel/unseen panel as Fig 3. Eqns (2) and (3) are used to calculate state values of all zones/cells within the base panel and the new panel. Cells in the CA model of the panel are set up to correspond to the mesh division and Gauss points based on the FEA mesh.

The second step: Each zone on the new panel is matched with its similar zone on the base panel using Eqn (7), the zone similarity rule.

The third step: The failure pattern on the CA zone/cell mesh of the base panel is figured based on the failure patterns observed in the lab experiment of the standard experimental panels. Then this cracked pattern is matched on the new panel: if a zone/cell on the base panel is cracked, the corresponding similar zone on the new panel is also assumed to be cracked;

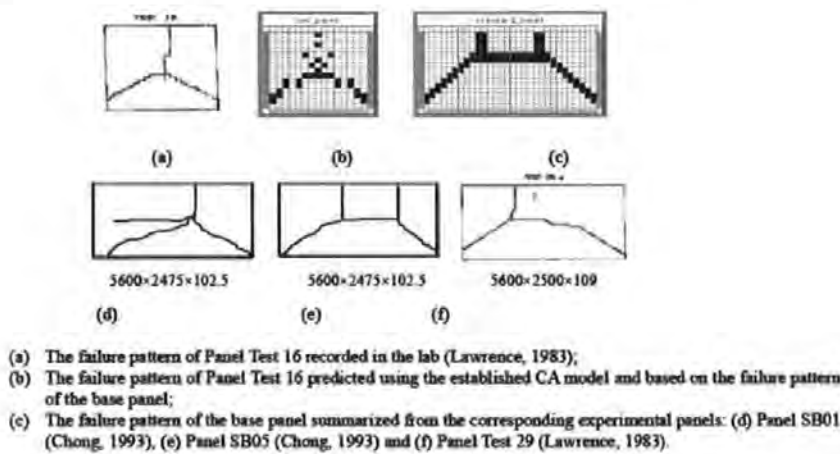Fig. 4 shows an example that successfully verifies the above procedure.

(a)   (b)   (c)

5600×2475×102.5   5600×2475×102.5   5600×2500×109

(d)   (e)   (f)

(a) The failure pattern of Panel Test 16 recorded in the lab (Lawrence, 1983);
(b) The failure pattern of Panel Test 16 predicted using the established CA model and based on the failure pattern of the base panel;
(c) The failure pattern of the base panel summarized from the corresponding experimental panels: (d) Panel SB01 (Chong, 1993), (e) Panel SB05 (Chong, 1993) and (f) Panel Test 29 (Lawrence, 1983).

FIG. 4. An Example of Predicting the Failure Pattern of the Panel

Page 529

concept of generalizated panel

The above technique has demonstrated that it is possilbe to directly predict the failure pattern of a laterally loaded masonry panel using the CA model and the exsiting lab records of a few standard panels. However, the predicted failure pattern does not relate the corresponding failure load which is the most important parameter for the design. The conventional methods are very difficult to deal with such a complex and highly nonlinear realtionship between the failure pattern and the failure load of the panel.

Because artificial neural networks (ANN) are suitable for complex nonlinear problems involving in a number of parameters and variables, this paper develops a new concept, called *generalized panel*, in order to establish an ANN model to express the relationship between the failure pattern and the corresponding failure load of the panel.

The predicted failure patterns of panels using the CA model can have different mesh sizes. This raises an issue for application of ANN, as the number of cells in input layer for an ANN model, which take their data from the CA model, must be a fixed size.

The concept of generalized panel is to map the failure patterns of panels predicted using the CA technique and expressed with the numerical patterns into a fixed CA mesh which can form the input data for the ANN model. This mapping satisfies the criteria for matching similar zones between the new panels and the generalized panel. In other words, if a zone/cell on the new panel is cracked, the corresponding similar zone on the generalized panel is also assumed to be cracked. In this process the value of a cracked zone/cell is set to 1, and to 0 if uncracked. Since the failure patterns of panels with different dimensions projected on the generalized panel may be the same, this paper multiplies the failure pattern projected on the generalized panel by a dimensionless factor (between 0 and 1) which considers the aspect ratio and the length of the panel, that is, the **dimensionless factor = the aspect ratio** ✕ **the length/the maximum length**. An example is shown in Fig. 5.


(a)   (b)
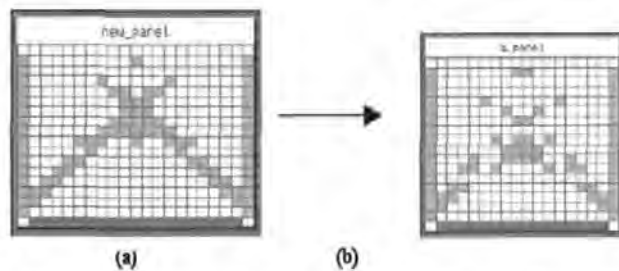
(a) The failure pattern predicted using the established CA model and based on the failure pattern of the base panel;
(b) The failure pattern projected on the generalized panel;

FIG. 5. An Example of Projecting the Predicted Failure Pattern into the Generalized Panel

In this research a generalized panel is defined by a panel which is divided to 16✕16 mesh. This process is applied to re-mesh all panels to a 16✕16 mesh and map the correct failure patterns into this mesh, regardless of these panel sizes.

The ANN and CA model of predicting failure load and failure pattern of panel

Fig. 6 gives out the ANN model used to predict the failure load of a new panel.
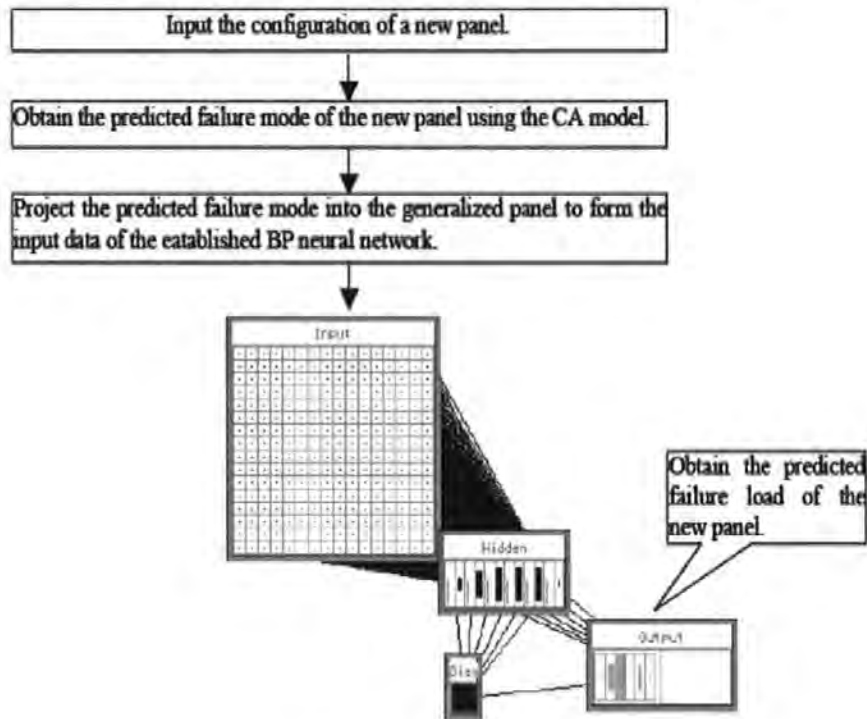
FIG. 6. The Structure of the Established BP Neural Networks

Specification on the BP neural network

The specification on the BP net shown in Fig. 6 is as follows:

Each set in the training and test data for the BP net consists of two parts, input and output. The input is the failure patterns of the panels obtained using the CA model, and the output is the failure loads of the panels. from the lab or the FEA using the stiffness/strength correctors if the corresponding lab record is not available. Failure loads for whole set of panels having various dimensions are obtained using the nonlinear FEA software and correctors. Failure loads for some panels tested in the laboratory by Chong (1993) are also added to this data. The data are used to train the neural net to learn the failure loads of these panels. The train NN is then applied to predict the failure load of the unseen panels.

The choice of the hidden layer of a BP net is usually based on the experience and the comparison of training results to a few different hidden layers with consideration on the learning rate and momentum. This paper deploys 1 hidden layer with 6 cells after verifying 1, 2 and 3 hidden layers with 6, 12 and 18 cells respectively. The learning rate is 0.6 and the momentum is 0.9.. The corresponding training error is 0.035 and the testing error is 0.068

using the trainig and test data established in this research. The other traing and testing errors are more than 0.0367 and 0.1077. Fig. 7 shows the training result of the established BP neural network (Fig. 6).
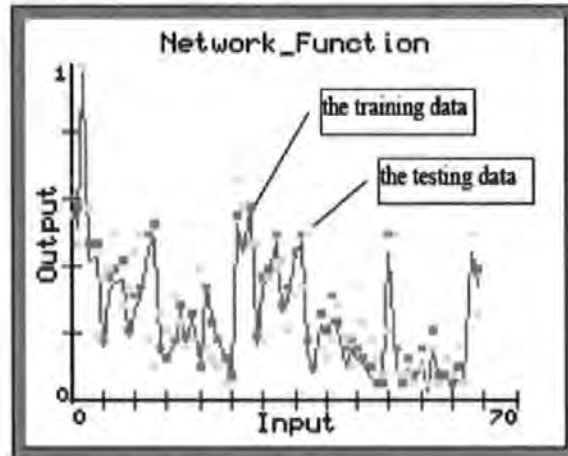

FIG. 7. The training result of the established BP neural network

The results predicted using the BP neural network

The Table 1 shows a group of results predicted using the trained BP neural net proposed in Fig. 6.

Table 1. The predicted result of the lab panels

The sizes of the panels tested in the lab (all panels are supported except for their free top edges)	The lab failure loads (kN/m^2)	The predicted failure loads using the proposed BP net (kN/m^2)	Errors
2500×2500	7.8	7.736	0.82 %
3750×2500	3.4	3.48	2.35 %
5000×2500	2.7	2.796	3.56 %
5600×2475	2.8	3.024	8%
6000×2500	2.3	2.416	5.04 %

It can be seen: Although the BP net gives outresults in the non- a less conservative prediction, the errors are in the range of allowance; this means the AI technique can replace the conventional techniques to directly predict the failure loads and failure patterns of panels. The table does not list the FEA failure loads for comparison as the author did not obtain the details of the panels enough for the FEA. However, when compared with the existing FEA

Page 532

results of laterally loaded masonry panels (Chong, 1993), it can confidently comment that the BP net can predict the failure load of the panel more accurately than does the FEA technique.

Conclusions

1. The new concept of *gegeralized panel* provides a functional model which can effectively transform a number of numerial patterns with different configurations into a unified numerical format which can be used as the input data of an analytical technique, particularly the AI techniques such as ANN.
2. The proposed ANN model can replace the conventional techniques such as the FEA to predict the failure load of the panel more accurately.
3. The technique developed in this paper can be used as an artificial experimental environment that can replace some of the physical tests for masonry panels, which could be very expensive.

Acknowledgments

References

Baker, L.R. (1982). "A Principal Stress Failure Criterion for Brickwork in Bi-Axial Bending". Proc. 6th IBMaC, Rome.

Chong, V.L. (1993). The Behaviour of Laterally Loaded Masonry Panels with Openings. Thesis (PhD). University of Plymouth, UK.

Edgell G. *The experimental results of laterally loaded masonry wall panels*. CERAM Building Technology.

Halpern, P. Sticks AND Stones (1989): A Guide to Structurally Dynamic Cellular Automata. *American Journal of Physics Teachers*, 57 (5).

Lawrence, S. J. (1983). "Behaviour of Brick Masonry Walls under Lateral Loading". Vols 1 and 2. Thesis (Ph.D.), University of OtherSouth Wales, Australia.

Lawrence, S.J. and Lu, J.P. (1991). "An Elastic Analysis of Laterally Loaded Masonry Walls with Openings". International Symposium on Computer Methods in Structural Masonry. Swansea, UK.

Lee, J. S., Pande, G. N., Middleton, J. and Kralj. (1996). "Numerical Modelling of Brick Masonry Panels Subject to Lateral Loadings". *Computer and Structures*, Vol. 61, No. 4, 735-745.

Lourenco, P. B.(1997). "An Anisotropic Macro-Model for Masonry Plates and Shells: Implementation and Validtion." *Rep. 03.21.1.3.07*. University of Technology, Delft, The Netherlands.

Lourenco, P. B.(2000). "Anisotropic Softening Model for Masonry Plates and Shells". *Journal of Structural Engineering*, ASCE. Vol. 126, No. 9, 1008-1016.

Mathew, A., Kumar, B., Sinha, B. P. and Redreschi, R. F. (1999). "Analysis of Masonry Panel under Biaxial Bending Using ANNs and CBR". *Journal of Computing in Civil Engineering*. Vol. 13, No. 3. University of Edinburgh, UK.

Rafiq, M. Y., Zhou, G. C. Bugmann, G. and Easterbrook, D. (2003). "Analysis of Brickwork Wall Panels Subjected to Lateral Loading Using Correctors". *Journal of Masonry International*, pp. 75-82, Vol 16, No 2, 2003.

Yaqub Rafiq, Chengfei Sui, Dave Easterbrook and Guido Bugmann (2006), "Prediction of the behaviour of masonry wall panels using Evolutionary Computation and Cellular Automata", *accepted in the14th EG-ICE workshop, Ascona, Switzerland, June.*

Rucker and Rudy. (1989). *CA Lab (Exploring Cellular Automata) – Rudy Rucker's Cellular Automata Laboratory*. Autodesk Inc., Sausalito, CA.

Soschinske, K. A. (1997). *Cellular Automata Simulation of Resin Flow Through a Fiber Reinforcement*. UMI Dissertation Service.

Zhou, G. C. (2002). "Application of Stiffness/Strength Corrector and Cellular Automata in Predicting Response of Laterally Loaded Masonry Panels". Thesis (PhD), University of Plymouth, UK.

Zhou, G. C., Rafiq, M. Y. and Easterbrook, (2002). "A Different Approach to the Analysis of Brickwork Wall Panels Subjected to Lateral Loading". *6th International Masonry Conference*, London, UK.

Zhou, G. C., Rafiq, M. Y. and Easterbrook, D. (2002). "Application of Cellular Automata in Analysing Laterally Loaded Masonry Panels". *6th International Masonry Conference*, London, UK.

Zhou,G. C., Rafiq M. Y. Easterbrook, D. J., and Bugmann, G. (2003). "Application of cellular automata in modelling laterally loaded masonry panel boundary effects", Masonry International. Vol 16 No 3, pp 104-114. ISSN 0950-2289

Zhou,G. C., Rafiq M. Y., Bugmann, G. and Easterbrook, D. J. (2006). "A Cellular Automata Model for Predicting Failure Pattern of Laterally loaded Masonry Wall Panel", accepted by Journal of Computin in Civol Engineering.

Page 534

Prediction of the Behaviour of Masonry Wall Panels Using Evolutionary Computation and Cellular Automata

Yaqub Rafiq, Chengfei Sui, Dave Easterbrook, and Guido Bugmann

University of Plymouth, Drake Circus, Plymouth, PL4 8AA, UK
{mrafiq, csui, deasterbrook, gbugmann}@plymouth.ac.uk

Abstract. This paper introduces methodologies that not only predict the failure load and failure pattern of masonry panels subjected to lateral loadings more accurately, but also closely matches deflection at various locations over the surface of the panel with their experimental results. In this research, Evolutionary Computation is used to model variations in material and geometric properties and also the effects of the boundary types on the behaviour of the panel within linear and non-linear ranges. A cellular automata model is used that utilises a zone similarity concept to map the failure behaviour of a single full scale panel *'the base panel'*, tested in the laboratory, to estimate variations in material and geometric properties and also boundary effects for any unseen panels.

1 Introduction

Due to the highly composite and anisotropic material properties of masonry, it has been difficult to accurately predict the behaviour of masonry panels. The research presented in this paper proposes a numerical model updating technique that studies the behaviour of masonry panels subjected to lateral loading within the full linear and non-linear ranges. The method uses evolutionary computation (EC) techniques to model variations in geometric and material properties over the entire surface of the panel. The EC search produces factors *'the corrector factors'*, which reflect the collective effects of the above mentioned variations. These factors are then used to vary the value of flexure rigidity at various locations over the entire surface of the panel. The modified flexure rigidity are then used in a specialised non-linear finite element analysis (FEA) program to predict the failure load, failure pattern and load deflection relationships over the full linear and non-linear ranges. The EC exploration also includes the effect that boundary types may have on the response of panels to lateral loading. Results obtained from the non-linear FEA are compared with the experimental results from a full scale panel tested in the laboratory. Finally a cellular automata (CA) is used to map information obtained from the single full scale panel 'base panel'[1] to an 'unseen panel'[2] for which an estimate in variations of material and geometric properties and boundary effects is produced. A non-linear FEA is then used to predict the failure behaviour of these unseen panels.

---

[1] The base panel is a panel for which displacement values are known at various load levels and locations over the surface of the panel and for which failure load and failure pattern are also known.

[2] The unseen panel is a panel for which the above parameters are normally not known.

Prediction of the Behaviour of Masonry Wall Panels Using EC and Cellular Automata   535

The generality of the methodologies proposed in this paper was tested on several *'unseen panels'* with and without openings and the results were found to have a reasonable match with their experimental results. A sample of this study is presented later in this paper.

2 Modelling and Measurement Error

Robert-Nicoud et al. [1] define modelling error $|e_{mod}|$ as the difference between the predicted response of a given model and that of an ideal model representing the real behaviour accurately. Raphael and Smith [2] categorised the modelling error into three components, e_1, e_2 and e_3. The component e_1 is the error due to the discrepancy between the behaviour of the mathematical model and that of the real structure. The component e_2 is introduced during the numerical computation of the solution to the partial differential equations representing the mathematical model. The component e_3 is the error due to the assumptions that are made during the simulation of the numerical model.

For masonry wall panels, assumptions regarding the choice of boundary conditions are very difficult to justify. This is because the true nature of the panel boundaries either for a wall tested in the laboratory or real structures does not comply with the known boundary types (fixed, simply supported etc.). Hence the error resulting from the use of incorrect boundary types would be relatively large.

Another factor that greatly affects the behaviour of masonry wall panels is the existence of a large error due to the component e_2 [2] introduced during the numerical computation process. This error is mainly due to the uncertainty in modelling the material and geometric properties of highly composite anisotropic material such as masonry. Yet, there is not an agreed material model for masonry to represent the true anisotropic nature of this material. There are very few commercial packages for modelling masonry structures. Adding to this error is the modelling complexity due to the propagation of cracks over the surface and along the depth of the masonry panel, when performing a non-linear FEA.

The value of e_1 for steel and reinforced concrete structures may be reduced through the use of more precise mathematical models [2]. However, due to the extremely complex nature of masonry material, the applicability of this approach in practice would be almost impossible. Another reason for ambiguity in this error is the lack of sufficient laboratory test data and the high cost of these tests for masonry wall panels. The majority of tests performed on masonry wall panels only report the failure load of the panel, as this is the major design requirement, and the failure pattern, which is the crack pattern observed during the laboratory tests. Recording load and deflection information is generally limited to a single location, the location of maximum deflection, over the entire surface of the panel. This makes it extremely difficult to understand the true behaviour and the boundary effects on the response of masonry wall panels. One of the mostly cited published data available is the data from 18 full scale masonry wall panels tested in the University of Plymouth (UoP) by Chong [3] that reports load deflection data at 36 locations over the surface of the panel. These data are used in this research.

2.1 Error Due to Incorrect Support Types (University of Plymouth Test Panels)

The panel's vertical sides were supported on a steel angle connected to the test frame abutment to simulate a simply supported support type, and the base of the wall was enclosed in a steel channel packed with bed joint mortar at both sides (refer to Fig.1 for support details). It was assumed that a combined effect of the support details and the self weight of the wall might provide sufficient restraint to the base of the panel to simulate a fixed support type.
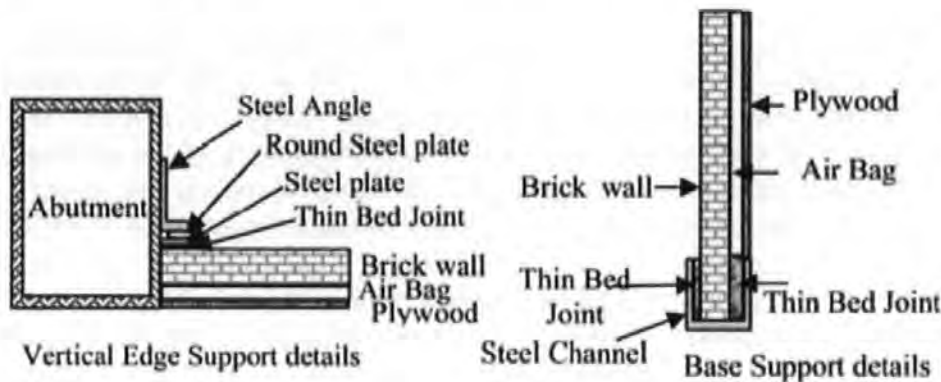

Fig. 1. Test panel support details

From Fig. 1, one can argue that the vertical edges of the panel are not truly simply supported and there is some degree for restrain to rotation. Similarly the base of the panel is by no means fully fixed and allows some degree of rotation. Due to the flexible nature of the edge support, some degree of movement perpendicular to the plane of the wall was observed at the right hand support.

2.2 Error Due to Applied Loads and Deflection Measurements

The load was applied to the wall by means of an air bag and it was assumed to be uniformly distributed over the entire surface of the panel. This assumption may be true when the air bag is fully inflated, but not at the lower load levels.

Fig. 2 shows the location of the measurement points (36 points in total) on the face of the base panel. This panel was a solid single leaf clay brick masonry wall panel. Linear Variable Differential Transformers (LVDTs) were placed at each gridline intersection to measure the wall movement perpendicular to the plane of the wall. Due to the unevenness of the surface, inherent to masonry panels, irregularities were observed in the deformed shape of the panel surface, as shown in Figs. 2(b) and 3. The reason for these irregularities could be the slippage of the LVDTs from their intended location and/or inaccuracy in the LVDT readings.

Controlling the load levels at each load increment and maintaining a uniform load over the entire surface of the panel by means of the airbag is another source of error that needs to be considered.
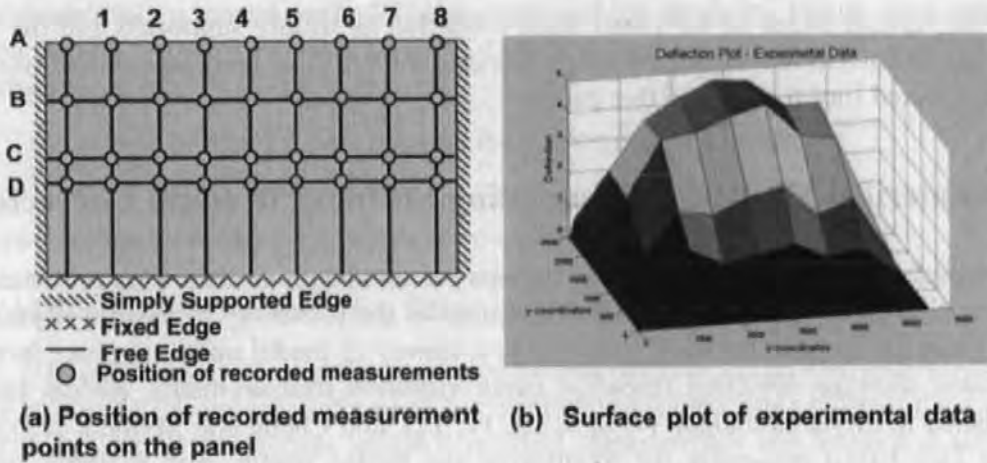
Prediction of the Behaviour of Masonry Wall Panels Using EC and Cellular Automata   537

(a) Position of recorded measurement points on the panel

(b) Surface plot of experimental data

Fig. 2. Position of recorded measurement points and 3D deformed shape of panel SBO1

(a) Deflection at various load levels

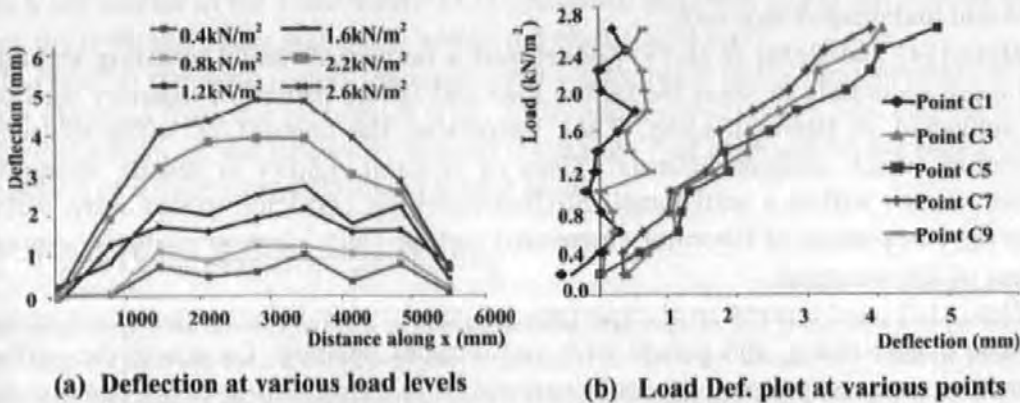(b) Load Def. plot at various points

Fig. 3. Measured load deflection along grid line C at various load levels

2.3 Numerical Computation Finite Element Modelling

As mentioned earlier, it was very difficult to find a FEA package that accurately models the masonry material properties, crack propagation and failure characteristics. Therefore, in this study a specialised non-linear FEA program, developed by Ma and May [4], was used. This FEA program was purely developed for research on masonry wall panels, but it lacks essential flexibility of the FEA packages.

In this analysis the following essential aspects were considered:

- The non-linearity failure criteria include both tension cracking and compression crushing of the masonry.
- The wall thickness was divided into 10 equal slices to monitor the crack propagation through the depth of the panel.
- Due to the inflexibility of this FEA program, degrees of freedom are only allowed to be either free or restrained. Spring stiffness was not provided to model support flexibility.

♦ The vertical edges of the panel were modelled as simply supported and the base edge as fully fixed. A full investigation into the effect of boundary modelling was conducted (not reported in this paper).

3 Numerical Model Updating Using Stiffness/Strength Correctors

A comprehensive literature review of various model updating methods is presented by Robert-Nicoud et al [1]. Siatta et al [5] discusses the reliability of system identification. Friswell and Mottershead [6] provide a survey of model updating procedures in structural damage detection research, using vibration measurements. Recent papers published in this area include [7, 8, 9, 10, 11, 12], and Cheng and Melhem [13] used fuzzy case-based reasoning for monitoring the bridge health. The majority of the research on model updating process involves computing sets of stiffness coefficients that help predict observed vibration modes of structures. The location and extent of damage are inferred through a comparison between the stiffness coefficients of damaged and undamaged structures.

Zhou [14] and Rafiq et al. [15] developed a numerical model updating technique that more accurately predicts the failure load and failure pattern of masonry wall panels subjected to lateral loading. They introduced the concept of stiffness/strength correctors which assigns different values of flexural rigidity or tensile strength to various zones within a wall panel. Stiffness/strength corrector values were derived from the comparison of laboratory measured and the finite element analysis computed values of displacement.

Zhou [14] used a number of experimental panels with different geometric properties and aspect ratios, and panels with and without opening, for which the stiffness correctors were determined. It was discovered from a comparison of the contour plots of corrector factors on these panels, that there appeared to be regions, termed 'zones', with similar patterns of corrector factors which are closely related to their relative positions from similar boundary types. In other words, zones within two panels appear to have almost identical corrector factors if they are located the same distance from similar boundary types.

Based on this finding, Zhou et al. [16] developed methodologies for zone similarity techniques. In order to achieve a more reasonable and automatic technique for establishing this zone similarity between the base panel and any new panel, a cellular automata (CA) model was developed to propagate the effect of panel boundaries to zones within the panel. The CA assigns a unique value, the so called 'state value' for each zone within the base panel and an unseen panel, based on their relative locations from various boundary types. The CA then identifies similar zones between the two panels by comparing similar state values of the two panels. Zones on two panels are considered to be similar if they are surrounded by similar boundary types and having similar distances from similar boundary types. Obviously the exact match is not possible. Therefore to find a good match for a zone on an unseen panel with a zone on the base panel, each zone on the unseen panel is compared with every zone on the base panel and the errors between the state value of a zone on the new panel and all zones on the base panel are calculated. The zone on the base panel with minimum error value is selected as the closest similar zone.

Prediction of the Behaviour of Masonry Wall Panels Using EC and Cellular Automata   539

Although the proposed methodologies improved the predicted failure load and failure pattern of a number of unseen panels, two important issues were not given enough attention:

   (i) the effects of panel aspect ratio on the response of the panel;
   (ii) the load deflection relationships

The research presented in this paper, has concentrated more these issues.

3.1 Methodologies for Reducing Error in Laboratory Data

Figs. 2(b) and 3 demonstrated the existence of irregularities in the load deflection data recorded in the laboratory and a need for minimising (correcting) error in the experimental data. A finite element analysis method approximates the numerical solution for differential equations, which are generally based on the displacement function that closely matches the theoretical deformed shape for structural elements. For plate and shell type structures, these displacement functions generally produce deformed shapes which are similar to the Timoshenko [17], analytical solutions of the differential equations for isotropic plates and shells within the elastic load level.

In order to compare results obtained from a non-linear finite element analysis and those obtained from the laboratory tests, an in depth investigation was carried out to reduce the error in the laboratory data to reflect the real response of the panel under the action of a uniformly distributed lateral load.

3.2 Three Dimensional Surface Fitting

The first step was to carry out a regression analysis on the 3D laboratory load deflection data to fit a surface that is a closer representation of an ideal response of laterally loaded panel under ideal conditions, which matches with the FEA model as closely as possible. On the 2D linear load deflection data, the objective was to minimise the local irregularities in the deformed shape of the panel as depicted in Fig 3.

In this investigation the following three different regression formulae were used:

   1. A polynomial function:

$$F_1 = \sum_{i=1}^{m} A_i * (ABS (X / L_x))^i \quad and \quad F_2 = \sum_{i=0}^{n} B_i * (Y / L_y)^i \tag{1}$$

$$W = A_0 * F_1 * F_2 + C$$

   2. A trigonometric function:

$$F_1 = COS^2 (ABS (\pi /2 *(X / (0.5*L_x)*A_1))^{A_2}) \quad and \quad F_2 = \sum_{i=1}^{m} B_i * (Y / L_y)^i \tag{2}$$

$$W = A_0 * F_1 * F_2 + C$$

   3. A Timoshenko like function [17].

Where: W is the deflection normal to the panel surface; Lx, Ly are panel length and height respectively; A_1, A_2 A_i, B_i and C are constant. Constant C is needed to model any movement in panel boundaries during the experiment; X and Y represent coordinates of point i.

540   Y. Rafiq et al.

Fig. 4. shows that all three models give a good fit for the experimental data while maintaining symmetry about the centreline of the panel. A more detailed investigation proved that the Timoshenko type surface gives a better fit with the experimental data at all measured points.
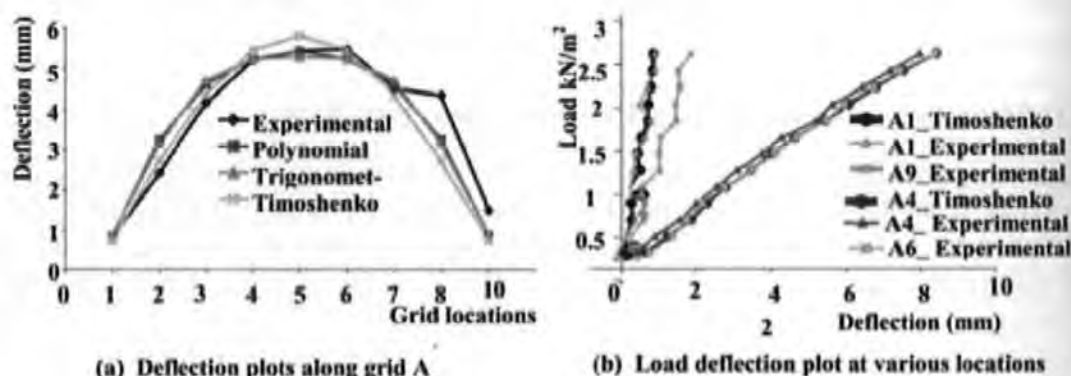

(a) Deflection plots along grid A   (b) Load deflection plot at various locations

Fig. 4. Load def. plots using various regression models (for nodal positions refer to Fig. 2a)

3.3 Evolutionary Computation Refined by Regression to Derive Correctors

In this research, the Genetic Algorithm (GA) was used to directly derive the corrector factors at various locations over the surface of the panel. At first the panel was divided into 36 locations to cover all measurement points (see Fig. 2). For simplicity a symmetrical half model was used. Corrector factors at each location were assigned to a GA variable (20 different variables for the symmetrical half model). Corrector factors, identified by the GA, were used to modify the flexural rigidity at each location on the panel. The objective function of the GA was designed to minimise the error between the modified experimental deflection (def_3D) and the deflection obtained by the FEA (def_FEA), over the entire surface of the panel.

Although the GA was able to find models that improved the predicted deflected shape of the panel, due to compensatory effects of many variables it was difficult to identify a suitable model. At this stage a regression analysis was used to refine corrector factors, selected from a number of the GA runs, to obtain a set of corrector factors that represent a best fit for the experimental deflected shape of the panel. Table 1 gives details of corrector factors derived by the GA and refined by regression. It should be noted that these corrector factors are used in the FEA to modify the flexural stiffness by multiplying these factors to the global elastic modulus (E) at each zone.

Table 1. Corrector factors derived by the GA and refined by Regression

	1	2	3	4	5	6	7	8	9
A	0.697	0.981	1.125	1.152	1.153	1.152	1.125	0.981	0.697
B	0.704	1.016	1.174	1.204	1.205	1.204	1.174	1.016	0.704
C	0.716	1.076	1.258	1.292	1.294	1.292	1.258	1.076	0.716
D	0.749	1.237	1.484	1.531	1.533	1.531	1.484	1.237	0.749

3.4 Boundary Modelling

A careful study of the corrector factors in Table 1 revealed that the flexural rigidities were mainly modified around the panel boundaries with relatively small changes inside the panel. It was therefore necessary to investigate the effect that boundary types may have on the behaviour of the panels.

At this stage it was decided to conduct a parametric study by changing the boundary types at the panel supports, and the GA was allowed to obtain corrector factors that produced a best fit with the modified experimental deformed shape. In this paper only the effect of the boundary at the base of the panel is discussed.

At first, the same boundary conditions as shown in Fig. 1 were assumed. The results from the FEA showed a kink around load level of 1.0 kN/m^2 (Fig. 5).
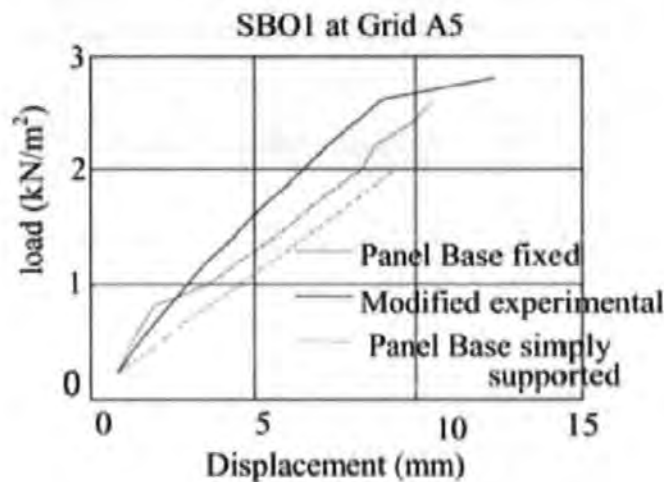
Fig. 5. Comparison of modified experimental with the predicted deflection using Table 1 Corrector Factors – Base simply supported and Fixed

Careful study revealed that this kink was due to the development of tensile cracks parallel to the bed joints, produced by the hogging moments along the panel base. As the tensile strength of the masonry is low parallel to the bed joints compared with that perpendicular to the bed joints, the first crack appears at a very low load level near the fixed support, which causes a kink in the load deflection curve. As this kink was not visible in the experimental load deflection data, it caused some concern.

The obvious choice for the next step was to change the boundary condition at the base of the panel to a simply supported type that allows full rotation of the base support. This eliminated the kink, but the stiffness of the panel was naturally reduced. This was reflected in the load deflection plots, (see Fig 5 for details).

A close investigation of Fig. 5 also revealed that the gradient of the predicted curves at various load levels were different from those of the experimental curves. In order to obtain a suitable set of corrector factors, it was decided to modify the objective function of the GA to include the gradient effect. The following errors were used:

542   Y. Rafiq et al.

1. Deflection error: minimise deviation of the FEA deflection values from the target values over the entire surface of the panel.
2. Gradient error: minimise deviation of the gradients of the FEA load deflection curve between two adjacent load levels.
3. Load error: minimise deviation of the FEA failure load from the target failure load.

A study of the corrector factors, derived from the simply supported base, revealed an increase in the corrector factors around the base of the panel. By changing the base of the panel to a fixed support (Table 2 corrector values) the opposite effect was observed. A close look at the results clearly strengthened the initial findings that the base of the panel is neither simply supported nor fixed, but there is only some degree of fixity at this edge.

Table 2. Corrector factors derived by the GA with panel base fixed

	1	2	3	4	5	6	7	8	9
A	1.283	1.278	1.278	1.278	1.278	1.278	1.278	1.278	1.283
B	1.187	1.182	1.181	1.181	1.181	1.181	1.181	1.182	1.187
C	0.927	0.921	0.920	0.920	0.920	0.920	0.920	0.921	0.927
D	0.223	0.218	0.218	0.218	0.218	0.218	0.218	0.218	0.223

From Fig. 5 it was observed that the FEA predicted failure load for simply supported base was much below the measured failure load. Although the failure load for the fixed base model was relatively increased, it was still below the measured values.

A closer look at this revealed that the decrease in failure load was due to the lower values of tensile strengths perpendicular to bed joints.

The results of the full boundary investigations revealed that:

♦ Boundary conditions shown in Fig 2 give closer results than the other models.
♦ Corrector factors derived by the GA for this model (refer to Table 2) give a better load deflection match at various locations over the surface of the panel.
♦ Changing the tensile strength perpendicular to the bed joints by 50% improved the predicted failure load of the panel.

4 Case Study

The corrector factors not only modeled the boundary effects, but also modelled variation in the material and geometric properties. One of the objectives of this research was to use these corrector factors to predict the behaviour of unseen panels with and without openings and panels for which the boundary conditions are different from the base panel. In this investigation it is important to note that the corrector factors derived in Table 2 are used to estimate the correctors at various locations on any unseen panel (Panel SBO2 in this study). The Cellular Automata 'zone similarity' technique [14,16] was used to estimate corrector values for unseen panels. These corrector

factors are then used in a non-linear FEA to predict the load deflection, failure load and failure pattern for the unseen panel.

To assess the validity of the numerical model updating techniques presented in this paper a panel which was the same size as the base panel SBO1, but with an opening at the middle of panel (Panel SBO2), was investigated. Results of this investigation are presented in Fig 6.
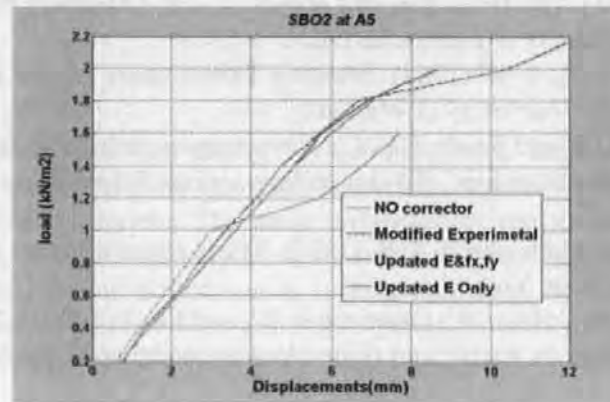

Fig. 6. Load deflection curve at maximum deflection location (A5)

5 Further Work

The challenging task is to extend this model updating technique to panels tested elsewhere, under different laboratory conditions and using different material constituents for construction of the panels. We were able to locate test data for a limited number of panels, tested elsewhere and would greatly appreciate the offer of further data, particularly on load deflection and tensile strength information for any type and size of masonry panels from researchers around the world.

The plan would be to investigate the suitability and generality of the corrector factors derived for the base panel to predict the failure criteria for as many unseen panels as possible.

6 Conclusions

This is perhaps the first time that an attempt has been made to use a numerical model updating technique to study the behaviour of a highly composite anisotropic material such as masonry within the full linear and non-linear range.

The research presented in this paper introduces a numerical model updating technique that has the potential to be extended to masonry material, which is highly composite and anisotropic.

In this research, corrector factors from a single panel tested in the laboratory were used for a number of unseen panels with different boundary types, size and configurations. The results produced more accurate prediction of the behaviour of the laterally loaded masonry wall panels.

544   Y. Rafiq et al.

References

1. Robert-Nicoud, Y., Raphael, B., and smith I. F. C. (2005). " System Identification through Model Composition and Stochastic Search", ASCE Journal of Computing in Civil Engineering, Vol. 19, No. 3, pp 239-247.

2. Raphael, B., and Smith, I. F. C., (2003) Fundamentals of computer aided engineering. Wiley, New York.

3. Chong, V. L. (1993). The Behaviour of Laterally Loaded Masonry Panels with Openings. Thesis (Ph.D). University of Plymouth, UK.

4. Ma, S. Y. A. and May, I. M. (1984). Masonry Panels under Lateral Loads. Report No. 3. Dept of Engineering, University of Warwich.

5. Saitta, S., Raphael, B. and Smith, I. F. C., "Data mining techniques for improving the reliability of system identification", Advanced Engineering Informatics, Vol. 19, No 4, 2005, pages 289-298.

6. Friswell, M. I., and Mottershead, J. E. (1995). Finite element model updating in structural dynamics, Kluwer, New York

7. Brownjohn, J. M. W., Moyo, P., Omenzetter, P., and Lu, Y. (2003). "Assessment of highway bridge upgrading by testing and finite-element model updating." J. Bridge Eng. 8 (3), 162–172.

8. Castello, D. A., Stutz, L. T., and Rochinha, F. A., (2002). "A structural defect identification approach based on a continuum damage model." Comput. Struct. 80, 417–436.

9. Teughels, A., Maeck, J., and Roeck, G. (2002). "Damage assessment by FE model updating using damage functions." Comput. Struct. 80, 1869–1879.

10. Modak, S. V., Kundra, T. K., and Nakra, B. C. (2002). "Comparative study of model updating studies using simulated experimental data."Comput. Struct. 80, 437–447.

11. Hemez, F. M., and Doebling, S. W. (2001). "Review and assessment of model updating for non-linear, transient dynamics." Mech. Syst. Signal Process. 15 (1), 45–74.

12. Hu, N., Wang, X., Fukunaga, H., Yao, Z. H., Zhang, H. X., and Wu, Z. S. (2001). "Damage assessment of structures using modal test data." Int. J. Solids Struct., 38, 3111–3126.

13. Cheng, Y. and Melhem, H. G., "Monitoring bridge health using fuzzy case-based reasoning", Advanced Engineering Informatics, Vol. 19, No 4, 2005, pages 299-315.

14. Zhou, G. C. (2002). Application of Stiffness/Strength Corrector and Cellular Automata in Predicting Response of Laterally Loaded Masonry Panels. School of Civil and Structural Engineering. Plymouth, University of Plymouth. PhD Thesis.

15. Rafiq, M. Y., Zhou G. C., Easterbrook, D. J., (2003). "Analysis of brick wall panels subjected to lateral loading using correctors." Masonry International 16(2): 75-82.

16. Zhou,G. C., Rafiq M. Y. Easterbrook, D. J., and Bugmann, G. (2003). "Application of cellular automata in modelling laterally loaded masonry panel boundary effects", Masonry International. Vol. 16 No 3, pp 104 -114.

17. Timoshenko, S. P., Woinowsky-Krieger, S. (1981) Theory of Plates and Shells,2nd Edition, McGraw-Hill.

Paper 21
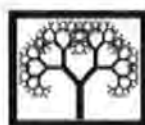
Using Artificial Intelligence Techniques to Predict the Behaviour of Masonry Panels

M.Y. Rafiq, C. Sui, G.C. Zhou, D.J. Easterbrook and G. Bugmann
School of Engineering
University Plymouth, United Kingdom

Abstract

Laboratory experimental data is often erroneous. This error is more apparent in data obtained from testing of anisotropic composite materials such as masonry wall panels. In this paper data colleted from the laboratory tests of masonry panels is presented. Methodologies for reducing (correcting) error in laboratory tested data are discussed. The concept of stiffness/strength corrector to model the variation in masonry properties in laterally loaded masonry panels was introduced by Zhou [1] and Rafiq et al [2] to model variation in masonry properties. A cellular automata (CA) technique was used to model the boundary effect and establish stiffness/strength corrector values for unseen panels, using zone similarity techniques introduced by Zhou et al [3] These stiffness/strength correctors are then used in a non-linear finite element analysis (FEA) to predict the failure load and failure pattern of these unseen panels. This paper demonstrates that methodologies for reducing error in experimental data can further improve the predicted failure load of the panels.

Keywords: corrector factor, cellular automata.

1 Introduction

Masonry is a material composed of two completely different constituents, which when combined together produce a highly variable composite material. However due to this highly composite nature of the constituents of this material it has been very difficult to accurately predict the behaviour of masonry elements. Research carried out by Lawrence [4] indicated that it is essential to consider an inherent random variation in masonry properties, in any theoretical analysis to produce a better prediction of the behaviour of laterally loaded masonry panels.

1

Research in the University of Plymouth by Zhou [1] and Rafiq et al [2], has proposed a novel approach for the analysis of masonry panels subjected to lateral loading, which gives a much closer prediction of both failure load and failure patterns. This method is based on the proper modelling of the variation in masonry properties in various locations within the panel and more importantly, properly modelling the effect of panel boundaries, which has been proved by this research to have a dominant effect on the behaviour of panels subjected to lateral loading. The research has introduced a new concept, "stiffness/strength corrector" Zhou [1], which quantifies the boundary effects and properly models the variation in masonry properties at various locations (zones) within a masonry wall panel. Derivation of these correctors was based on a closer mapping of laboratory experimental results, carried out by Chong [4], with those obtained from a non-linear finite element analysis of full-scale masonry wall panels subjected to a uniformly distributed lateral load. The finite element program was originally developed by Ma and May [5] and further developments were introduced by Chong [4] and Zhou [1] and Zhou et al [3], used a cellular automata (CA) to model the effect of various boundary (edge support) types. This research used a single leaf brick panel for which stiffness/strength correctors were determined as the 'base panel', i.e. the panel from which all other panel correctors could be predicted. This research also introduced the concept of zone similarities, using CA, which enable, corrector values at various zones inside the base panel to be mapped on to any unseen panel with various boundary types and for panels with or without opening, to determine corrector values. The corrector values were then used in a non-liner FEA program to estimate the failure load and failure pattern for unseen masonry panels.

Research by Zhou [1] demonstrated that it was possible to achieve an improvement of about 20% in the failure load capacity of the laterally loaded masonry wall panels. Although considerable improvements were achieved in the failure load and failure pattern of the masonry panels, errors in the experimental results made comparison of the analytical and experimental load deflection results inconclusive.

The research presented in this paper extends the previous research by introducing methodologies for minimising the error in the laboratory test data and concentrates on reducing the error between analytical and measured load deflection data at various locations on a panel. Case studies will be presented to demonstrate that it is possible to improve load deflection and failure load capacity of the panels. The research also introduces a methodology for handling scaling effects when establishing corrector values for unseen panels which are different in their size to those of the base panel.

2 A brief overview of the previous research

Figure 1 shows location of the measurement points on the base panel. This panel was a solid single leaf clay brick masonry wall panel. Linear Variable Differential Transformers (LVDTs) were placed at each gridline intersection. The panel was loaded using an air bag, which was a common procedure for applying uniform

2

lateral load on the face of the panel. The panel was simply supported along its vertical edges, fixed at its base and free at the top. The load was gradually increased on the panel and deflection data was recorded at intervals of 0.2 kN/m². It was observed that at the initial stage of the test the right hand edge of the panel was moved until the sides of the panel were fully in contact with the supporting edges. Figures 2 shows a 3 dimensional surface plot of the experimental load deflection data at every measurement location and Figure 3 shows a line plot of the load deflection data along gridline C (across the width of the panel) at various load levels.

Evidence of movement in the right hand support is clear in Figures 2 and 3. Irregularities in the surface plot in Figure 2 and in line plot in Figure 3 clearly show inaccuracies in the laboratory recording data. This error in more pronounced at lower load values (up to 1.6 kN/m²). From the surface plot of deflection in Figure 2 it is also clear that their was no data available at locations near the bottom support of the panel. This has resulted an a flat surface near that area which is not a true representation of the deflected shape for this type of panel.

Figure 4 shows individual load deflection plots at various recording points along gridline C. The evidence of irregularities at locations near the boundaries of the panel (Points C1 and C9) is more pronounced. Figure 4 better demonstrate the existence of error in recording data as at certain load levels the deflection is moving in the wrong direction as the load is increased. Moreover, it was expected that the deflected shape of the panel should be symmetrical about its vertical centreline (about gridline 5). From Figures 2 and 3 it is clear that this was not the case with the measured data. Methodologies for minimising the error in the laboratory data to reflect the real response of panels under applied lateral load are discussed in the following section.
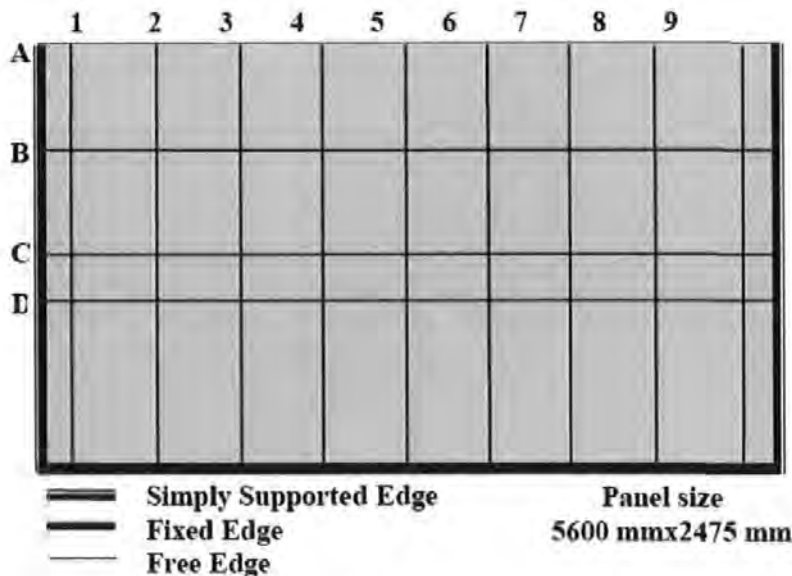

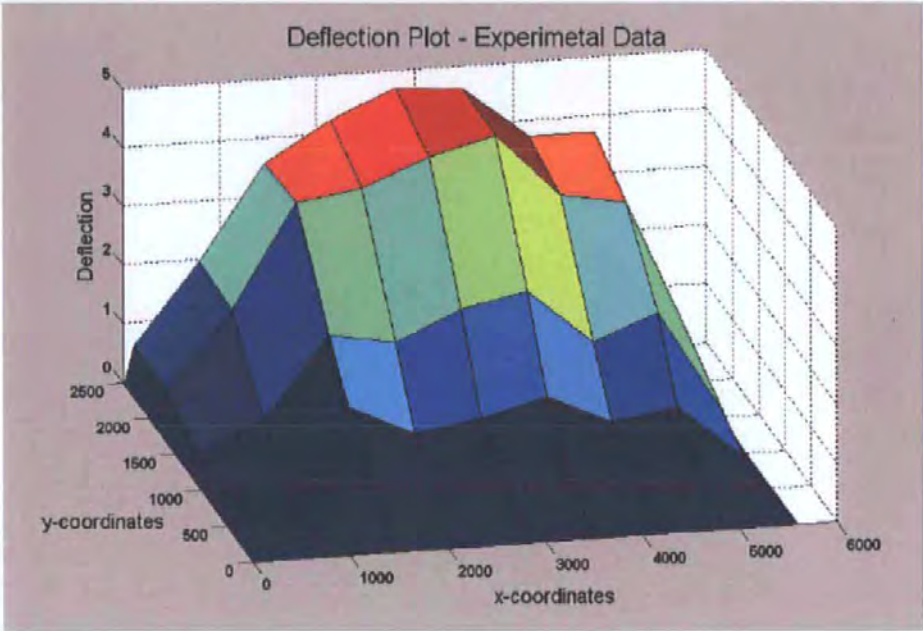Figure 1 position of recorded measurement points on the 'base panel'

3

Figure 2. surface plot of experimental deflection data (at 1.8 kN/m^2)
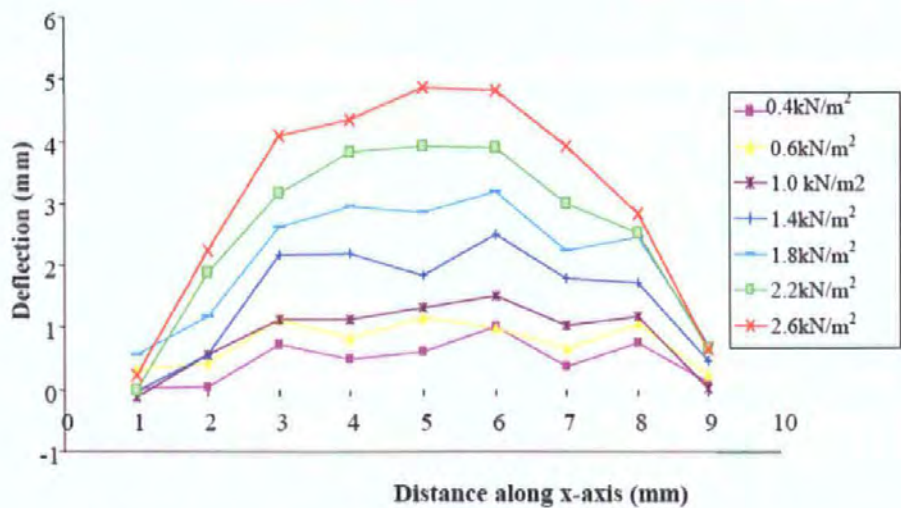

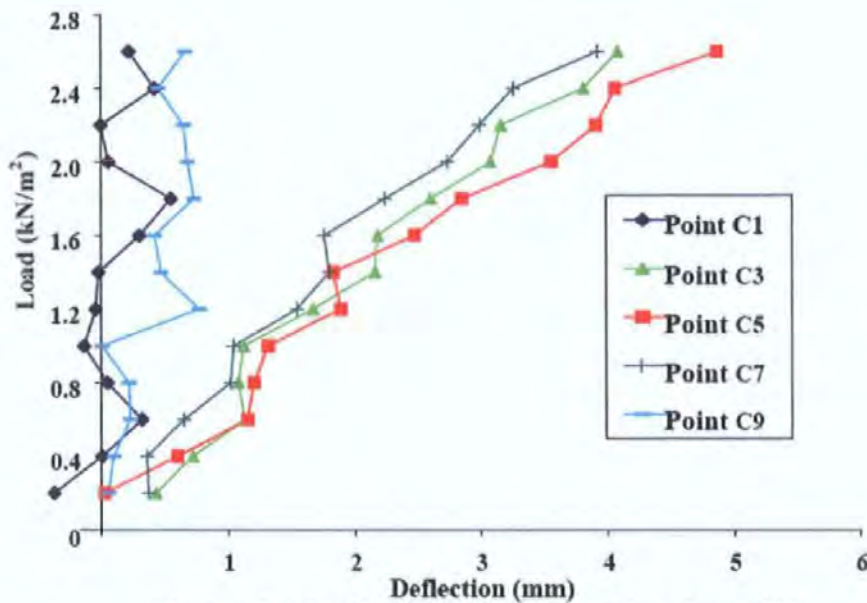Figure 3 Measured deflection along grid line C at various load levels

4

Figure 4 Load Deflection plot at various points along grid C

3   Methodologies for reducing errors in laboratory data

An in depth investigation was carried out to reduce the error in the laboratory data to reflect the real response of the panel under the uniformly distributed lateral load in order to be able to compare a like with like situation both for the FAE and experimental results. The first step was to carry out a regression analysis both on the 3D data and 2D linear data to find a better fit between the expected experimental data and the FEA model in order to minimise discrepancies in actual experimental data as depicted in Figure 4.

3.1   Three dimensional surface

In this analysis the following three different regression models were investigated to fit the experimental data:

Polynomial function;
Trigonometric function; and
Timoshenko [6] like function.

The result of the three analyses is presented in Figure 5. From Figure 5 it is clear that all three curves give a good fit to the experimental data while maintaining symmetry about the centreline of the panel. A more detailed investigation proved that the Timoshenko type surface was a better fit with the experimental data and with the real situation.
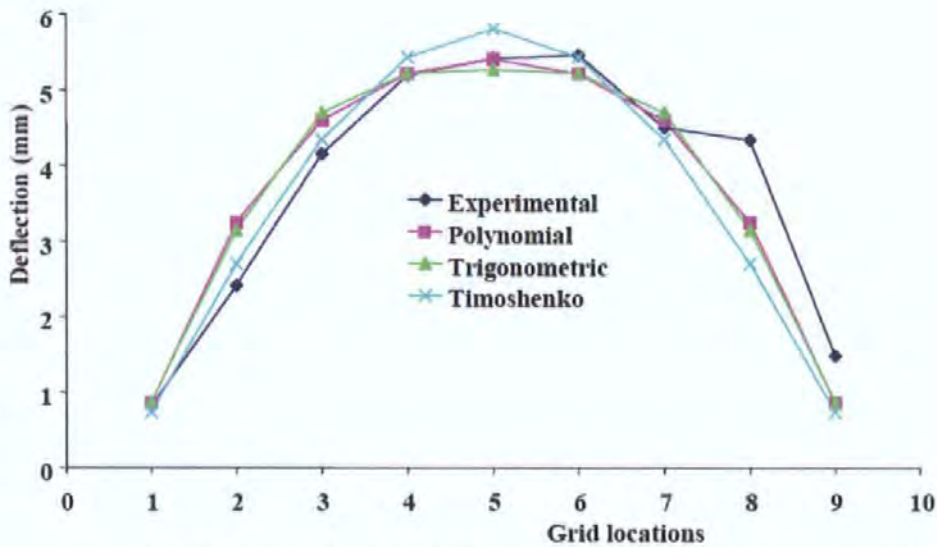
5

Figure 5 Load deflection plots along grid A using various regression rules

Figure 6 shows a comparison of load deflection plot of the experimental data with that of the chosen Timoshenko type regression results. Once again, from Figure 6 it is clear that the chosen curve not only gives a better fit with the experimental data at various load levels, but also eliminates the unexpected irregularities in the load deflection plots near the boundaries of the panel.

The final relationship used to simulate the expected deformed shape of the base panel under a uniformly distributed load is given below:

$F1 = A_1* \cosh (\pi *Y/L_x)+A_2*\pi *Y/ L_x *\sinh (\pi *Y/ L_x)+A_3*\sinh (\pi *Y/ L_x)$
$- A_3*Y *\pi/ L_x *\cosh (\pi *Y/ L_x)$
and
$F2 = \pi^4/96* \sin (\pi *X/ L_x)$
And finally the final deformed shape is represented by:
$Z = A_0*F_2 + F_1*\sin (pi*X/L_x) + C$

Where:

A$_0$, A$_1$, A$_2$ and A$_3$ are constants
L_x and L_y represent the width and height of the panel respectively and
X and Y represent X and Y coordinates of any point on the panel
Z is the vertical deflection at location (X,Y)
The constant C was introduced here to model possible movement at the edges of the panel.

The Timoshenko type regression formula allows a better satisfaction of the panel boundary conditions, such as $\frac{\partial Z}{\partial x} |_{(x=o \text{ and } x=Lx)}=0$ and $\frac{\partial Z}{\partial y} |_{y=0}=0$.
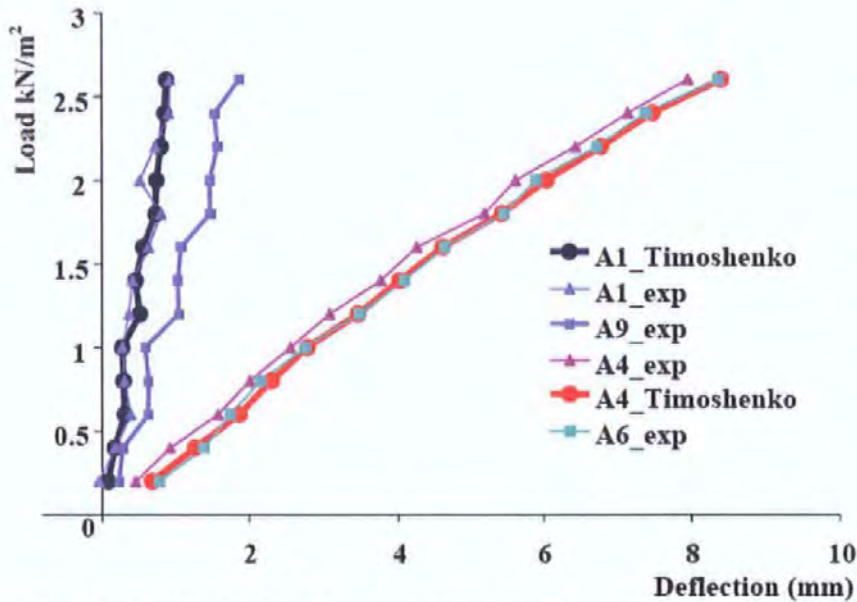
6

Figure 6   Load deflection plots – a comparison of experimental and corrected deflection along Grid A

3.2   Modified corrector values

As discussed earlier, the stiffness/strength corrector concept introduced by Zhou [1] was based on a closer mapping of laboratory experimental results, with those obtained from a non-linear finite element analysis of full-scale masonry wall panels subjected to a uniformly distributed lateral loads. In order to maintain symmetry and eliminate irregularities in experimental load deflection data near the panel boundaries, as discussed in the previous section, in this research stiffness/strength corrector values are based on the comparison of the FEA results with those obtained from a Timoshenko type regression results. The following section describes how the corrector values are improved using several iterations.

3.3   Iteration method

The corrector values derived by Zhou [1] were calculated as:

$$\Psi = \frac{W_{FEA}}{W_{Exp}}, \quad \text{and} \quad D_\Psi = D * \Psi$$

Where:
  W = deflection at any point on the panel
  D = Flexural Rigidity and
  Ψ = corrector values

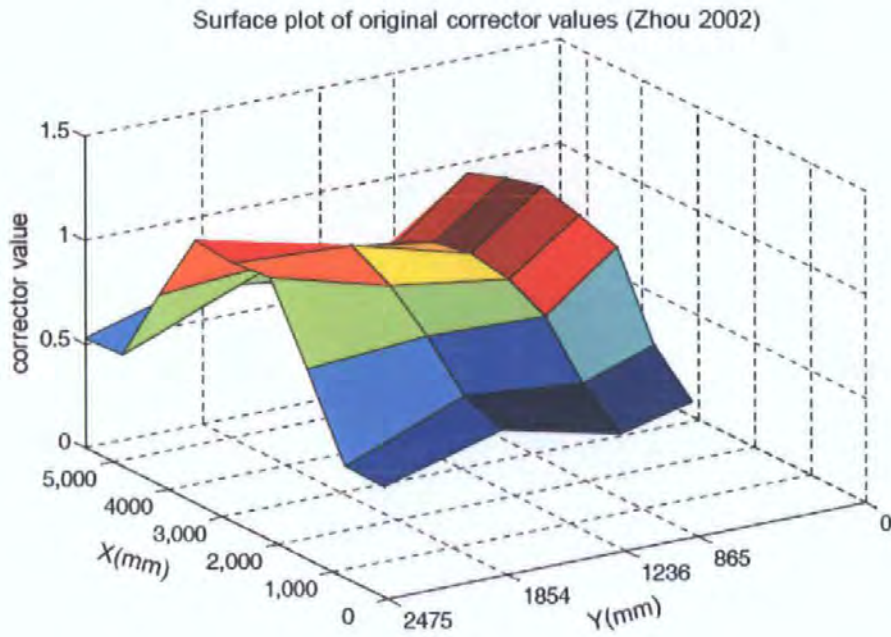A surface plot of Zhou's corrector values is given in Figure 7.

7

Figure 7 surface plot of correctors obtained by Zhou [1]

Zhou's corrector values were based on a direct comparison (a single step) of the FEA and experimental deflection values. In order to further improve the accuracy of the corrector values after a comprehensive study the following modification was introduced:

$$\psi_i = \frac{W_{FEA}^{i-1}}{W_{Exp}}, \quad \text{and} \quad D\psi_i = D\psi_{i-1} * (\psi_i)^m$$

Where:

i = number of iteration

m = a constant 0< m < 1.0 to refine the search for better match between experimental and FEA results.

The result of the investigation demonstrated that values of m<0.4 and up to 4 Iteration gives much better results.

Figure 8 shows corrector values obtained by the iteration method.

8

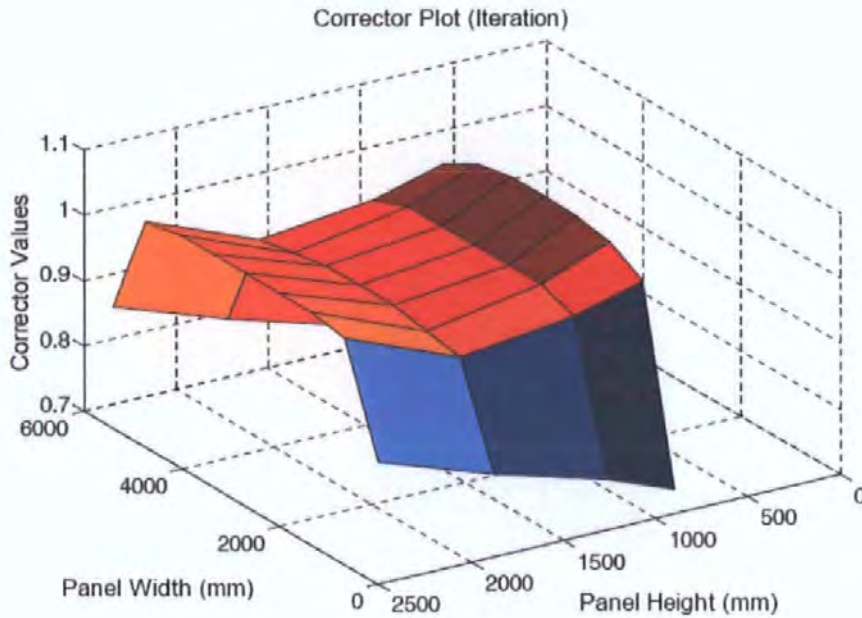Figure 8 Surface plot of correctors obtained by iteration for different m

3.4 The Genetic Algorithm approach

A further investigation was carried out using genetic algorithms (GAs). In this investigation corrector values were directly determined by the GA. The variables in the GA were 36 corrector values at the locations of the laboratory measured deflection points and the objective was to minimise the total error between measured and FEA results at all locations on the panel. Although the GA minimised the error considerably, due to the high dimensionality of the problem (36 dimensions in this case) it was difficult to find a unique solution. It was decided to combine the GA and regression analysis results to get a better result.

3.5 Combining the GA and regression

In this method corrector values from several runs of the GA were collected and a regression analysis was performed in order to minimise the error between the FEA results and the measured deflection at each location on the panel individually. The results of this investigation are presented in Figure 9, and this was adopted as the corrector values for the base panel.
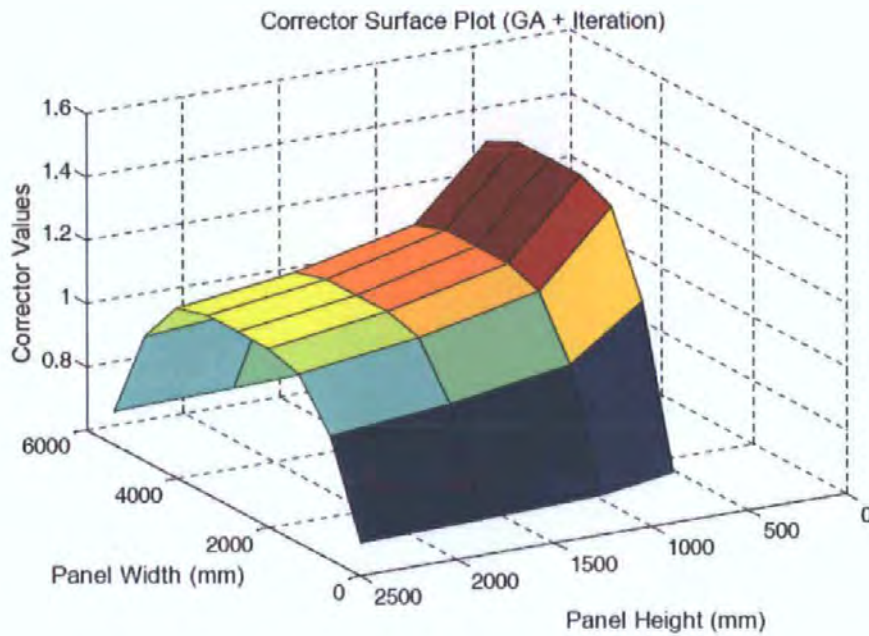
9

Figure 9 Surface plot of correctors obtained by the GA and iteration

4   Case studies

4.1   The base panel

Using the corrector values shown in Figure 9, the base panel was analysed using non-linear FEA program. The predicted failure load was 2.6 kN/m^2 which was an excellent match with the experimental failure load of 2.7 kN/m^2. Figure 10 shows a contour plot of the analytical failure pattern of this panel at 2.6 kN/m^2 load level. Once again this is similar to the experimental failure pattern shown in Figure 11.
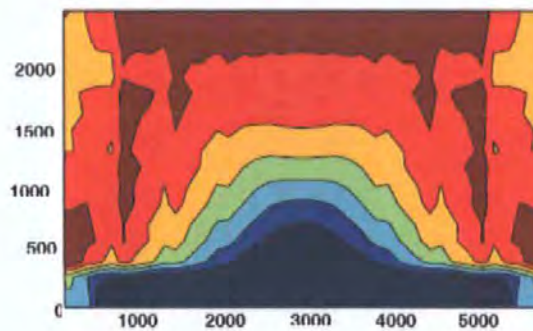

Figure 10 Predicted failure pattern of the base panel

10

Figure 11 Experimental failure pattern of base panel

Figure 12 shows a comparison of the modified experimental and analytical load deflected shapes. There is a close similarity between the two surfaces.
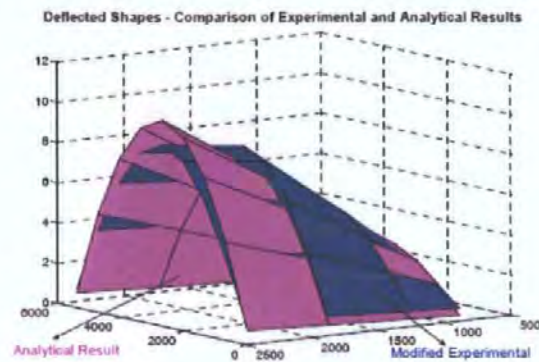

Figure 12 Surface plot of the experiment and analytical deflected shapes

4.2 Unseen panel with different size and boundary conditions

To demonstrate the generality and applicability of the methodologies described in this paper, cellular automata was used to establish corrector values at different locations on this unseen panel using similarity rules discussed in Zhou et al [3]. The corrector values were taken from the base panel as shown in Figure 9. The unseen panel was analysed using the same non-linear FEA program. The results of the analysis are discussed in this section.

Figures 13 and 14 show the analytical and experimental failure patterns of this unseen panel respectively. From the comparison of these two Figures it is clear that the analytical method was able to predict the failure pattern correctly. The analytical predicted failure load for this panel was 7.5 kN/m^2, which compares well with the experimental failure load of 7.0 kN/m^2.

Figure 15 shows a comparison of the experimental and analytical load deflected shapes. Both deflected shapes are similar, but the analytical model seems to be a bit

11

stiffer than the actual panel. This could also be the effect of scaling factor as this unseen panel was half the size of the base panel. This aspect needs further investigation. It is worthwhile mentioning that the experimental records of this unseen panel showed that the right hand side of this panel had moved. This aspect has not been considered in the analysis.
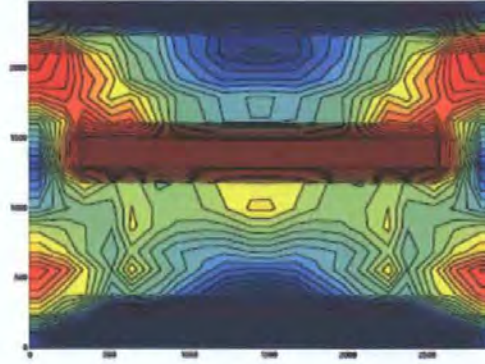

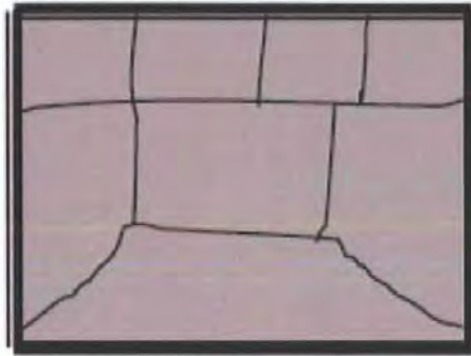Figure 13 Predicted failure pattern of an unseen panel

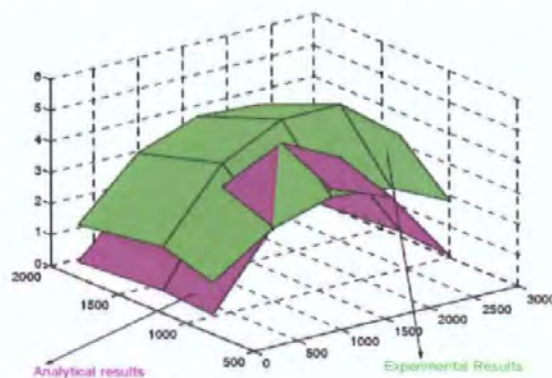Figure 14 Experimental failure pattern of an unseen panel

Figure 15 Surface plots of the experiment and analytical deflected shapes

12

5 Conclusions

Based on this investigation the following conclusions can be drawn:

- The failure load values were greatly improved.
- Load deflection curves at various locations on the panel were closely related to the experimental results.
- The failure pattern was similar to those of the experimental results and those of Zhou [1].
- The corrector values for 'unseen' panels, which were determined by the Cellular Automata, using zone similarity concepts greatly improved the prediction of failure load and load deflection values.
- Scaling rules proposed in this research was effective to model scaling effects due to changes between the 'base panel' and any 'unseen' panels.

References

[1]   Zhou, G. C. (2002). Application of Stiffness/Strength Corrector and Cellular Automata in Predicting Response of Laterally Loaded Masonry Panels. School of Civil and Structural Engineering. Plymouth, University of Plymouth. PhD Thesis.

[2]   Rafiq, M. Y., G. C. Zhou, et al. (2003). "Analysis of brick wall panels subjected to lateral loading using correctors." Masonry International 16(2): 75-82.

[3]   Zhou, G. C., M. Y. Rafiq, et al. (2003). "Application of cellular automata in modelling laterally loaded masonry panel boundary effects." Masonry International (3): 104-114.

[4]   Chong, V. L. (1993). The Behaviour of Laterally Loaded Masonry Panels with Openings. Thesis (Ph.D). University of Plymouth, UK.

[5]   Ma, S. Y. A. and May, I. M. (1984). Masonry Panels under Lateral Loads. Report No. 3. Dept of Engineering, University of Warwick.

[6]   Timoshenko, S. P., Woinowsky-Krieger, S. (1981). Theory of plates and shells, 2nd Edition, McGraw-Hill. ISBN 0-07-085820-9.

13